HEATHROW AIRPORT 2019 AIR QUALITY ASSESSMENT

Report for: Heathrow Airport Limited

Ref. HAL1011301PO

Ricardo ref. ED16750 Issue: 1 19 December 2023

Ricardo Energy & Environment, Gemini Building, Fermi Avenue, Harwell, Oxfordshire, OX11 0QR, UK | +44(0)1235 75 3000 | ee.ricardo.com
Registered company no. 08229264 | VAT no. GB 212 8365 24

Customer:
Heathrow Airport Limited

Customer reference:
HAL1011301PO

Contact:
Charles Walker, Bright Building, 1st Floor, Manchester Science Park, Pencroft Way, Manchester, M15 6GZ, UK.

T: +44 (0) 1235 753 115
E: charles.walker@ricardo.com

Author:
Charles Walker

Approved by:
Gareth Horton

Signed

Ricardo reference:
ED16750

Date:
19 December 2023

CONTENTS

Appendices

1. INTRODUCTION

1.1 CONTEXT

This report presents an assessment of air quality in the neighbourhood of Heathrow Airport in the year 2019. It considers the impacts of the operation of the airport (including road traffic to and from the airport), as well as non-airport sources of air pollution, to estimate both the overall picture of air quality and the airport's contribution to it.

This study is one of a series of assessments that have been carried out for Heathrow Airport. A major study for 2013 included an emission inventory[1], dispersion modelling study[2], and model evaluation against monitoring data[3]. Since 2013, annual aircraft inventories have been produced and from 2015 they were expanded to include all airfield sources[4,5]. However, they did not include off-airfield sources, including airport carparks, nor did they calculate concentrations.

This work updates the major 2013 study to 2019 with a full emission inventory (adding to the airfield inventory already issued[4]), dispersion modelling and model evaluation. 2019 was chosen in preference to either 2020 or 2021 as the latter 2 years were impacted by the Covid-19 pandemic.

1.2 AIR QUALITY

In England, concentrations of key pollutants in outdoor air are regulated by the Air Quality Standards Regulations 2010[6]. (Similar regulations exist for Wales, Scotland, and Northern Ireland.)

These Air Quality Standards Regulations set 'limit values', 'target values' and 'long-term objectives' for ambient concentrations for several pollutants, including NO_2, PM_{10} and $PM_{2.5}$, identified as priority pollutants in an airport context[7]. The objectives relevant to these pollutants are shown in Table 1.

Table 1 Air quality standards regulations for selected pollutants

Pollutant	Objective	Concentration measured as	Date to be achieved by (and maintained thereafter)
PM_{10}	50 µg m^{-3} not to be exceeded more than 35 times a year	24-hour mean	31 December 2004
PM_{10}	40 µg m^{-3}	Annual mean	31 December 2004
$PM_{2.5}$	20 µg m^{-3}	Annual mean	1 January 2020
$PM_{2.5}$	Target of 20% reduction in concentrations at urban background	Annual mean	Between 2010 and 2020
Nitrogen dioxide (NO_2)	200 µg m^{-3} not to be exceeded more than 18 times a year	Hourly mean	1 January 2010
Nitrogen dioxide (NO_2)	40 µg m^{-3}	Annual mean	1 January 2010

[1] John Cookson and Martin Peirce (2014) Heathrow Airport 2013 Emission Inventory. Ricardo-AEA/R/ 3411.

[2] Hazel Peace, Charles Walker, Martin Peirce (2015) Heathrow Airport 2013 Air Quality Assessment. Ricardo-AEA/R/3438.

[3] Charles Walker, Martin Peirce and Hazel Peace (2015) Heathrow Airport 2013 Air Quality Assessment: Model Evaluation Airport Air Quality Modelling for 2008/9: Results and Model Evaluation. Ricardo-AEA/R/3439.

[4] Charles Walker (2022) Heathrow Airport Airfield Emission Inventories 2015 to 2020.

[5] Charles Walker (2023) Heathrow Airport Airfield Emission Inventory 2021

[6] https://www.legislation.gov.uk/uksi/2010/1001/contents/made

[7] DfT (2006) *Project for the Sustainable Development of Heathrow: Report of the Airport Air Quality Technical Panels.*

The legal limits on the concentrations of key pollutants have proved to be challenging to meet in urban areas across the UK (and Europe). In the airport context, the air quality limit that appears most challenging in the UK is the 40 µg m^{-3} limit for annual-mean nitrogen dioxide (NO_2) concentrations. Air Quality Management Areas are declared for areas exceeding one of the air quality legal limits. The whole of the London Borough of Hillingdon south of the Chiltern-Marylebone railway line, in which Heathrow Airport sits, has been declared an Air Quality Management Area (AQMA)[8], though it should be emphasised that the airport is only one contributor to air quality problems within any AQMA. The impacts of airports on local air quality are a major constraint on airport growth in many parts of the world and were a key issue in the Airports Commission's deliberations into provision of additional runway capacity in the UK.

The Air Quality Strategy for England[9], published in April 2023, sets out further tightening of the $PM_{2.5}$ standards. These are shown in Table 2.

Table 2 The environmental targets (fine particulate matter) (England) regulations 2023

Pollutant & metric	Target	Target year
$PM_{2.5}$ annual mean concentration	Interim target: 12 µg m^{-3}	2028
$PM_{2.5}$ annual mean concentration	Legally binding target: 10 µg m^{-3}	2040
$PM_{2.5}$ population exposure	Interim target: 22% reduction in exposure compared to 2018	2028
$PM_{2.5}$ population exposure	Legally binding target: 35% reduction in exposure compared to 2018	2040

Most NO_2 in the air arises as a side-effect of combustion, the high temperatures oxidising a small fraction of the nitrogen in the air. Broadly speaking, near Heathrow there are three main categories of source:

- Road traffic – some of which will be travelling to or from the airport.
- Heathrow Airport itself – especially aircraft engines and the ground support vehicles and equipment that service the aircraft.
- Other sources both local and more distant, such as domestic and commercial heating, industrial processes, and other vehicles and equipment powered by combustion engines.

In addition, although airports are not considered to be a major source of particulate matter (PM_{10}) emissions, achieving the current objectives of the Air Quality Standards Regulations[6] for this pollutant presents challenges for many areas of the UK. In addition, in view of the Air Quality Strategy cap[9] on $PM_{2.5}$ concentrations, the list of key pollutants for an airport emissions inventory needs to include both PM_{10} and $PM_{2.5}$. Furthermore, there is growing concern over ultrafine particle emissions from aircraft and although no current regulations exist for ultrafine particles, they are under consideration, within the European Commission, as an emerging pollutant[10].

1.3 THE ROLE OF MODELLING

While it is possible to measure concentrations of pollutants of concern, and several monitoring stations are operating in the area around Heathrow, these are expensive to run, and it is impractical to have enough to provide a full picture of local air quality. It is therefore necessary to turn to modelling to fill out the picture. A modelling study has several benefits:

- It can fill in the spatial gaps between monitors, allowing air quality to be assessed at all locations of interest. For example, the area impacted by air quality limit exceedances can be calculated and the number of households covered by the area as well.
- It makes it possible to see which sources are responsible for how much pollution ("source apportionment"). For example, if there is an exceedance of a limit value, how much is due to the airport, how much due non-airport road traffic and how much due remote sources?

[8] https://uk-air.defra.gov.uk/aqma/details?aqma_ref=28

[9] https://www.gov.uk/government/publications/the-air-quality-strategy-for-england

[10] Systematic assessment of monitoring of other air pollutants not covered under Directives 2004/107/EC and 2008/50/EC, October 2022

- It provides a basis for forecasting how air quality will behave in the future. Even in the case of 'business as usual', there will be changes in the number and types of aircraft using the airport, for example. In addition, where there are proposals for changes to airport infrastructure, such as a new runway, modelling is necessary to understand the effects of such developments.
- Bringing the last two points together, modelling can inform action planning, i.e., implementing measures aimed at improving air quality and eliminating exceedances, by helping to understand whether proposed measures are likely to be effective and cost-effective.

1.4 ABOUT THIS ASSESSMENT

The study reported here was designed with these purposes in mind. The work falls into three main parts:

- First, an emissions inventory is calculated to estimate how much of the pollutants is emitted from the different sources.
- Second, dispersion modelling calculates how the emissions are carried through the air, due to meteorological conditions such as wind speed and direction, and the resulting concentrations of pollution in the air.
- These modelled concentrations are compared with monitoring data as a check on the accuracy of the model.

The final total concentrations are also compared with the air quality limit values to see if there is a risk of them being exceeded.

The main body of this report presents the methodology and results of the emissions inventory and dispersion modelling (including an analysis of the airport's activity). It also includes a brief comparison with monitoring data. A more detailed model evaluation, and conclusions about the suitability of the model, are discussed in Appendix 1.

2. METHODOLOGY

The methodology for the present work closely resembles that of the 2013 work[1,2,3], but as new data has become available and operational changes have occurred, an update was desirable.

The 2013 methodology followed the recommendations of the Project for the Sustainable Development of Heathrow (PSDH)[11], a project sponsored by the Department for Transport to formulate the best practical methodology for airport air quality assessments.

The methodology is also consistent with the International Civil Aviation Organization's Airport Air Quality Manual[12], meeting the requirements of the 'Advanced' approach with elements of the 'Sophisticated' approach where data is available.

Since the methodology is largely the same as that used for the 2013 work, only those aspects which are materially different are described in this report.

2.1 AIRFIELD SOURCES

Airfield emissions include:

- Aircraft and APU
- Ground Support Equipment (GSE)
- Stationary sources (heating plant and fire training ground)

Emissions from these sources have been discussed and reported previously[4], so are not reproduced in this report.

2.1.1 Spatial representation of emissions

Taxiways, stand locations and hold areas have been updated to reflect the airfield layout in 2019, as shown in Figure 1.

[11] Department for Transport (2006) Project for the Sustainable Development of Heathrow. Report of the Airport Air Quality Technical Panels.

[12] International Civil Aviation Organization (2011) Airport Air Quality Manual. Doc 9889, ISBN 978-92-9231-862-8.

Figure 1 Airfield layout

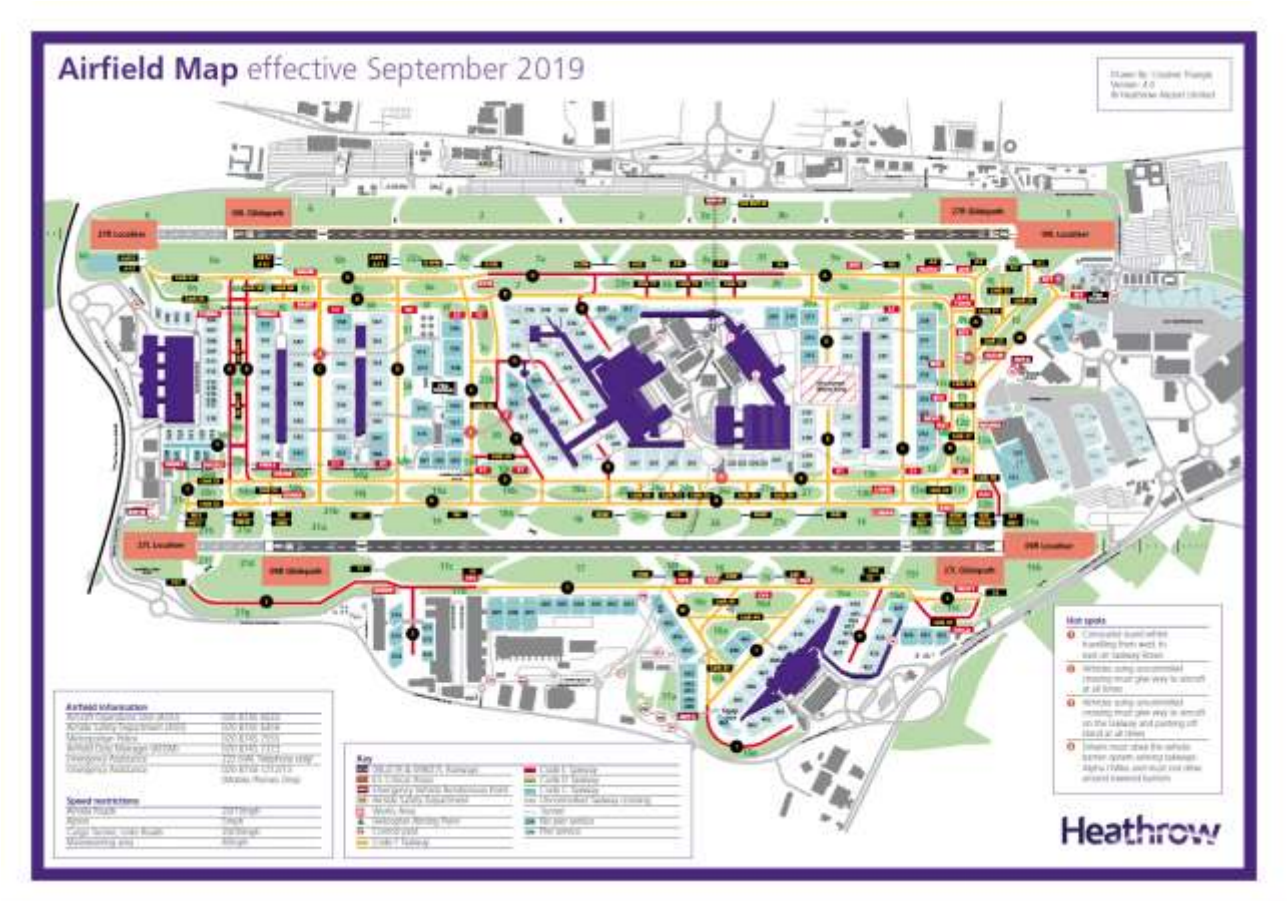

Sample ground radar data for 2019 were obtained from Heathrow's OPAS system. These were used to disaggregate taxiing and hold emissions and to provide runway entry and exit block probabilities.

Climb angles were derived from NTK data for 2019 as described in the emission inventory report[4]. Analysis of NTK arrivals data confirmed that approach angles are very close to 3°, so all aircraft were assumed to approach at an angle of 3°.

2.1.2 Runway utilisation and easterly/westerly split

Runway utilisation, especially the split between easterly and westerly operations, varies from year to year depending on weather conditions. Table 3 shows the runway utilisation for 2019, compared with 2008/9 and 2013. Compared with 2013, there are more westerlies and fewer easterlies in 2019. The easterly/westerly split in 2019 was similar to that seen in 2008/9.

Table 3 Number of movements[1] by runway

	Movements			Percentage		
Runway	2008/9	2013	2019	2008/9	2013	2019
09L	66,964	76,885	60,194	14.1%	16.3%	12.6%
09R	67,863	81,013	66,382	14.3%	17.2%	13.9%
Total easterly	134,827	157,898	126,576	28.3%	33.5%	26.5%
27L	171,327	154,869	175,880	36.0%	32.8%	36.8%
27R	169,627	159,171	175,604	35.7%	33.7%	36.7%

	Movements			Percentage		
Total westerly	340,954	314,040	351,484	71.7%	66.5%	73.5%

[1] ATMs and non-ATMs

2.2 LANDSIDE ROAD NETWORK

For the Heathrow Expansion project[13], Mott MacDonald produced modelled road traffic flow data for 2017, 2024, 2026, 2029, 2035 and 2050. The data included estimated traffic flows and congested speeds for weekday AM peak, PM peak, inter-peak, and off-peak and weekend daily period. The flow data were broken down by vehicle type (car, taxi, LGV, rigid HGV, articulated HGV, bus, coach, and motorcycle) separately for airport and non-airport traffic, for each section of road. The data for 2017 and 2024 were interpolated to derive 2019 road traffic data.

Hourly profiles of traffic by road class were provided with the road traffic data.

Schematically, the emissions (g/hour) on a given link for vehicles in each category are calculated as the product of traffic volume (vehicles/hour), link length (km) and emission factor (g/km).

The emission factors for a given pollutant vary with speed and vehicle category, and therefore the above calculation was undertaken for each specific vehicle type using the relevant speed-related emission factor.

Road vehicle emission factors, which vary with vehicle type, fuel type, emission standard and speed were taken from COPERT[14] (version 5.3).

Separate emission factors are available for a finer categorisation of vehicles than available in the traffic model output (for example, making the distinction between petrol and diesel cars). National[15] and London traffic-composition[16] data from the NAEI are used to apportion the modelled traffic volumes amongst the pertinent sub-categories (for example, by engine size and age). This approach makes the tacit assumption that the composition of traffic on the roads around Heathrow Airport at the sub-category level is not materially different from the national or London average (for example, the age distribution and engine size of vehicles).

A proportion of vehicles on the network will be near the start of a journey, so will not have reached the optimum operating range for engine (and catalyst if fitted). This leads to additional emissions, which are often expressed as a cold start 'penalty' per trip. Such emissions are widely distributed over the network, and the NAEI makes estimates for the national network. However, the airport is a spatial focus for cold-start emissions arising from vehicles leaving the airport after having been parked there, and this contribution is estimated as part of the airport inventory. This is further discussed in Section 2.3. The remaining cold start emissions associated with other vehicles on the network are taken from the NAEI, accepting that this may involve a certain amount of double counting.

For particulate matter, non-exhaust sources of emissions are also included: brake wear, tyre wear and road abrasion. The emission factors for brake and tyre wear were derived using the methodology adopted by the NAEI, as described in the Air Quality Expert Group report on particles[17]. Brake and tyre wear emissions factors are speed-dependent and vary with vehicle type. For road abrasion, constant emission factors of 0.0075 g/km for light duty vehicles and 0.038 g/km for heavy duty vehicles, taken from the NAEI, have been included. As the exhaust contribution to particle emissions is subject to increasingly more stringent regulation, the non-exhaust contributions have become a major component of the calculated mass of particulate matter emitted by road vehicles.

The road network used in the modelling is shown in Figure 2.

[13] https://www.heathrow.com/company/about-heathrow/expansion
[14] https://www.emisia.com/utilities/copert/
[15] https://naei.beis.gov.uk/resources/rtp_fleet_projection_NAEI_2017_Base2019r_v1_1.xlsx
[16] https://naei.beis.gov.uk/resources/rtp_fleet_projection_TfL_London_data_2018_v1.1.xlsx
[17] AQEG (2005) Particulate Matter in the United Kingdom. Defra 2005.

Figure 2 Road network for which emissions are calculated for the 2019 inventory.

2.3 CARPARKS, CAR RENTALS, TAXIS, AND COLD STARTS

The methodology for carparks, car rentals, taxis and cold starts remains the same as 2013. However, public carpark activity data (including car rentals and taxis) were obtained from specific output from Mott MacDonald's road traffic model. Staff carpark activity data were derived from staff carpark occupancy data that provided by HAL for 2019.

Emission factors were also updated for running emissions (for example, car travel within carpark) as discussed in Section 2.2. Cold start emission factors for were taken from the NAEI[18]. Running emissions were allocated to the location of the carparks, car rental areas and taxi ranks respectively. Cold start emissions were allocated to the carparks and Local Heathrow roads on the network surrounding the airport.

[18] https://naei.beis.gov.uk/resources/RoadtransportEFs_NAEI19_v1.xlsx

2.4 BACKGROUND AND RURAL SOURCES

The concentrations from 'background' area sources, also referred to as NAEI sources, are calculated using the same methodology as in the 2013 work[2]. Emissions for 2019 are taken from the NAEI[19]. Additionally, emissions from large point sources (principally Part A processes) were obtained from the NAEI[20]. These were modelled as individual stack sources.

The contribution from all sources not modelled explicitly (the 'rural' term) was taken from Defra's modelled background pollution data[21].

2.5 DISPERSION MODELLING

2.5.1 ADMS-Airport

Dispersion modelling was carried out using ADMS-Airport[22] version 5.4, licensed to Ricardo by Cambridge Environmental Research Consultants (CERC). ADMS-Airport is one of a suite of ADMS dispersion models. It was developed to include specific features of emission sources at airports. It shares with other members of the ADMS family the underlying description of atmospheric dispersion governed by atmospheric turbulence, which exploits advances made over the last few decades in understanding the transport and diffusion of pollutants in the lower levels of the atmosphere. The performance of its representation of basic atmospheric dispersion has been evaluated extensively against field trial data, and results can be found on the CERC website www.cerc.co.uk.

2.5.2 Annual-Mean Modelling for NO_2 Concentrations

The ADMS family of models includes a module for calculating the production of NO_2 from gas-phase reactions in the atmosphere following the release of NO_x (which is mainly in the form of NO initially). The method relies on an approximation to enable the impact of non-linear chemical reactions to be expressed within a Lagrangian framework. Using ADMS in this way to calculate NO_2 concentrations requires that all sources of NO_x be included in the same code run, which can be unwieldy and lead to long run times if concentrations are required on an extensive grid of receptors.

Alternative approximate methods of deriving annual-mean NO_2 concentrations are available and the 'Jenkin' method, as discussed in Appendix 1, was applied in the current work. This method has practical advantages - although this is not the sole reason for its choice - in that it allows the ADMS-Airport runs to be carried out separately for sub-sets of the NO_x sources, with the results then added together at the annual-mean level before calculating NO_2 concentrations. This brings flexibility to the modelling study and keeps the run-time of individual ADMS-Airport runs at a manageable level.

2.5.3 Model Options

ADMS-Airport has various model options that can be used singly or in combination to represent particular features of the dispersion situation. Besides the decision not to use the chemistry module for NO_x-to-NO_2 conversion discussed above, other specific modelling choices made for this study are listed below:

- **Building wakes**

  ADMS-Airport has provision to calculate the near-field concentration in the wake of an individual building (or combinations of buildings), but this level of detail in the modelling was deemed unnecessary for most of the sources on the airport. The presence of buildings on the airport has been accounted for in the modelling of heating-plant stack sources only. However, the effect of building wakes was considered when choosing the depths of volume sources use to represent APU and GSE emissions.
- **Coastal and topographical effects**

[19] https://naei.beis.gov.uk/data/mapping-archive
[20] https://naei.beis.gov.uk/mapping/mapping_2019/NAEIPointsSources_2019.xlsx
[21] https://uk-air.defra.gov.uk/data/modelled-data?base_year=2019
[22] http://www.cerc.co.uk/environmental-software/ADMS-Airport-model.html

No coastal or topographical effects on dispersion are included other than through their influence, if any, on the meteorological data used for the airport. The topography around Heathrow airport does not warrant the use of the complex-topography module.

- **Deposition**

  The dry deposition velocities and scavenging coefficients appropriate to the pollutants considered are small enough that attenuation of the airborne plume due to both dry and wet deposition can be ignored over the distance scales relevant to the current study.

- **Urban canopy flow module**

  The urban canopy flow module modifies the standard ADMS vertical profiles of atmospheric velocity and turbulence to take account of the effects of buildings in an urban area. The module was used where appropriate in the modelling, as recommended by CERC for the Heathrow Expansion Project[13]. However, the module is not compatible with all sources, particularly aircraft jet sources.

- **Aerodynamic Roughness Length**

  Aerodynamic Roughness Length is a length scale related to the height, shape and packing density of projections from the surface (crops, hedges, buildings etc), and governs the variation of wind speed with height above the surface (in the absence of thermal gradients) at heights above the 'canopy' created by the surface projections. The value of 0.5 m used previously for all sources was retained for this study.

- **Minimum Monin-Obukhov Length**

  The basic ADMS dispersion modelling can account for the fact that in a built-up area the waste heat per unit plan area is sufficient to affect the thermal structure of the lower levels of the atmosphere and consequently the dispersion of pollutants. Thus, the ADMS user can set a constraint on how 'stable' the atmosphere can become (where stable conditions inhibit the vigour of the turbulence responsible for atmospheric diffusion), and this is represented in terms of setting a lower limit on positive values of the Monin-Obukhov length (which is the distance scale from the surface at which buoyancy effects and shear effects become comparable). The value of 30 m, recommended for mixed urban/industrial complexes modelling, was used for this study.

2.6 METEOROLOGICAL DATA

The ADMS-Airport model was run using hourly sequential wind speed and direction data from the Heathrow site for the calendar year 2019. Figure 3 shows the wind rose for 2019 alongside those of 2013 and 2008/9 that were used in previous studies. The wind roses for the three periods are similar in terms of frequency of different wind directions and frequency of low wind speeds. This suggests that any differences between annual mean concentrations in the two years are unlikely to be due to weather conditions to any great extent. However, as noted in Table 3, the fraction of easterly operations is somewhat lower in 2019 than in 2013, and this will affect the spatial configuration of runway sources with knock-on effects on concentrations.

Figure 3 Wind roses

(a) 2019

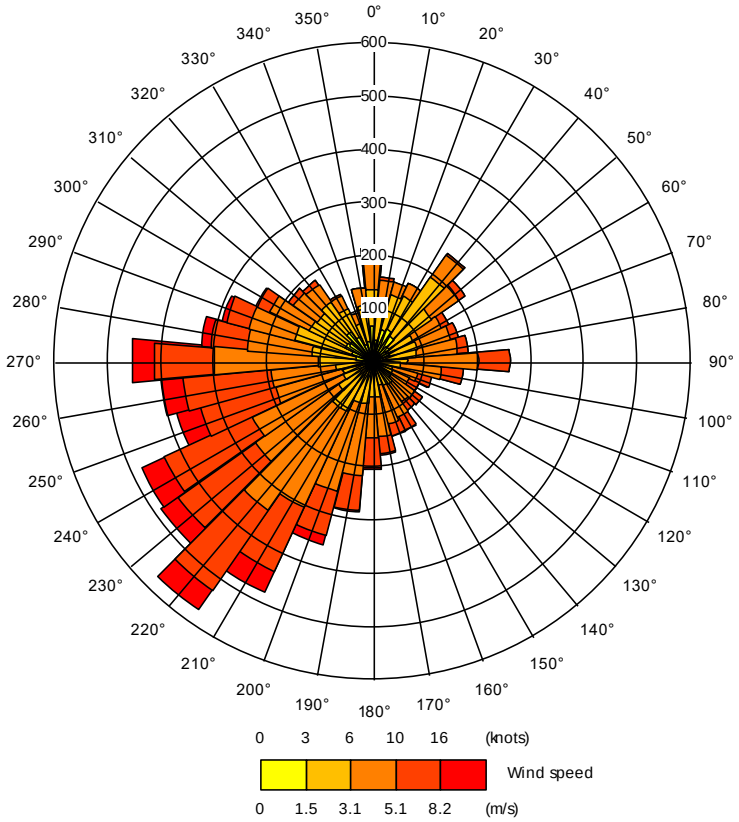

(b) 2013

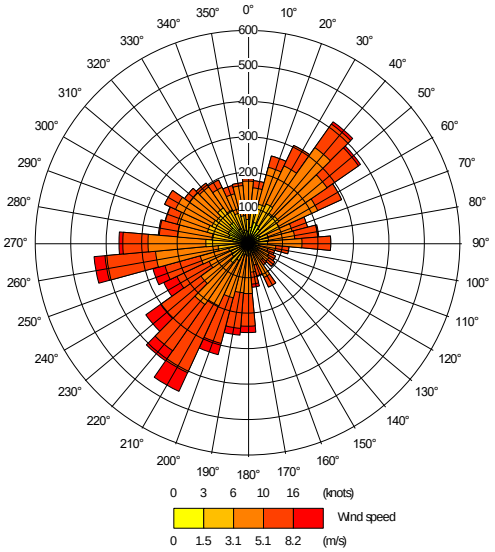

(c) 2008/9

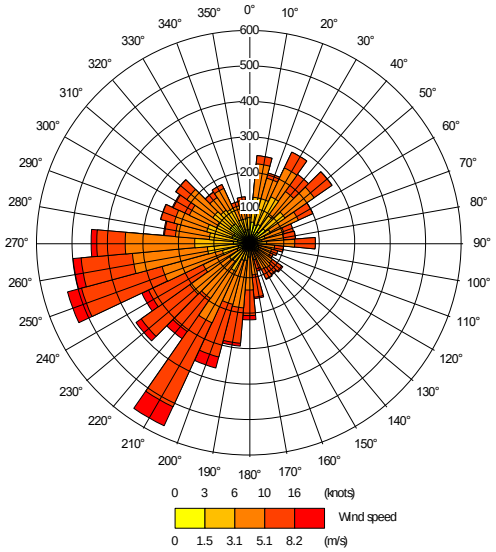

The radial scales denotes the number of hours per year.

Table 4 gives some statistical information on the meteorological data. As seen from Figure 3, the wind blows predominantly from the SW, particularly at higher wind speeds, which is commonly the case in the UK in the absence of specific mesoscale effects. This explains the greater frequency of usage of runways 27L and 27R (westerly operation) compared to runways 09L and 09R (easterly operation). For 2019, the westerly/easterly split was 73.5%/26.5%.

Table 4 Characteristics of the Heathrow meteorological data for 2019

Parameter	Value
Data capture[1]	82%
No. calm hours	148
Mean wind speed	4.0
Mean temperature	11.9

[1] The fraction of hours with valid data for all parameters used by ADMS.

2.7 RECEPTORS

The focus of attention in this study is to assess how well the model predicts concentrations in residential areas around the airport, particularly at locations strongly influenced by sources related directly to the operation of the airport. This includes receptors that are appreciably influenced by emissions from within the airport perimeter itself but also receptors influenced strongly by road traffic emissions, where the traffic itself has a major airport-related component.

The concentration contribution from airfield sources falls off rapidly with distance from the airport boundary, so that airport contribution to annual mean NO_x concentrations drops to only a few percent of the total on a distance scale of a few kilometres from the key airport sources. This sets the spatial scale of the area over which direct airport-related impacts on local air quality need to be assessed. Consequently, a ‘study area’ was defined, representing the area over which concentration contours were calculated, including concentrations close to modelled roads. This was chosen to be a rectangular area 9 km E-W by 9 km N-S, with SW corner at OS grid reference (503000, 172000), as marked on Figure 4. This study area is the same as that used in the 2008/9 and 2013 studies, which helps in comparing results with the previous studies.

Figure 4 Study Area

3. EMISSIONS

Airfield emissions have been discussed and reported previously[4], so are only summarised in this report.

3.1 NO_X EMISSIONS

Table 5 shows the calculated annual NO_x emissions for 2019 and 2013 for each major source category.

Table 5 NO_x emissions (tonnes) by source category

	2013	2019	Difference (%)[1]
On airfield			
Aircraft – ground level[2]	1,524.36	1,906.85	25.09
Aircraft – elevated[3]	2,567.94[a] 2,761.41[b]	2,750.68	7.12 [a]
GSE	186.79	95.07	-49.10
Stationary sources	85.83	99.07	15.42
Off airfield			
Airport related traffic	386.82[c]	252.15[d] 82.45[e]	-78.68[e]
Non-airport traffic	1,829.76[c]	1,683.10[f] 408.89[e]	-77.65[e]
Carparks	11.98	17.50	46.11

[1] Difference (%) = 100 * (2019 value – 2013 value) / 2013 value
[2] Emissions from aircraft on the ground, including main engines, APU, and engine testing emissions.
[3] From wheels off to 3,000 feet above ground (departure) and from 3,000 feet to touchdown (arrival)
[a] The 2013 emissions were originally reported up to an altitude of 1,000 m. These have been recalculated to 3,000 feet for comparison with 2019.
[b] From wheels off to 1,000 m above ground (departure) and from 1,000 m to touchdown (arrival), as reported originally
[c] The 2013 emissions were originally reported within an 11 km × 11 km rectangular major road network area
[d] Total for airport-related trips within the 15 km × 15 km rectangular major road network area
[e] Emissions within the 11 km × 11 km rectangular major road network area for comparison with 2013
[f] Total for non-airport trips within the 15 km × 15 km rectangular major road network area

It can be seen in the table above that aircraft make a dominant contribution to the airport NO_x emissions. It should be borne in mind that this is for aircraft emissions in the LTO cycle (so cruise emissions are excluded because they have no impact on local air quality), and road network emissions are presented only on major roads within the 15 km × 15 km area around the airport. Choosing a larger road network area would change the balance of calculated emissions.

3.2 PM_{10} AND $PM_{2.5}$ EMISSIONS

Table 6 and Table 7 show the calculated annual PM_{10} and $PM_{2.5}$ (collectively referred to as PM) emissions respectively, for 2019 and 2013 for each major source category. It is worth noting that for aircraft exhaust emissions the $PM_{2.5}$ mass has been assumed equal to the PM_{10} mass, but this is not the case for brake and tyre wear emissions.

Focusing on airport-related sources, emissions from airport-related traffic on the road network are roughly equal to half of those from aircraft. This contrasts with NO_x where aircraft emissions were more dominant. However, it should be repeated that choosing a different road network area would change the balance of calculated emissions.

Table 6 PM_{10} emissions (tonnes) by source category

	2013	2019	Difference (%)[1]
On airfield			
Aircraft – ground level[2]	35.51	36.55	2.95
Aircraft – elevated[3]	14.38[a] 15.46[b]	12.15	-15.47[a]

	2013	2019	Difference (%)[1]
GSE	10.95	6.37	-41.79
Stationary sources	6.88	39.47	473.97
Off airfield			
Airport related traffic	44.63[c]	18.97[d] 6.65[e]	-85.10[e]
Non-airport traffic	211.86[c]	124.79[f] 30.69[e]	-85.51[e]
Carparks	1.43	1.21	-15.15

[1] Difference (%) = 100 * (2019 value – 2013 value) / 2013 value
[2] Emissions from aircraft on the ground, including main engines, APU, and engine testing emissions.
[3] From wheels off to 3,000 feet above ground (departure) and from 3,000 feet to touchdown (arrival)
[a] The 2013 emissions were originally reported up to an altitude of 1,000 m. These have been recalculated to 3,000 feet for comparison with 2019.
[b] From wheels off to 1,000 m above ground (departure) and from 1,000 m to touchdown (arrival), as reported originally
[c] The 2013 emissions were originally reported within an 11 km × 11 km rectangular major road network area
[d] Total for airport-related trips within the 15 km × 15 km rectangular major road network area
[e] Emissions within the 11 km × 11 km rectangular major road network area for comparison with 2013
[f] Total for non-airport trips within the 15 km × 15 km rectangular major road network area

Table 7 $PM_{2.5}$ emissions (tonnes) by source category

	2013	2019	Difference (%)[1]
On airfield			
Aircraft – ground level[2]	28.11	28.68	2.02
Aircraft – elevated[3]	14.38[a] 15.46[b]	12.15	-15.47[a]
GSE	7.87	4.45	-43.49
Stationary sources	6.88	38.68	462.48
Off airfield			
Airport related traffic	26.32[c]	12.36[d] 4.24[e]	-83.90[e]
Non-airport traffic	125.17[c]	79.34[f] 19.37[e]	-84.52[e]
Carparks	0.97	0.84	-13.35

[1] Difference (%) = 100 * (2019 value – 2013 value) / 2013 value
[2] Emissions from aircraft on the ground, including main engines, APU, and engine testing emissions.
[3] From wheels off to 3,000 feet above ground (departure) and from 3,000 feet to touchdown (arrival)
[a] The 2013 emissions were originally reported up to an altitude of 1,000 m. These have been recalculated to 3,000 feet for comparison with 2019.
[b] From wheels off to 1,000 m above ground (departure) and from 1,000 m to touchdown (arrival), as reported originally
[c] The 2013 emissions were originally reported within an 11 km × 11 km rectangular major road network area
[d] Total for airport-related trips within the 15 km × 15 km rectangular major road network area
[e] Emissions within the 11 km × 11 km rectangular major road network area for comparison with 2013
[f] Total for non-airport trips within the 15 km × 15 km rectangular major road network area

4. MONITORING DATA

Within the study area, 17 sites with continuous monitoring data for the 2019 period were identified, with 14 of the sites having continuous NO_x/NO_2 analysers, 16 having continuous PM_{10} analysers and 9 with continuous $PM_{2.5}$ analysers. Excluding Bath Road, monitoring at which only began in November 2019, the model evaluation was based on comparison with monitoring data at this set of sites. The extent of the study area and the set of sites used in the evaluation are shown in Figure 5.

Figure 5 Monitoring site locations.

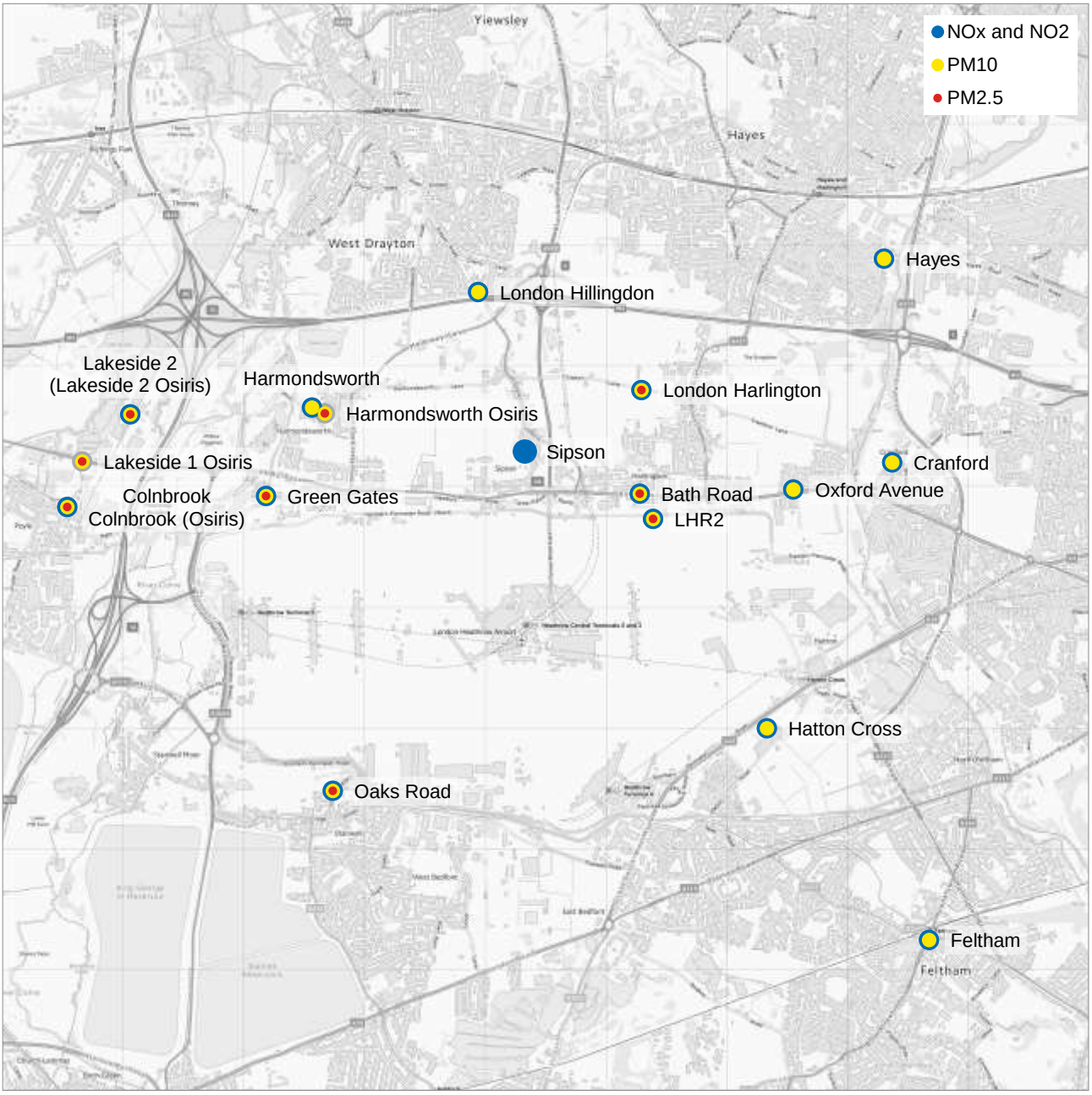

Contains OS data © Crown copyright and database right 2023.

Table 8 presents relevant characteristics of the monitoring sites, including a short name that will be used in the discussions in the remainder of the report, the site OS co-ordinates and the range of pollutants monitored at the site. It also gives a brief description of the environment local to the site. It is common for monitoring sites to be given a classification (rural, urban background, roadside etc) relating to the type of environment that the site can be taken to represent. For sites potentially affected significantly by airport sources, this classification scheme is less useful. From a model-evaluation perspective, the key distinguishing feature amongst sites is the extent to which they are influenced by various sources of emissions. The monitoring sites included in this evaluation span a useful range from this perspective, from sites where the sources on the airport have a major influence (such as LHR2), sites where emissions from a nearby road have a dominant influence (such as Hillingdon and Hayes) and sites located within residential areas with an appreciable (but not dominant) airport contribution and/or nearby road contribution (for example, Sipson, Harlington, Harmondsworth, Oxford Avenue, Cranford and Hatton Cross).

Table 8 Monitoring site information.

Site name	Short name	Easting	Northing	Pollutants	Location
Heathrow Bath Road	Bath Road	508280	176941	NO, NO_2, PM_{10}, $PM_{2.5}$	Approx. 15 m north of centre of A4 Bath Road.
Heathrow Green Gates	Green Gates	505184	176921	NO, NO_2, PM_{10}, $PM_{2.5}$	In parkland adjacent to residential area, approx. 400 m north of west end of runway 09L.
Heathrow LHR2	LHR2	508391	176732	NO, NO_2, PM_{10}, $PM_{2.5}$	Within boundary fence of airport. Approx. 180 m north of runway 27R centreline, 500 m from the end. Approx. 19 m south of centre of Northern Perimeter Road, near junction with Neptune Road.
Heathrow Oaks Road	Oaks Rd	505737	174481	NO, NO_2, PM_{10}, $PM_{2.5}$, O_3	Alongside residential road in residential area adjacent to parkland. Approx. 200 m south of Southern Perimeter Road.
Hillingdon Harmondsworth	Harmonds-worth	505564	177654	NO, NO_2, PM_{10}	Alongside minor road on outskirts of Harmondsworth village, adjacent to residential and commercial areas and parkland. Approx. 900 m north of airport perimeter road.
Hillingdon Harmondsworth Osiris	Harmonds-worth Osiris	505671	177605	PM_{10}, $PM_{2.5}$, PM_1	Alongside residential cul-de-sac on outskirts of Harmondsworth village. Approx. 800 m north of airport perimeter road.
Hillingdon Hayes	Hayes	510305	178887	NO, NO_2, PM_{10}	On the corner of busy North Hyde Road and side-road North Hyde Gardens in mixed residential, commercial, and industrial area. Approx. 10 m from edge of North Hyde Road, approx. 1 m from kerb of North Hyde Gardens.
London Hillingdon 3 Oxford Avenue	Oxford Ave	509553	176975	NO, NO_2, PM_{10}	In residential area, approx. 10 m from centre of residential road Oxford Avenue, and approx. 30 m north of centre of A4 Bath Road. Approx. 300 m north-east of Northern Perimeter Road.
Hillingdon Sipson	Sipson	507328	177289	NO, NO_2	At the end of Ashby Way, a cul-de-sac in a residential area adjacent to parkland. Approx. 300 m north of the A4 (T) Bath Road.
Hounslow 2 - Cranford	Cranford	510372	177199	NO, NO_2, PM_{10}, O_3, SO_2	In residential area adjacent to parkland.
Hounslow Feltham	Feltham	510678	173245	NO, NO_2, PM_{10}	On the corner of A444 Hounslow Roads and side-road B3377 Hanworth Road in Feltham Town Centre.
Hounslow Hatton Cross	Hatton Cross	509334	174998	NO, NO_2, PM_{10}	At end of Myrtle Grove cul-de-sac, adjacent to parkland. Approx. 100 m south-east of A30 (T) Great South-West Road.

Site name	Short name	Easting	Northing	Pollutants	Location
London Harlington	Harlington	508295	177800	NO, NO_2, PM_{10}, $PM_{2.5}$, O_3, CO	Alongside minor road amidst farmland, approx. 300 m west of outskirts of Harlington and 1 km north of airport perimeter road.
London Hillingdon	Hillingdon	506941	178610	NO, NO_2, PM_{10}, O_3, SO_2, CO	At end of Sipson Road cul-de-sac, in a residential area bounded on the south by the M4. Approx. 40 m north of the nearest lane of the M4.
Slough Colnbrook	Colnbrook	503537	176831	NO, NO_2, PM_{10}	In grounds of Pippins primary school, between residential and industrial areas. Approx. 500 m west of the M25.
Slough Colnbrook Osiris	Colnbrook	503537	176831	PM_{10}, $PM_{2.5}$, PM_1	In grounds of Pippins primary school, between residential and industrial areas. Approx. 500 m west of the M25.
Slough Lakeside 1 Osiris	Lakeside 1 Osiris	503662	177207	PM_{10}, $PM_{2.5}$, PM_1	Alongside the A4 Colnbrook By-Pass.
Slough Lakeside 2	Lakeside 2	504060	177598	NO, NO_2, PM_{10}	Within Industrial units on Lakeside Road, Slough.
Slough Lakeside 2 Osiris	Lakeside 2 Osiris	504060	177598	PM_{10}, $PM_{2.5}$, PM_1	Within Industrial units on Lakeside Road, Slough.

Table 9 presents a summary of NO_x and NO_2 measurements at the continuous monitoring sites and Table 10 presents the equivalent summary of PM_{10} and $PM_{2.5}$ measurements.

All the NO_x/NO_2 analysers included are of the chemiluminescence type, which is the EU reference method for NO_2. The EU sets an accuracy objective of 15% at the 95% confidence level for NO_x/NO_2 continuous analysers[23], and the AQEG report on nitrogen dioxide in the UK[24] states that it is likely that the great majority of UK national network measurements meet this uncertainty requirement. For sites operated to LAQN standards, a working uncertainty of 10% (at 2 standard deviations) has been suggested[25], based on observation and analysis. Technical guidance for air quality review and assessment[26] suggests that the overall uncertainty of the measurements (considering both accuracy and precision) from a continuous analyser is expected to be about ±10% (2 standard deviations) for long-period averages that are well above the instrument detection limit, provided that appropriate QA/QC methods are applied.

All downloaded data were fully ratified by the data compilers before being published.

Table 9 Measured NO_x and NO_2 concentrations – 2019 (µg m^{-3})

Short name	NO_x (µg m^{-3})	NO_2 (µg m^{-3})	Data capture (%)
Bath Road[1]	118.2	47.9	11.6
Green Gates	55.9	30.6	98.8
LHR2	98.3	42.5	95.5
Oaks Rd	44.6	26.3	83.8

[23] CEN (2003) Ambient air quality – measurement methods for the determination of the concentration of nitrogen dioxide and nitrogen monoxide by chemiluminescence. PR 14211.

[24] AQEG (2004) Nitrogen dioxide in the United Kingdom. www.defra.gov.uk/environment/quality/air/airquality/publications/nitrogen-dioxide

[25] Fuller G, Johnson P and Cue A (2002) Air quality in London 2001. Environmental Research Group, King's College London.

[26] Defra (2009) Part IV of the Environment Act 1995 Environment. (Northern Ireland) Order 2002 Part III. Local Air Quality Management. Technical Guidance. LAQM.TG(09) February 2009.

Short name	NO_x (µg m^{-3})	NO_2 (µg m^{-3})	Data capture (%)
Harmondsworth	40.6	23.7	96.6
Hayes	94.0	41.2	99.6
Oxford Ave	60.1	33.1	99.4
Sipson	50.3	29.7	97.4
Cranford	44.3	26.9	99.5
Feltham	53.2	29.1	97.8
Hatton Cross	49.2	27.9	86.6
Harlington	50.9	30.7	99.0
Hillingdon	87.2	44.7	91.1
Colnbrook	42.3	24.5	99.6
Lakeside 2	54.7	27.6	89.4

[1] Monitoring at Bath Road began in November 2019

Table 10 Measured PM_{10} and $PM_{2.5}$ concentrations – 2019 (µg m^{-3})

Short name	PM_{10} (µg m^{-3})	Data capture (%)	$PM_{2.5}$ (µg m^{-3})	Data capture (%)
Bath Road[1]	13.5	10.5	9.0	10.5
Green Gates	13.0	98.3	8.4	98.3
LHR2	13.4	99.9	8.7	99.9
Oaks Rd	14.9	80.6	9.5	80.6
Harmondsworth	15.0	97.4	n/a	n/a
Harmondsworth Osiris[2]	14.5	90.1	5.3	90.0
Hayes	27.7	97.6	n/a	n/a
Oxford Ave	23.5	95.0	n/a	n/a
Cranford	16.7	99.2	n/a	n/a
Feltham	19.6	98.6	n/a	n/a
Hatton Cross	19.6	92.1	n/a	n/a
Harlington	15.1	97.1	9.5	97.1
Hillingdon	n/a	0.0	n/a	n/a
Colnbrook	16.4	96.4	n/a	n/a
Colnbrook Osiris[2]	14.9	51.5	6.9	51.5
Lakeside 1 Osiris[2]	12.0	50.7	6.4	50.7
Lakeside 2	15.0	97.4	n/a	n/a
Lakeside 2 Osiris[2]	14.0	58.9	6.6	59.2

[1] Monitoring at Bath Road began in November 2019
[2] Osiris monitors are not reference analysers and as such the data should only be considered indicative.

5. MODEL EVALUATION

A detailed model evaluation is discussed in Appendix 1. It concluded that the model performed well for airfield sources. However, it did not perform particularly well for road sources. For NOx, the model underpredicted the contribution from roads by a factor of 2.5. The 2013 study also found that roads sources were being underpredicted by the model (by a factor of 1.5).

Although large, this level of discrepancy is not very unusual. It may be related to the diesel emission scandal, where manufacturers routinely cheated the emissions tests. This has led to real-world emissions being significantly higher that the official figures would suggest. There are also other factors that may give rise to higher real-world emissions, for example, abatement technologies require time to reach their optimal operating temperatures and with Heathrow being a focal point for journey starts emissions may be higher than expected due to cold running. Significant amounts for stop-start driving conditions can also have a large impact on vehicle emissions.

To account for the underprediction of roads sources, an adjustment factor was applied to the roads component of the NOx modelling.

PM_{10} and $PM_{2.5}$ concentrations were found to be dominated by background concentrations. A large component of which is the unmodelled rural background. No adjustment was made to PM_{10} or $PM_{2.5}$ concentrations.

6. CONCENTRATIONS

6.1 SELECTION OF RECEPTOR LOCATIONS

Concentrations are presented at several receptor locations, namely:

- The seventeen continuous monitor locations near Heathrow
- Selected points to represent residential properties around the perimeter of the airport (PerimA to PerimH)
- Selected points to represent residential properties alongside the M4 motorway (M4A to M4D).

These are shown in Figure 6.

Figure 6 Locations of selected receptors

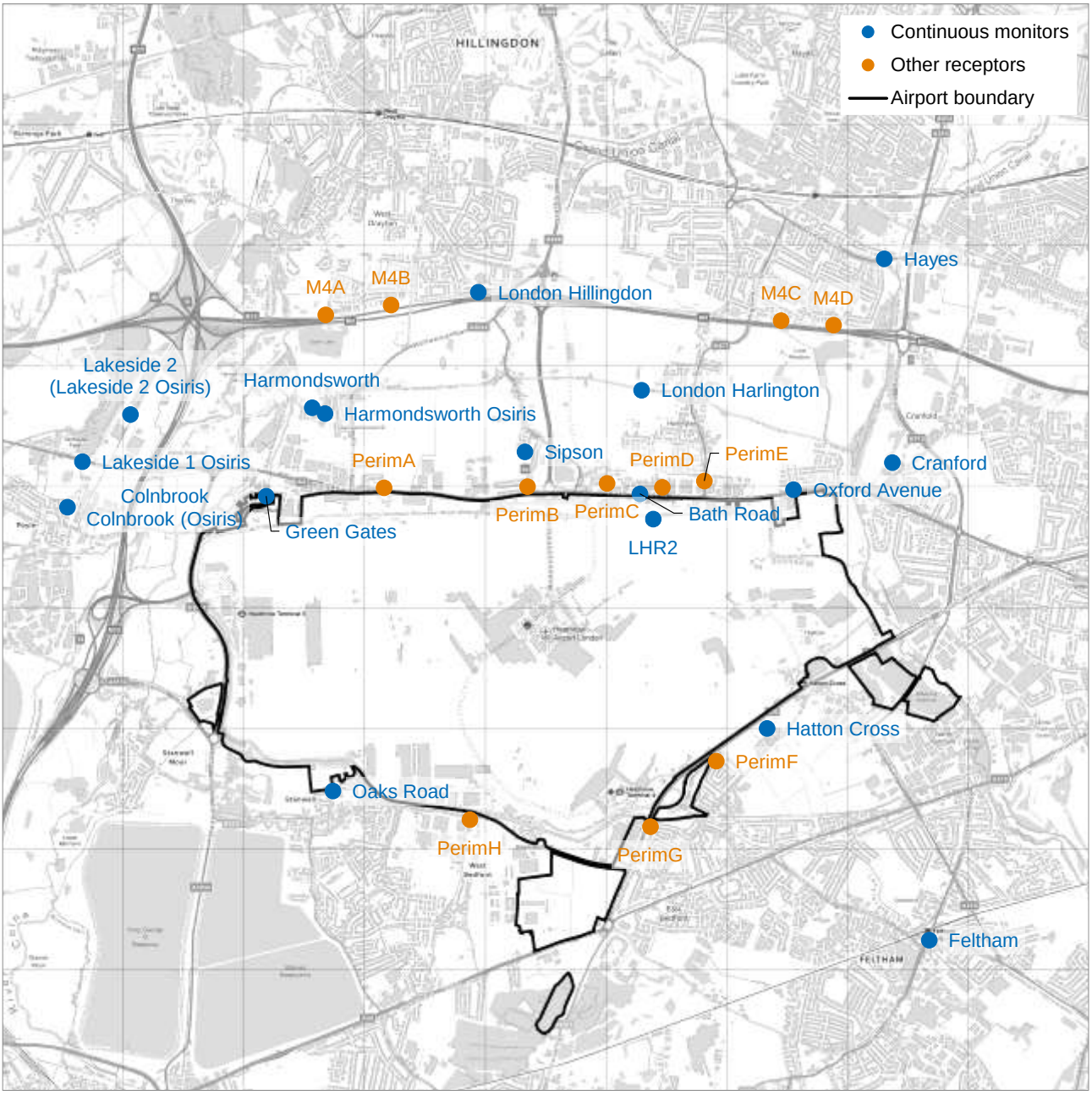

Contains OS data © Crown copyright and database right 2023.

Properties alongside the M4 motorway are at particular risk of air quality exceedances. Concentrations fall off quickly with distance from the motorway, so concentrations are sensitive to the exact location of the receptor. Accordingly, concentrations were calculated for 29 receptor locations along the M4, representing the facades of the buildings closest to the motorway. The four motorway receptor locations reported here (M4A to M4D) represent the highest modelled concentrations along different stretches of the motorway. These four receptor locations are all approximately 30 m from the edge of the nearest carriageway.

6.2 NO_X AND NO_2 CONCENTRATIONS

Although the focus of interest from a human health standpoint is annual mean NO_2 concentrations, discussion of the relative contribution from various sources is best conducted in terms of annual mean NO_x concentrations. These are related directly to NO_x emission rates, whereas the relationship between NO_2 and NO_x concentrations is non-linear because of gas-phase reactions in the atmosphere.

Focusing first on concentrations at the set of key receptor locations shown in Figure 6, Table 11 shows the split of total NO_x concentrations between airport-related and non-airport source categories. (The table also shows annual mean NO_2 concentrations for later discussion in Section 6.2.3.)

The estimated total NO_x concentrations at receptor locations span a large range, from 46.3 µg m^{-3} (Colnbrook) to 117.9 µg m^{-3} (M4A). A major part of this variation derives from the variation in the airport contribution, which ranges from 4.3 µg m^{-3} at Colnbrook to 48.9 µg m^{-3} at LHR2.

Table 11 Airport and non-airport contributions to annual mean NO_x concentrations

Receptor	Contribution to NO_x (µg m^{-3})			Contribution to NO_x (%)			NO_2 (µg m^{-3})
	Airport[1]	Non-airport[2]	Total	Airport[1]	Non-airport[2]	Total	
Bath Road	27.5	47.9	75.4	36.5	63.5	100.0	36.3
Green Gates	10.6	42.9	53.5	19.8	80.2	100.0	29.0
LHR2	48.9	41.6	90.6	54.0	46.0	100.0	40.6
Oaks Road	12.7	34.8	47.5	26.7	73.3	100.0	25.8
Harmondsworth	6.5	42.8	49.3	13.1	86.9	100.0	26.9
Harmondsworth Osiris	6.7	42.0	48.6	13.7	86.3	100.0	26.6
Hayes	7.4	62.4	69.8	10.6	89.4	100.0	35.1
Oxford Avenue	18.0	42.2	60.3	29.9	70.1	100.0	30.8
Sipson	15.4	38.0	53.4	28.9	71.1	100.0	28.4
Cranford	8.9	40.4	49.3	18.0	82.0	100.0	26.3
Feltham	4.9	55.3	60.2	8.2	91.8	100.0	31.2
Hatton Cross	19.4	42.2	61.6	31.6	68.4	100.0	31.3
Harlington	11.1	44.0	55.1	20.2	79.8	100.0	29.0
Hillingdon	13.6	78.1	91.8	14.9	85.1	100.0	45.3
Colnbrook	4.3	42.0	46.3	9.3	90.7	100.0	25.5
Lakeside 1 Osiris	8.1	53.0	61.2	13.3	86.7	100.0	32.2
Lakeside 2	5.4	47.9	53.3	10.1	89.9	100.0	29.2
PerimA	19.1	50.7	69.8	27.4	72.6	100.0	35.4
PerimB	24.9	45.7	70.6	35.2	64.8	100.0	35.0
PerimC	22.1	44.2	66.4	33.4	66.6	100.0	32.7
PerimD	23.2	45.7	68.9	33.7	66.3	100.0	33.3
PerimE	26.7	56.5	83.2	32.1	67.9	100.0	38.9
PerimF	19.0	43.1	62.1	30.6	69.4	100.0	31.3
PerimG	16.8	67.7	84.5	19.9	80.1	100.0	40.7
PerimH	15.9	50.8	66.7	23.9	76.1	100.0	33.4
M4A	15.7	102.1	117.9	13.3	86.7	100.0	55.6
M4B	16.0	97.0	113.0	14.2	85.8	100.0	53.5
M4C	18.5	91.8	110.3	16.8	83.2	100.0	51.0

Receptor	Contribution to NO_x (µg m^{-3})			Contribution to NO_x (%)			NO_2 (µg m^{-3})
	Airport[1]	Non-airport[2]	Total	Airport[1]	Non-airport[2]	Total	
M4D	17.4	88.0	105.4	16.5	83.5	100.0	49.1

[1] Includes aircraft, APUs, GSE, airport-related traffic on the road network, carparking and stationary sources.
[2] Includes non-airport traffic on the road network, large point sources, NAEI area sources and rural background.

6.2.1 Airport-related NO_x

As in past air quality studies, LHR2 is estimated to have by far the largest airport-related NO_x contribution, resulting from its proximity to the runway (it is the only one of the receptor locations to be on the airfield). The Bath Road monitoring site and PerimE (on Harlington High Street) show the next largest estimated airport-related NO_x contributions.

Table 12 shows a breakdown of the airport-related contribution. Clearly, the large airport contribution at LHR2 derives from aircraft main engines and the landside road network (as well as being close to the runway, it is close to a junction on the Northern Perimeter Road). In general, GSE makes a relatively small contribution, because the layout of the airfield places these sources further from receptor locations than the runway sources.

Table 12 Breakdown of the airport contribution to annual mean NO_x concentrations by source category

Receptor	Contribution to NO_x (µg m^{-3})					Contribution to NO_x (%)				
	Aircraft[1]	GSE	Road traffic	Other[2]	Total	Aircraft[1]	GSE	Road traffic	Other[2]	Total
Bath Road	17.7	0.7	8.0	1.1	27.5	64.3	2.6	29.0	4.1	100.0
Green Gates	4.0	0.5	5.8	0.3	10.6	37.7	4.3	54.7	3.3	100.0
LHR2	32.0	0.9	15.1	1.0	48.9	65.3	1.9	30.9	2.0	100.0
Oaks Road	8.7	0.6	3.0	0.3	12.7	68.8	4.7	23.7	2.7	100.0
Harmondsworth	3.0	0.3	3.0	0.2	6.5	46.2	4.6	46.2	3.0	100.0
Harmondsworth Osiris	3.2	0.3	2.9	0.2	6.7	48.4	4.9	43.5	3.2	100.0
Hayes	3.8	0.2	3.2	0.2	7.4	51.6	2.3	43.2	2.8	100.0
Oxford Avenue	12.3	0.4	4.6	0.8	18.0	68.0	2.3	25.3	4.4	100.0
Sipson	8.9	0.6	5.5	0.4	15.4	57.5	4.1	35.8	2.6	100.0
Cranford	6.0	0.2	2.1	0.5	8.9	67.8	2.6	24.2	5.3	100.0
Feltham	3.0	0.2	1.6	0.2	4.9	60.5	3.8	31.6	4.1	100.0
Hatton Cross	12.8	0.6	5.4	0.7	19.4	65.7	2.9	27.8	3.5	100.0
Harlington	7.3	0.4	3.1	0.3	11.1	65.7	3.5	27.9	3.0	100.0
Hillingdon	3.2	0.2	10.0	0.2	13.6	23.6	1.7	73.4	1.2	100.0
Colnbrook	1.8	0.1	2.2	0.1	4.3	42.4	2.8	52.5	2.4	100.0
Lakeside 1 Osiris	1.7	0.1	6.3	0.1	8.1	20.4	1.4	77.0	1.2	100.0
Lakeside 2	1.7	0.1	3.5	0.1	5.4	31.5	2.4	64.2	1.9	100.0
PerimA	6.8	0.8	10.9	0.6	19.1	35.7	4.1	57.0	3.2	100.0
PerimB	12.8	0.8	10.5	0.8	24.9	51.4	3.4	42.0	3.2	100.0
PerimC	14.5	0.7	6.3	0.7	22.1	65.4	3.1	28.4	3.2	100.0

Receptor	Contribution to NO_x (µg m^{-3})					Contribution to NO_x (%)				
	Aircraft[1]	GSE	Road traffic	Other[2]	Total	Aircraft[1]	GSE	Road traffic	Other[2]	Total
PerimD	17.1	0.7	4.8	0.7	23.2	73.5	2.9	20.5	3.0	100.0
PerimE	17.6	0.6	7.7	0.8	26.7	65.8	2.3	29.0	2.9	100.0
PerimF	11.9	0.8	5.5	0.8	19.0	62.7	4.0	28.9	4.3	100.0
PerimG	7.8	0.9	7.4	0.7	16.8	46.3	5.4	44.3	4.0	100.0
PerimH	6.8	0.6	7.5	1.0	15.9	42.7	4.0	47.0	6.2	100.0
M4A	2.2	0.2	13.2	0.1	15.7	14.2	1.1	83.8	0.9	100.0
M4B	2.6	0.2	13.0	0.2	16.0	16.4	1.3	81.4	1.0	100.0
M4C	5.2	0.2	12.8	0.3	18.5	28.1	1.3	69.1	1.4	100.0
M4D	5.1	0.2	11.8	0.3	17.4	29.1	1.3	68.0	1.5	100.0

[1] Aircraft main engines and APU
[2] Carparking and stationary sources

Figure 7 shows contour plots of the airport-related NO_x concentrations around the airport. The NO_x contribution from aircraft and other airfield sources falls off to less than 5 µg m^{-3} more than about 2 km from the airport boundary, except along motorways and major roads.

Appendix 1 gives the corresponding contour plot of total NO_x.

Figure 7 Airport-related contribution[1] to annual mean NO_x concentrations in 2019 outside the airport boundary

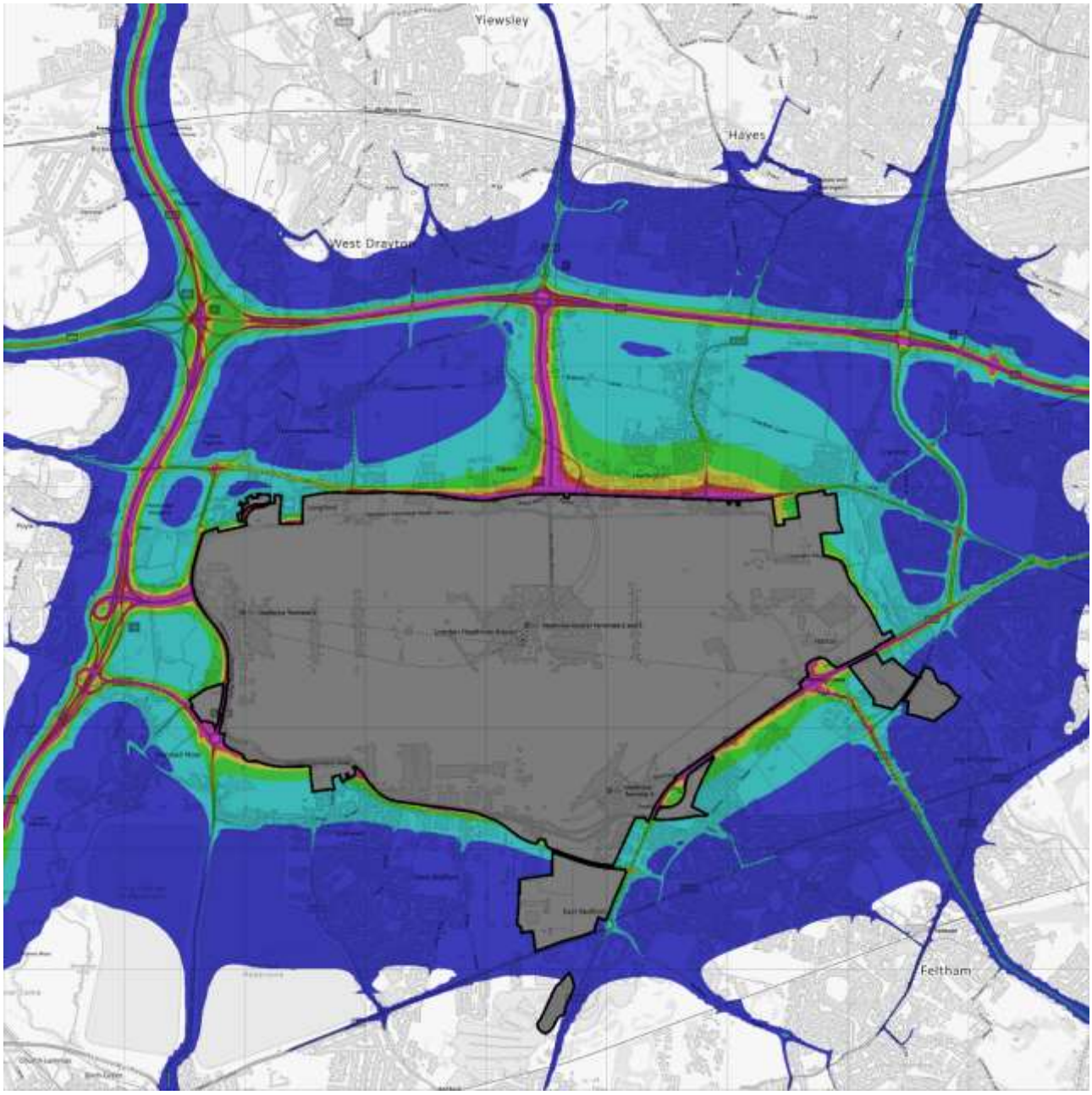

30 µg m^{-3}
25 µg m^{-3}
20 µg m^{-3}
15 µg m^{-3}
10 µg m^{-3}
5 µg m^{-3}

[1] Includes aircraft, APUs, GSE, airport-related traffic on the road network, carparking and stationary sources.

6.2.2 Non-airport NO_x

A breakdown of the non-airport contribution to NO_x concentrations is given in Table 13. The greatest non-airport contributions are at the receptor locations close to the M4 motorway, namely Hillingdon, M4A, M4B, M4C and M4D. The variability in the estimated non-airport contribution largely depends on distance from major roads. Other non-airport sources ("background") are much less variable, reflecting the fact that they are more distant and less spatially defined.

Table 13 Breakdown of the non-airport NO_x contribution by source category

Receptor	Annual mean NO_x contribution (µg m^{-3})		
	Road traffic	Background[1]	Total
Bath Road	17.1	30.7	47.9
Green Gates	14.7	28.2	42.9
LHR2	10.8	30.8	41.6
Oaks Road	8.1	26.7	34.8
Harmondsworth	13.1	29.6	42.8
Harmondsworth Osiris	12.3	29.6	42.0
Hayes	25.8	36.6	62.4
Oxford Avenue	11.9	30.4	42.2
Sipson	8.5	29.5	38.0
Cranford	9.1	31.3	40.4
Feltham	22.1	33.2	55.3
Hatton Cross	11.8	30.4	42.2
Harlington	12.9	31.1	44.0
Hillingdon	47.8	30.3	78.1
Colnbrook	12.4	29.7	42.0
Lakeside 1 Osiris	24.4	28.7	53.0
Lakeside 2	20.0	28.0	47.9
PerimA	18.3	0.0	50.7
PerimB	12.9	0.0	45.7
PerimC	10.6	0.0	44.2
PerimD	11.0	0.0	45.7
PerimE	21.9	0.0	56.5
PerimF	10.3	0.0	43.1
PerimG	33.4	0.0	67.7
PerimH	18.4	0.0	50.8
M4A	70.5	0.0	102.1
M4B	64.1	0.0	97.0
M4C	54.1	0.0	91.8
M4D	50.3	0.0	88.0

[1] Sources from the NAEI not already included in the airport and road network source categories.

6.2.3 NO_2 concentrations

Annual mean NO_2 concentrations at the chosen receptor locations are shown in Table 11 (Section 6.2). There are a number of exceedances of the 40 µg m^{-3} limit, especially along the M4 motorway, reaching as high as 55.6 µg m^{-3} at the M4A receptor location near the M4.

Figure 8 displays annual mean concentrations of NO_2 outside the airport. This shows that off-airport annual mean NO_2 concentrations above 40 µg m^{-3} (red and magenta) are mainly associated with roads and motorways. Around the perimeter of the airport, concentrations above 40 µg m^{-3} are confined to within about 50 m of the boundary, and concentrations above 36 µg m^{-3} are mostly limited to within about 100 m of the boundary.

Concentrations above 40 µg m^{-3} are also found along roads throughout the study area. For A-roads and smaller, these are mainly confined to within a few metres of the carriageway. However, for the M4 and M25, the 40 µg m^{-3} contour extends up to around 200 m from the motorway.

Figure 8 Annual mean NO_2 concentrations in 2019 outside the airport boundary

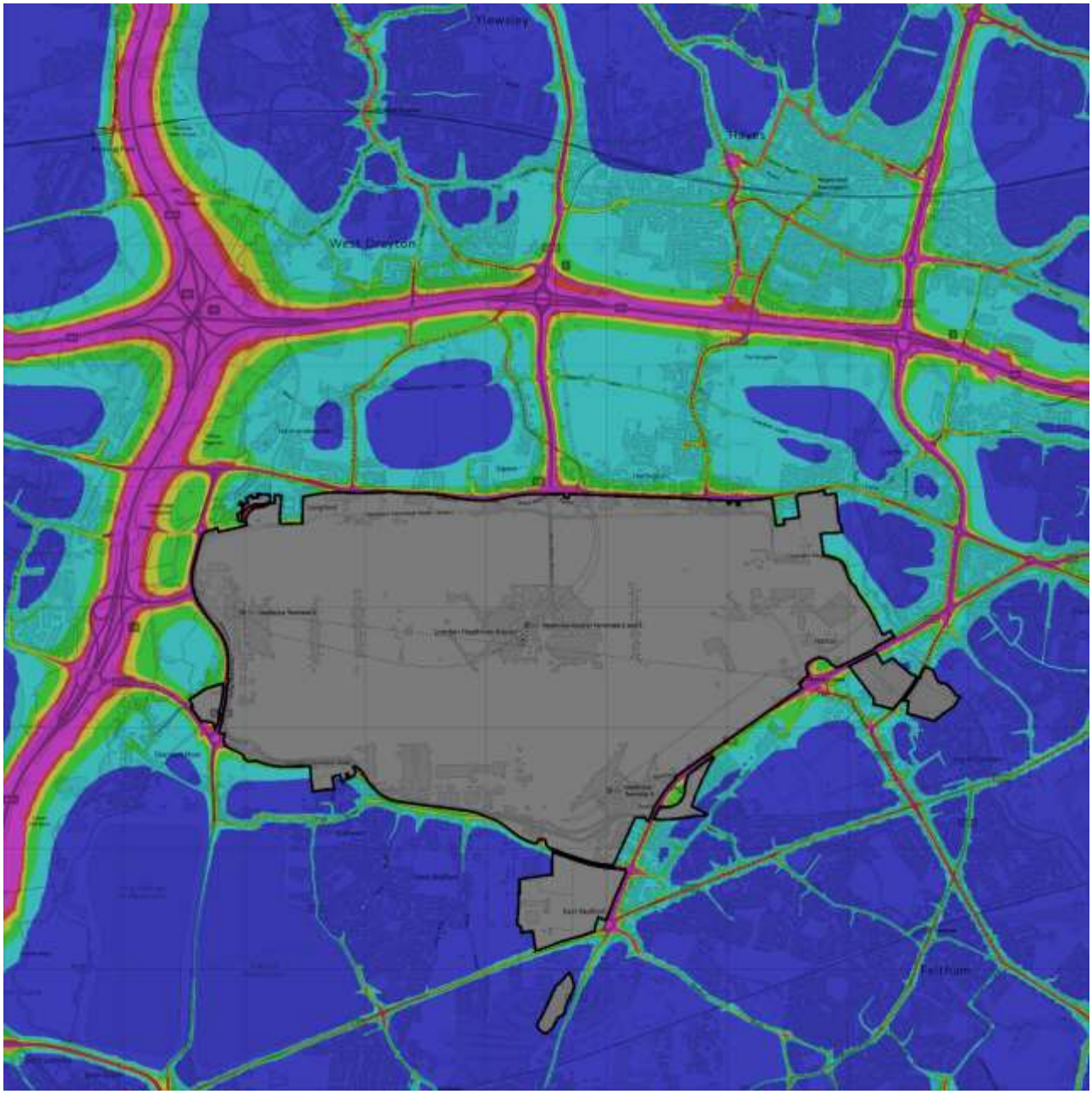

Concentrations within the airport boundary are not shown in the above figure, to emphasise that the spatial representation of the emissions on the airport and the spatial detail in the dispersion modelling has been aimed at the estimation of concentrations in residential areas around the airport. In addition, the Air Quality Standards (AQS) objectives apply at locations with relevant public exposure, which would exclude locations within the airport boundary from the annual mean NO_2 objective. On airport locations are subject to separate workplace exposure limits[27]. Annual mean NO_2 concentrations within the airport boundary are shown in Appendix 1, but the caveats on spatial resolution given above should be borne in mind.

6.2.4 Comparison with 2013

Table 14 compares the NO_x and NO_2 concentrations in 2019 with those in 2013 and Table 15 compares the airport and non-airport contribution to NO_x concentrations.

Table 14 Comparison of modelled NO_x and NO_2 concentrations for 2019 and 2013

Receptor	NO_x (µg m^{-3})			NO_2 (µg m^{-3})		
	2019	2013	Difference (%)[1]	2019	2013	Difference (%)[1]
Bath Road	75.4	n/a	n/a	36.3	n/a	n/a
Green Gates	53.5	58.8	-8.9	29.0	35.0	-17.1
LHR2	90.6	110.9	-18.3	40.6	53.2	-23.6
Oaks Road	47.5	61.9	-23.2	25.8	35.7	-27.8
Harmondsworth	49.3	56.0	-12.1	26.9	33.7	-20.2
Harmondsworth Osiris	48.6	n/a	n/a	26.6	n/a	n/a
Hayes	69.8	86.0	-18.9	35.1	45.4	-22.8
Oxford Avenue	60.3	70.7	-14.8	30.8	39.8	-22.7
Sipson	53.4	61.9	-13.7	28.4	36.2	-21.6
Cranford	49.3	59.9	-17.8	26.3	35.2	-25.3
Feltham	60.2	n/a	n/a	31.2	n/a	n/a
Hatton Cross	61.6	79.8	-22.8	31.3	43.0	-27.2
Harlington	55.1	65.0	-15.2	29.0	37.5	-22.8
Hillingdon	91.8	94.4	-2.8	45.3	50.5	-10.3
Colnbrook	46.3	55.7	-16.9	25.5	33.5	-23.8
Lakeside 1 Osiris	61.2	n/a	n/a	32.2	n/a	n/a
Lakeside 2	53.3	n/a	n/a	29.2	n/a	n/a

[27] EH40/2005 Workplace exposure limits, Health and Safety Executive, January 2020

Receptor	NO_x (µg m^{-3})			NO_2 (µg m^{-3})		
	2019	2013	Difference (%)[1]	2019	2013	Difference (%)[1]
PerimA	69.8	67.7	3.1	35.4	38.7	-8.5
PerimB	70.6	74.4	-5.1	35.0	41.3	-15.3
PerimC	66.4	68.4	-2.9	32.7	38.5	-15.0
PerimD	68.9	70.1	-1.6	33.3	39.0	-14.6
PerimE	83.2	96.5	-13.8	38.9	49.4	-21.3
PerimF	62.1	82.8	-25.0	31.3	44.3	-29.3
PerimG	84.5	90.8	-6.9	40.7	47.6	-14.5
PerimH	66.7	81.6	-18.3	33.4	43.8	-23.8
M4A	117.9	96.2	22.5	55.6	51.4	8.1
M4B	113.0	92.6	22.0	53.5	49.9	7.2
M4C	110.3	104.2	5.9	51.0	53.7	-5.0
M4D	105.4	101.8	3.6	49.1	52.8	-7.1

[1] Difference (%) = 100 * (2019 value – 2013 value) / 2013 value

Table 15 Comparison of modelled airport and non-airport contribution to NO_x concentrations for 2019 and 2013

Receptor	Airport NO_x (µg m^{-3})			Non-airport NO_x (µg m^{-3})		
	2019	2013	Difference (%)[1]	2019	2013	Difference (%)[1]
Bath Road	27.5	n/a	n/a	47.9	n/a	n/a
Green Gates	10.6	7.7	37.1	42.9	51.0	-15.9
LHR2	48.9	53.6	-8.7	41.6	57.3	-27.3
Oaks Road	12.7	18.5	-31.3	34.8	43.4	-19.7
Harmondsworth	6.5	5.9	9.9	42.8	50.1	-14.6
Harmondsworth Osiris	6.7	n/a	n/a	42.0	n/a	n/a
Hayes	7.4	5.1	43.6	62.4	80.9	-22.8
Oxford Avenue	18.0	15.9	13.4	42.2	54.8	-23.0
Sipson	15.4	14.3	7.5	38.0	47.5	-20.1
Cranford	8.9	7.7	15.6	40.4	52.2	-22.7
Feltham	4.9	n/a	n/a	55.3	n/a	n/a
Hatton Cross	19.4	24.6	-21.0	42.2	55.2	-23.7
Harlington	11.1	9.8	14.0	44.0	55.2	-20.3
Hillingdon	13.6	15.2	-10.3	78.1	79.2	-1.4
Colnbrook	4.3	4.8	-9.9	42.0	51.0	-17.5
Lakeside 1 Osiris	8.1	n/a	n/a	53.0	n/a	n/a
Lakeside 2	5.4	n/a	n/a	47.9	n/a	n/a
PerimA	19.1	11.5	65.4	50.7	56.2	-9.8

Receptor	Airport NO_x (µg m^{-3})			Non-airport NO_x (µg m^{-3})		
	2019	2013	Difference (%)[1]	2019	2013	Difference (%)[1]
PerimB	24.9	21.8	14.1	45.7	52.6	-13.0
PerimC	22.1	18.7	18.4	44.2	49.7	-11.0
PerimD	23.2	19.9	16.5	45.7	50.2	-8.8
PerimE	26.7	25.8	3.4	56.5	70.7	-20.1
PerimF	19.0	25.1	-24.4	43.1	57.7	-25.3
PerimG	16.8	18.9	-11.3	67.7	71.9	-5.7
PerimH	15.9	21.8	-26.9	50.8	59.8	-15.1
M4A	15.7	15.6	1.1	102.1	80.6	26.6
M4B	16.0	14.7	9.1	97.0	78.0	24.5
M4C	18.5	15.4	20.4	91.8	88.7	3.4
M4D	17.4	14.5	19.7	88.0	87.2	0.9

[1] Difference (%) = 100 * (2019 value – 2013 value) / 2013 value

With the exception of the M4 sites and PerimA, the total modelled concentrations are lower in 2019 than in 2013 for both NO_x and NO_2. This is also the case for the non-airport contribution to NOx concentrations.

Comparison of the airport contribution to NOx concentrations paints a more complex picture. Differences range from 31.3% lower in 2019 than in 2013 at Oaks Road to 65.4% higher in 2019 at PerimA. This is mainly a reflection of the differences in westerly/easterly split for the two years and the fact that airfield emissions have increased whereas other sources have decreased between 2013 and 2019. Figure 9 shows how the spatial pattern of airport-related contribution to annual mean NOx concentrations have changed between 2013 and 2019.

Figure 9 Airport-related contribution[1] to annual mean NO_x concentrations – Comparison of 2019 with 2013

2019

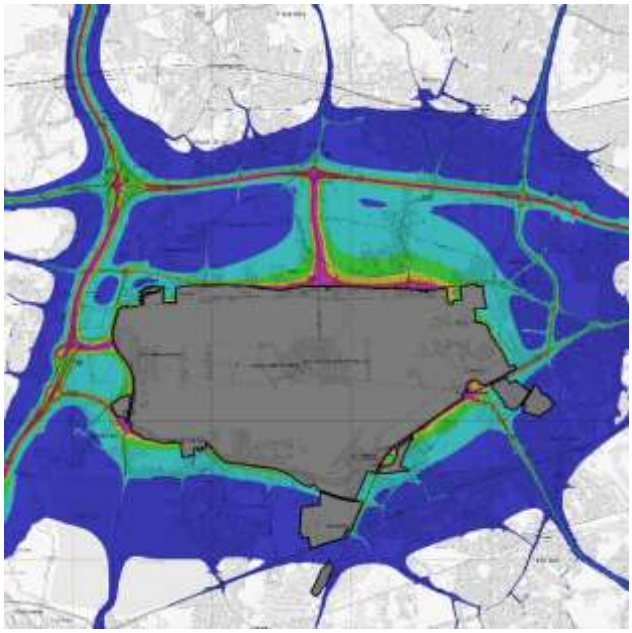

2013

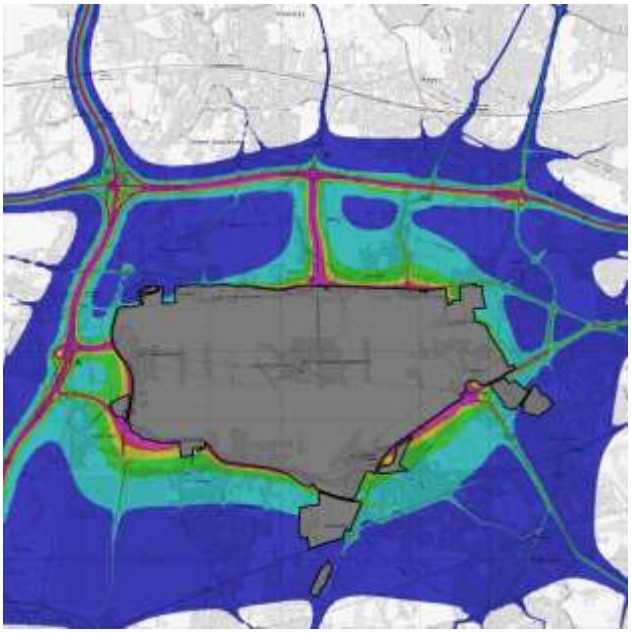

Contains OS data © Crown copyright and database right 2023.
[1] Includes aircraft, APUs, GSE, airport-related traffic on the road network, carparking and stationary sources.

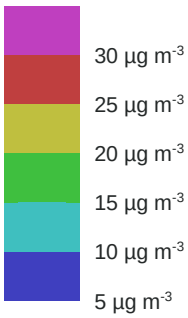

Figure 10 compares the annual mean NO_2 concentrations in 2019 with 2013. Other than a clear reduction in both roadside and non-roadside concentrations, the figure shows the removal of the emissions from the Great Western railway line, which passes east–west about 1 km north of the M4 motorway. This is due to The Great West Electrification Project that introduced electrification infrastructure and modern electric trains to the Great Western Mainline route. It was completed in 2020. Diffusion tube monitoring data also suggests that the concentrations in 2013 may have been overestimated.

Figure 10 Annual mean NO_2 concentrations – Comparison of 2019 with 2013

2019

2013

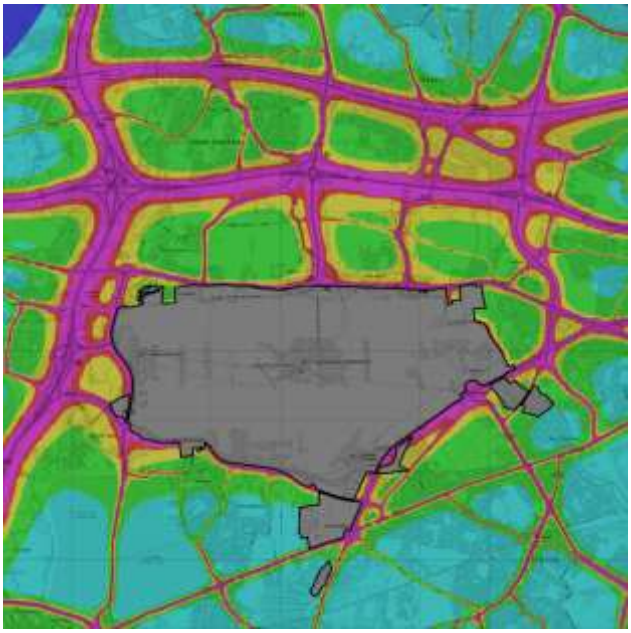

Contains OS data © Crown copyright and database right 2023.
[1] Includes aircraft, APUs, GSE, airport-related traffic on the road network, carparking and stationary sources.

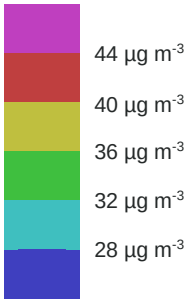

6.3 PM CONCENTRATIONS

Table 16 gives the estimated PM_{10} concentrations for 2019 at the set of receptor locations introduced in earlier sections, showing the split between airport-related and non-airport contributions. Table 17 gives the equivalent data for $PM_{2.5}$.

Table 16 Airport and non-airport contributions to annual mean PM_{10} concentrations

Receptor	Contribution to PM_{10} (µg m^{-3})			Contribution to PM_{10} (%)		
	Airport[1]	Non-airport[2]	Total	Airport[1]	Non-airport[2]	Total
Bath Road	0.9	19.5	20.4	4.3	95.7	100.0
Green Gates	0.5	18.6	19.0	2.4	97.6	100.0
LHR2	1.6	19.1	20.7	7.5	92.5	100.0
Oaks Road	0.4	18.6	19.0	2.1	97.9	100.0
Harmondsworth	0.2	19.1	19.3	1.1	98.9	100.0
Harmondsworth Osiris	0.2	19.1	19.3	1.1	98.9	100.0
Hayes	0.3	22.2	22.4	1.1	98.9	100.0
Oxford Avenue	0.7	19.5	20.1	3.2	96.8	100.0
Sipson	0.5	19.0	19.5	2.5	97.5	100.0
Cranford	0.3	20.3	20.6	1.4	98.6	100.0
Feltham	0.2	21.0	21.2	0.9	99.1	100.0
Hatton Cross	0.8	19.3	20.1	4.2	95.8	100.0
Harlington	0.3	19.4	19.8	1.8	98.2	100.0
Hillingdon	0.4	21.0	21.4	1.7	98.3	100.0
Colnbrook	0.1	19.7	19.8	0.8	99.2	100.0
Lakeside 1 Osiris	0.3	19.4	19.7	1.5	98.5	100.0
Lakeside 2	0.2	19.4	19.6	0.9	99.1	100.0
PerimA	0.6	20.6	21.2	2.8	97.2	100.0
PerimB	0.7	20.7	21.4	3.1	96.9	100.0
PerimC	0.5	20.8	21.3	2.4	97.6	100.0
PerimD	0.5	21.1	21.6	2.2	97.8	100.0
PerimE	0.6	21.7	22.3	2.7	97.3	100.0
PerimF	0.5	21.1	21.6	2.5	97.5	100.0
PerimG	0.6	22.1	22.7	2.6	97.4	100.0
PerimH	0.6	20.7	21.3	2.7	97.3	100.0
M4A	0.4	22.4	22.8	1.8	98.2	100.0
M4B	0.4	22.8	23.2	1.7	98.3	100.0
M4C	0.5	24.4	24.8	1.8	98.2	100.0
M4D	0.4	24.3	24.8	1.7	98.3	100.0

[1] Includes aircraft, APUs, GSE, airport-related traffic on the road network, carparking and stationary sources.
[2] Includes non-airport traffic on the road network, large point sources, NAEI area sources and rural background.

Table 17 Airport and non-airport contributions to annual mean $PM_{2.5}$ concentrations

Receptor	Contribution to $PM_{2.5}$ (µg m^{-3})			Contribution to $PM_{2.5}$ (%)		
	Airport[1]	Non-airport[2]	Total	Airport[1]	Non-airport[2]	Total
Bath Road	0.6	13.1	13.6	4.4	95.6	100.0
Green Gates	0.3	12.5	12.8	2.5	97.5	100.0
LHR2	1.0	12.8	13.8	7.2	92.8	100.0
Oaks Road	0.3	12.7	13.0	2.3	97.7	100.0
Harmondsworth	0.2	12.7	12.9	1.2	98.8	100.0
Harmondsworth Osiris	0.2	12.7	12.9	1.3	98.7	100.0
Hayes	0.2	14.4	14.6	1.3	98.7	100.0
Oxford Avenue	0.5	12.9	13.4	3.6	96.4	100.0
Sipson	0.3	12.7	13.1	2.7	97.3	100.0
Cranford	0.2	13.4	13.6	1.7	98.3	100.0
Feltham	0.1	13.9	14.0	1.1	98.9	100.0
Hatton Cross	0.6	13.0	13.6	4.5	95.5	100.0
Harlington	0.3	12.9	13.2	2.0	98.0	100.0
Hillingdon	0.3	13.8	14.1	1.9	98.1	100.0
Colnbrook	0.1	13.2	13.3	0.8	99.2	100.0
Lakeside 1 Osiris	0.2	13.0	13.2	1.5	98.5	100.0
Lakeside 2	0.1	12.9	13.0	0.9	99.1	100.0
PerimA	0.4	13.8	14.2	3.0	97.0	100.0
PerimB	0.5	13.8	14.3	3.5	96.5	100.0
PerimC	0.4	13.9	14.3	2.8	97.2	100.0
PerimD	0.4	14.0	14.4	2.7	97.3	100.0
PerimE	0.5	14.3	14.8	3.2	96.8	100.0
PerimF	0.4	14.1	14.5	3.0	97.0	100.0
PerimG	0.5	14.8	15.3	3.1	96.9	100.0
PerimH	0.4	14.0	14.5	3.1	96.9	100.0
M4A	0.3	14.8	15.1	2.0	98.0	100.0
M4B	0.3	14.9	15.2	1.9	98.1	100.0
M4C	0.3	15.7	16.1	2.2	97.8	100.0
M4D	0.3	15.7	16.0	2.0	98.0	100.0

[1] Includes aircraft, APUs, GSE, airport-related traffic on the road network, carparking and stationary sources.
[2] Includes non-airport traffic on the road network, large point sources, NAEI area sources and rural background.

The estimated total annual mean PM_{10} concentrations at all the sites are well below the 40 µg m^{-3} limit value. For PM_{10}, however, the limit on the annual number of daily exceedances of a 24-hour mean concentration of 50 µg m^{-3} (no more than 35) is generally more onerous, and it is common practice to take an annual mean value of 31.5 µg m^{-3} to be equivalent to the shorter-period limit. Clearly, estimated annual mean PM_{10}

concentrations are also well below this surrogate limit. For $PM_{2.5}$, estimated annual mean concentrations are well below the 25 µg m^{-3} objective and limit value which come into force in 2010 and 2015 respectively. However, they are above the interim target of 12 µg m^{-3} set for 2028.

6.3.1 Airport-related PM

Clearly from Table 16, the estimated contribution from airport-related sources is small, ranging from 0.15 µg m^{-3} (Colnbrook) to 1.56 µg m^{-3} (LHR2) for PM_{10} and from 0.11 µg m^{-3} (Colnbrook) to 1.00 µg m^{-3} (LHR2) for $PM_{2.5}$. For PM_{10}, the highest contribution at off-airport receptor locations is 0.88 µg m^{-3} at Bath Road and, for $PM_{2.5}$, the highest contribution is 0.61 µg m^{-3} at Hatton Cross. These represent a very small contribution to the total. Both aircraft and the landside road network make appreciable contributions to the airport contribution, depending on the location of the receptor. This is shown in Table 18, which gives a breakdown of the airport-related contribution to PM_{10} by source category. (The relative breakdown for $PM_{2.5}$ is shown in Table 19.)

Table 18 Breakdown of the airport contribution to annual mean PM_{10} concentrations by source category

Receptor	Contribution to PM_{10} (µg m^{-3})					Contribution to PM_{10} (%)				
	Aircraft[1]	GSE	Road traffic	Other[2]	Total	Aircraft[1]	GSE	Road traffic	Other[2]	Total
Bath Road	0.41	0.05	0.31	0.11	0.88	46.4	5.3	35.7	12.6	100.0
Green Gates	0.18	0.03	0.20	0.04	0.46	39.9	6.7	43.8	9.7	100.0
LHR2	0.75	0.06	0.61	0.13	1.56	48.2	3.9	39.4	8.5	100.0
Oaks Road	0.15	0.04	0.11	0.09	0.39	39.1	10.3	27.3	23.3	100.0
Harmondsworth	0.06	0.02	0.09	0.04	0.21	31.0	9.5	42.5	17.0	100.0
Harmondsworth Osiris	0.07	0.02	0.09	0.04	0.22	32.0	10.1	40.7	17.2	100.0
Hayes	0.09	0.01	0.11	0.05	0.25	34.5	4.6	42.7	18.2	100.0
Oxford Avenue	0.35	0.03	0.18	0.10	0.65	53.7	4.2	27.3	14.8	100.0
Sipson	0.18	0.04	0.19	0.07	0.48	37.7	8.8	38.5	14.9	100.0
Cranford	0.15	0.02	0.07	0.06	0.30	48.9	5.3	24.2	21.6	100.0
Feltham	0.07	0.01	0.05	0.05	0.19	37.8	6.5	27.7	28.1	100.0
Hatton Cross	0.51	0.04	0.19	0.11	0.84	59.9	4.5	22.1	13.4	100.0
Harlington	0.16	0.03	0.10	0.07	0.35	44.9	7.4	28.7	19.1	100.0
Hillingdon	0.06	0.02	0.25	0.04	0.36	16.8	4.4	69.0	9.8	100.0
Colnbrook	0.05	0.01	0.07	0.02	0.15	35.9	5.4	43.5	15.1	100.0
Lakeside 1 Osiris	0.05	0.01	0.23	0.02	0.30	15.3	2.6	74.9	7.2	100.0
Lakeside 2	0.05	0.01	0.09	0.02	0.17	27.9	5.2	54.3	12.6	100.0
PerimA	0.10	0.05	0.37	0.07	0.58	16.3	9.0	62.8	11.8	100.0
PerimB	0.13	0.06	0.37	0.11	0.66	19.2	8.4	56.0	16.4	100.0
PerimC	0.13	0.05	0.23	0.11	0.51	25.2	9.0	45.0	20.8	100.0
PerimD	0.15	0.04	0.18	0.11	0.48	30.9	9.3	37.5	22.3	100.0
PerimE	0.15	0.04	0.30	0.10	0.60	25.4	6.9	50.4	17.3	100.0
PerimF	0.13	0.05	0.19	0.16	0.53	24.3	9.7	36.1	29.8	100.0

Receptor	Contribution to PM_{10} (µg m^{-3})					Contribution to PM_{10} (%)				
	Aircraft[1]	GSE	Road traffic	Other[2]	Total	Aircraft[1]	GSE	Road traffic	Other[2]	Total
PerimG	0.09	0.06	0.26	0.18	0.60	15.7	10.1	44.2	30.1	100.0
PerimH	0.08	0.04	0.26	0.18	0.57	14.3	7.6	46.2	32.0	100.0
M4A	0.03	0.01	0.34	0.03	0.41	6.5	2.9	83.8	6.8	100.0
M4B	0.03	0.01	0.31	0.03	0.39	7.9	3.6	80.4	8.2	100.0
M4C	0.05	0.02	0.33	0.06	0.45	11.4	3.6	72.5	12.5	100.0
M4D	0.05	0.02	0.30	0.06	0.42	11.8	3.6	71.3	13.2	100.0

[1] Aircraft main engines and APU
[2] Carparking and stationary sources

Table 19 Breakdown of the airport contribution to annual mean $PM_{2.5}$ concentrations by source category

Receptor	Contribution to $PM_{2.5}$ (µg m^{-3})					Contribution to $PM_{2.5}$ (%)				
	Aircraft[1]	GSE	Road traffic	Other[2]	Total	Aircraft[1]	GSE	Road traffic	Other[2]	Total
Bath Road	0.26	0.03	0.20	0.11	0.60	43.8	5.5	33.0	17.7	100.0
Green Gates	0.13	0.02	0.13	0.04	0.32	40.6	6.8	40.1	12.5	100.0
LHR2	0.45	0.04	0.38	0.13	1.00	45.3	4.3	37.9	12.6	100.0
Oaks Road	0.12	0.03	0.07	0.09	0.30	40.2	9.2	21.8	28.8	100.0
Harmondsworth	0.05	0.01	0.06	0.03	0.16	32.4	8.9	37.4	21.3	100.0
Harmondsworth Osiris	0.05	0.02	0.06	0.03	0.16	33.6	9.4	35.6	21.4	100.0
Hayes	0.06	0.01	0.07	0.04	0.19	34.7	4.3	37.1	23.9	100.0
Oxford Avenue	0.25	0.02	0.11	0.09	0.48	53.3	4.0	23.3	19.3	100.0
Sipson	0.13	0.03	0.12	0.07	0.35	37.9	8.5	34.3	19.3	100.0
Cranford	0.11	0.01	0.05	0.06	0.23	47.4	4.8	20.4	27.3	100.0
Feltham	0.05	0.01	0.03	0.05	0.15	36.5	5.9	22.3	35.3	100.0
Hatton Cross	0.36	0.03	0.12	0.11	0.61	58.6	4.4	19.3	17.8	100.0
Harlington	0.11	0.02	0.06	0.06	0.26	43.3	7.0	25.2	24.5	100.0
Hillingdon	0.05	0.01	0.18	0.03	0.27	17.8	4.1	65.7	12.5	100.0
Colnbrook	0.04	0.01	0.04	0.02	0.11	36.1	5.2	39.0	19.7	100.0
Lakeside 1 Osiris	0.03	0.01	0.14	0.02	0.20	17.0	2.7	70.1	10.3	100.0
Lakeside 2	0.03	0.01	0.06	0.02	0.12	28.7	5.0	50.1	16.3	100.0
PerimA	0.10	0.04	0.24	0.06	0.43	22.2	8.5	55.1	14.2	100.0
PerimB	0.13	0.04	0.23	0.10	0.50	25.6	7.9	47.2	19.3	100.0
PerimC	0.13	0.03	0.14	0.10	0.40	31.9	8.0	35.7	24.3	100.0
PerimD	0.15	0.03	0.11	0.10	0.39	37.6	7.9	28.6	25.8	100.0

Receptor	Contribution to $PM_{2.5}$ (µg m^{-3})					Contribution to $PM_{2.5}$ (%)				
	Aircraft[1]	GSE	Road traffic	Other[2]	Total	Aircraft[1]	GSE	Road traffic	Other[2]	Total
PerimE	0.15	0.03	0.19	0.10	0.47	32.6	6.2	40.0	21.2	100.0
PerimF	0.13	0.04	0.12	0.15	0.44	29.4	8.2	27.5	34.9	100.0
PerimG	0.09	0.04	0.17	0.17	0.48	19.7	8.8	35.2	36.3	100.0
PerimH	0.08	0.03	0.16	0.18	0.45	18.1	6.7	35.8	39.4	100.0
M4A	0.03	0.01	0.24	0.03	0.30	8.8	2.8	79.6	8.8	100.0
M4B	0.03	0.01	0.22	0.03	0.30	10.4	3.3	76.1	10.3	100.0
M4C	0.05	0.01	0.23	0.05	0.35	14.8	3.3	66.4	15.6	100.0
M4D	0.05	0.01	0.21	0.05	0.33	15.3	3.3	65.0	16.4	100.0

[1] Aircraft main engines and APU
[2] Carparking and stationary sources

Figure 11 displays the spatial variation of the airport-related contribution to annual mean PM_{10} concentrations around the airport, showing that the contribution at non-roadside receptor locations drops below 1 µg m^{-3} within about 100 m of the airport boundary. Along the M4 and M25, the contribution also drops below 1 µg m^{-3} within about 100 m of the motorway. Contour plots of total PM_{10} and $PM_{2.5}$ concentrations are given in Section 6.3.3.

Figure 11 Airport-related contribution[1] to annual mean PM_{10} concentration in 2019 outside the airport boundary

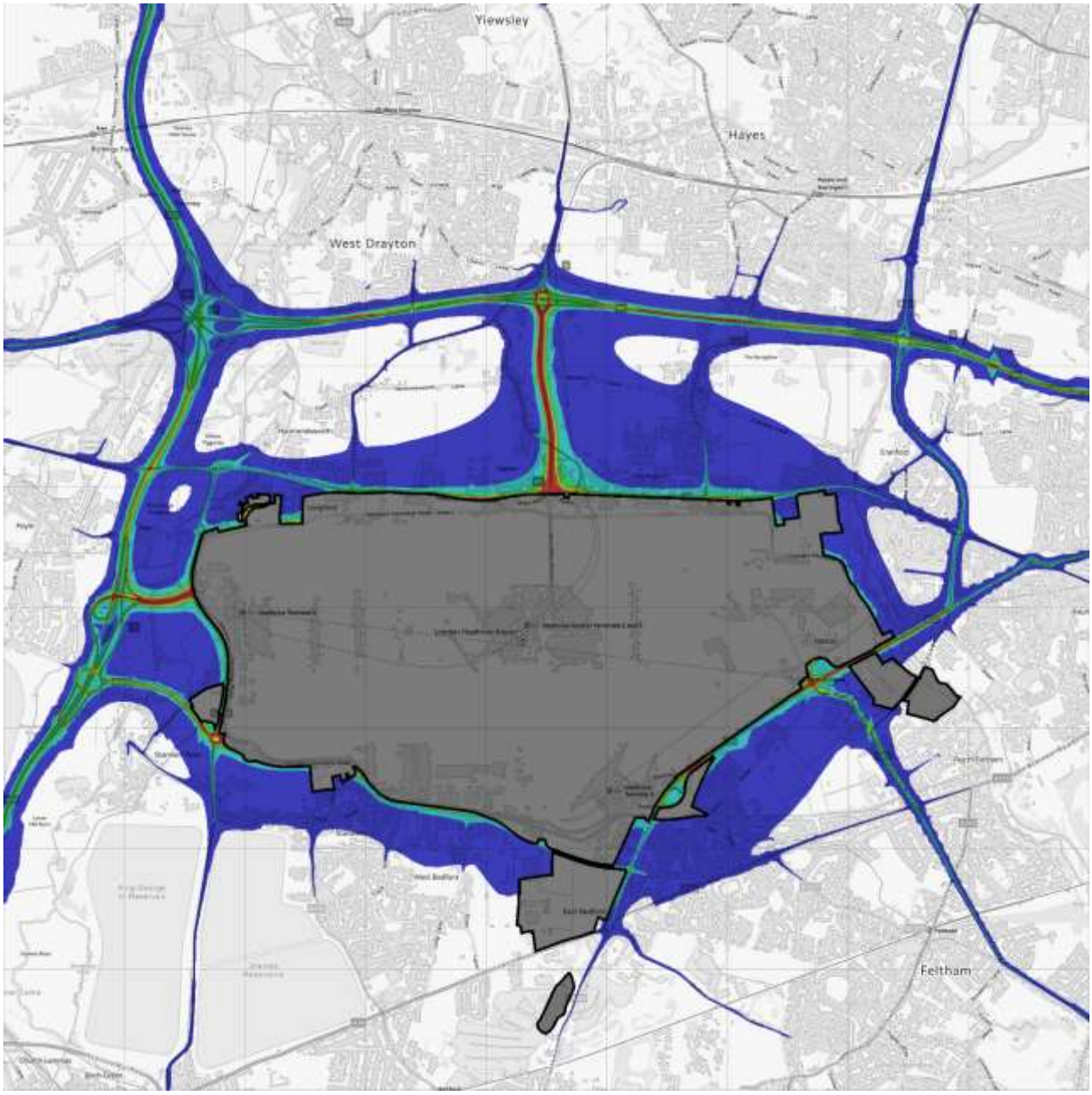

[1] Includes aircraft, APUs, GSE, airport-related traffic on the road network, carparking and stationary sources.

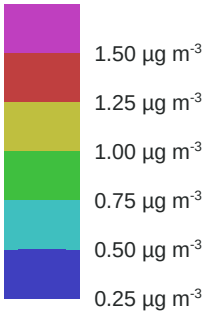

Figure 12 Airport-related contribution[1] to annual mean $PM_{2.5}$ concentration in 2019 outside the airport boundary

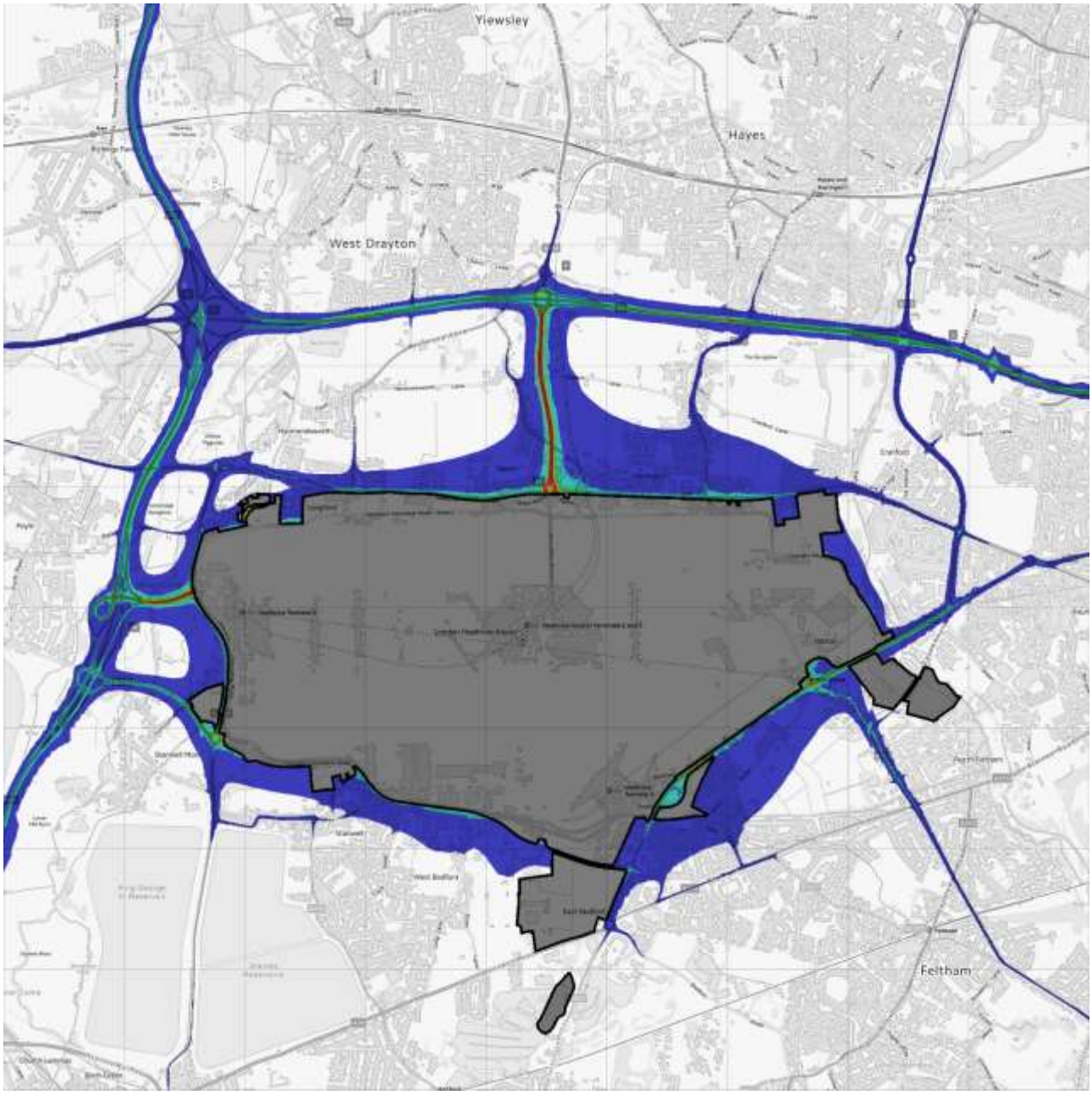

[1] Includes aircraft, APUs, GSE, airport-related traffic on the road network, carparking and stationary sources.

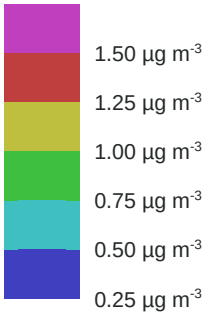

6.3.2 Non-airport PM

The contribution from non-airport sources is relatively constant across the set of receptor locations, with the consequence that the total concentration is also relatively constant. Even so, it is instructive to examine its contributions by source. Table 20 shows the pertinent breakdown, separately for PM_{10} and $PM_{2.5}$.

Table 20 Breakdown of the non-airport PM contribution by source category

Receptor	Annual mean PM_{10} contribution ($\mu g\ m^{-3}$)			Annual mean $PM_{2.5}$ contribution ($\mu g\ m^{-3}$)		
	Road traffic	Background[1]	Total	Road traffic	Background[1]	Total
Bath Road	0.7	18.8	19.5	0.4	12.6	13.1
Green Gates	0.4	18.1	18.6	0.3	12.2	12.5
LHR2	0.4	18.8	19.1	0.2	12.6	12.8
Oaks Road	0.3	18.4	18.6	0.2	12.5	12.7
Harmondsworth	0.3	18.7	19.1	0.2	12.5	12.7
Harmondsworth Osiris	0.3	18.8	19.1	0.2	12.5	12.7
Hayes	0.9	21.3	22.2	0.6	13.8	14.4
Oxford Avenue	0.5	19.0	19.5	0.3	12.7	12.9
Sipson	0.2	18.8	19.0	0.2	12.6	12.7
Cranford	0.3	20.0	20.3	0.2	13.2	13.4
Feltham	0.8	20.2	21.0	0.5	13.4	13.9
Hatton Cross	0.4	18.9	19.3	0.3	12.7	13.0
Harlington	0.4	19.0	19.4	0.3	12.6	12.9
Hillingdon	1.1	19.9	21.0	0.8	13.0	13.8
Colnbrook	0.3	19.4	19.7	0.2	13.0	13.2
Lakeside 1 Osiris	0.7	18.6	19.4	0.5	12.5	13.0
Lakeside 2	0.5	19.0	19.4	0.3	12.6	12.9
PerimA	0.6	20.0	20.6	0.4	13.4	13.8
PerimB	0.4	20.3	20.7	0.3	13.6	13.8
PerimC	0.4	20.5	20.8	0.2	13.6	13.9
PerimD	0.4	20.7	21.1	0.2	13.7	14.0
PerimE	0.9	20.8	21.7	0.5	13.8	14.3
PerimF	0.3	20.7	21.1	0.2	13.9	14.1
PerimG	1.1	20.9	22.1	0.7	14.1	14.8
PerimH	0.7	20.1	20.7	0.4	13.6	14.0
M4A	1.7	20.7	22.4	1.2	13.6	14.8
M4B	1.5	21.3	22.8	1.0	13.8	14.9
M4C	1.5	22.9	24.4	1.0	14.7	15.7
M4D	1.3	23.0	24.3	0.9	14.8	15.7

[1] Sources from the NAEI not already included in the airport and road network source categories.

Clearly, the background contribution is dominant and virtually constant across the area of interest, reflecting the fact that background sources are distant and coarsely defined spatially. The small distance of some of the receptor locations from the M4 or other major roads leads to the comparatively large contribution at these sites from road vehicles on the network.

6.3.3 Total PM concentrations

Figure 13 displays annual mean concentrations of PM_{10} outside the airport. It shows that off-airport annual mean PM_{10} concentrations are well below both the 40 µg m^{-3} limit value and the 31.5 µg m^{-3} level that is indicative of shorter-period limit.

Figure 14 displays annual mean concentrations of $PM_{2.5}$ outside the airport. It shows that off-airport annual mean $PM_{2.5}$ concentrations are well below the 20 µg m^{-3} limit value. However, they are above the above the interim target of 12 µg m^{-3} set for 2028 throughout most of the study area.

Figure 13 Annual mean PM_{10} concentrations in 2019 outside the airport boundary

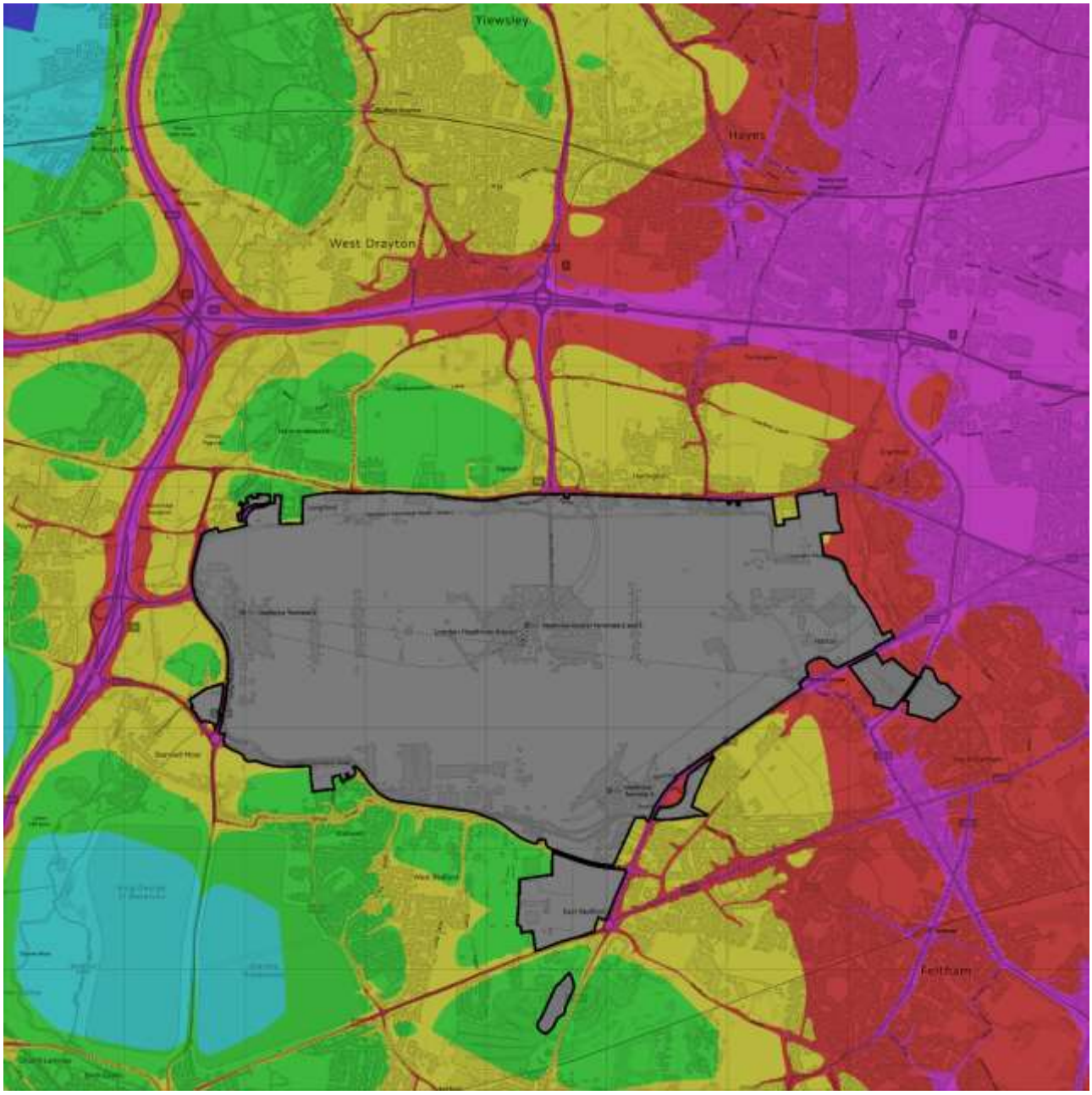

Contains OS data © Crown copyright and database right 2023.
The annual mean AQS limit value for PM_{10} is 40 µg m^{-3}.
The 50 µg m^{-3} daily mean AQS limit value for PM_{10} is roughly equivalent to an annual mean of 31.5 µg m^{-3}.

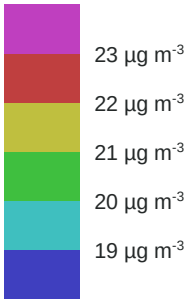

Figure 14 Annual mean $PM_{2.5}$ concentrations in 2019 outside the airport boundary

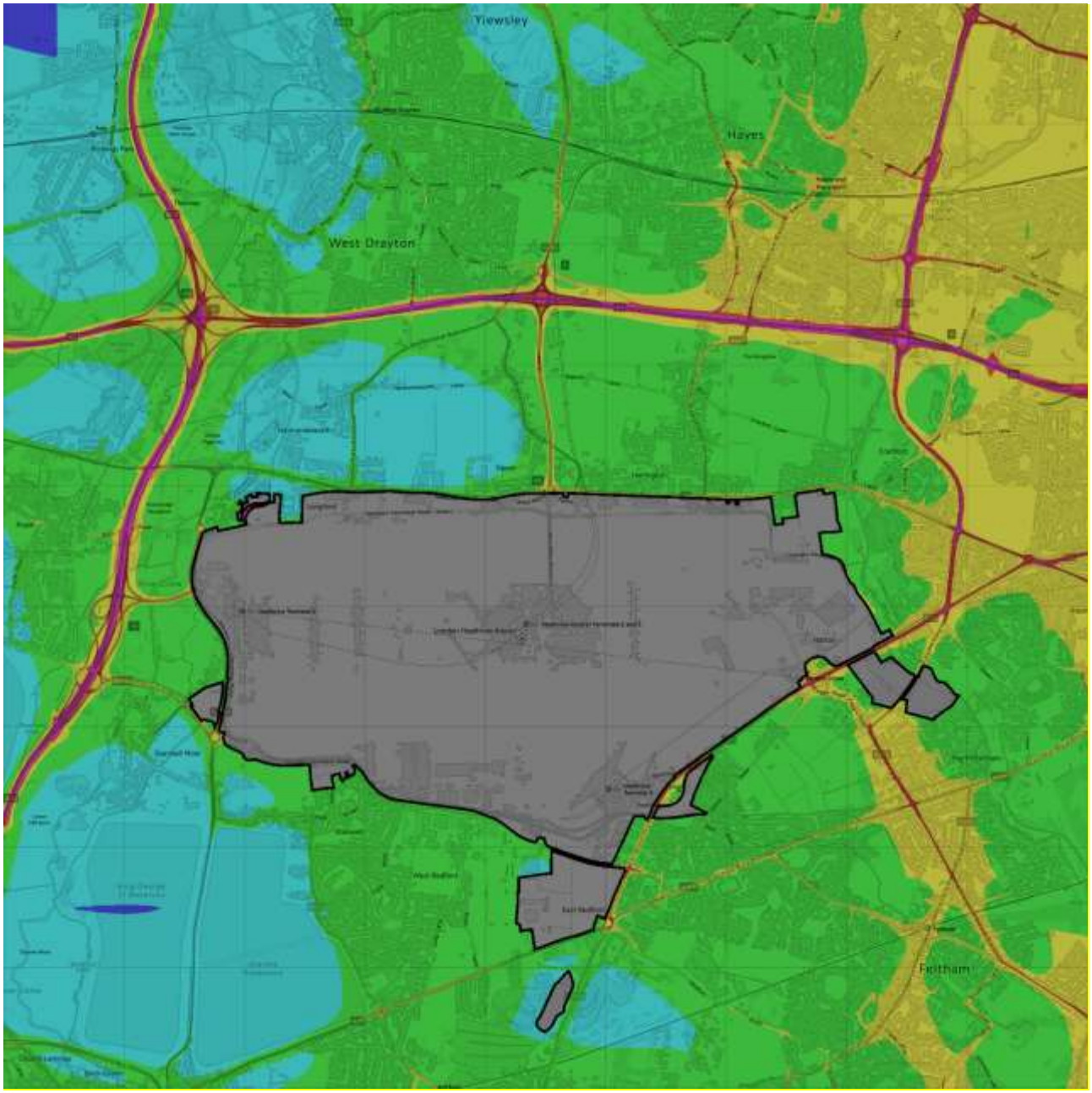

The annual mean AQS limit value for PM2.5 is 20 µg m−3.

17 µg m^{-3}
16 µg m^{-3}
15 µg m^{-3}
14 µg m^{-3}
13 µg m^{-3} (the interim target for 2028)

6.3.4 Comparison with 2013

Table 21 compares annual mean PM concentrations for 2019 with those in 2013 and Table 22 compares the airport and non-airport contribution to PM_{10} concentrations only. The relative differences for $PM_{2.5}$ are similar.

Table 21 Comparison of modelled PM concentrations for 2019 and 2013

Receptor	PM_{10} (µg m^{-3})			$PM_{2.5}$ (µg m^{-3})		
	2019	2013	Difference (%)[1]	2019	2013	Difference (%)[1]
Bath Road	20.4	n/a	n/a	13.6	n/a	n/a
Green Gates	19.0	20.2	-5.9	12.8	15.0	-14.4
LHR2	20.7	23.5	-11.8	13.8	16.9	-17.9
Oaks Road	19.0	19.9	-4.3	13.0	14.8	-12.2
Harmondsworth	19.3	19.8	-2.8	12.9	14.7	-12.6
Harmondsworth Osiris	19.3	n/a	n/a	12.9	n/a	n/a
Hayes	22.4	20.8	7.7	14.6	15.2	-4.0
Oxford Avenue	20.1	20.9	-3.7	13.4	15.2	-11.9
Sipson	19.5	20.0	-2.6	13.1	14.8	-11.7
Cranford	20.6	19.9	3.6	13.6	14.6	-7.2
Feltham	21.2	n/a	n/a	14.0	n/a	n/a
Hatton Cross	20.1	21.2	-4.9	13.6	15.4	-11.8
Harlington	19.8	20.4	-3.2	13.2	15.0	-12.2
Hillingdon	21.4	23.0	-6.8	14.1	16.6	-15.3
Colnbrook	19.8	20.1	-1.4	13.3	14.9	-10.7
Lakeside 1 Osiris	19.7	n/a	n/a	13.2	n/a	n/a
Lakeside 2	19.6	n/a	n/a	13.0	n/a	n/a
PerimA	21.2	20.8	1.9	14.2	15.3	-7.0
PerimB	21.4	20.9	2.1	14.3	15.3	-6.7
PerimC	21.3	20.4	4.4	14.3	15.0	-5.0
PerimD	21.6	20.6	4.6	14.4	15.1	-5.1
PerimE	22.3	22.4	-0.4	14.8	16.2	-8.5
PerimF	21.6	21.6	-0.3	14.5	15.7	-7.5
PerimG	22.7	23.0	-1.4	15.3	16.5	-7.3
PerimH	21.3	21.7	-1.6	14.5	15.8	-8.1
M4A	22.8	23.3	-1.9	15.1	16.8	-10.4
M4B	23.2	22.9	1.1	15.2	16.6	-8.5
M4C	24.8	23.6	5.2	16.1	16.9	-4.9
M4D	24.8	23.4	6.0	16.0	16.7	-4.2

[1] Difference (%) = 100 * (2019 value – 2013 value) / 2013 value

Table 22 Comparison of modelled airport and non-airport contribution to PM_{10} concentrations for 2019 and 2013

Receptor	Airport PM_{10} (µg m^{-3})			Non-airport PM_{10} (µg m^{-3})		
	2019	2013	Difference (%)[1]	2019	2013	Difference (%)[1]
Bath Road	0.9	n/a	n/a	19.5	n/a	n/a
Green Gates	0.5	0.5	-15.6	18.6	19.7	-5.6
LHR2	1.6	3.5	-55.8	19.1	20.0	-4.0
Oaks Road	0.4	0.8	-52.3	18.6	19.1	-2.2
Harmondsworth	0.2	0.4	-46.1	19.1	19.5	-2.0
Harmondsworth Osiris	0.2	n/a	n/a	19.1	n/a	n/a
Hayes	0.3	0.3	-0.1	22.2	20.6	7.8
Oxford Avenue	0.7	0.8	-16.4	19.5	20.1	-3.2
Sipson	0.5	0.8	-43.3	19.0	19.2	-0.8
Cranford	0.3	0.4	-16.2	20.3	19.6	3.9
Feltham	0.2	n/a	n/a	21.0	n/a	n/a
Hatton Cross	0.8	1.1	-24.2	19.3	20.0	-3.8
Harlington	0.3	0.5	-31.8	19.4	19.9	-2.5
Hillingdon	0.4	1.2	-69.1	21.0	21.8	-3.4
Colnbrook	0.1	0.3	-50.8	19.7	19.8	-0.6
Lakeside 1 Osiris	0.3	n/a	n/a	19.4	n/a	n/a
Lakeside 2	0.2	n/a	n/a	19.4	n/a	n/a
PerimA	0.6	0.7	-11.0	20.6	20.1	2.3
PerimB	0.7	1.3	-50.1	20.7	19.6	5.6
PerimC	0.5	1.0	-47.7	20.8	19.4	7.1
PerimD	0.5	1.1	-56.2	21.1	19.5	8.0
PerimE	0.6	1.3	-54.6	21.7	21.1	3.0
PerimF	0.5	1.4	-60.9	21.1	20.3	3.7
PerimG	0.6	1.0	-42.9	22.1	21.9	0.6
PerimH	0.6	1.3	-56.9	20.7	20.3	2.0
M4A	0.4	1.2	-67.1	22.4	22.0	1.8
M4B	0.4	1.1	-66.0	22.8	21.8	4.6
M4C	0.5	1.1	-58.2	24.4	22.5	8.2
M4D	0.4	1.0	-58.4	24.3	22.3	8.9

[1] Difference (%) = 100 * (2019 value – 2013 value) / 2013 value

The total modelled concentrations of both PM_{10} and $PM_{2.5}$ are lower in 2019 than in 2013. This is also the case for the airport and non-airport contributions to PM concentrations.

In contrast to NO_x, aircraft PM emissions have decreased between 2013 and 2019, whereas PM emissions from stationary sources have increased significantly due to increased use of the biomass.

However, when combined with a dramatic reduction in PM emissions from road traffic (and GSE), the airport contributions to PM concentrations are lower in 2019 than in 2013. The comparisons for PM_{10} are shown in Figure 15 and for $PM_{2.5}$ in Figure 16.

Figure 15 Airport-related contribution[1] to annual mean PM_{10} concentrations – Comparison of 2019 with 2013

2019

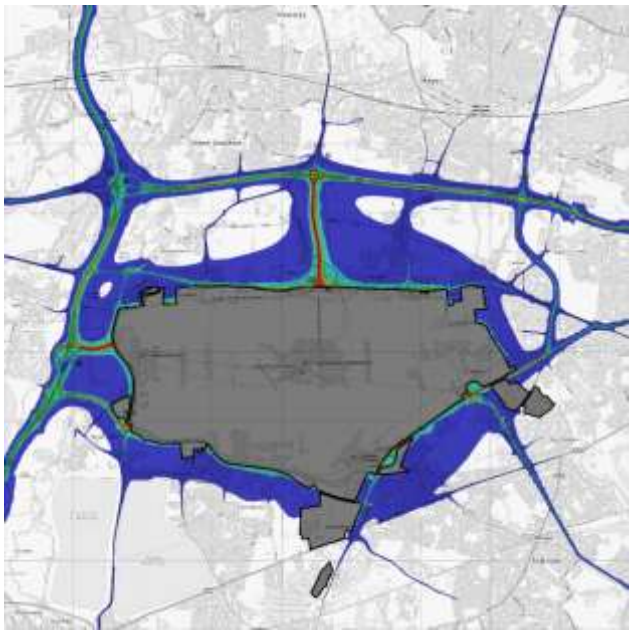

2013

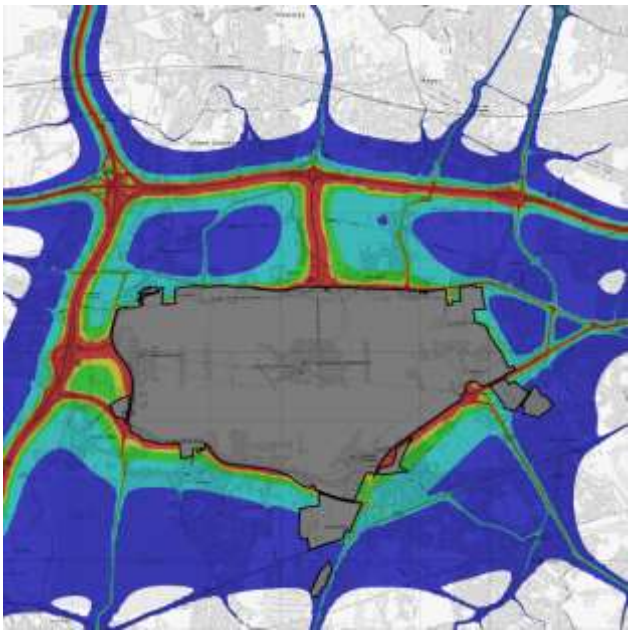

[1] Includes aircraft, APUs, GSE, airport-related traffic on the road network, carparking and stationary sources.

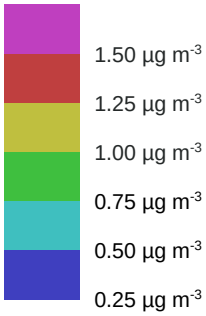

Figure 16 Airport-related contribution[1] to annual mean $PM_{2.5}$ concentrations – Comparison of 2019 with 2013

2019

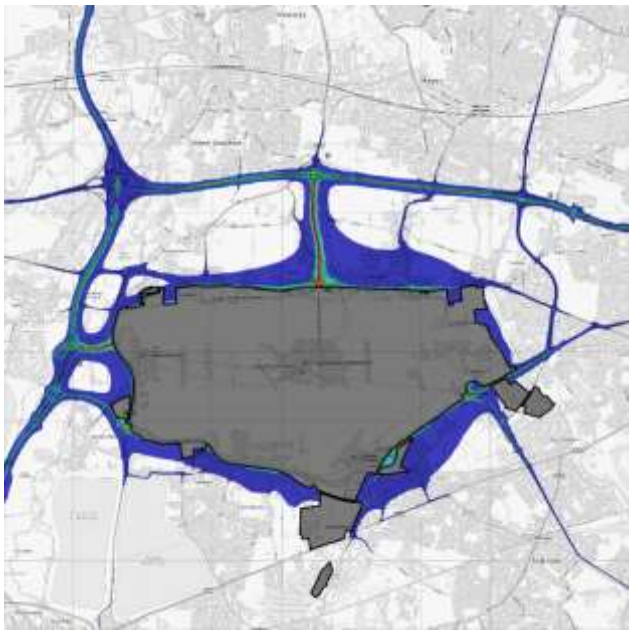

2013

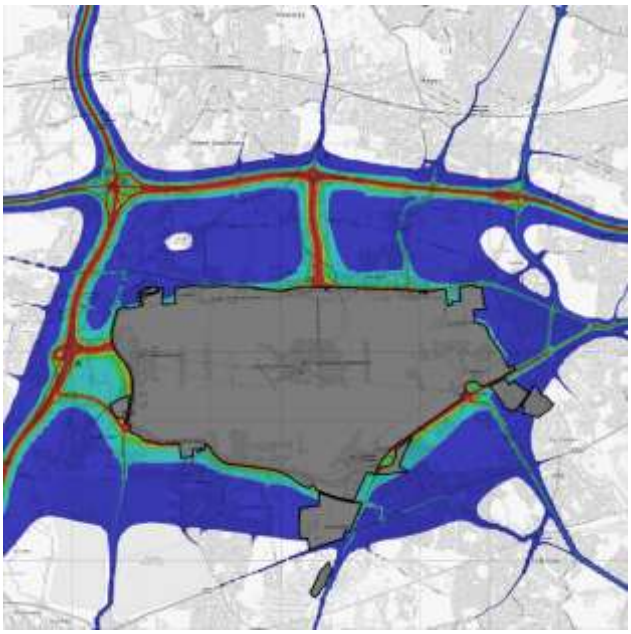

Contains OS data © Crown copyright and database right 2023.
[1] Includes aircraft, APUs, GSE, airport-related traffic on the road network, carparking and stationary sources.

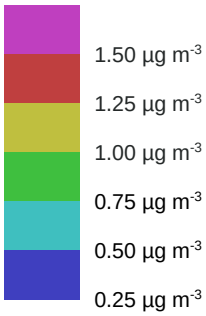

Figure 17 and Figure 18 compare the modelled annual mean PM_{10} and $PM_{2.5}$ concentrations in 2019 with 2013, respectively. Figure 17 reflects the increase in background PM_{10} concentrations, which is particularly evident to the northeast towards London, whereas Figure 18 reflects changes in the gradient of background $PM_{2.5}$ concentrations, with increases to the east and reductions to the west. Both figures reflect the reduction in the road-network contribution to PM concentrations. The removal of the emissions from the Great Western railway line is also evident.

It should be noted that the PM concentrations have not been adjusted to account for the model overprediction. PM concentrations are dominated by background sources and one reason for their increase is the popularity of wood burning stoves. However, the emission estimates for these are highly uncertain and these uncertainties may provide an explanation for the model overprediction.

Figure 17 Annual mean PM_{10} concentrations – Comparison of 2019 with 2013

2019

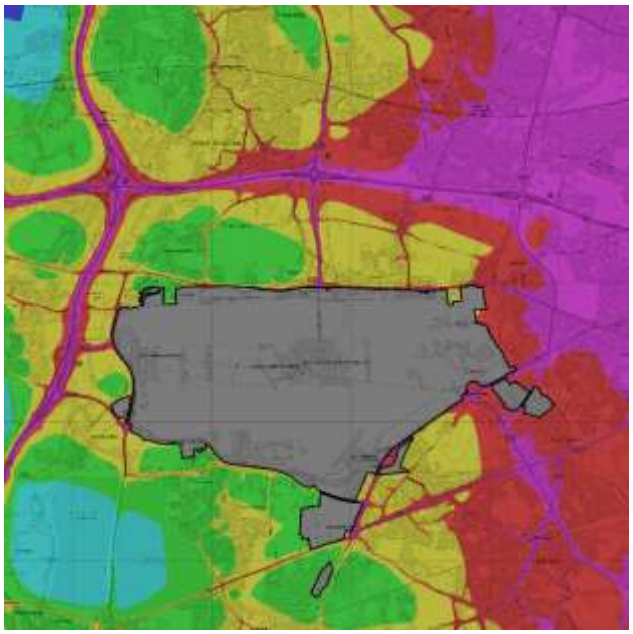

2013

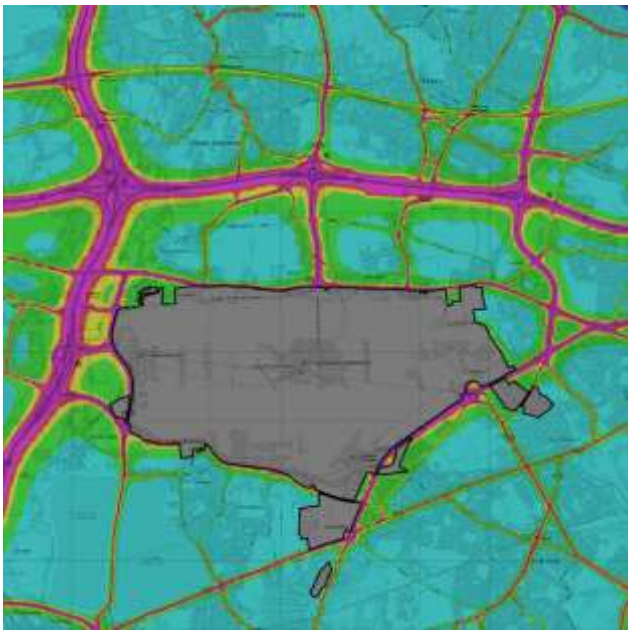

The annual mean AQS limit value for PM_{10} is 40 µg m^{-3}.

The 50 µg m^{-3} daily mean AQS limit value for PM_{10} is roughly equivalent to an annual mean of 31.5 µg m^{-3}.

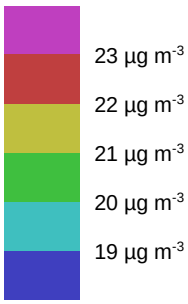

Figure 18 Annual mean $PM_{2.5}$ concentrations – Comparison of 2019 with 2013

2019

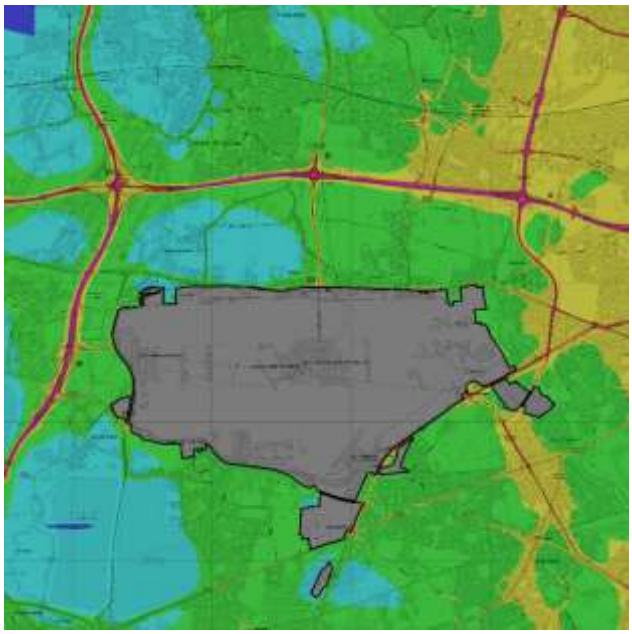

2013

Contains OS data © Crown copyright and database right 2023.
The annual mean AQS limit value for $PM_{2.5}$ is 20 µg m^{-3}.

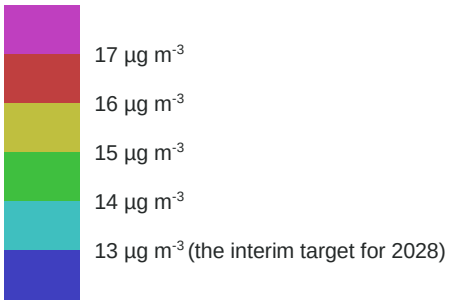

7. SUMMARY AND CONCLUSIONS

While a detailed comparison of the modelling results with monitoring is described in Appendix 1, it is useful to present a brief comparison here.

Table 23 presents a summary of modelled and measured NO_x and NO_2 concentrations at the continuous monitoring sites. Figure 19 shows the measured NO_2 concentrations overlaid on a contour map of modelled NO_2. There are areas of exceedance of the annual mean NO_2 limit of 40 µg m^{-3} predicted within approximately 200 m of the motorways and within a few metres of A-roads. There are also exceedances predicted within 50 m of the airport boundary.

Table 23 Comparison of modelled annual mean NO_x and NO_2 concentrations (after adjustment) with measured values for continuous NO_x/NO_2 analysers

Receptor	Modelled NO_x (µg m^{-3})	Measured NO_x (µg m^{-3})	Modelled NO_2 (µg m^{-3})	Measured NO_2 (µg m^{-3})
Green Gates	53.5	55.9	29.0	30.6
LHR2	90.6	98.3	40.6	42.5
Oaks Road	47.5	44.6	25.8	26.3

Receptor	Modelled NO_x ($\mu g\ m^{-3}$)	Measured NO_x ($\mu g\ m^{-3}$)	Modelled NO_2 ($\mu g\ m^{-3}$)	Measured NO_2 ($\mu g\ m^{-3}$)
Harmondsworth	49.3	40.6	26.9	23.7
Hayes	69.8	94.0	35.1	41.2
Oxford Avenue	60.3	60.1	30.8	33.1
Sipson	53.4	50.3	28.4	29.7
Cranford	49.3	44.3	26.3	26.9
Feltham	60.2	53.2	31.2	29.1
Hatton Cross	61.6	49.2	31.3	27.9
Harlington	55.1	50.9	29.0	30.7
Hillingdon	91.8	87.2	45.3	44.7
Colnbrook	46.3	42.3	25.5	24.5
Lakeside 2	53.3	54.7	29.2	27.6

Figure 19 Modelled and measured annual mean NO_2 concentrations in 2019.

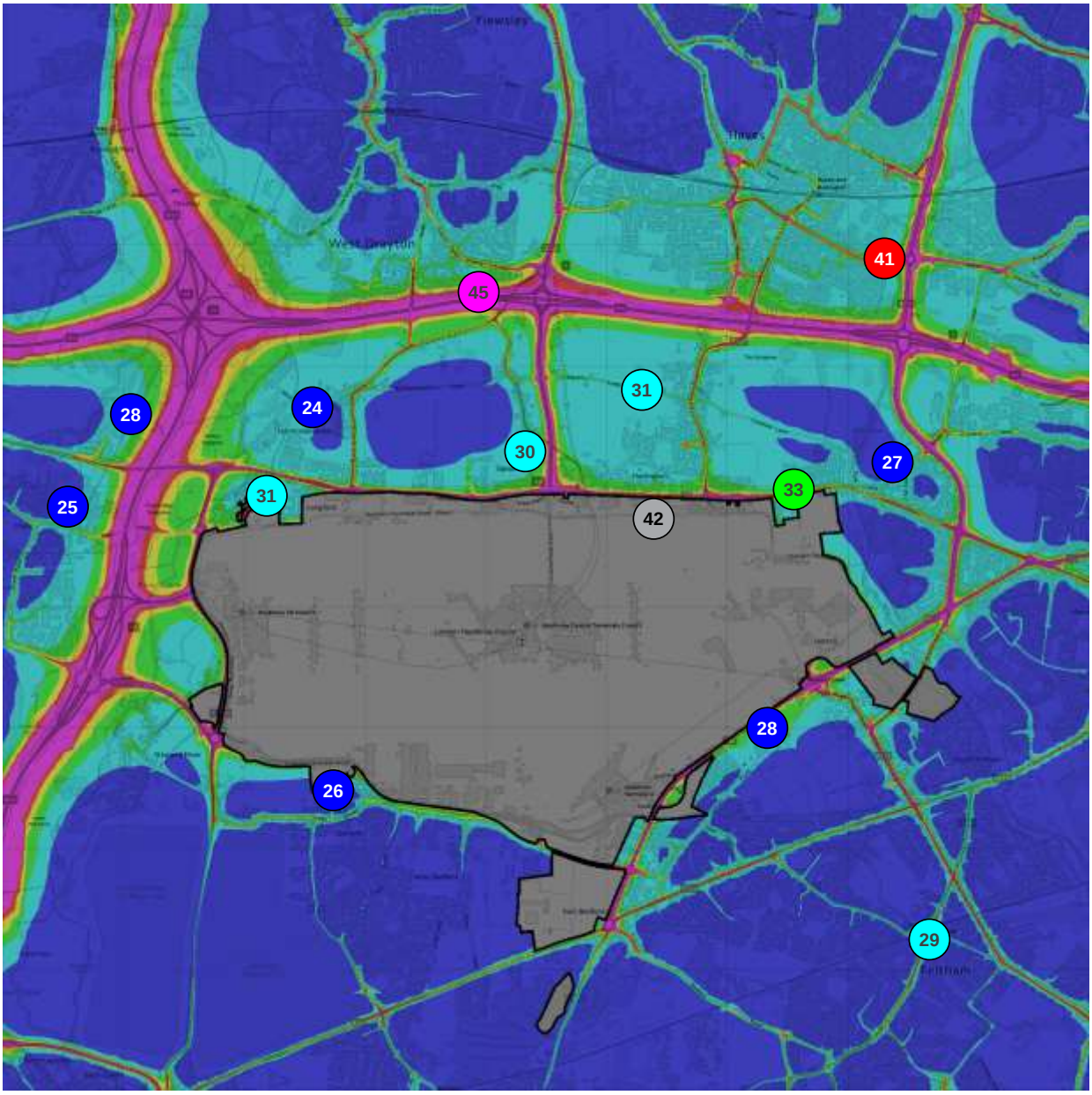

Contours show modelled concentrations.
Spot values at monitoring locations are measured NO_2 concentrations in µg m^{-3}.

44 µg m^{-3}

40 µg m^{-3} (the annual mean limit value for NO_2)

36 µg m^{-3}

32 µg m^{-3}

28 µg m^{-3}

Figure 20 to Figure 32 present breakdowns of modelled annual mean NOx concentrations (source apportionments) at the continuous monitoring sites. With the exception of LHR2 and Hillingdon, they show that the background is the largest contributor to annual mean NOx. As expected for an airfield site, the major

contributor at LHR is aircraft and at Hillingdon the largest contributor is road traffic, particularly non-airport traffic on the M4. At the two sites that recorded exceedances of the annual mean NO_2 standard, Hillingdon and Hayes, the airport (airfield and airport-related traffic) contribution to annual mean NOx is 15% and 11%, respectively. The airfield contribution alone at Hillingdon and Hayes is 4% and 6%, respectively.

Figure 20 Source apportionment of annual mean NO_x concentrations at Green Gates

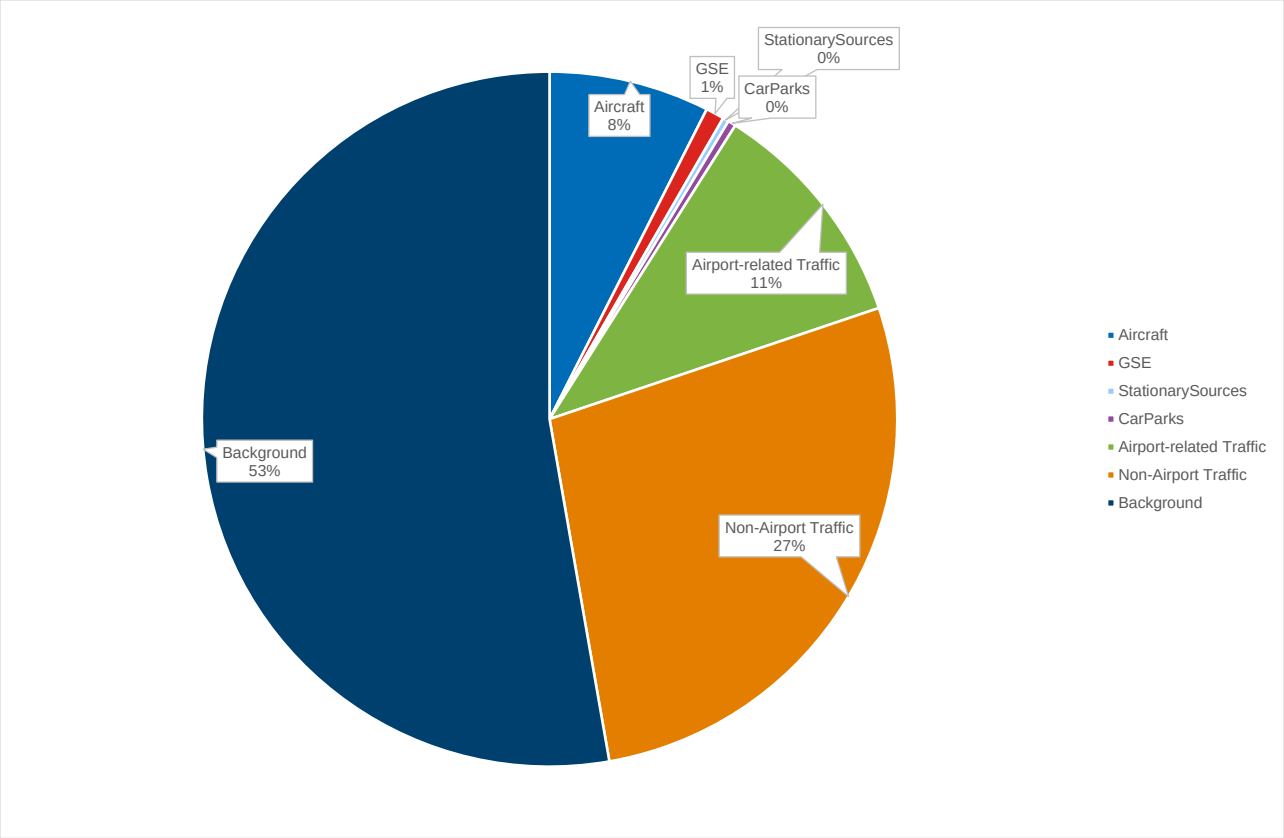

Figure 21 Source apportionment of annual mean NO_x concentrations at LHR2

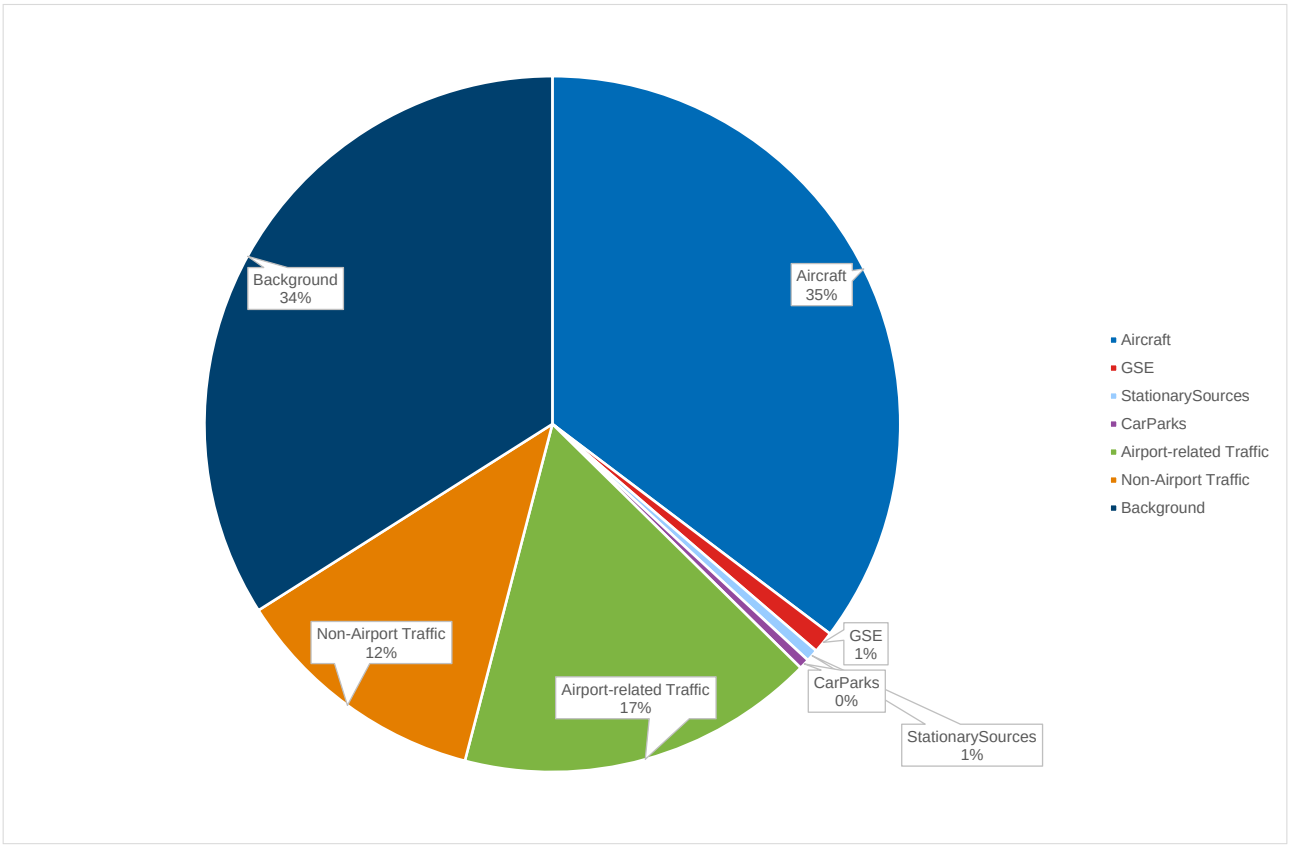

Figure 22 Source apportionment of annual mean NO_x concentrations at Oaks Road

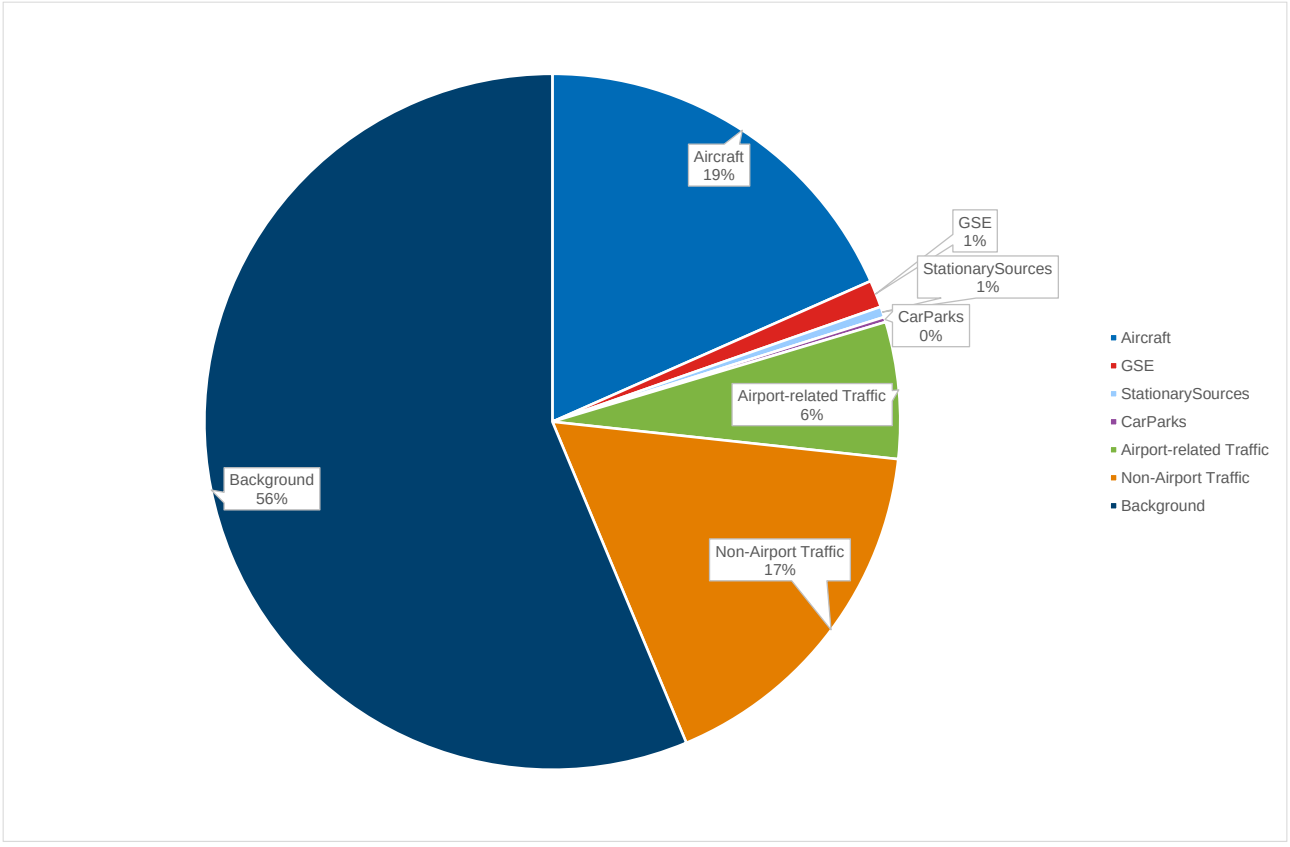

Figure 23 Source apportionment of annual mean NO_x concentrations at Harmondsworth

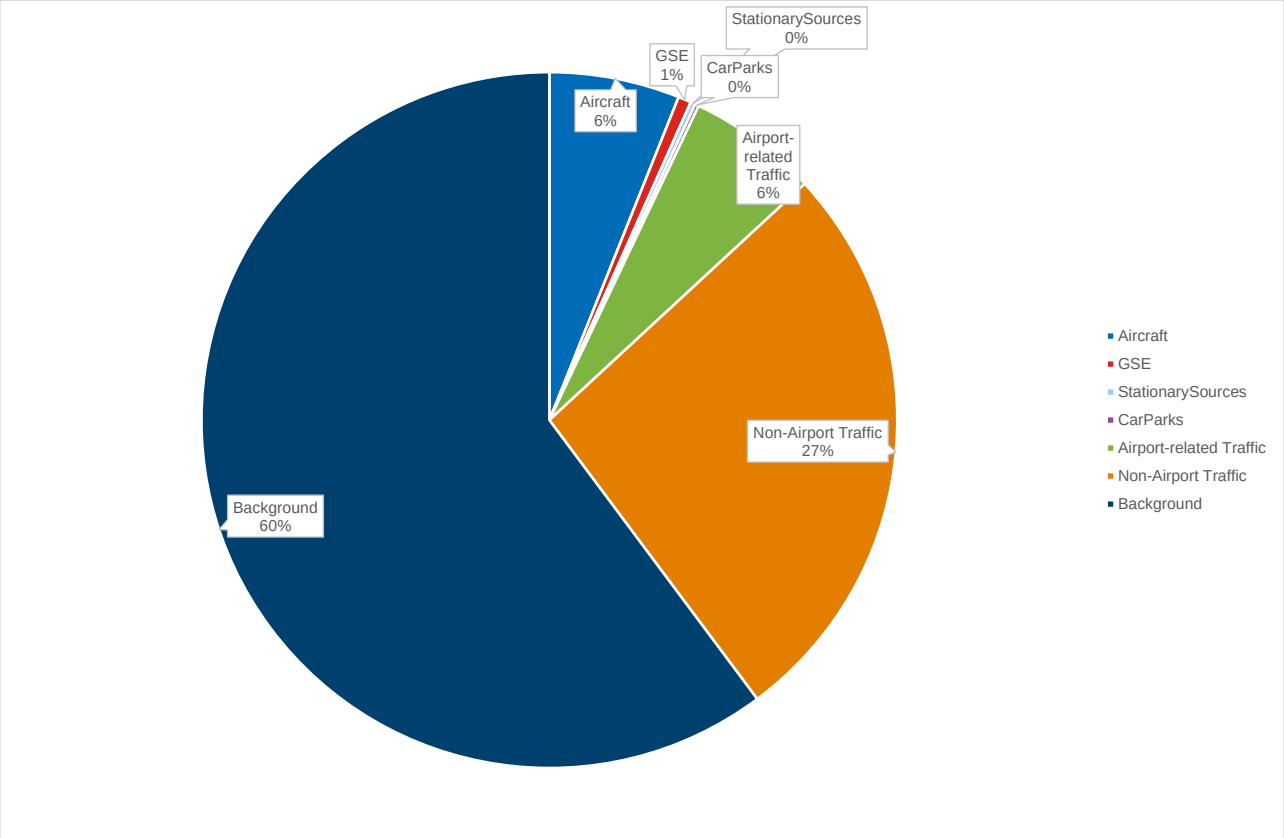

Figure 24 Source apportionment of annual mean NO_x concentrations at Hayes

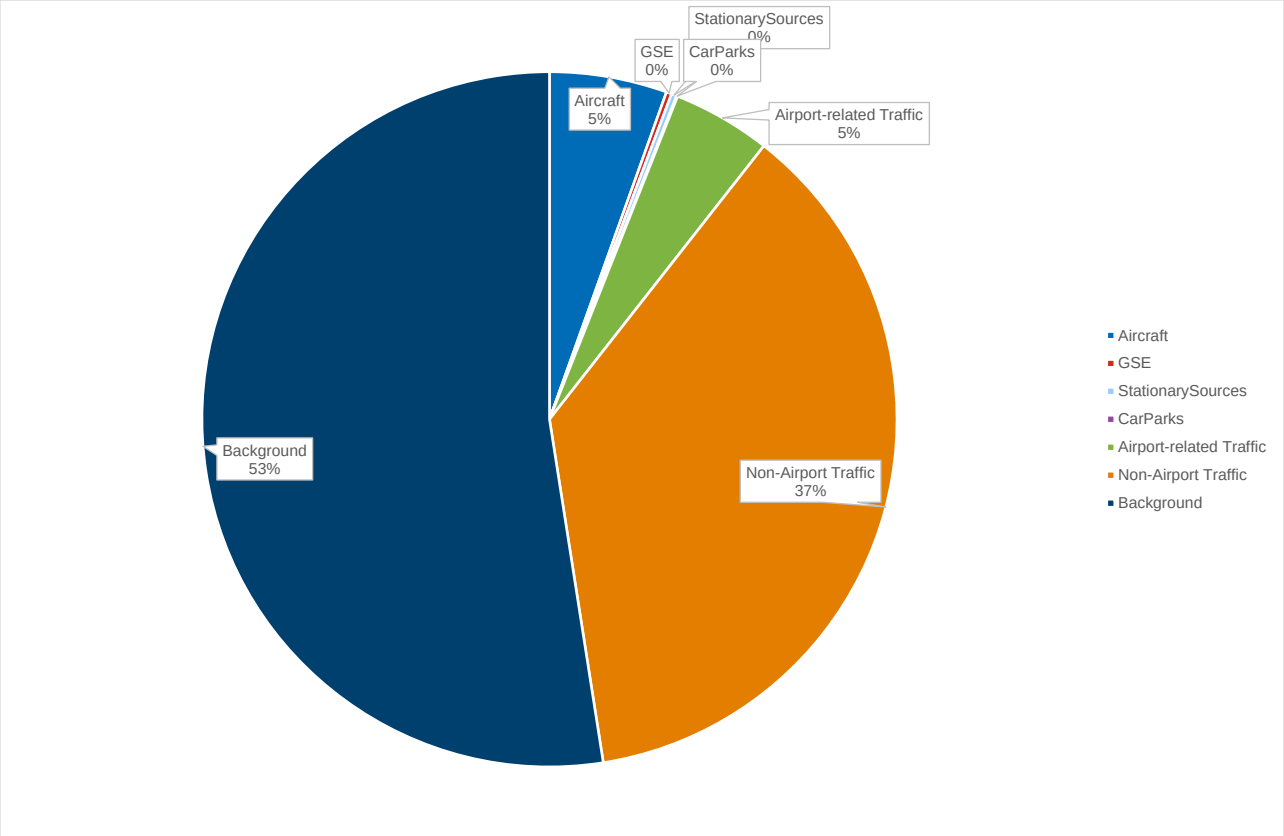

Figure 25 Source apportionment of annual mean NO_x concentrations at Oxford Avenue

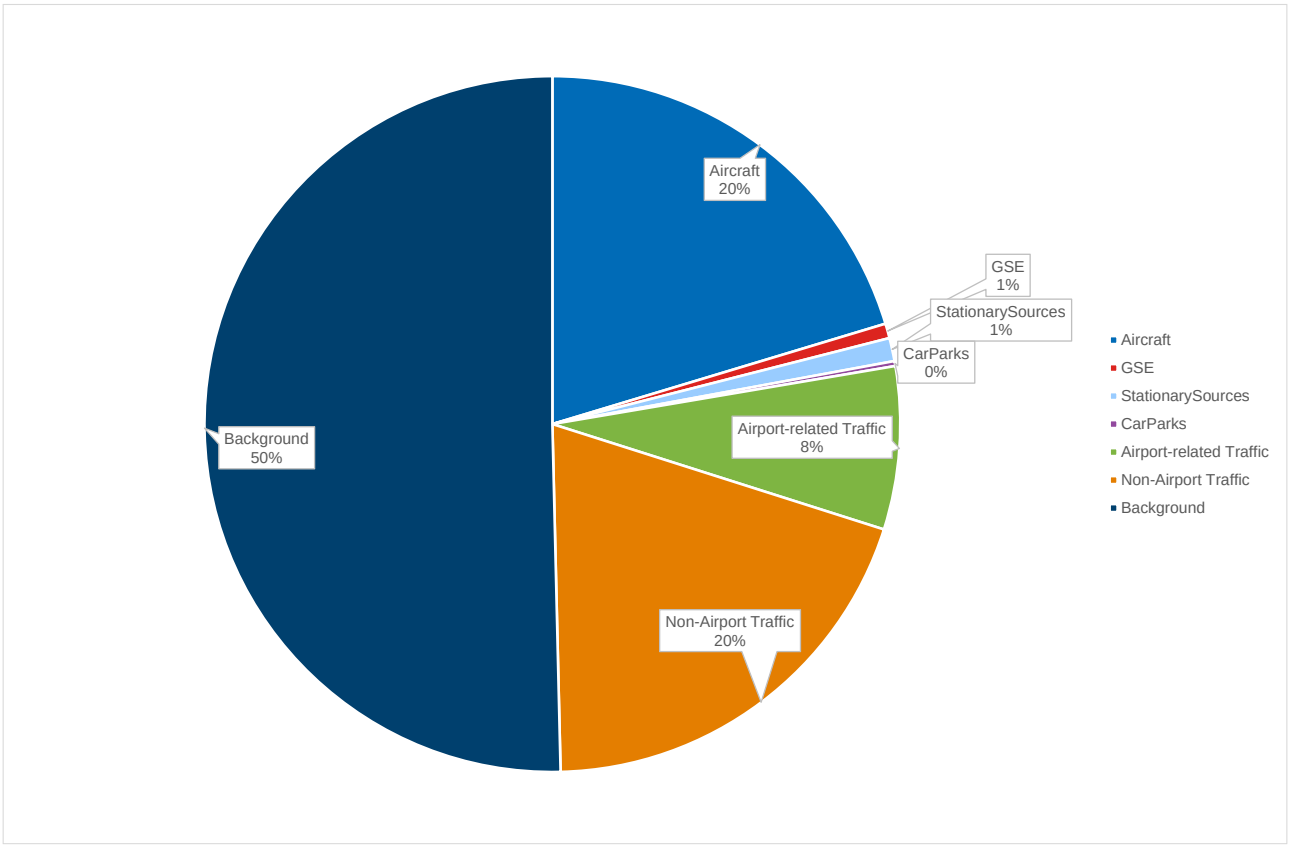

Figure 26 Source apportionment of annual mean NO_x concentrations at Sipson

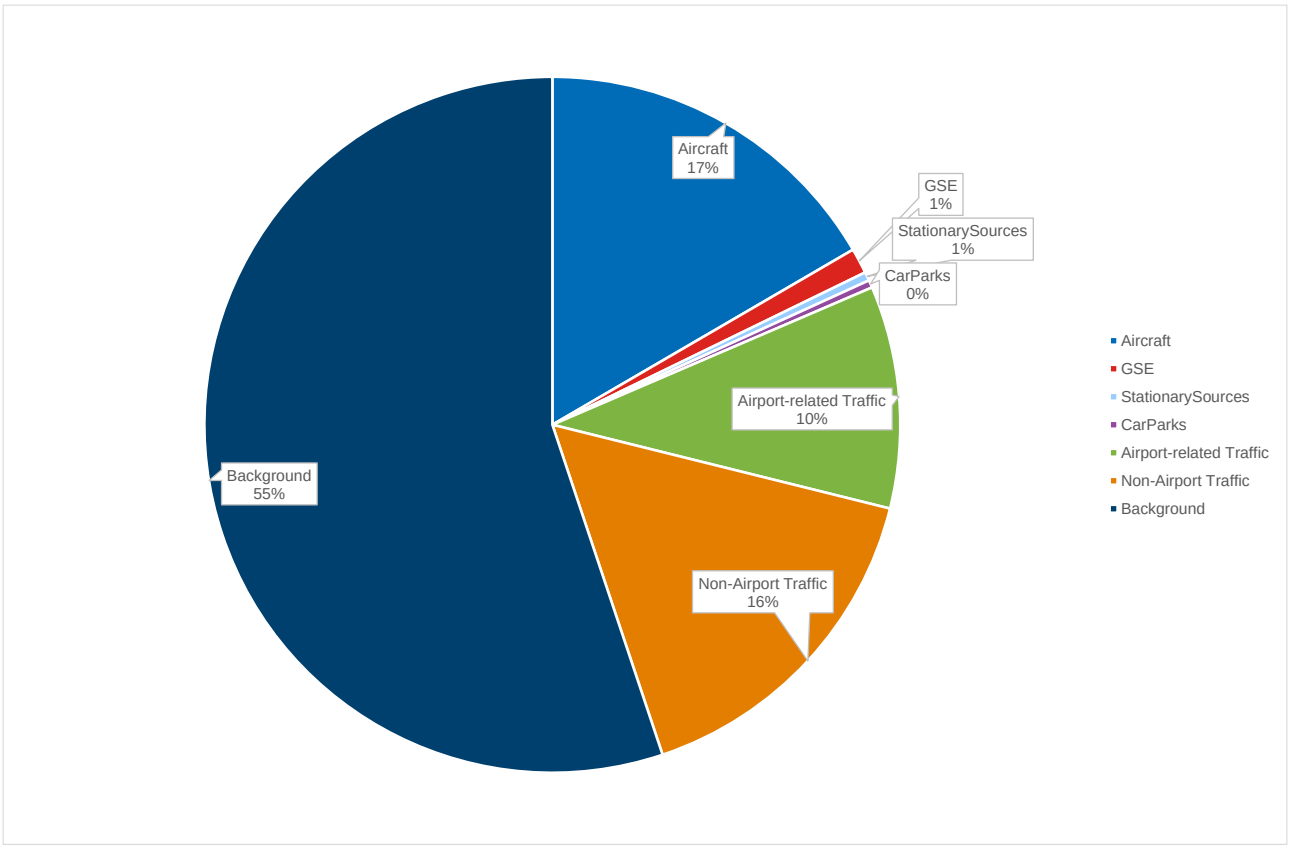

Figure 27 Source apportionment of annual mean NO_x concentrations at Cranford

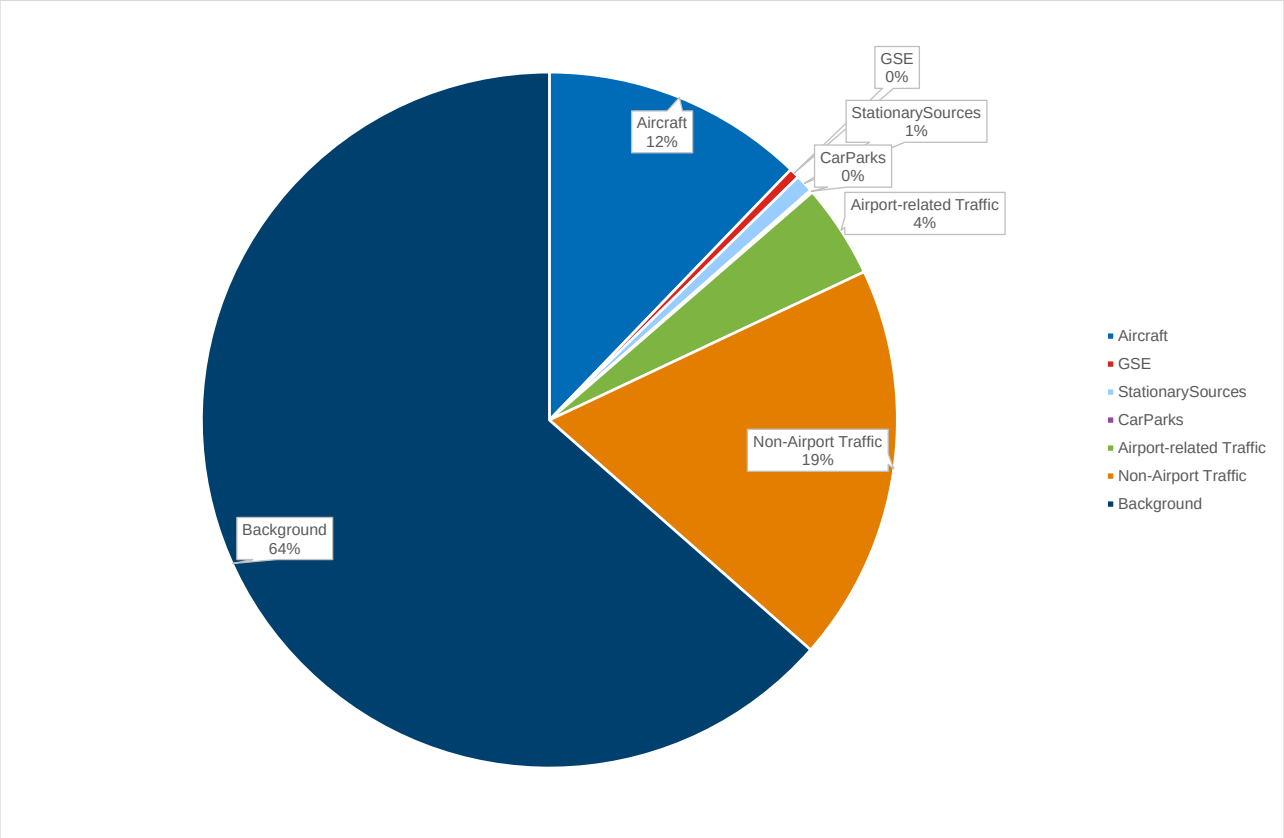

Figure 28 Source apportionment of annual mean NO_x concentrations at Feltham

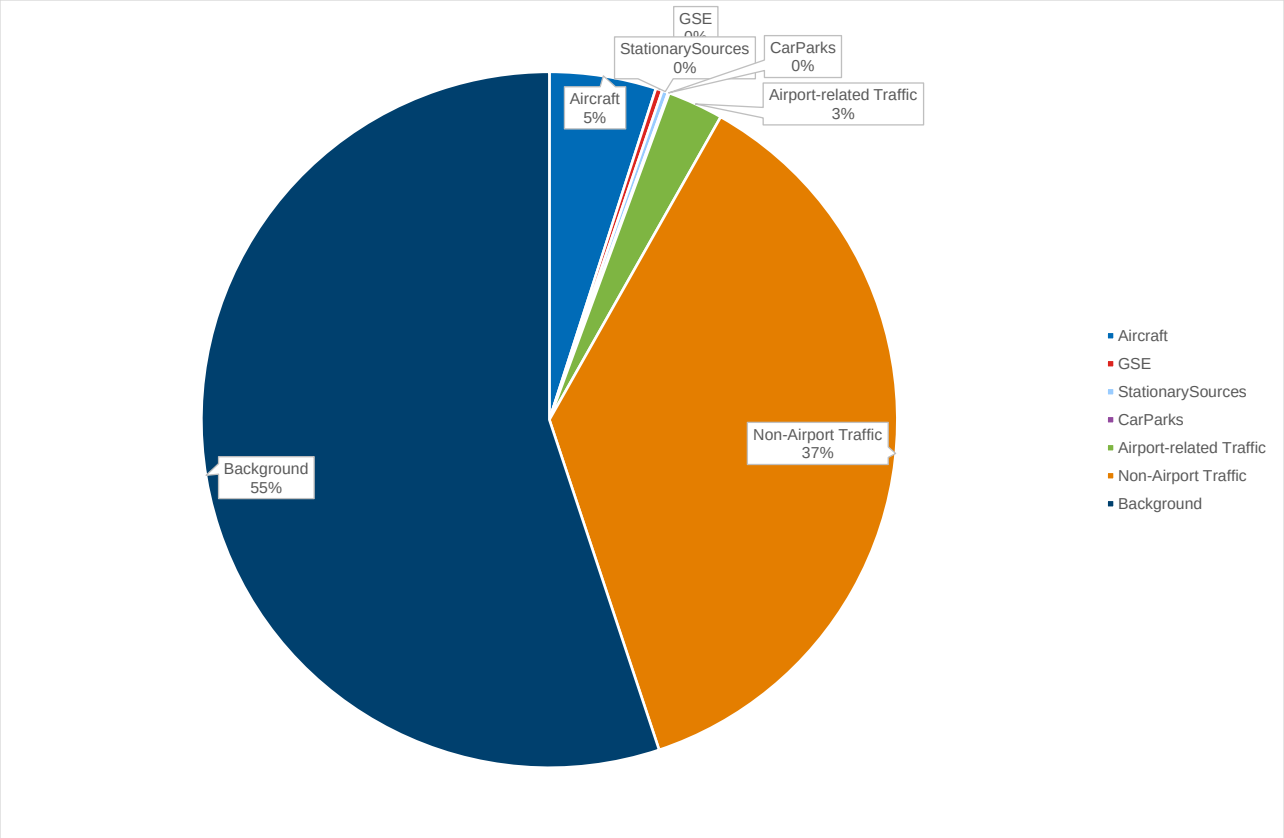

Figure 29 Source apportionment of annual mean NO_x concentrations at Hatton Cross

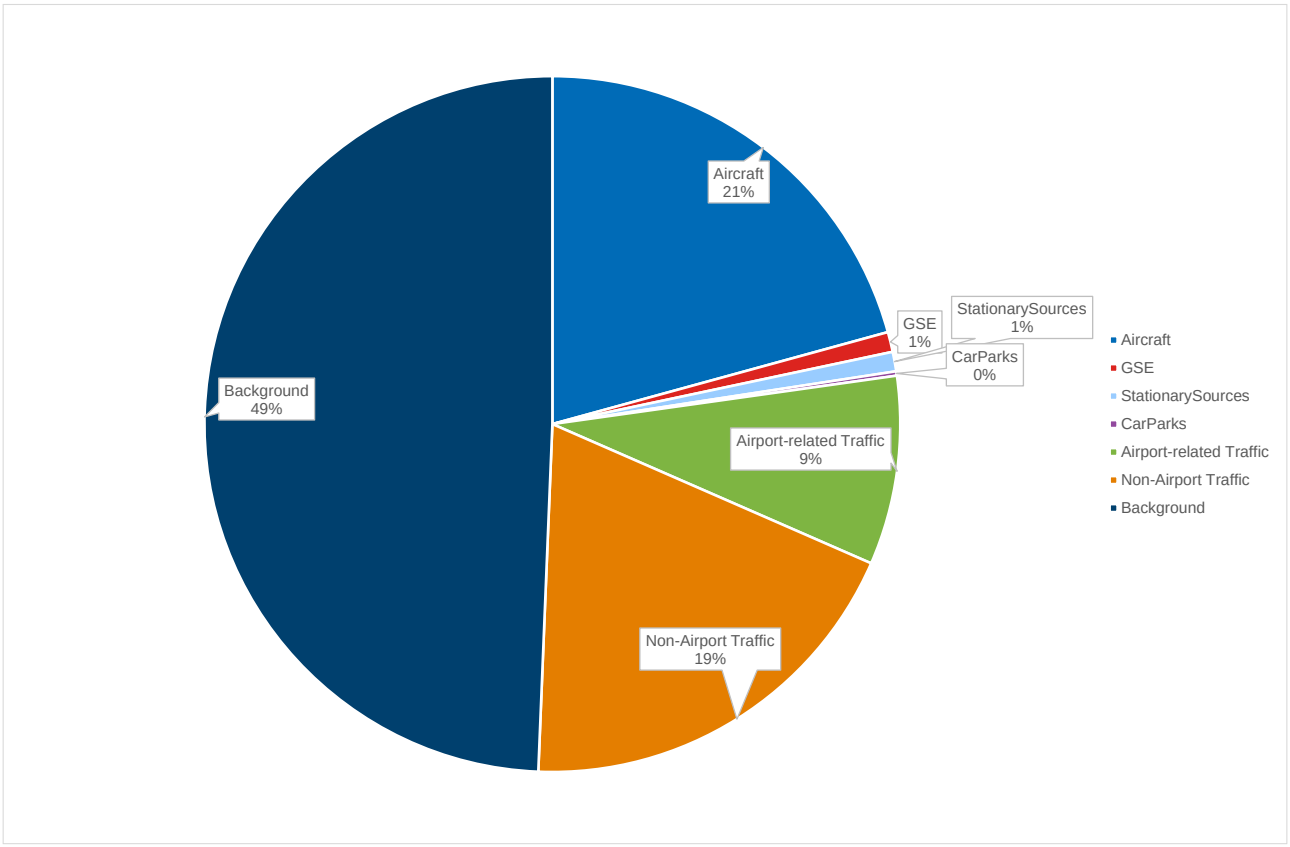

Figure 30 Source apportionment of annual mean NO_x concentrations at Harlington

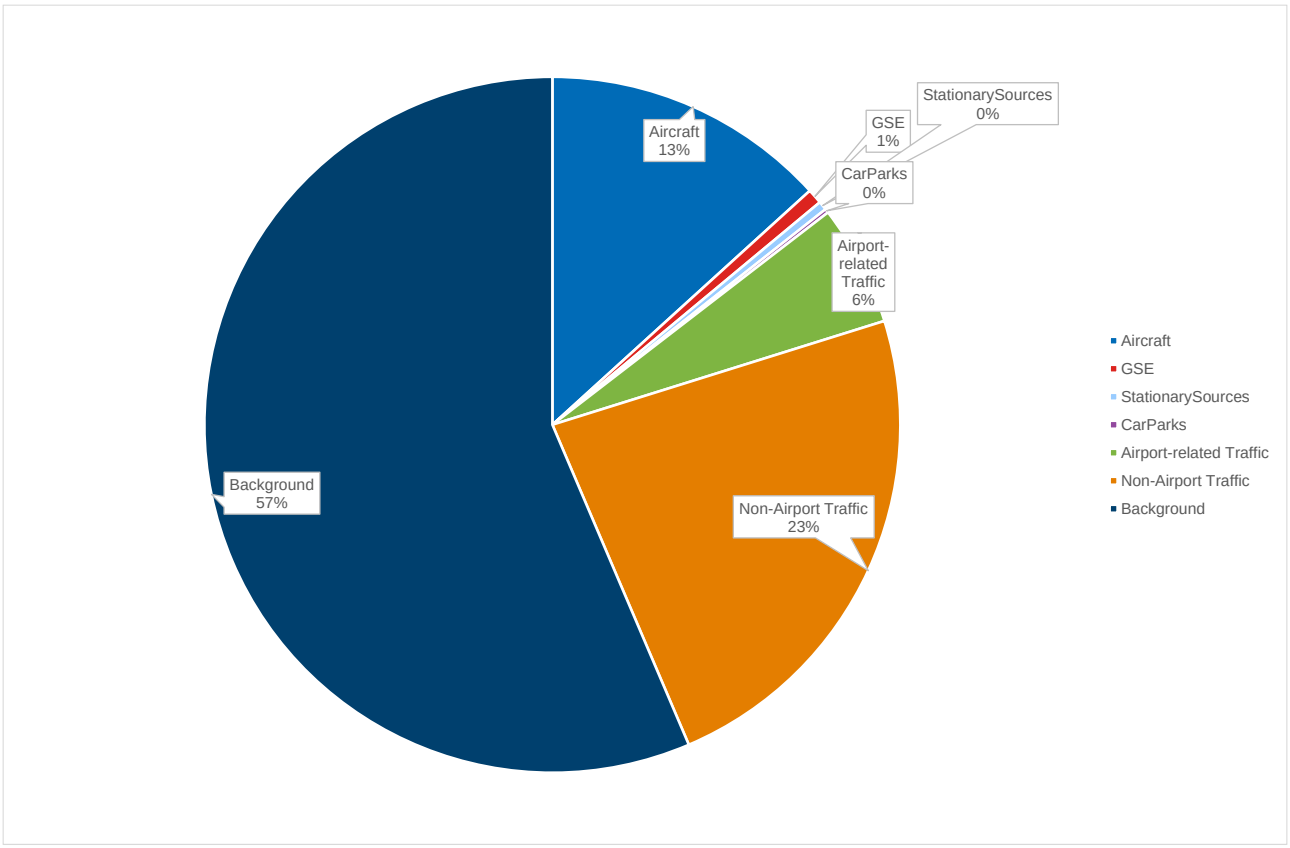

Figure 31 Source apportionment of annual mean NO_x concentrations at Hillingdon

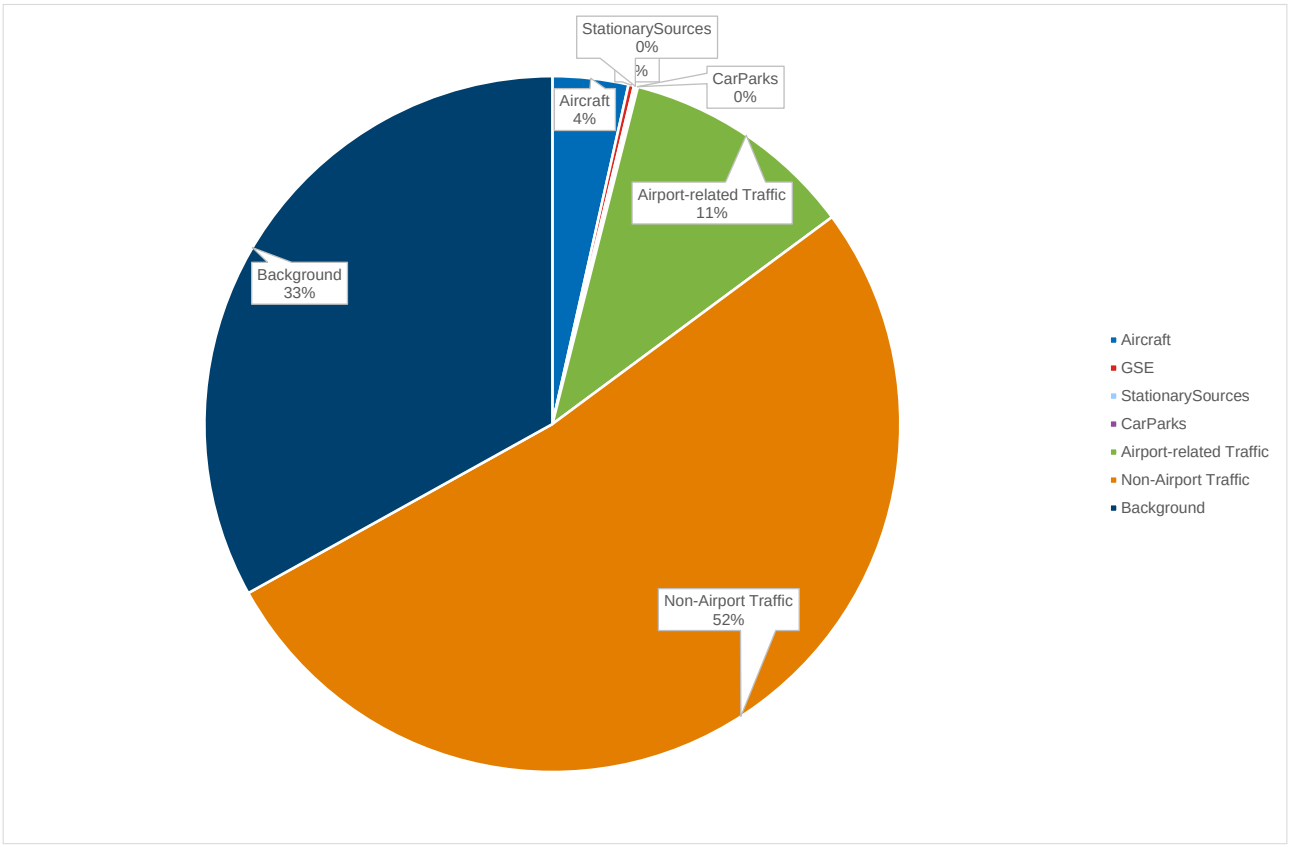

Figure 32 Source apportionment of annual mean NO_x concentrations at Lakeside 2

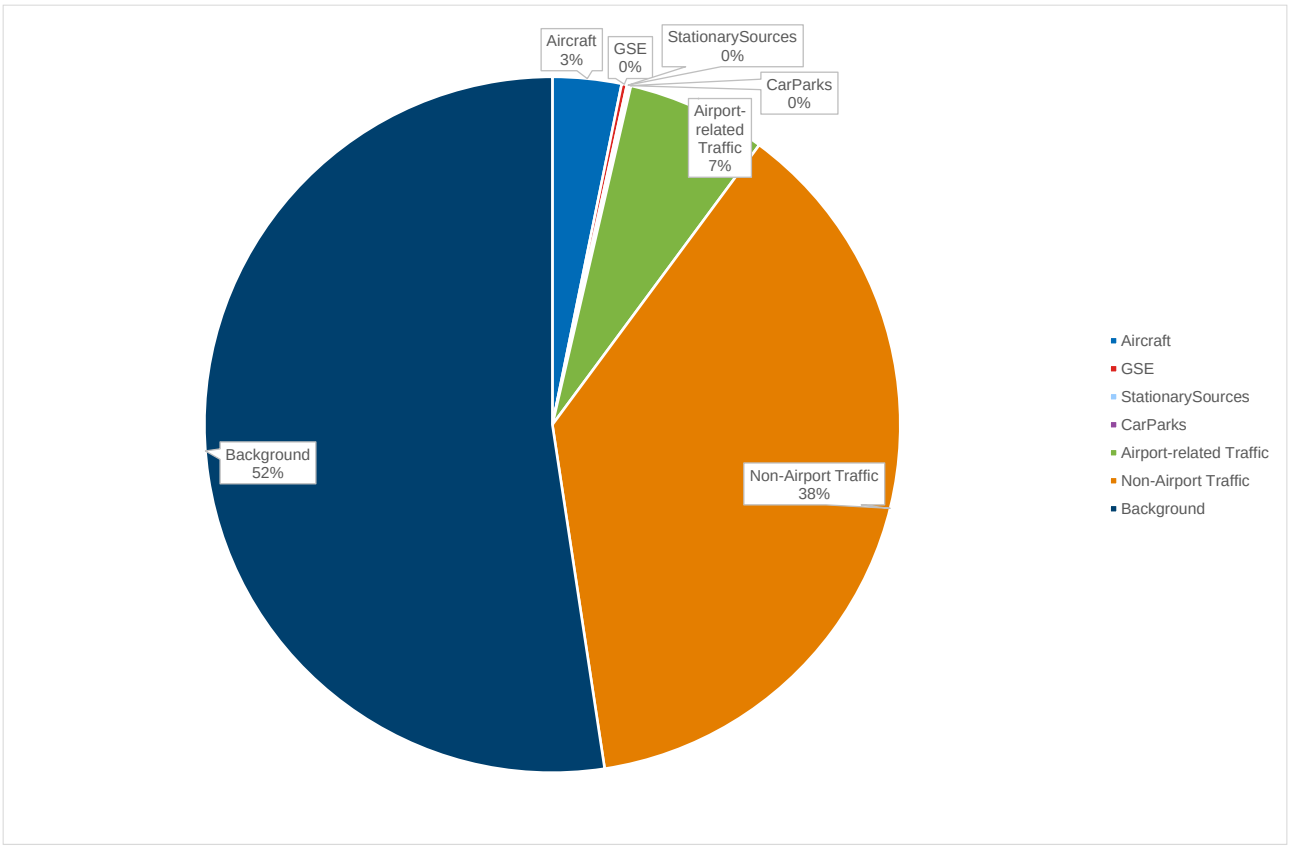

Table 24 presents a summary of modelled and measured PM_{10} and $PM_{2.5}$ concentrations at the continuous monitoring sites.

Table 24 Comparison of modelled annual mean PM_{10} and $PM_{2.5}$ concentrations with measured values for continuous PM analysers

Receptor	Modelled PM_{10} ($\mu g\ m^{-3}$)	Measured PM_{10} ($\mu g\ m^{-3}$)	Modelled $PM_{2.5}$ ($\mu g\ m^{-3}$)	Measured $PM_{2.5}$ ($\mu g\ m^{-3}$)
Green Gates	19.0	13.0	12.8	8.4
LHR2	20.7	13.4	13.8	8.7
Oaks Road	19.0	14.9	13.0	9.5
Harmondsworth	19.3	15.0	12.9	n/a
Harmondsworth Osiris	19.3	14.5	12.9	5.3
Hayes	22.4	27.7	14.6	n/a
Oxford Avenue	20.1	23.5	13.4	n/a
Cranford	20.6	16.7	13.6	n/a
Feltham	21.2	19.6	14.0	n/a
Hatton Cross	20.1	19.6	13.6	n/a
Harlington	19.8	15.1	13.2	9.5
Colnbrook	19.8	16.4	13.3	n/a
Lakeside 1 Osiris	19.7	12.0	13.2	6.4
Lakeside 2	19.6	15.0	13.0	6.6

Figure 33 and Figure 34 show a comparison between modelled and measured concentrations for NO_x and NO_2 respectively and Figure 35 shows the comparison for PM. Having been suitably adjusted, modelled NO_x and NO_2 concentrations are overall in close agreement with monitoring data. On average PM_{10} agrees with monitoring data, but there is variation from site to site, while $PM_{2.5}$ is overpredicted at all locations where it is monitored.

Figure 33 Modelled versus measured NO_x concentrations.

Unadjusted

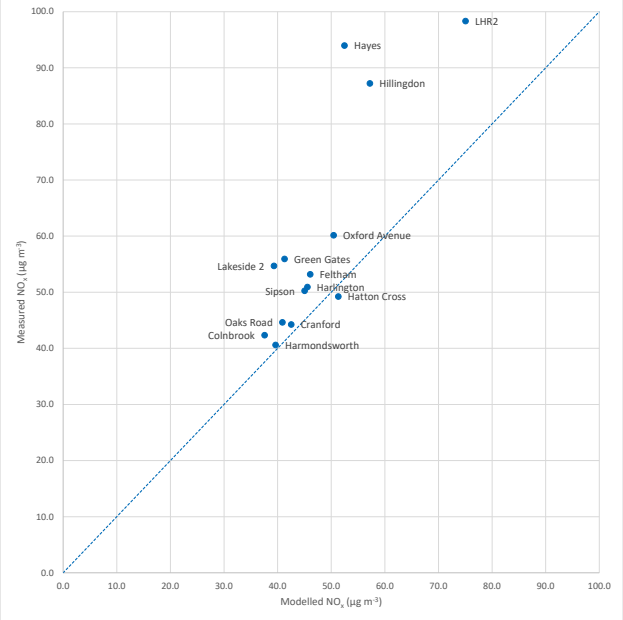

Adjusted

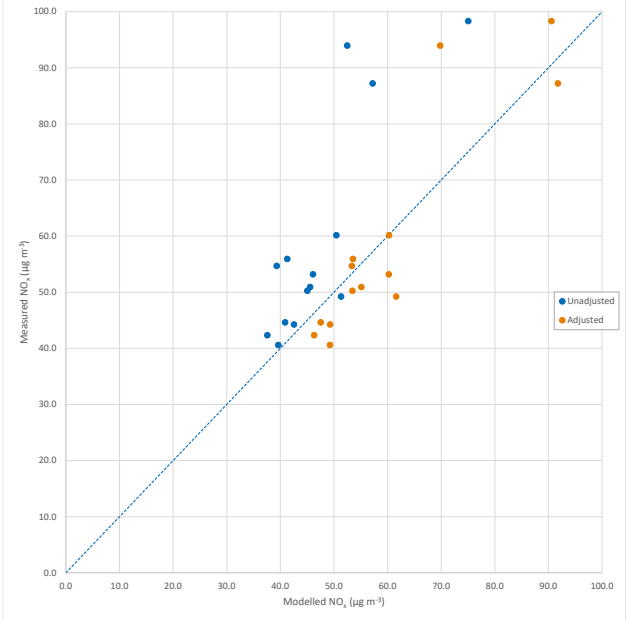

Figure 34 Modelled versus measured NO_2 concentrations.

Unadjusted

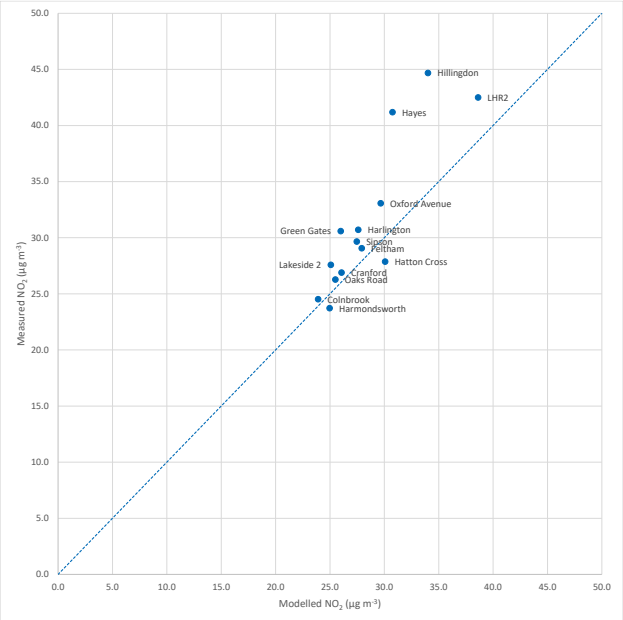

Adjusted

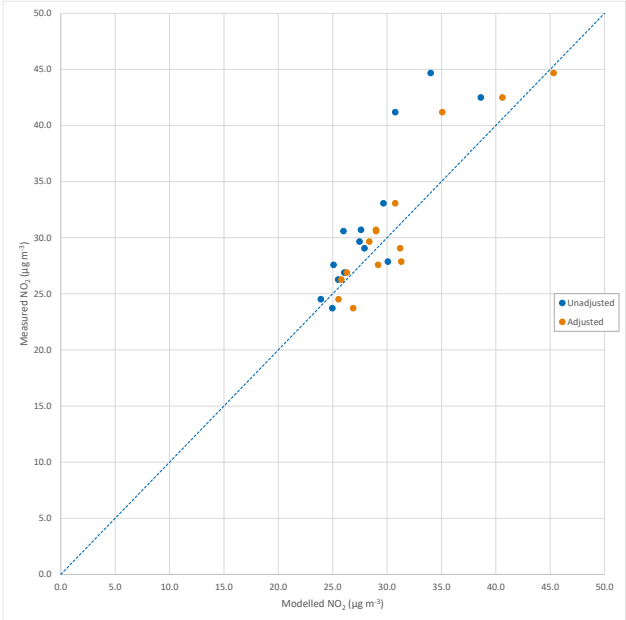

Figure 35 Modelled versus measured PM concentrations.

PM_{10}

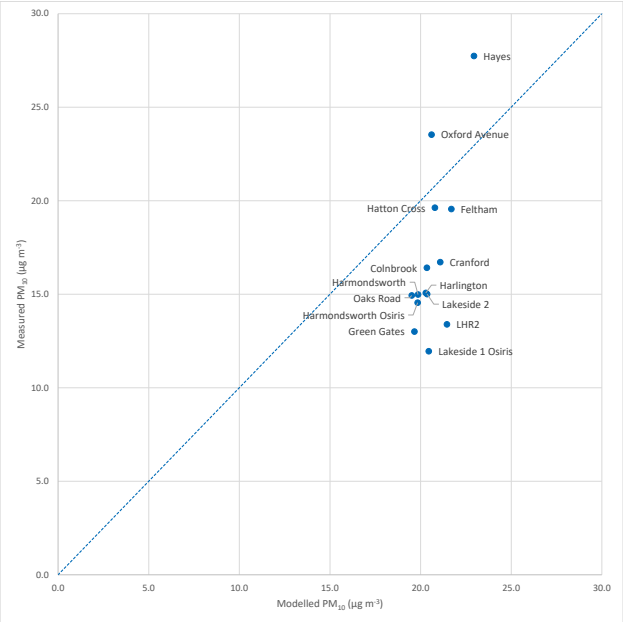

$PM_{2.5}$

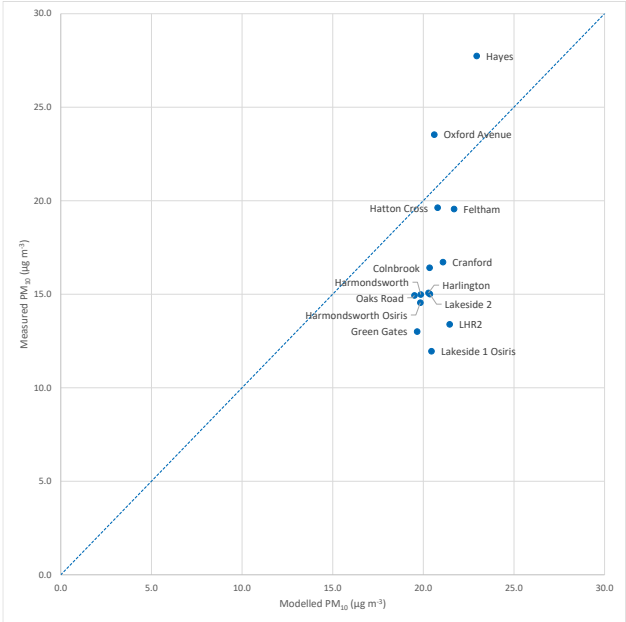

APPENDICES

Appendix 1 Model Evaluation

NO_x

TOTAL ANNUAL MEAN

The key aim in the model evaluation exercise is to assess how well the combined emission quantification and dispersion modelling methodologies can predict annual mean NO_x and NO_2 concentrations.

Table 25 compares the modelled annual mean NO_x concentrations at the continuous NO_x/NO_2 analysers with the measured values. It also gives the breakdown of the model total by source category. The average of the modelled values is 47.5 µg m^{-3}, whereas the average over the measurements is 59.0 µg m^{-3}.

It is judged more appropriate to discuss model–monitoring differences in terms of fractional discrepancies (*(modelled−measured)/measured*) rather than absolute discrepancies (*modelled−measured*), and the corresponding values are shown in Table 25. The average fractional discrepancy (also referred to below as the bias) is −16.3% (i.e., the model underestimates on average by 16.3% across the set of sites). The standard deviation of the fractional discrepancy is 13.8% (13 sites), which is a measure of the site-to-site variability in the measured values that has not been captured by the model. If the measurement uncertainty (one standard deviation) for long-period averages is around 5% (Section 4), this indicates that the observed bias is highly unlikely to be explained by statistical measurement fluctuations for a finite sample of 13 sites. Similarly, a large fraction of the site-to-site variability not explained by the model is unlikely to be attributable to measurement uncertainties.

For comparison, in the model evaluation carried out for the 2013 study, the modelled annual mean concentration averaged across monitoring sites was 62.0 µg m^{-3} compared to a measured average of 73.6 µg m^{-3}, a fractional discrepancy of only −13.5%.

Figure 36 presents a scatter plot of modelled versus measured annual mean values. The correlation coefficient for the two data sets (which measures the extent to which they are linearly related) is 0.69.

Table 25 Comparison of modelled annual mean NO_x concentrations with measured values for continuous NO_x/NO_2 analysers

Receptor name	Modelled annual mean NO_x concentration (µg m^{-3})							Measured NO_x (µg m^{-3})	Model bias (%)
	Aircraft	Background	Carparks	GSE	Roads	Stationary sources	Total		
Green Gates	4.0	28.2	0.2	0.5	8.2	0.1	41.3	55.9	-26.2
LHR2	32.0	30.8	0.4	0.9	10.4	0.5	75.0	98.3	-23.7
Oaks Road	8.7	26.7	0.1	0.6	4.5	0.2	40.9	44.6	-8.4
Harmondsworth	3.0	29.6	0.1	0.3	6.5	0.1	39.6	40.6	-2.5
Hayes	3.8	36.6	0.0	0.2	11.7	0.2	52.5	94.0	-44.2
Oxford Avenue	12.3	30.4	0.1	0.4	6.6	0.6	50.4	60.1	-16.2
Sipson	8.9	29.5	0.2	0.6	5.7	0.2	45.0	50.3	-10.4
Cranford	6.0	31.3	0.1	0.2	4.5	0.4	42.5	44.3	-3.9
Feltham	3.0	33.2	0.0	0.2	9.5	0.2	46.1	53.2	-13.4
Hatton Cross	12.8	30.4	0.1	0.6	6.9	0.6	51.3	49.2	4.3
Harlington	7.3	31.1	0.1	0.4	6.4	0.2	45.5	50.9	-10.6
Hillingdon	3.2	30.3	0.1	0.2	23.2	0.1	57.2	87.2	-34.4
Colnbrook	1.8	29.7	0.0	0.1	5.9	0.1	37.6	42.3	-11.3
Lakeside 2	1.7	28.0	0.0	0.1	9.4	0.1	39.3	54.7	-28.1

Figure 36 Scatter plot of modelled versus measured annual mean NO_x concentration (also shows the 1:1 line)

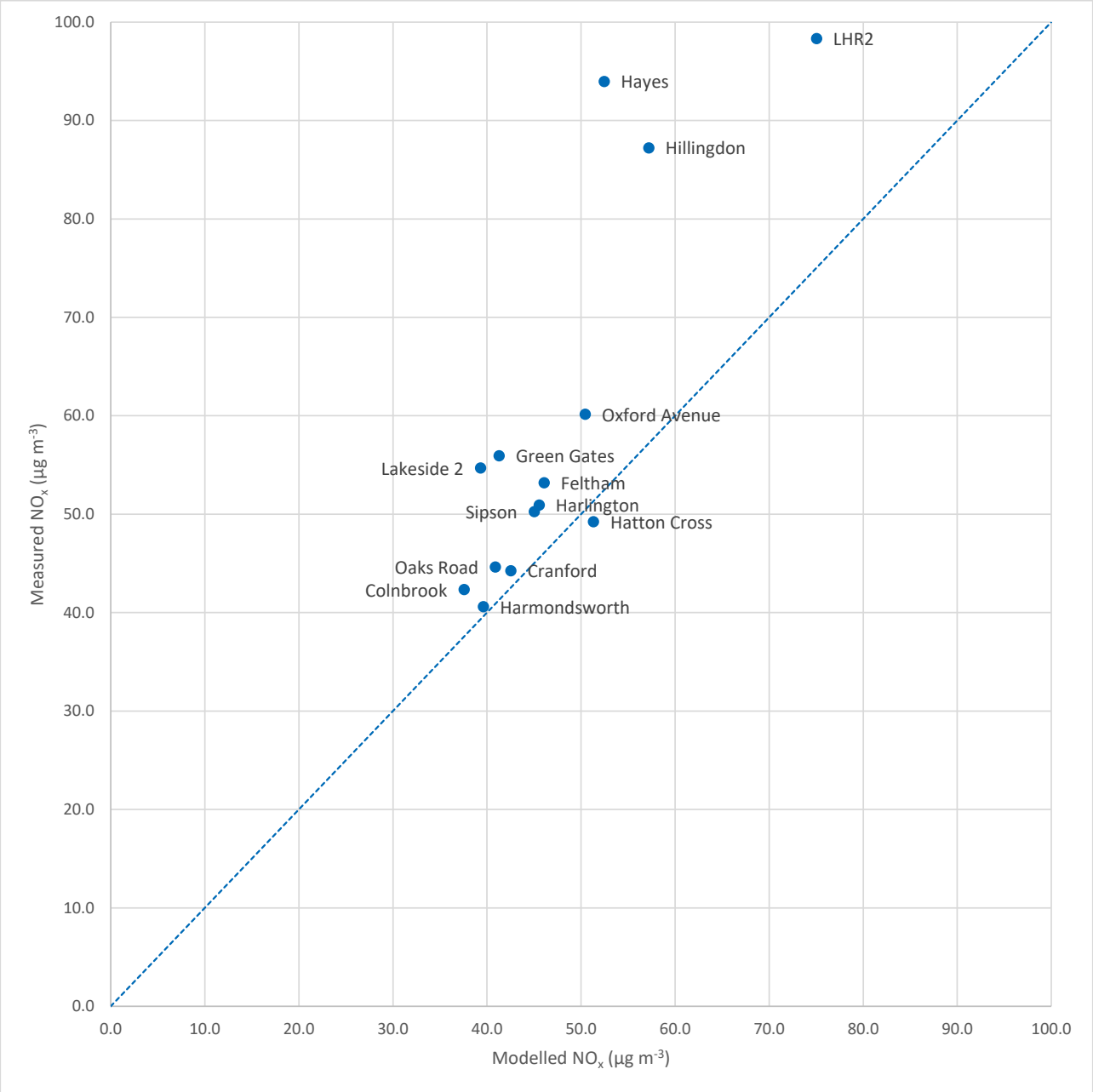

For the three sites with the highest total contribution from airfield sources, LHR2, Hatton Cross and Oxford Avenue, the fractional discrepancy is −23.7%, 4.3% and −16.2% respectively. For the three sites with the largest road-network contribution, Hillingdon, Hayes and LHR2, the fractional discrepancy is −34.4%, −44.2% and −23.7% respectively, suggesting that there is a greater systematic underestimation of the road-network contribution. This highlights the importance of evaluating the model separately for the various source contributions, given that the balance between contributions may change in the future. This is the objective of the more detailed analysis described below.

Table 25 shows that all sites have a major combined contribution from the background (NAEI area sources, large point sources and the rural background), which is fairly constant across the set of sites, so inaccuracies in this contribution could act to partly offset inaccuracy in the contributions from airfield and road-network sources. Again, this emphasises the importance of evaluating the performance of the modelling of airfield and road vehicle sources separately from that of the background contributions.

The availability of monitoring results from the Oaks Road site, upwind of the airport along the principal south-westerly wind direction, presents the opportunity to isolate the contribution from airfield sources by taking

concentration differences between a monitor north of the airport and Oaks Road, focusing on wind directions that point to and from the two sites. A similar type of analysis was carried out 2013 model evaluation[3]. In taking concentration differences, the assumption is made that the rural background contribution does not have a significant concentration gradient between the two monitors. Similar difference analyses can enhance the evaluation of the road-network contribution at near-road sites.

The dispersion modelling results were obtained separately for each hour of the period, allowing average concentration differences to be calculated for selected ranges of wind direction (and wind speed). It is important to bear in mind when comparing concentration *differences* that the under/overestimation of the difference may have a contribution from the over/underestimation of the concentration being subtracted. Thus, there is benefit in using 'clear' differences, i.e., in situations where the sources of interest have a much larger contribution at one site than at the other.

The 1 km spatial resolution of the background area sources in the study area restricts the angular resolution of model results from these sources, which is a limitation for the squares within a few km of any given receptor location. However, the source categories represented in the area emissions (such as domestic and commercial combustion) are not highly focused spatially (and the emission densities are not large), so the limited spatial resolution is not likely to be a significant limitation (but it should be borne in mind in the angular comparisons presented below).

The measurement errors associated with concentration differences cannot be ignored. If the measurement biases of the analysers are uncorrelated, then the error in the (absolute) difference is greater than the error in the value at each site (taken to be around 5%). However, if the sites belong to the same network or are operated to the same QA/QC procedures it is expected that there will be some correlation between the systematic errors at each site. It is judged unlikely that the uncertainty in annual mean differences for the sites around Heathrow will be less than 2 µg m^{-3} or higher than 5 µg m^{-3} (at 1 standard deviation), although these estimates have not been based on any specific data or analysis.

EVALUATION OF THE MODELLING FOR AIRFIELD SOURCES

In is useful to consider key sources such as the airport and roads separately. This section deals with airfield sources, while the following section deals with road traffic sources.

Table 26 shows wind directions and data related to the particular wind directions for pairs of sites. The modelled and measured concentrations are the difference between the two concentrations from the two sites. Further detailed analysis of each pair of receptors is discussed in the following sections.

Considering only those sites paired with Oaks Road for southerly wind directions only, the values of the contribution to annual mean concentration difference for sectors dominated by airfield sources range over an order of magnitude across six sites north of the airfield (from 2.3 µg m^{-3} to 32.3 µg m^{-3}), and the average (absolute) discrepancy between modelled and measured values at the six sites is only −0.0 µg m^{-3}, with a standard deviation of 0.5 µg m^{-3}. Expressed in fractional terms, the mean fractional discrepancy is +5% (overestimation), with a standard deviation of 13.4%. This level of discrepancy is comparable to the uncertainties in concentration difference measurements, so provides no evidence that the modelling for airfield sources either overestimates or underestimates significantly.

Considering sites paired with Hatton Cross, the average (absolute) discrepancy between modelled and measured values at the six sites is -2.4 µg m^{-3}, with a standard deviation of 1.7 µg m^{-3}. Again, this level of discrepancy is comparable to the uncertainties in concentration difference measurements, so provides no evidence that the modelling for airfield sources either overestimates or underestimates significantly.

Table 26 Comparison of modelled and measured contributions to the annual mean difference in NO_x concentration between pairs of analysers, for sector ranges chosen to highlight the airfield source contribution.

(a) Southerly wind sectors

Site difference	Sector range[1]	Modelled NO_x (µg m^{-3})	Measured NO_x (µg m^{-3})	Discrepancy (µg m^{-3})	Model bias (%)
LHR2 - Oaks Road	170° - 270°	32.4	32.3	0.1	0.4
Sipson - Oaks Road	120° - 240°	10.3	10.2	0.1	0.7

Site difference	Sector range[1]	Modelled NO_x (µg m^{-3})	Measured NO_x (µg m^{-3})	Discrepancy (µg m^{-3})	Model bias (%)
Harlington - Oaks Road	160° - 240°	7.7	8.4	-0.7	-8.8
Harmondsworth - Oaks Road	110° - 190°	2.9	2.3	0.6	25.9
Green Gates - Oaks Road	100° - 180°	3.7	3.3	0.5	14.3
Oxford Avenue - Oaks Road	200° - 260°	13.7	14.0	-0.2	-1.6
LHR2 - Hatton Cross	170° - 270°	27.0	32.6	-5.5	-17.0
Sipson - Hatton Cross	120° - 240°	9.4	11.8	-2.4	-20.6
Harlington - Hatton Cross	160° - 240°	7.0	9.3	-2.3	-24.5
Harmondsworth - Hatton Cross	110° - 190°	2.6	3.3	-0.7	-21.9
Green Gates - Hatton Cross	100° - 180°	3.4	4.7	-1.3	-27.2
Oxford Avenue - Hatton Cross	200° - 260°	11.5	14.4	-2.9	-20.3

(b) Northerly wind sectors

Site difference	Sector range[1]	Modelled NO_x (µg m^{-3})	Measured NO_x (µg m^{-3})	Discrepancy (µg m^{-3})	Model bias (%)
Oaks Road - Harlington	330° - 90°	5.6	6.1	-0.5	-7.7
Oaks Road - Harmondsworth	330° - 90°	7.8	10.3	-2.5	-24.3
Oaks Road - Sipson	330° - 90°	7.0	7.0	0.0	0.0

[1] Angle is the direction from which the wind blows, clockwise from north; sector ranges are inclusive.

LHR2–Oaks Road

LHR2 is only 180 m from the centreline of the northern runway (27R), so receives a major contribution from runway sources, offering the potential for a good test of the 'moving-jet' module in ADMS-Airport (see the 2008/9 modelling methodology report[28]). In addition, there are no major sources immediately upwind of Oaks Road for the range of angles over which the wind blows airfield sources towards LHR2, so the difference is 'clear'.

A form of presentation of the concentration differences that has proved useful in other similar analyses is to plot the mean concentration as a function of wind direction (i.e., with all hours of the period sorted by 10° wind sector and the concentration then averaged over the hours for a given sector), which will be termed a '**concentration difference rose**'. This is displayed as a 'radar' plot in Figure 37, in which the angle in the plot corresponds to wind sector and the radial distance is the mean concentration for the sector[29]. This figure shows good agreement in the modelled and measured differences in the angular range 120° to 270°, when the wind blows from the airport towards LHR2. However, the model substantially underestimates the concentration difference when the wind blows from the north-east quadrant. In fact, for this quadrant, it predicts higher concentrations at Oaks Road than at LHR2, whereas the monitoring data suggests the opposite.

[28] Underwood B Y, Walker C T and Peirce M J (2010) Air Quality Modelling for Heathrow Airport 2008/9: methodology. AEAT/ENV/R/2915.

[29] It is important to note that in this form of presentation the concentration for a given wind sector has not been weighted by the relative probability that the wind blows in that sector. This avoids making the comparisons for sectors with low frequency difficult to read. However, it is important to recognise that discrepancies in some angular ranges have much less impact on the period-mean than in others. Table 26, on the other hand, includes the frequency weighting, as do the figures showing contribution as a function of wind speed.

Figure 37 The average difference in NO_x concentration (µg m^{-3}) between LHR2 and Oaks Road as a function of wind direction

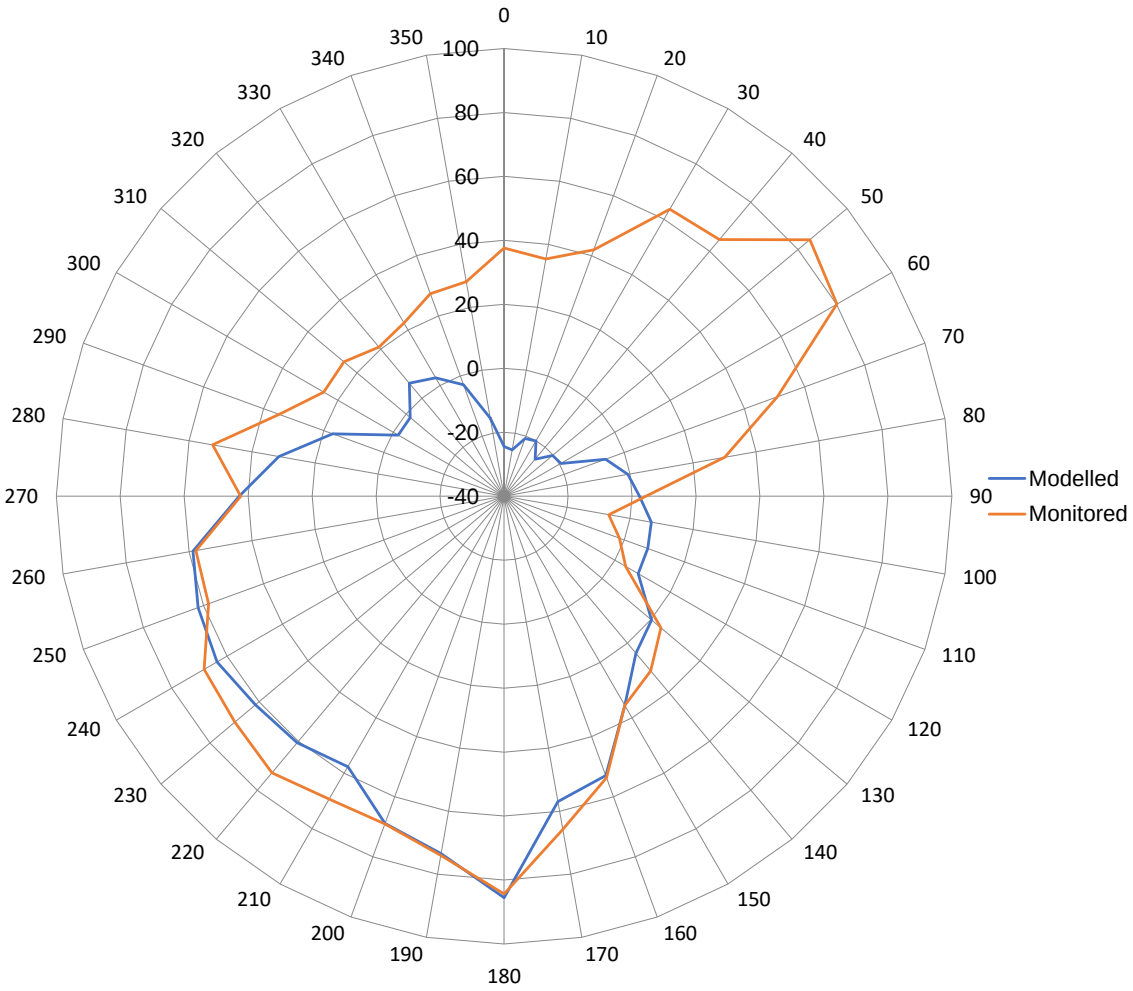

For angles in approximately the 120°–180° range, LHR2 'sees' emissions from the start of take-off roll on the nearby runway 27R. Although in general this runway is not used when the wind is in these directions, the westerly preference means there are a small number of departures picked up in this way, and in fact take-off roll is the largest non-background contributor at LHR2 in these wind directions.

For angles above about 180°, LHR2 'sees' emissions from a major part of the take-off roll on runway 27R and from other parts of the airfield including the Central Terminal Area (CTA), Terminal 5 (T5) aprons and runway 27L (although the contribution from these sources is significantly smaller than that from 27R). Thus, the good agreement persists over a major part of the spatial distribution of airfield sources.

A particular feature of Figure 37 is the peak in the monitoring difference for northeast winds that is not reflected in the model difference, this is thought to be related to road traffic and is discussed more in the following section.

The comparison for LHR2–Oaks Road differences can now be made quantitative, by evaluating the contribution to the total annual mean concentration difference from wind directions that give a significant airfield contribution at LHR2, choosing sectors 170° to 270° inclusive; this range of angles is marked on Figure 38. Although sectors 120° to 160° also point from the runway to LHR2, as mentioned above aircraft generally depart on the southern runway (09R) for this range of angles, so the contribution to annual mean concentrations is small. The LHR2–Oaks Road entry in Table 26 gives the modelled and measured contributions from the selected sectors to the annual mean concentration difference, showing a discrepancy of only −0.6% (negative, so the model is underestimating) on a contribution of around 32.3 µg m^{-3}.

Figure 38 The 170° to 270° sector range as seen from LHR2 and Oaks Road

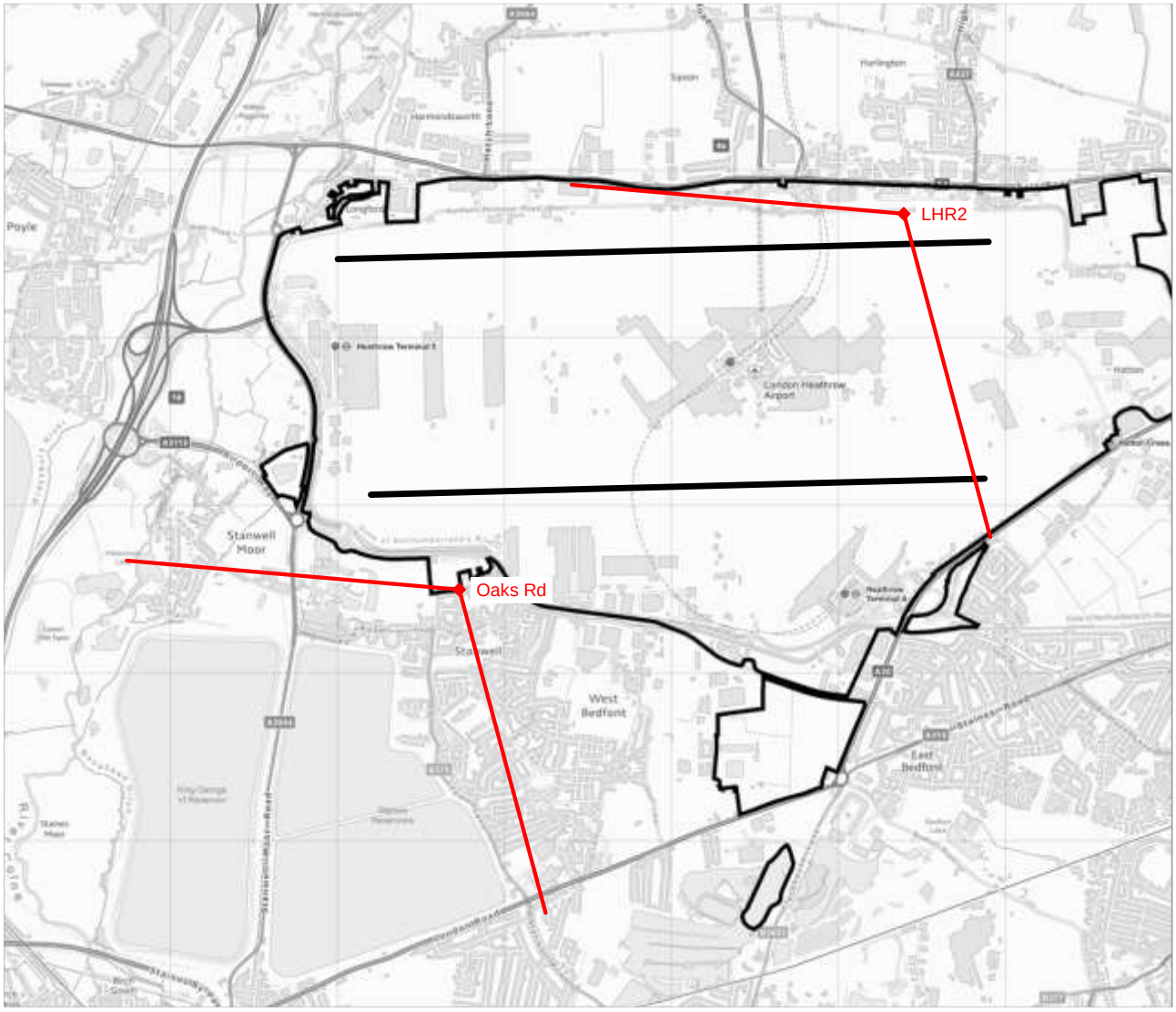

Table 27 shows the breakdown by source category of the modelled contribution to the annual mean NO_x concentration difference in the 170° to 270° range. The airfield sources account for 95% of the total model difference and clearly, aircraft sources dominate the airfield contribution.

Table 27 Breakdown by source category of the contribution to the annual mean LHR2–Oaks Road NO_x concentration difference from wind direction sectors 170° to 270° inclusive

Site	Aircraft	Background	Carparks	GSE	Roads	Stationary Sources	Total	Monitored
LHR2	29.5	5.5	0.2	0.9	1.9	0.2	38.2	45.8
Oaks Rd	0.0	4.3	0.0	0.0	1.4	0.0	5.7	11.8
Difference	29.5	1.2	0.2	0.9	0.4	0.2	32.4	32.3

A further level of evaluation can be carried out by investigating how the concentration contribution from the selected angular range is distributed as a function of wind speed. For this purpose, the hours for which the wind direction lies in the chosen range are partitioned amongst a set of wind speed categories separated by

around 0.5 m/s[30], with averages then taken for each category; the mean concentration for a given category is multiplied by the fraction of all hours in the year for which the wind lies in the given speed category (and angle range) to generate the contribution to the total annual mean concentration difference from the category.

The resulting set of values are shown in Figure 39, which will be termed a '**contribution/wind speed**' plot. The figure demonstrates a good level of agreement across all wind speed ranges.

Figure 39 LHR2–Oaks Road concentration difference contribution from wind sectors 170° to 270° inclusive as a function of wind speed

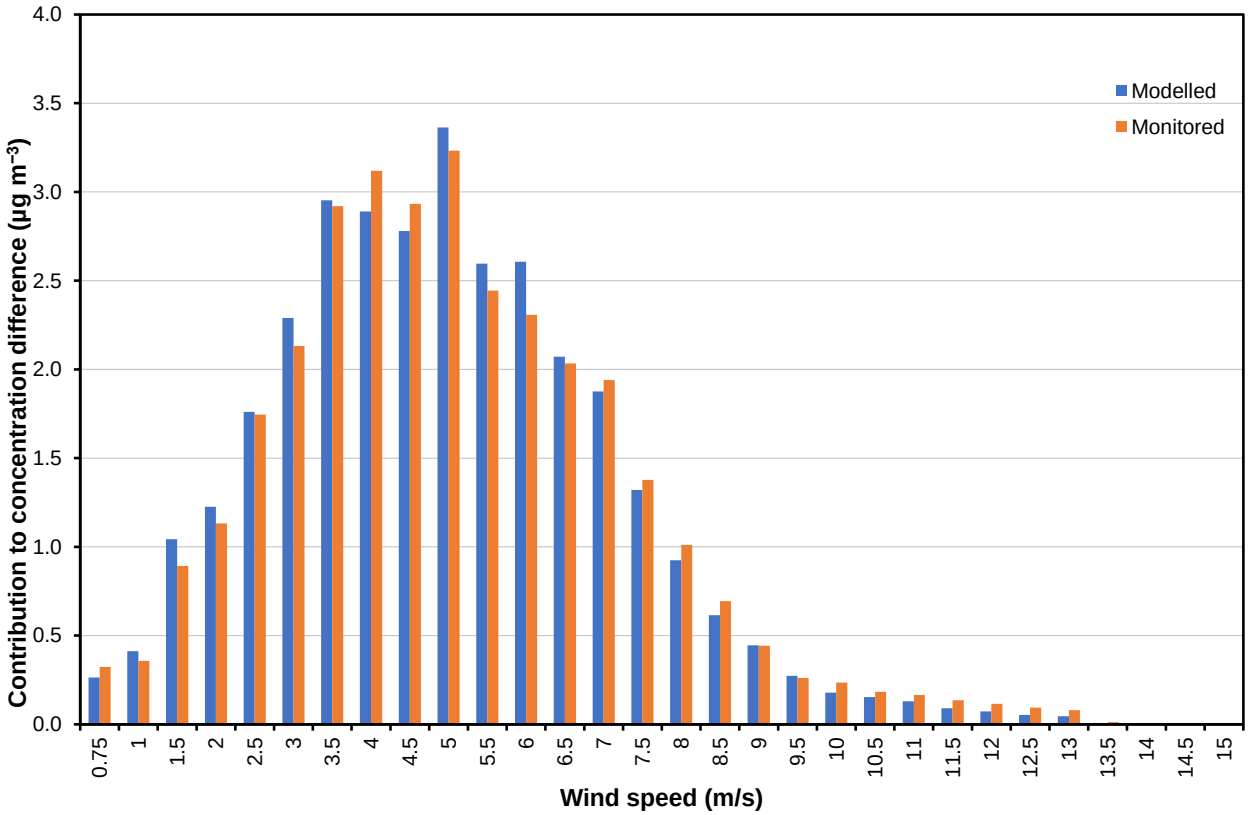

Figure 40 shows the difference in NO_x concentration between LHR2 and Oaks Road presented as a bi-variate polar plot (bi-polar plot for short). This presentation method is a visually appealing way of showing concentration differences jointly as a function of wind direction and wind speed. The plots are generated by assigning the hourly concentration differences to the set of joint wind sector and wind speed categories, then taking the average over the set of hours within each joint category.

[30] Wind speed in the meteorological data is given in terms of a discrete set of values, which are the m/s equivalent of a whole number of knots. In the analysis, hours with reported wind speed of zero or 0.5 m/s were assigned to a single bin with representative speed 0.75 m/s in line with the procedure in ADMS-Airport in which wind speeds of less than 0.75 m/s are set to 0.75 m/s, with the wind direction set to that in the previous hour (or the latest preceding hour with speed above 0.75 m/s).

Figure 40 Bi-polar plots for LHR2–Oaks Road

(a) Modelled

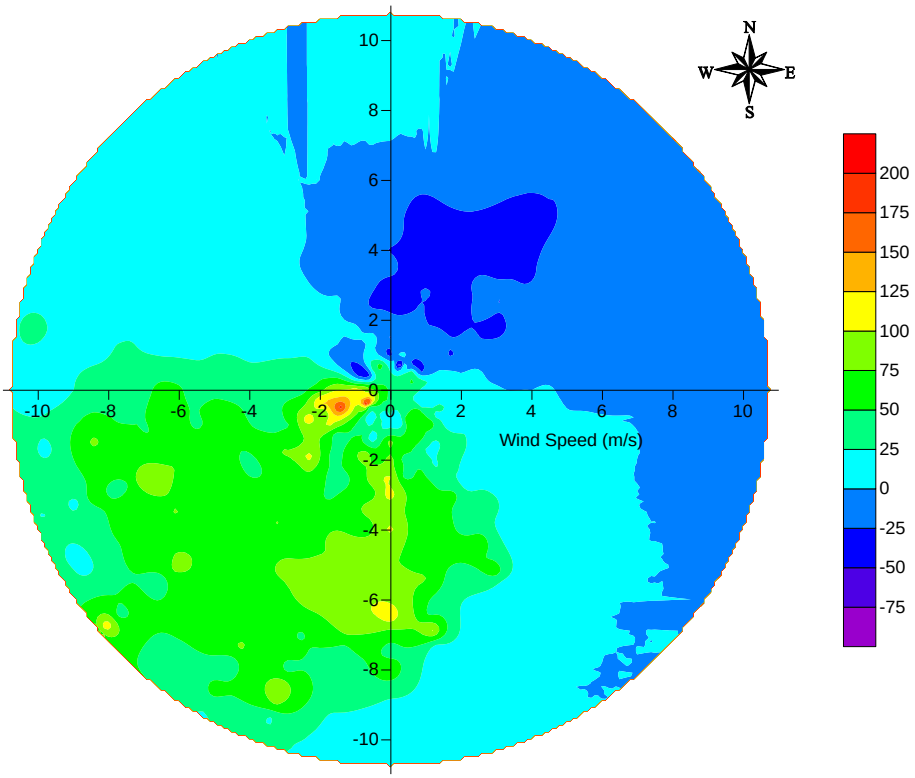

(b) Measured

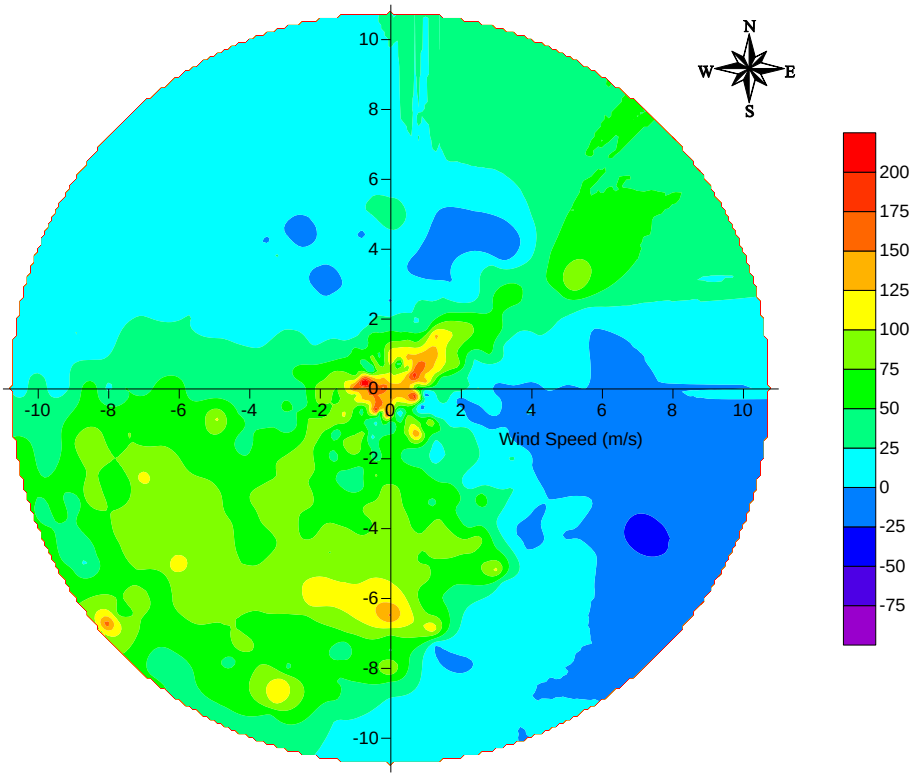

The set of average LHR2–Oaks Road concentration differences for the joint categories are then represented on a bi-polar plot in which the radial distance represents wind speed[31], the angle clockwise from the *y* (up-down) direction on the page represents wind angle (the direction from which the wind blows, clockwise from north) and the colour represents a concentration range. The plots have been smoothed to make the visual comparisons easier to comprehend[32]. Although the plots give a good visual impression of major features of the concentration distribution, it is important not to over-interpret them. Some of the joint categories contain few hours and the concentrations from them are therefore subject to greater sampling fluctuations. Under the action of the smoothing algorithm, concentration outliers may generate localised spatial features which, although visually striking, may simply reflect a sampling fluctuation. However, broad features of the plot reflect the results from many hours and are thus more reliable.

A key feature of both plots is that the concentration difference is large and positive for winds blowing from the SW quadrant, which point from airfield sources towards LHR2. Difference concentrations are above 50 µg m^{-3} across most of the quadrant, both in the measurement and the model results.

The relatively high concentration at high wind speeds is considered diagnostic of an elevated source, so in this instance reflects the influence of plume rise for hot engine exhaust plumes. However, the comparison in Figure 40 cannot be interpreted as showing that the plumes are elevated according to measurement but at ground-level according to modelling. Ground-level plumes generally lead to a rapid decline in concentration with increasing wind speed, whereas both monitoring and modelling plots show concentration remaining high up to the highest wind speeds. A contribution to the difference in the plots, nevertheless, may arise from inaccuracies in the modelling of plume rise, with an indication that the model gives too little plume rise at low wind speed and too much at high wind speed. Generally, the heights of rise are of order tens of metres, and even quite small differences in plume height can have a significant impact on ground-level concentrations.

Furthermore, there is a need for caution in interpreting the variation of concentration with wind speed as simply related to plume elevation: other factors may be at work. For example, emissions may not arise equally in all wind speeds (because of a difference in average wind speed for hours of the day with quite different emission rates) and the distribution of atmospheric ‘stability’ conditions (which affect the rate of dispersion) may not be the same at each wind speed. In addition, the influence of sampling fluctuations needs to be borne in mind for the highest wind speeds, which are relatively infrequent.

It is worth bearing in mind that the concentrations in the bi-polar plot are not weighted by the relative number of hours in the bin (i.e., those hours for which the analysis was undertaken), whereas high wind speeds are relatively infrequent. Thus, the contribution to annual mean concentrations from the highest wind speeds is relatively small, as shown in the difference/wind speed plot (Figure 39).

The discrepancy in the difference concentration for wind directions in the northeast quadrant is clearly visible in the bi-polar plot and will be discussed in the following section.

LHR2–Hatton Cross

The monitoring station at Hatton Cross, to the southeast of the airport, can also be used to evaluate the modelling of airfield sources in the same way as Oaks Road. Figure 41 shows the difference rose for LHR2-Hatton Cross.

[31] It is important to keep in mind when interpreting the plots that radial distance represents wind speed not spatial distance. All concentrations on a given plot relate to the specific locations of the monitoring sites.

[32] The smoothing is applied only for presentational purposes in this type of figure. All numerical analyses are carried out with un-smoothed data.

Figure 41 The average difference in NO_x concentration (µg m^{-3}) between LHR2 and Hatton Cross as a function of wind direction

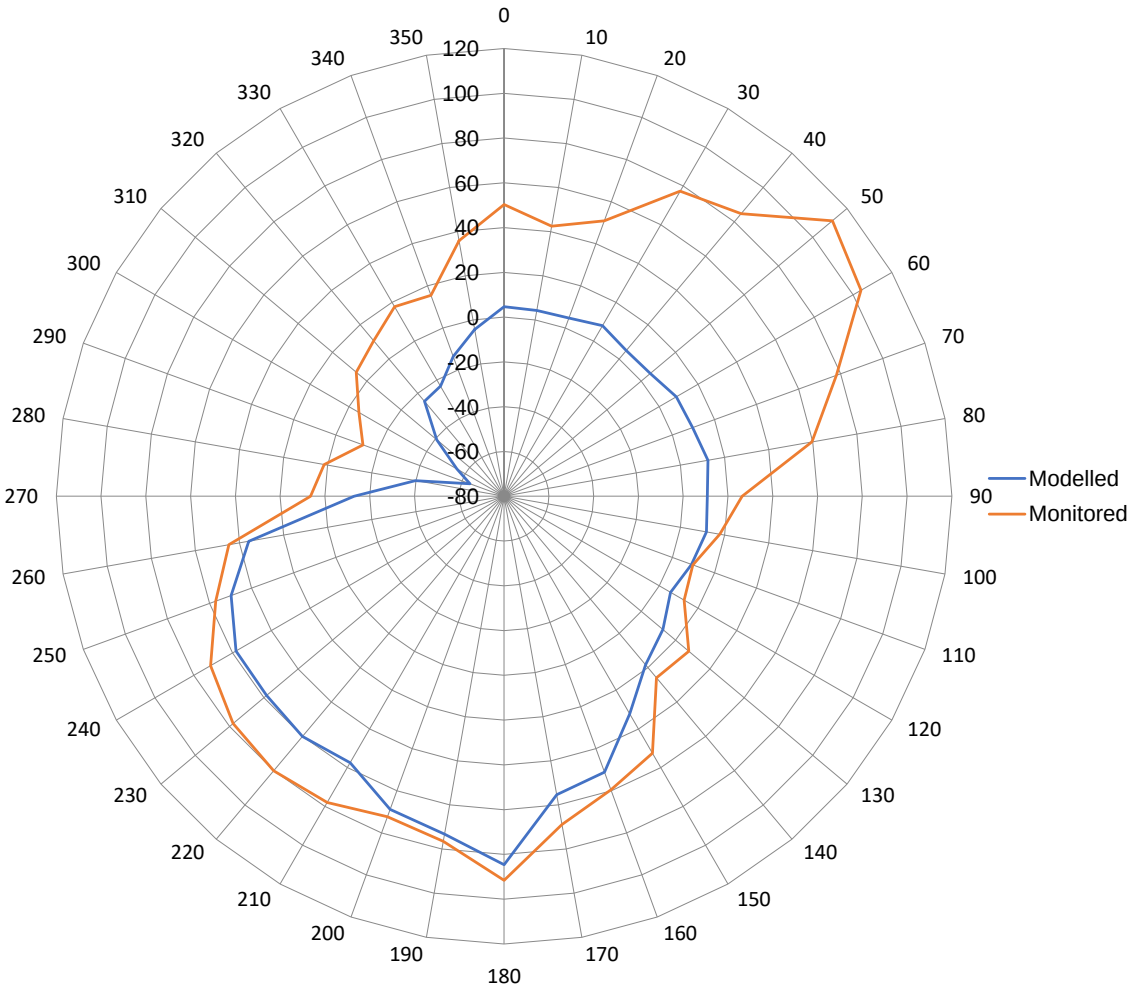

This shows a similar picture to the LHR2−Oaks Road comparison in Figure 39. The shape of the monitored difference is broadly similar. However, the discrepancy between modelled and monitored for northeast winds is less pronounced. This is thought to be related to road traffic and is discussed more in the following section.

Sipson–Oaks Road (Hatton Cross)

It is also possible to directly examine the model performance for airfield sources at receptor locations further than LHR2 from the runway.

Figure 42 shows the difference rose for Sipson–Oaks Road. Focusing first on wind directions pointing from airfield sources to the Sipson monitoring site (with sectors 120° to 240° inclusive accounting for most of the airfield contribution), the figure shows good agreement between model results and monitoring data across the range of sectors. The relevant entry in Table 26 compares the modelled and measured contribution to the annual mean concentration difference from this range of angles, confirming the good agreement, with the model value 0.3% higher than the measured value (i.e., a difference of <0.1 µg m^{-3}). Table 28 gives the breakdown by source category of the contribution from this angle range to the annual mean concentration difference, showing that aircraft account for 81% of the concentration difference according to the model.

Figure 42 The average difference in NO_x concentration (µg m^{-3}) between Sipson and Oaks Road as a function of wind direction

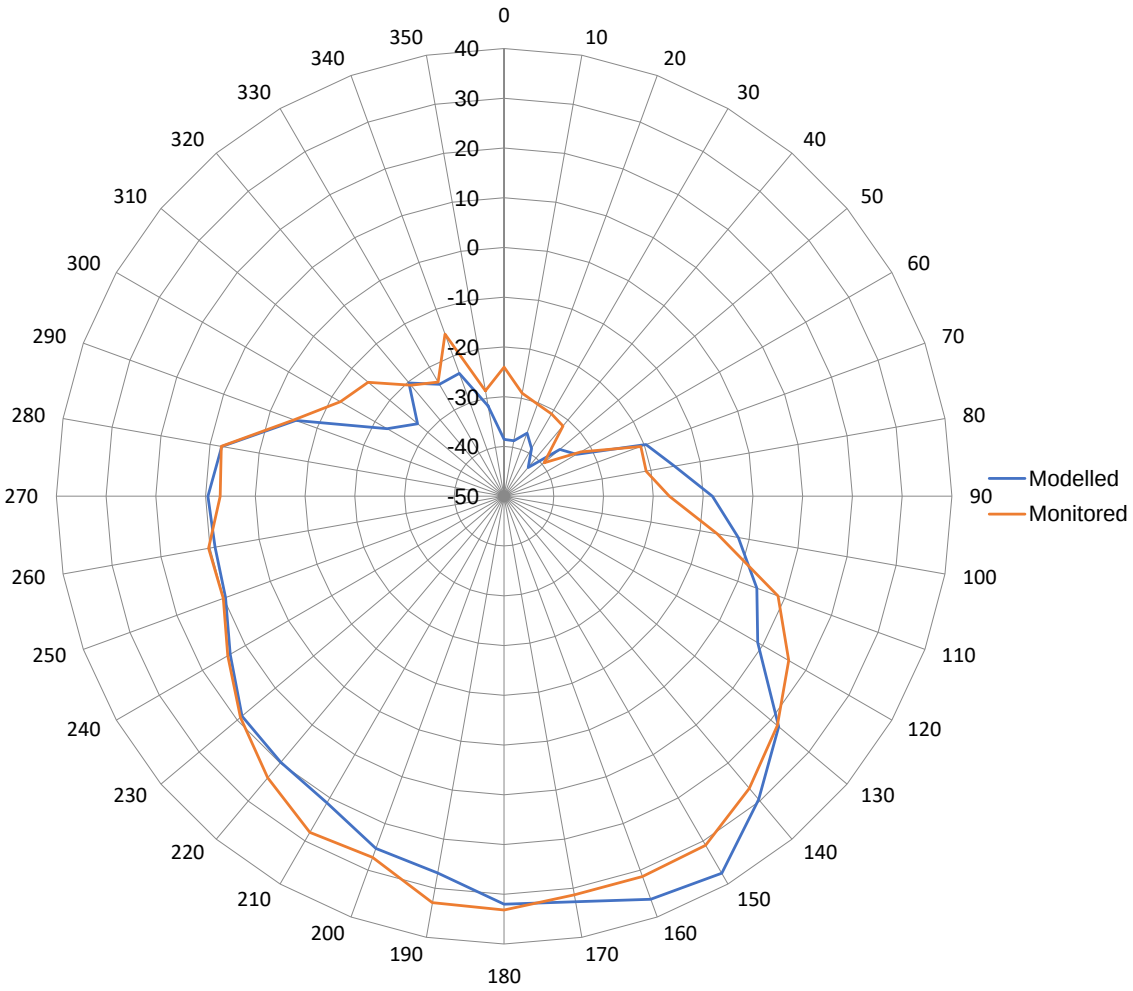

Table 28 Breakdown by source category of the contribution to the annual mean Sipson–Oaks Road NO_x concentration difference from wind direction sectors 120° to 240° inclusive

Site	Aircraft	Background	Carparks	GSE	Roads	Stationary Sources	Total	Monitored
Sipson	8.4	4.9	0.2	0.6	2.0	0.2	16.2	22.7
Oaks Rd	0.0	4.8	0.0	0.0	1.1	0.0	5.9	11.2
Difference	8.4	0.1	0.2	0.6	0.9	0.2	10.3	10.2

Figure 43 gives the contribution/wind speed plot for the sector range 120° to 240°. As was the case for LHR2-Oaks Road, the figure demonstrates a good level of agreement across all wind speed ranges.

Figure 43 Sipson–Oaks Road concentration difference contribution from wind sectors 120° to 240° inclusive as a function of wind speed

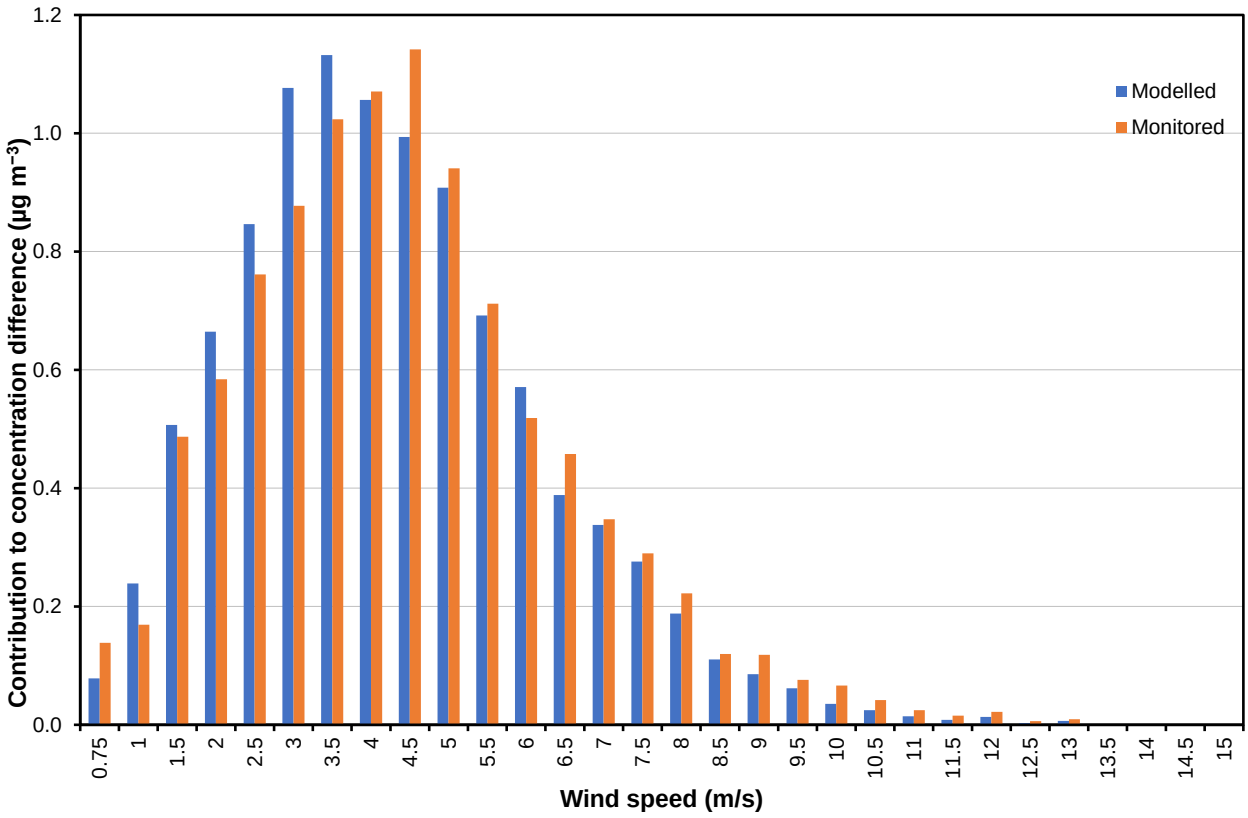

The bi-polar plots in Figure 44 are an alternative way of displaying the features discussed above. Focusing first on the areas of green, which represent a positive difference between Sipson and Oaks Road for winds blowing from the southern quadrant (i.e., from the airport). The model reproduces moderately well the measured concentration-difference magnitude, angular range, and distribution as a function of wind speed.

Figure 44 Bi-polar plots for Sipson–Oaks Road

(a) Modelled

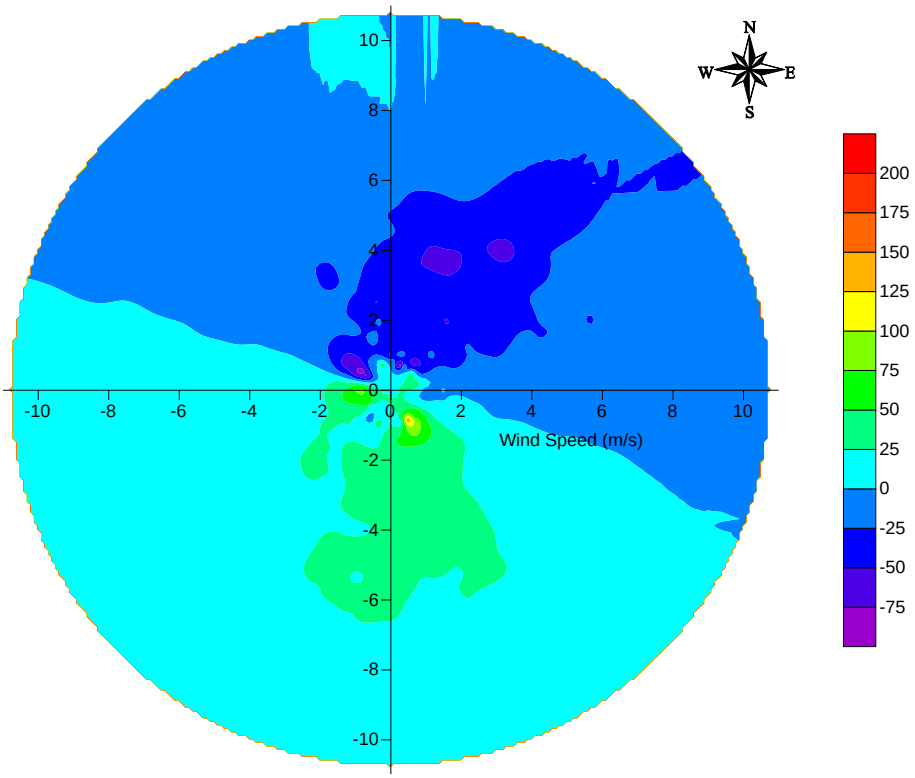

(b) Measured

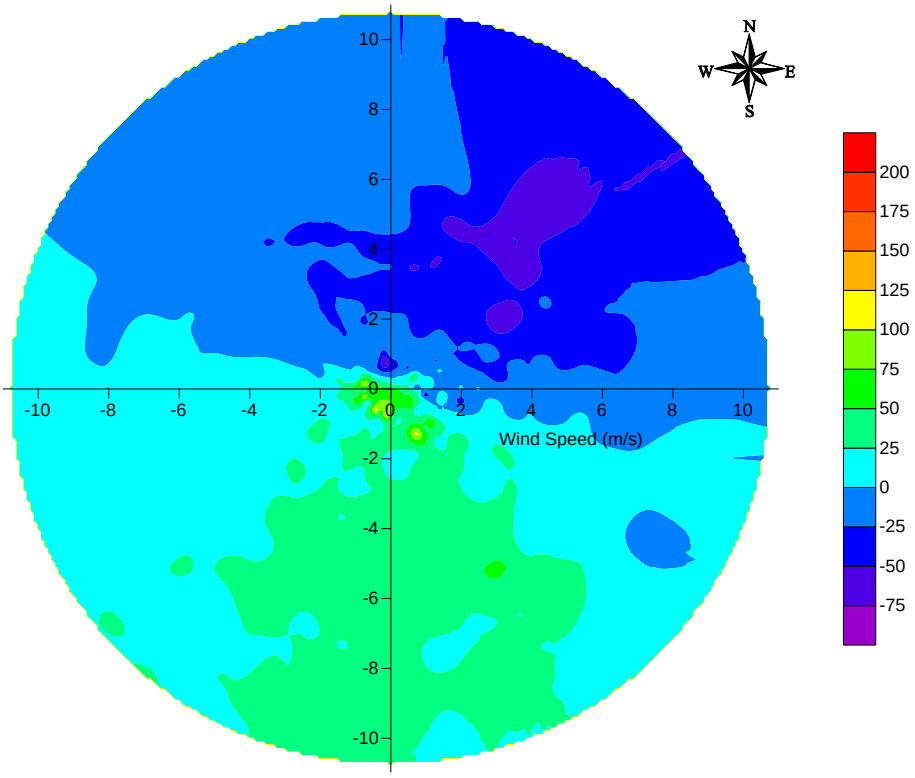

Figure 45 presents the difference rose for Sipson–Hatton Cross. It shows a similar picture to the Sipson–Oaks Road comparison in Figure 42.

Figure 45 The average difference in NO_x concentration (µg m^{-3}) between Sipson and Hatton Cross as a function of wind direction

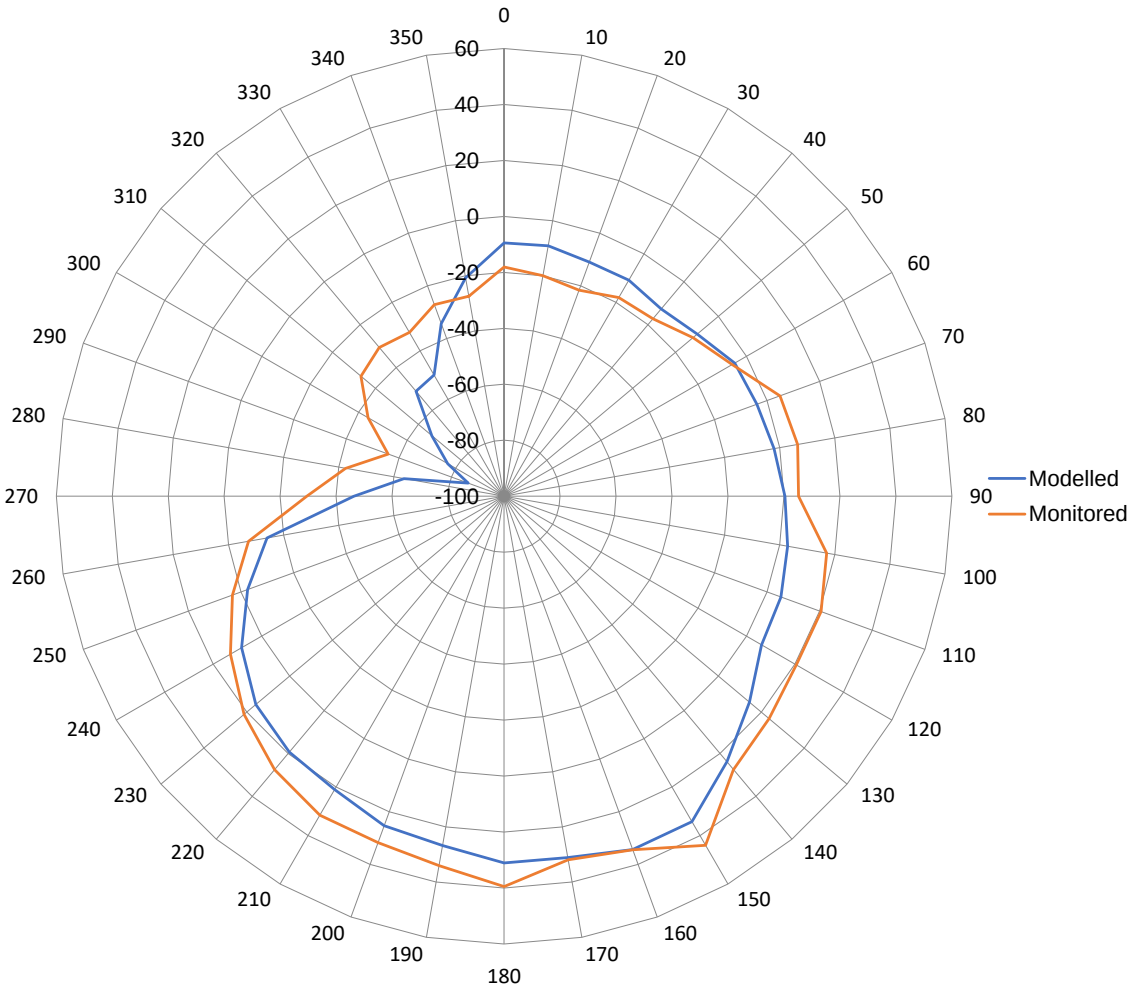

Harlington–Oaks Road (Hatton Cross)

The Harlington–Oaks Road difference rose is displayed in Figure 46, with airfield sources contributing principally over the sectors 160° to 240° inclusive. The model agreement is good in these sectors, with just a little underestimation. Although wind angles a little greater than this point from western end of the northern runway, the concentration contribution is small because departures will be on 27R (the eastern end of the northern runway) for these angles and there will be little emission density at the western end.

Figure 46 The average difference in NO_x concentration (µg m^{-3}) between Harlington and Oaks Road as a function of wind direction

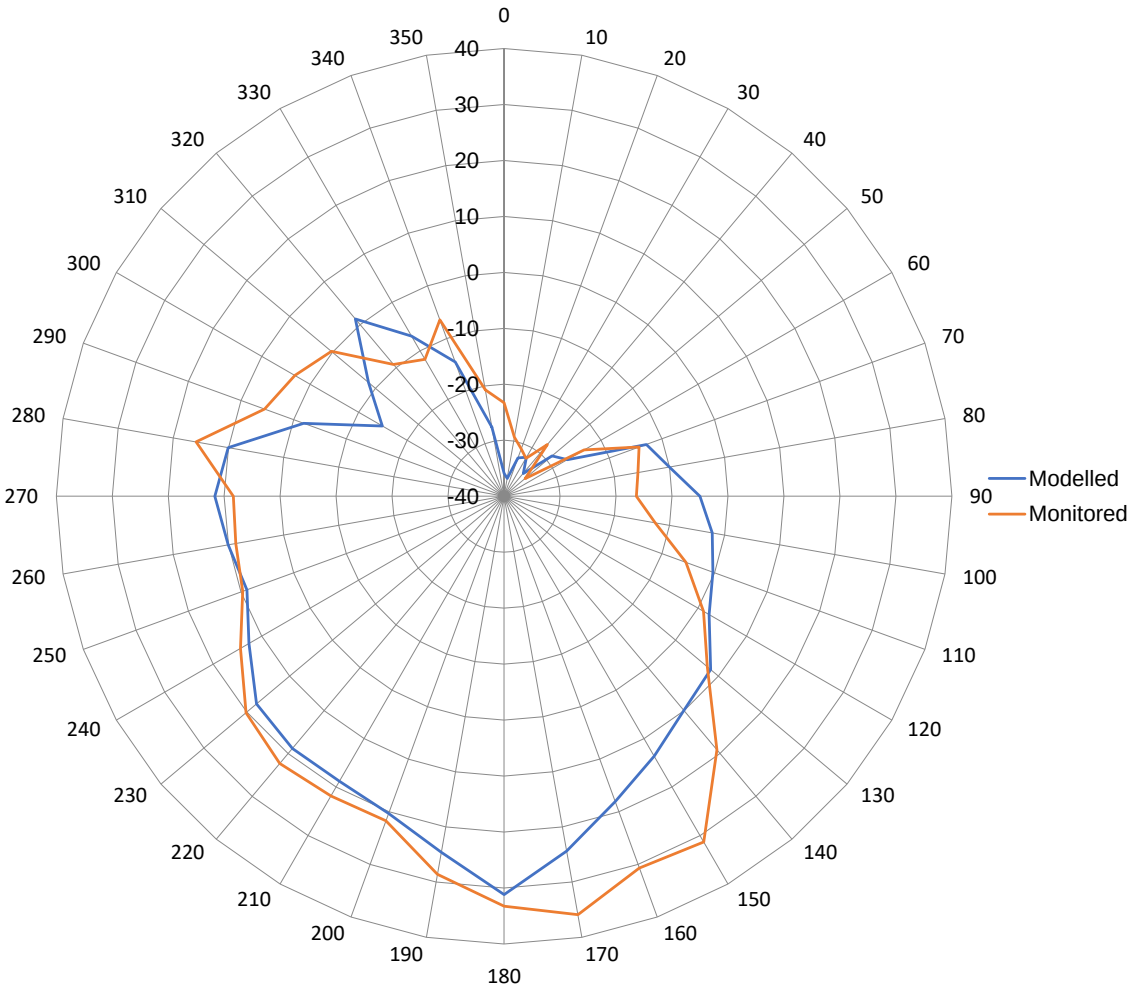

The wind directions pointing from the airport to the Harlington site will also carry pollutants from road vehicles on the Northern Perimeter Road and on the A4, but the breakdown of the difference by source contribution (Table 29) shows that the road network contributes very little of the total difference in annual mean concentrations, whereas airfield sources contribute 95%, according to the modelling, with aircraft emissions accounting for the majority fraction (around 88%). Thus, the Harlington–Oaks Road difference provides a good test of the modelling for the airfield contribution to NO_x concentrations in the residential areas of Harlington.

Table 29 Breakdown by source category of the contribution to the annual mean Harlington–Oaks Road NO_x concentration difference from wind direction sectors 160° to 240° inclusive

Site	Aircraft	Background	Carparks	GSE	Roads	Stationary Sources	Total	Monitored
Harlington	6.7	4.0	0.1	0.4	1.0	0.2	12.4	18.1
Oaks Rd	0.0	3.8	0.0	0.0	1.0	0.0	4.8	9.3
Difference	6.7	0.3	0.1	0.4	0.0	0.2	7.7	8.4

In contrast to the situation for Sipson, some wind angles that correspond to departures on 27R point to Harlington from parts of the runway that still have significant NO_x emission density from take-off roll, so the airfield contribution in Harlington is comparatively large despite the site being further from the runway.

The Harlington–Oaks Road entry in Table 26 above shows that the model underestimates the contribution from sectors 160° to 240° by 9%, which is equivalent to 0.8 µg m^{-3}, and comparable to the expected uncertainty in concentration differences.

The contribution/wind speed plot for this range of angles is displayed in Figure 47. It shows underestimation in a low range of wind speeds, but generally good agreement above 2 m/s. In contrast to the LHR2–Oaks Road and Sipson–Oaks Road plots, which showed good agreement for all wind speeds, including low speeds. This may be related to the model's performance for road traffic sources.

Figure 47 Harlington–Oaks Road concentration difference contribution from wind sectors 160° to 240° inclusive as a function of wind speed

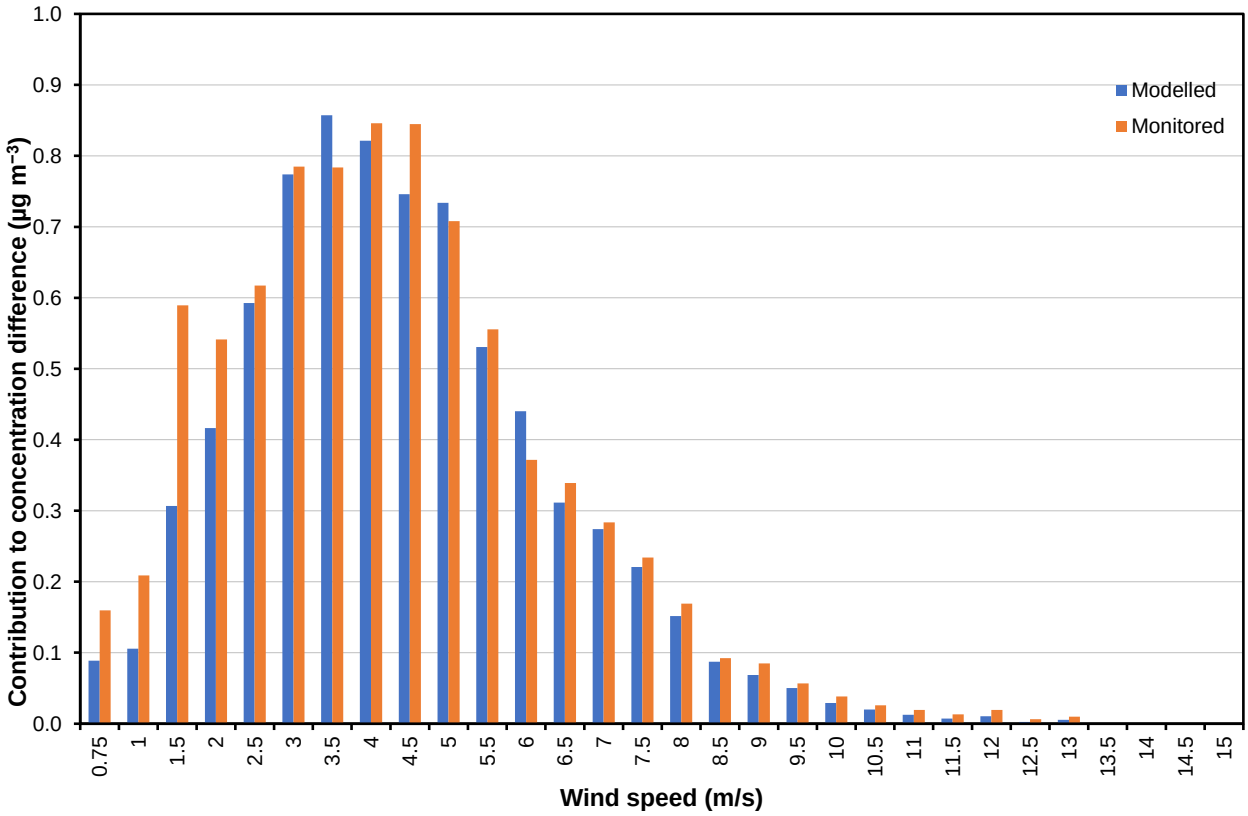

The difference rose for Harlington–Hatton Cross is given in . For southerly winds, the model agreement is reasonable, with a little underestimation.

Figure 48 The average difference in NO_x concentration (µg m^{-3}) between Harlington and Hatton Cross as a function of wind direction

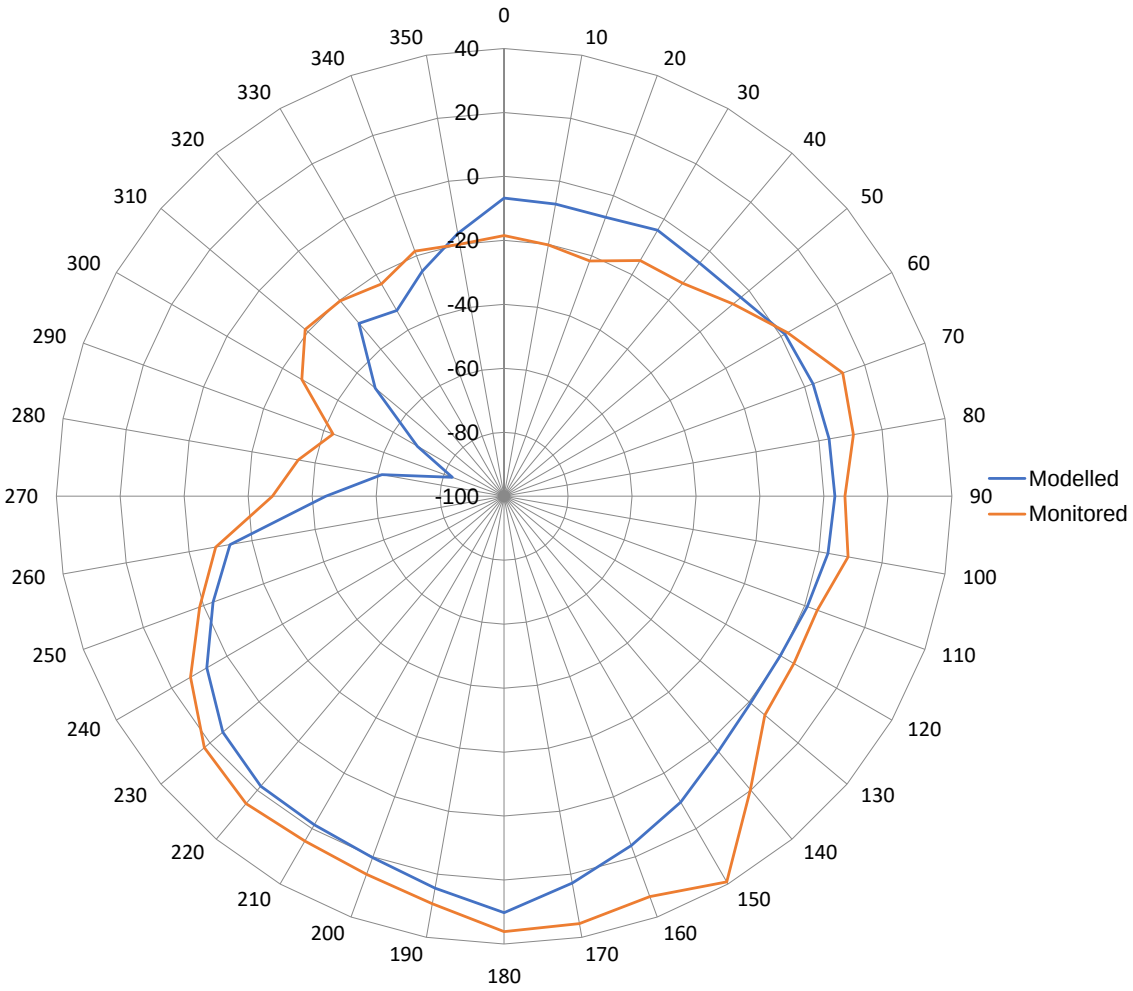

Harmondsworth–Oaks Road (Hatton Cross)

The Harmondsworth–Oaks Road difference rose is displayed in Figure 49, with airfield sources contributing principally over the sectors 110° to 190° inclusive. Harmondsworth, being further west than Sipson or Harlington, has a relatively small airfield contribution despite being closer than Harlington to the runway. Wind directions that lead to departures on 27R — which generate the highest emission density on the northern runway — do not point from the runway to the Harmondsworth site: for the range of angles pointing from airfield sources to the site, aircraft currently depart from the southern runway (09R). The comparison of modelled and measured contributions to the annual mean from this range of sectors is shown in Table 26 above, with the model overestimating in this case by 26%, equivalent to 0.6 µg m^{-3}.

Figure 49 The average difference in NO_x concentration (µg m^{-3}) between Harmondsworth and Oaks Road as a function of wind direction

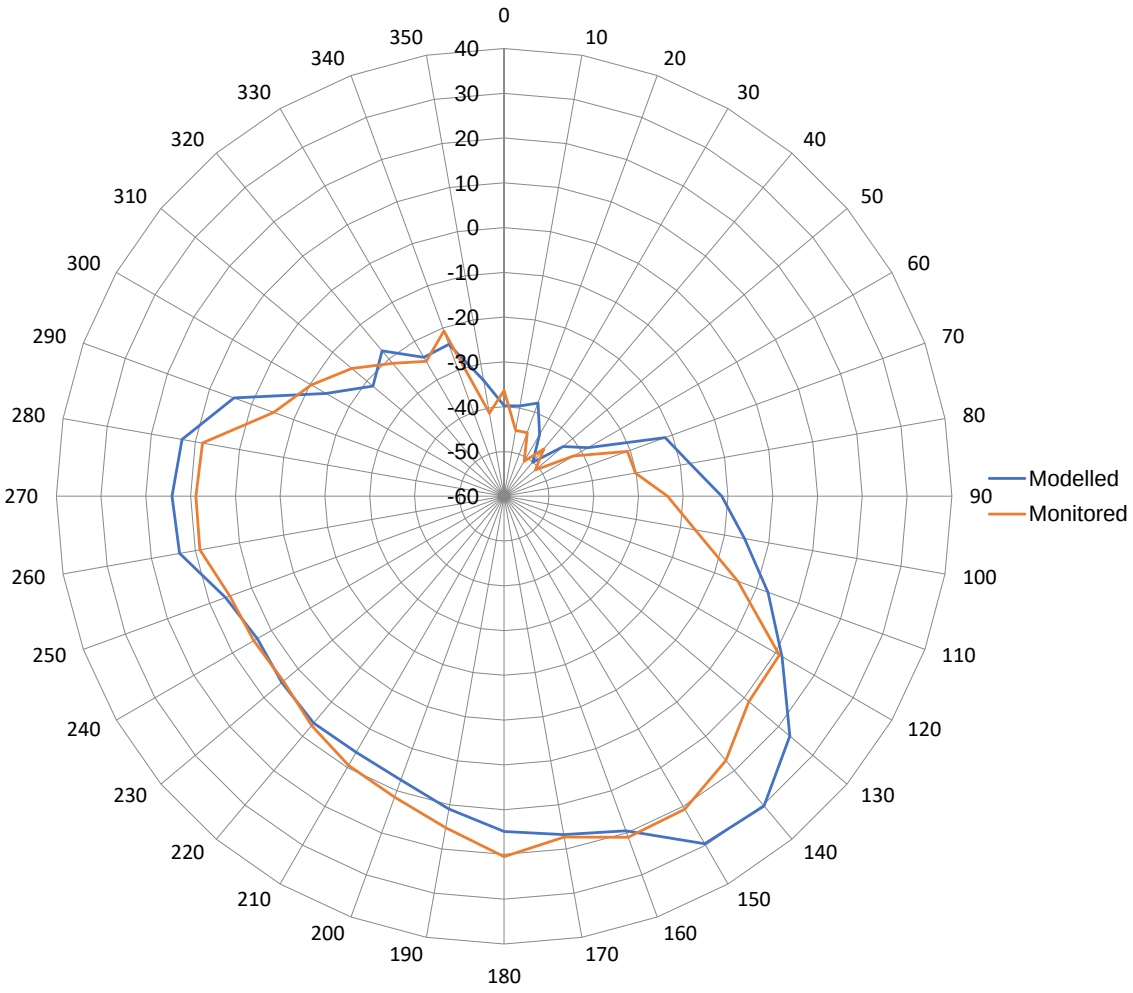

Table 30 Breakdown by source category of the contribution to the annual mean Harmondsworth–Oaks Road NO_x concentration difference from wind direction sectors 110° to 190° inclusive

Site	Aircraft	Background	Carparks	GSE	Roads	Stationary Sources	Total	Monitored
Harmondsworth	2.4	2.7	0.0	0.3	0.4	0.1	6.0	8.6
Oaks Rd	0.0	2.6	0.0	0.0	0.4	0.0	3.0	5.4
Difference	2.4	0.1	0.0	0.3	0.1	0.1	2.9	2.3

The difference rose for Harmondsworth–Hatton Cross is given in Figure 50. The picture is similar to that for Harmondsworth–Oaks Road, although the is less evidence of the model overpredicting the contribution from airfield sources.

Figure 50 The average difference in NO_x concentration (µg m^{-3}) between Harmondsworth and Hatton Cross as a function of wind direction

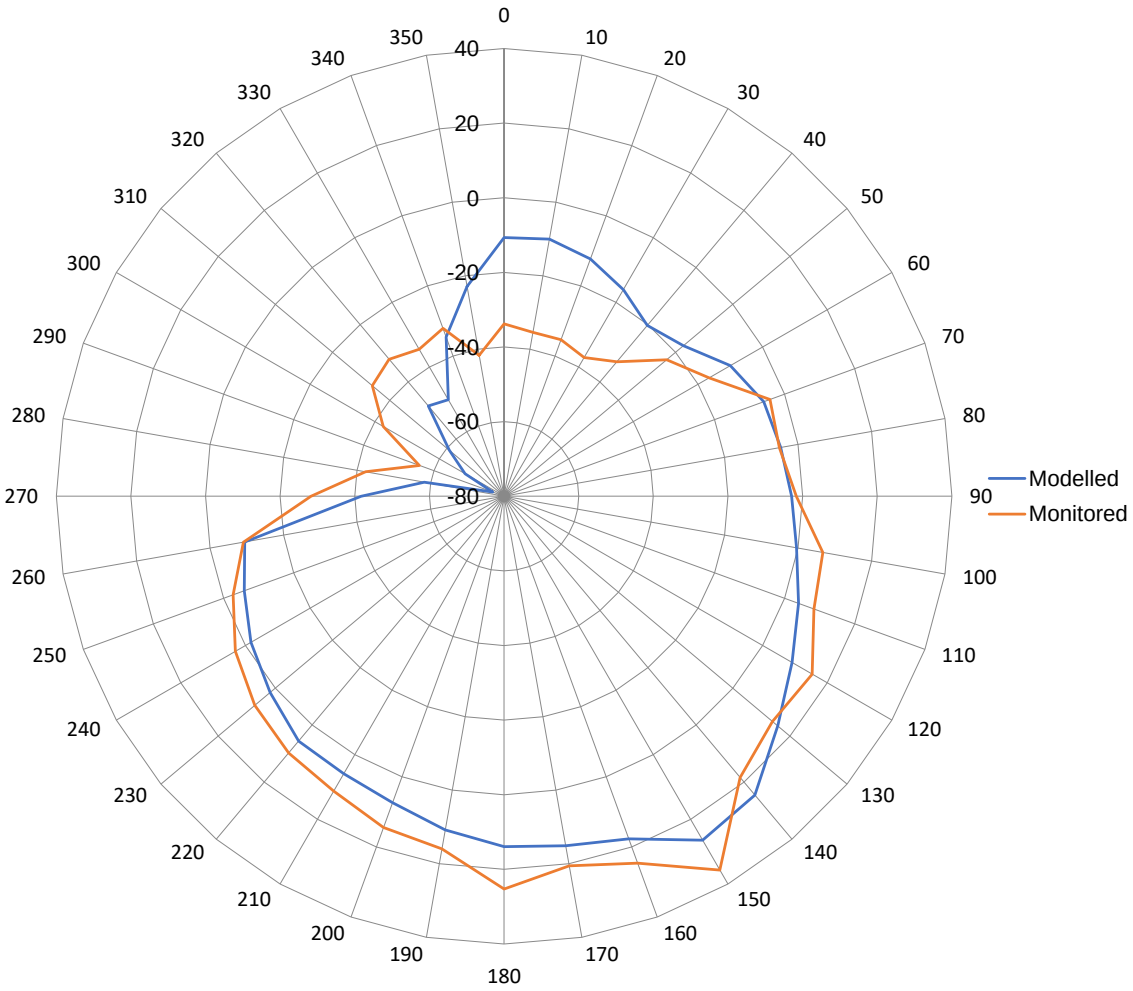

Green Gates–Oaks Road (Hatton Cross)

There is particular interest in the Green Gates site because the intended introduction of full runway alternation during easterly operations is likely to increase NO_x/NO_2 concentrations in Longford, close to where the Green Gates monitor is located.

The Green Gates–Oaks Road difference rose is shown in Figure 51, with airfield sources mainly contributing for wind sectors 100° to 180°. This is again similar to the other wind roses, with some slight underestimation in the southwest quadrant and some slight overestimation in the southeast quadrant. As with Harmondsworth, when the wind is in the southwest quadrant it does not blow from the airport towards Green Gates. The total NO_x contribution to annual mean concentrations from airfield sources is relatively small, for similar reasons to those given above for Harmondsworth, with aircraft mainly taking off on the southern runway when the wind blows from airfield sources to the site.

The breakdown by source of the contribution to the annual mean concentration difference from sectors with an airfield contribution is given in Table 31, with airfield sources accounting for 96% of the total difference.

Figure 51 The average difference in NO_x concentration (µg m^{-3}) between Green Gates and Oaks Road as a function of wind direction

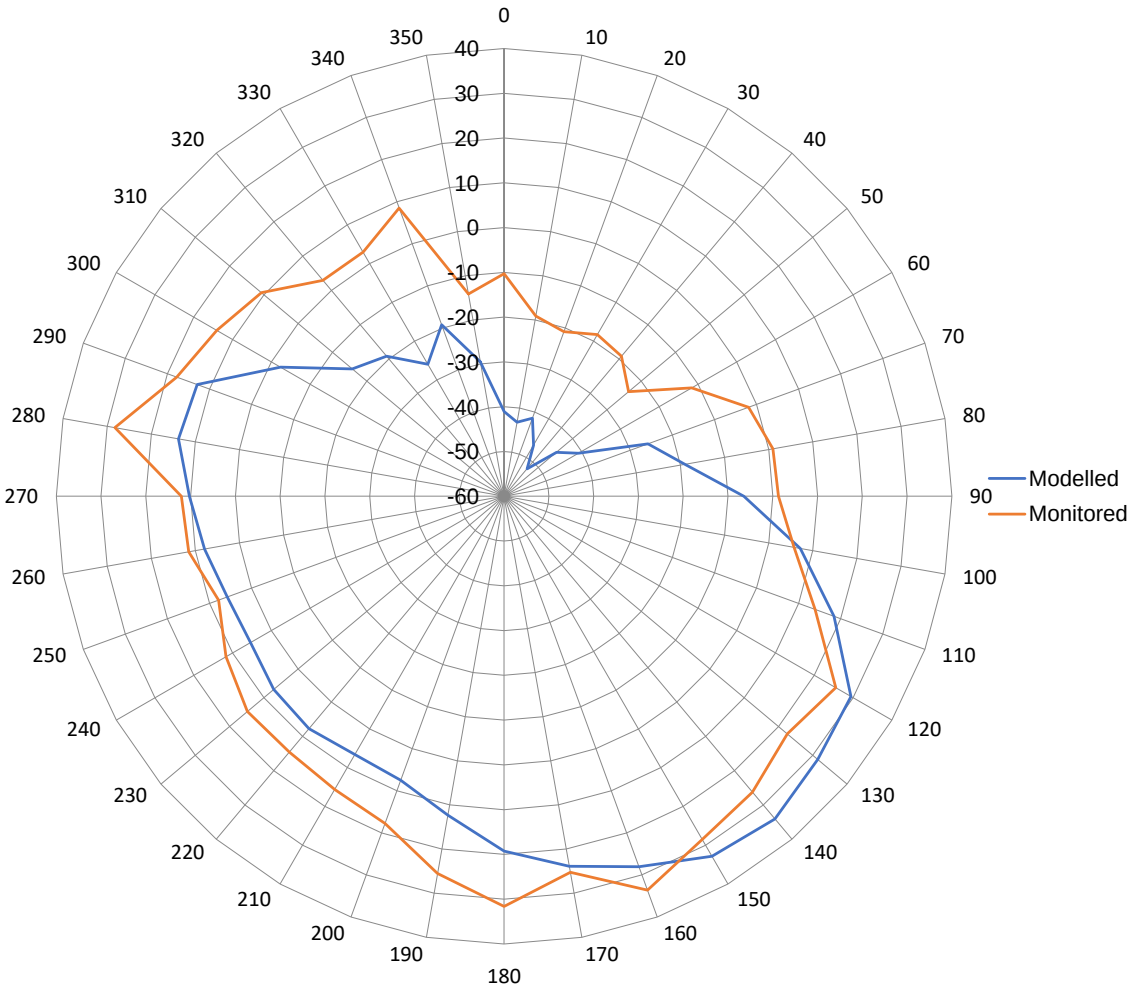

Table 31 Breakdown by source category of the contribution to the annual mean Green Gates–Oaks Road NO_x concentration difference from wind direction sectors 100° to 180° inclusive

Site	Aircraft	Background	Carparks	GSE	Roads	Stationary Sources	Total	Monitored
Green Gates	3.3	2.3	0.1	0.4	0.5	0.1	6.7	10.0
Oaks Rd	0.1	2.5	0.0	0.0	0.4	0.0	2.9	6.0
Difference	3.2	-0.1	0.1	0.4	0.2	0.0	3.7	3.3

The difference rose for Green Gates–Hatton Cross is given in Figure 52. It shows the model underestimating the difference in most wind directions.

Figure 52 The average difference in NO_x concentration (µg m^{-3}) between Green Gates and Hatton Cross as a function of wind direction

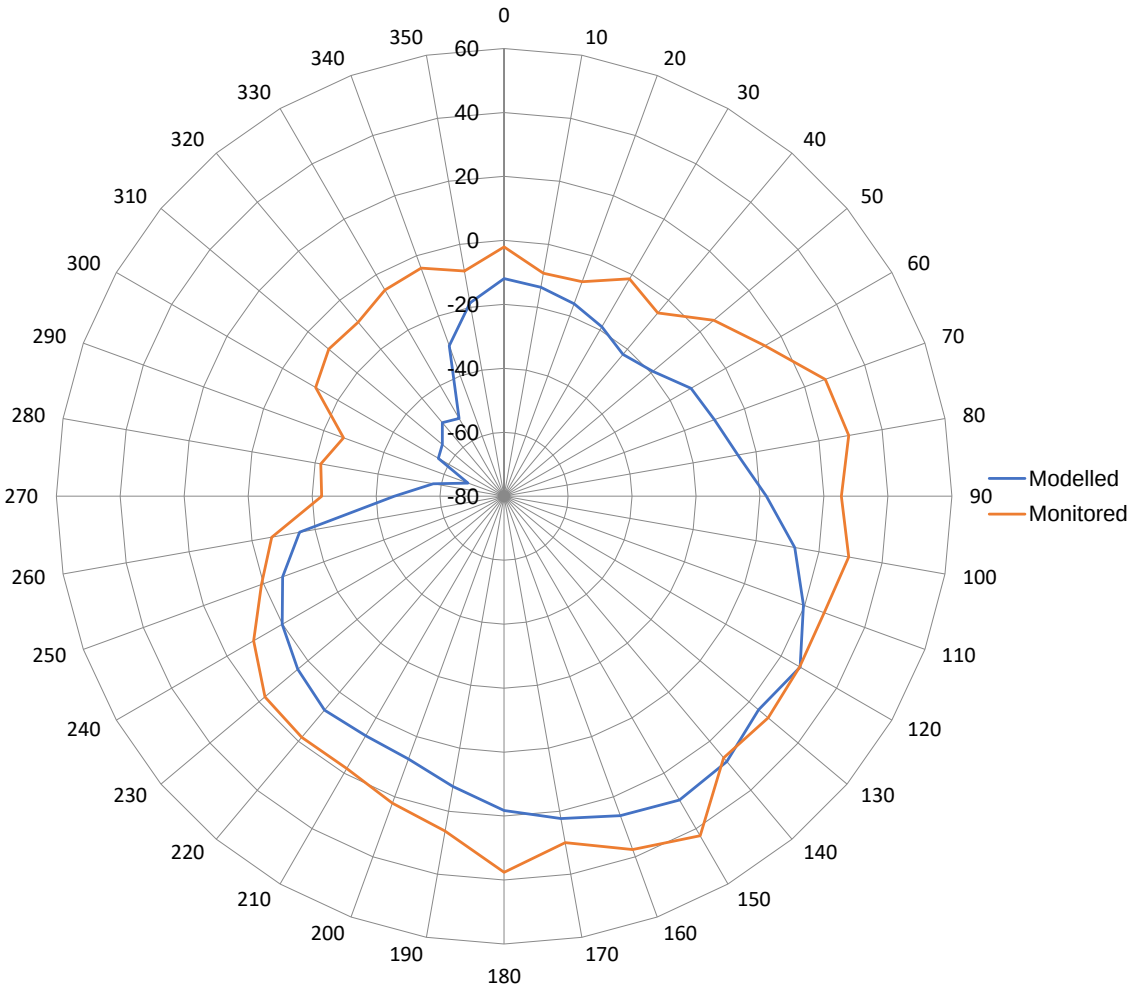

Oxford Avenue–Oaks Road (Hatton Cross)

The Oxford Avenue site receives a substantial contribution to annual mean NO_x concentrations from airfield sources, being downwind of major airfield sources along the dominant wind direction. In addition, it lies quite close to the A4.

Figure 53 shows the Oxford Avenue–Oaks Road difference rose, with airfield sources mainly contributing over the 210° to 260° sector range. Elevated concentration differences are shown over this sector range in both the modelling and monitoring results, with the modelled difference a little less than the measured difference. Table 32 gives the breakdown by source of the contribution to the annual mean concentration difference from these sectors, showing that airfield sources account for 89% of the total, with the road network accounting for 9%.

Figure 53 The average difference in NO_x concentration (µg m^{-3}) between Oxford Avenue and Oaks Road as a function of wind direction

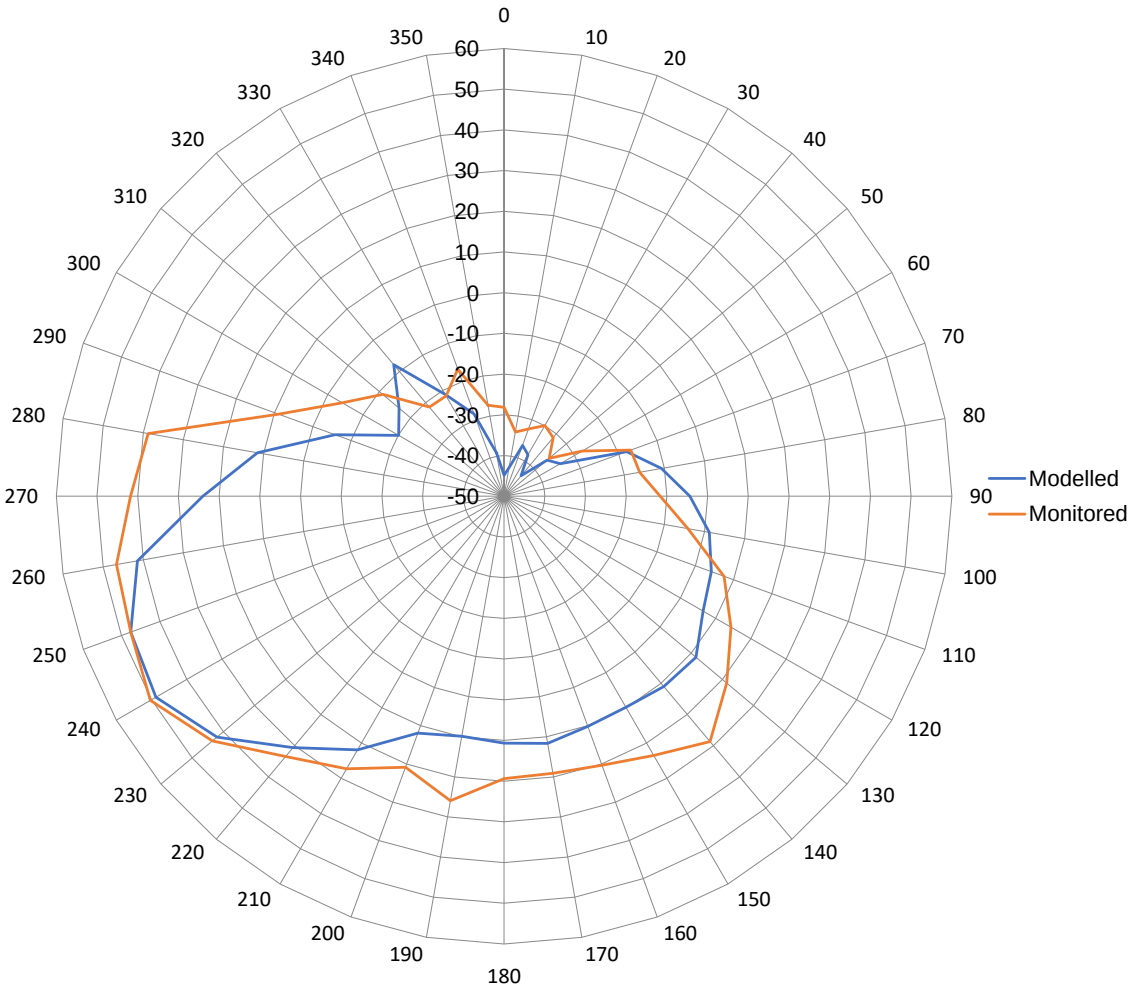

Table 32 Breakdown by source category of the contribution to the annual mean Oxford Avenue–Oaks Road NO_x concentration difference from wind direction sectors 200° to 260° inclusive

Site	Aircraft	Background	Carparks	GSE	Roads	Stationary Sources	Total	Monitored
Oxford Avenue	11.2	3.2	0.1	0.4	2.3	0.4	17.6	23.1
Oaks Rd	0.0	2.8	0.0	0.0	1.1	0.0	3.9	8.3
Difference	11.2	0.4	0.1	0.4	1.2	0.4	13.7	14.0

The difference rose for Oxford Avenue–Hatton Cross is given in Figure 50. Like Oxford Avenue–Oaks Road, the model is slightly underestimating the difference in most wind directions.

Figure 54 The average difference in NO_x concentration (µg m^{-3}) between Oxford Ave and Hatton Cross as a function of wind direction

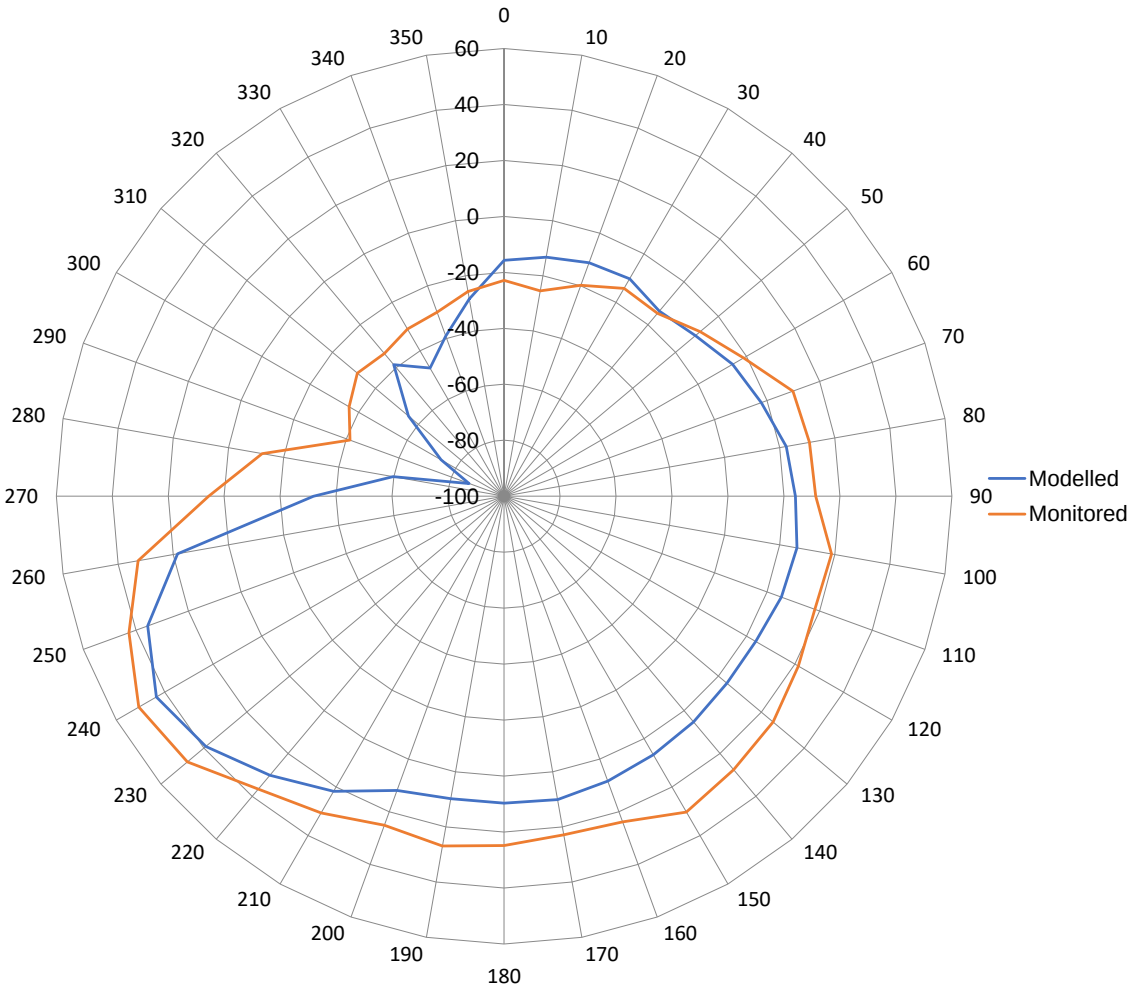

Oaks Road–Harlington (Sipson, Harmondsworth)

It is also possible to test the modelling for airfield sources by taking differences between Oaks Road and a site north of the airport for northerly wind sectors. The model–monitoring comparison is more difficult to interpret in this case because the concentrations include a substantial contribution from the road network at both sites, but they provide useful additional information.

An appropriate range of sectors to capture the airfield contribution at Oaks Road is 330° to 90° and the differences between Oaks Road and three northerly sites, Harlington, Harmondsworth and Sipson, are examined over this range. Table 26 shows the relevant comparison of modelled and measured differences, indicating that the model overestimates the difference slightly, on average by 1.0 µg m^{-3}.

The general features of the comparisons are similar for all three northerly sites, so only the Oaks Road–Harlington differences will be examined in more detail. In a sense, the difference rose can deduced by reversing the signs of the concentrations in Figure 46, but because of the nature of the polar plot this is difficult to read for northerly quadrants, so is re-plotted with signs reversed in Figure 55 (i.e. Oaks Road minus Harlington as opposed to Harlington minus Oaks Road).

Figure 55 The average difference in NO_x concentration (µg m^{-3}) between Oaks Road and Harlington as a function of wind direction

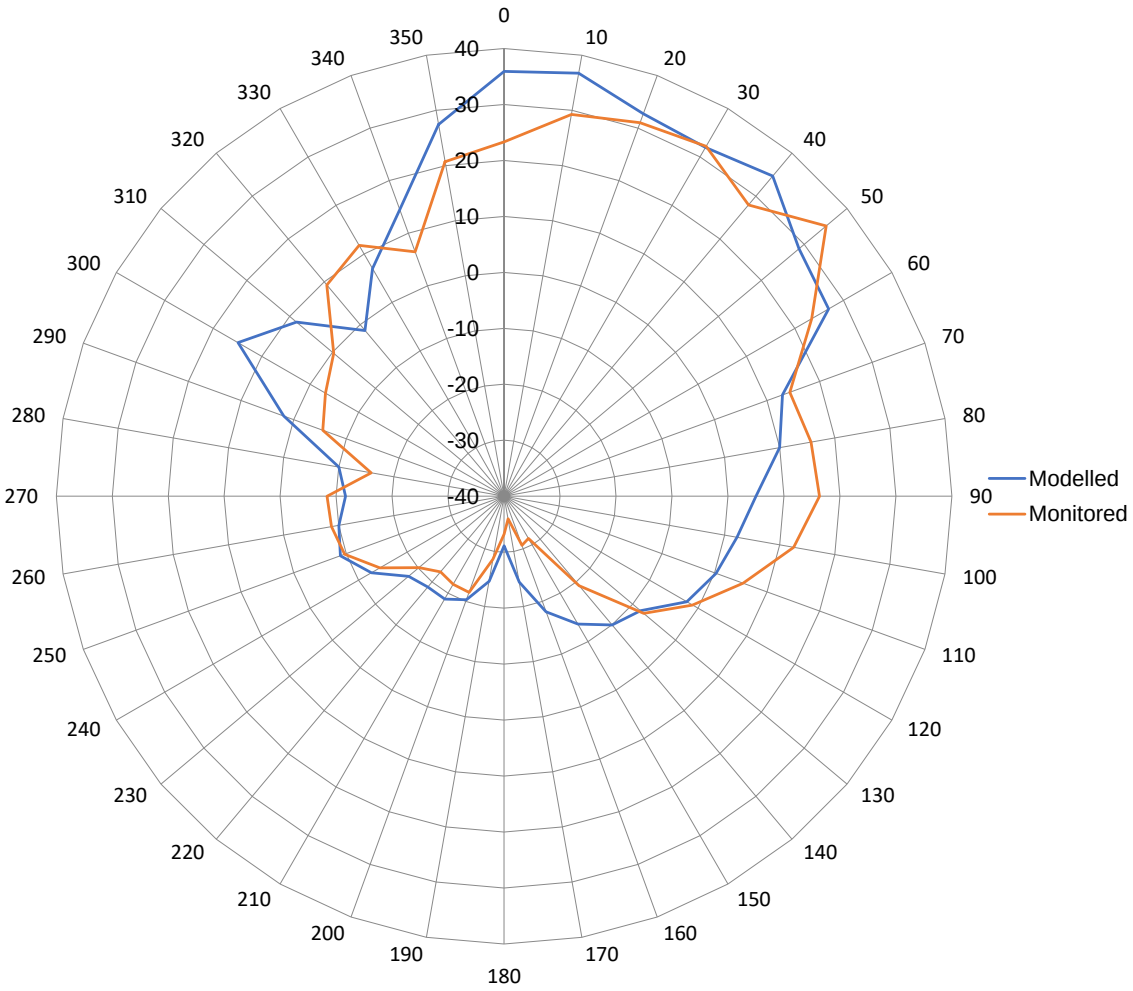

This reveals a moderate overestimation for wind angles around 330° to 70°: these sectors point to Oaks Road from the T5 aprons and from take-off roll on the southern 09R runway. This might indicate an overestimation of the airfield contribution at Oaks Road, but caution is needed, given that the modelled contribution at Harlington from these directions (which has a significant road-network contribution) may be underestimated. Section 3.3 discusses the general under-prediction of the contribution from the road network across the study area.

Figure 56 gives the contribution/wind speed comparison for the whole 330° to 90° range, showing even more strongly than in the differences for southerly winds (for example Figure 39) that model overestimation at low wind speed is partly offset by an underestimation at higher wind speeds. In this instance, the overestimation at low wind speeds has a greater effect on annual mean concentrations because the probability of low wind speeds is higher for northerly winds than it is for southerly winds, as illustrated in Figure 57. In the discussion of the LHR2–Oaks Road differences, it was speculated that underestimation of plume rise at low wind speed for main engine exhaust emissions (and overestimation at high wind speed) may be contributing to the discrepancy. In a similar vein, the lack of plume rise modelling for APU emissions on the aprons may also be playing a part. It is worth noting that the frequency of northerly winds is relatively low and quite strongly angle-dependent (see wind rose in Figure 3). Thus, uncertainties in the meteorological data for wind direction may contribute to modelling–monitoring differences.

Figure 56 Oaks Road–Harlington concentration difference contribution from wind sectors 330° to 90° inclusive as a function of wind speed

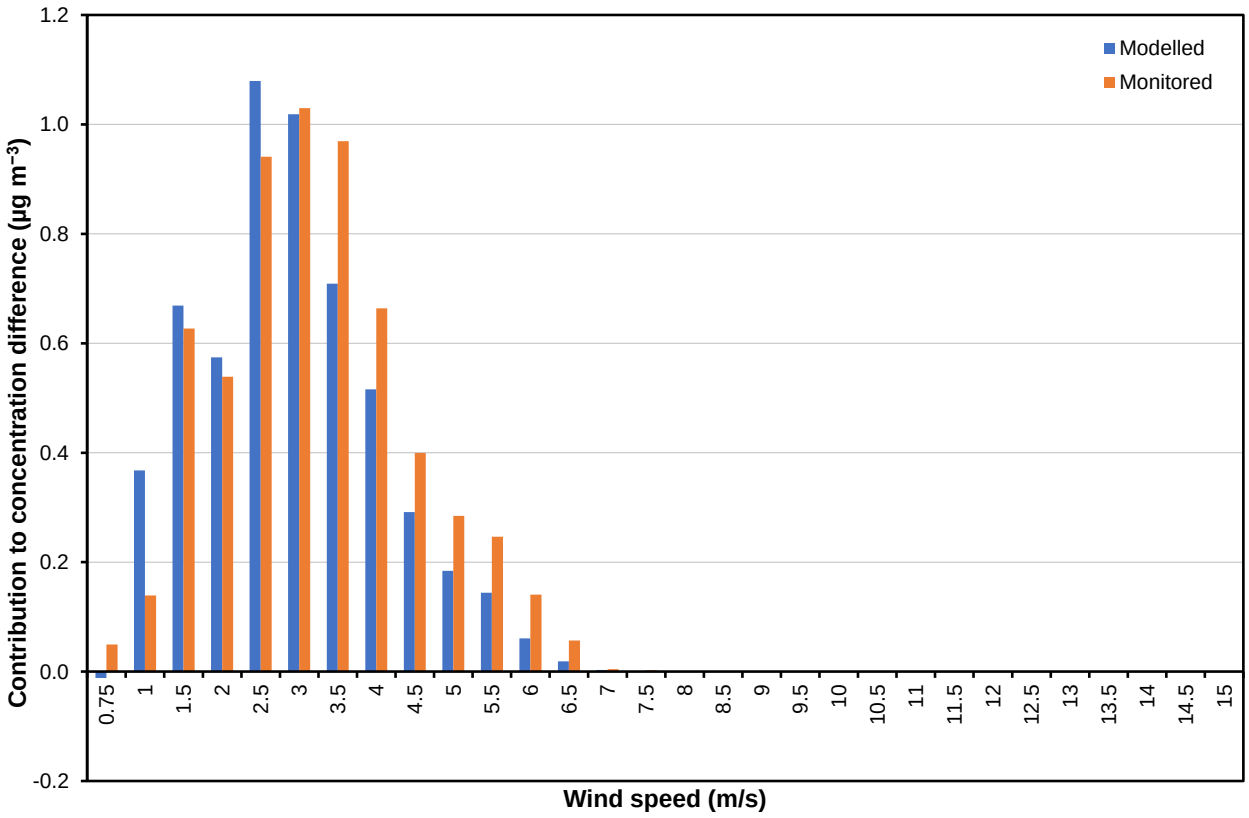

Figure 57 Wind speed frequency distribution shown separately for southerly (170°–270°) and northerly (330°–90°) sectors.

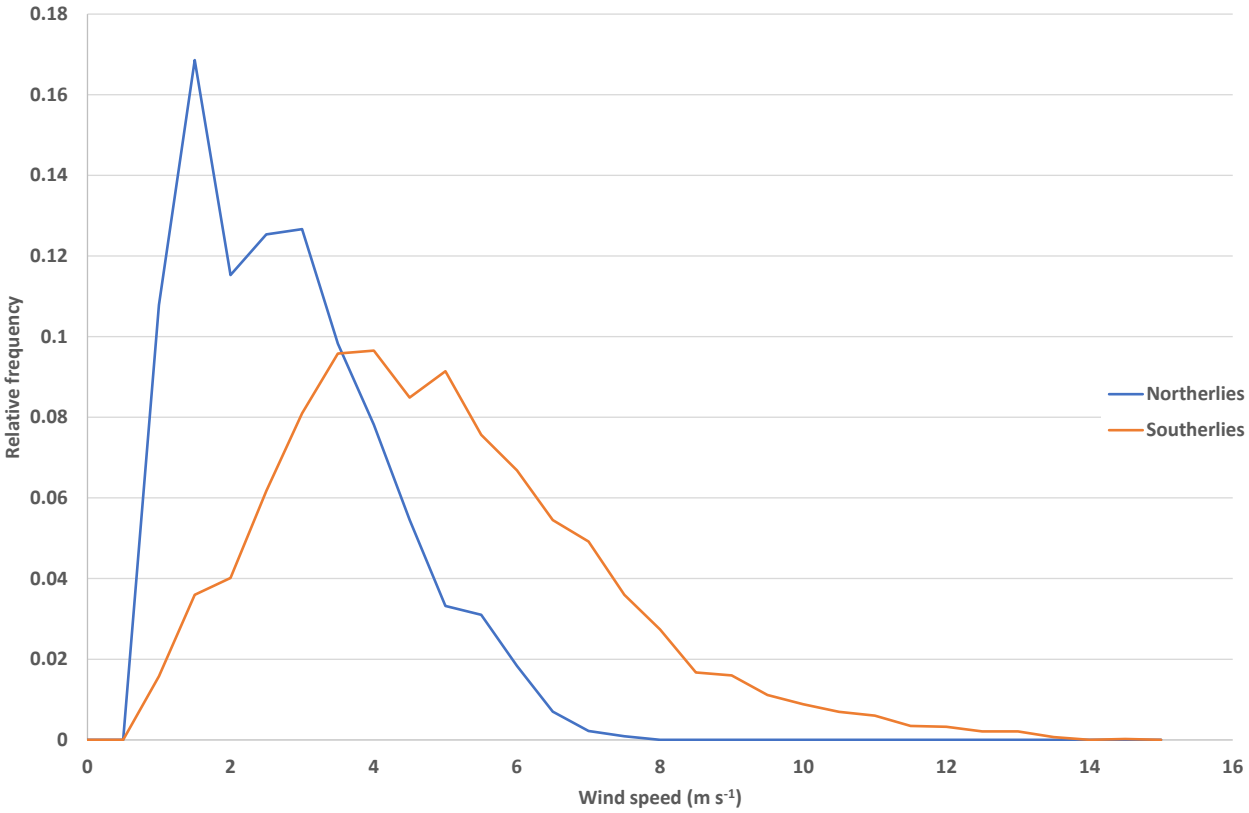

Summary for airfield sources

It is useful to summarise the position for airfield sources before moving on to comparisons for the road-network contribution.

The comparisons presented in this section indicate that the model gives a good account of the impact of airfield sources on annual mean NO_x concentrations at receptor locations in the residential areas north of the airport. Particularly, it represents well the variation in the airfield concentration contribution with distance from the principal sources on the airport and the variation with east–west location in relation to the ends of the northern runway. This gives confidence that the model provides a robust basis for investigating the potential impact on residential areas of operational changes on the airport that affect the magnitude and spatial distribution of NO_x emissions, for example the introduction of full runway alternation in easterly operations (which would then allow departures on runway 09L) and the construction of a third runway north of the current runways.

These comparisons jointly test the methodology for quantifying airfield emissions and the dispersion modelling methodology that translates emissions into airborne concentrations. This raises the possibility that significant errors in emissions quantification may be fortuitously cancelling errors in dispersion modelling. The good agreement found above, however, applied in situations where different source groups (runway, apron, etc.) were dominant, so any fortuitous cancellation would have to apply across a range of sources.

Concentration contours for the airfield contribution to annual mean NOx concentrations

The above tests give confidence in the model's ability to predict the spatial variation of the airfield contribution to total NO_x concentrations in the residential areas around the airport. To show this variation, concentration contour plots have been generated based on the model values at a set of grid points, as described in the modelling methodology report.

Figure 58 gives the contour plot for annual mean contribution from airfield sources. The shape of the contours reflects the spatial distribution of NO_x emissions on the airport — with particularly high emission intensity at the eastern end of the northern runway — coupled with the strongly anisotropic wind rose (with its south-westerly dominance). The current restriction of departures on runway 09L (the western end of the northern runway) adds to the anisotropy of the contours. Values of the airfield contribution to the annual mean NO_x concentration above 30 µg m^{-3} are restricted to within the main body of the airport, with values in the nearest residential communities typically within the range 10–20 µg m^{-3}.

Figure 58 Airfield contribution to annual mean NO_x concentrations

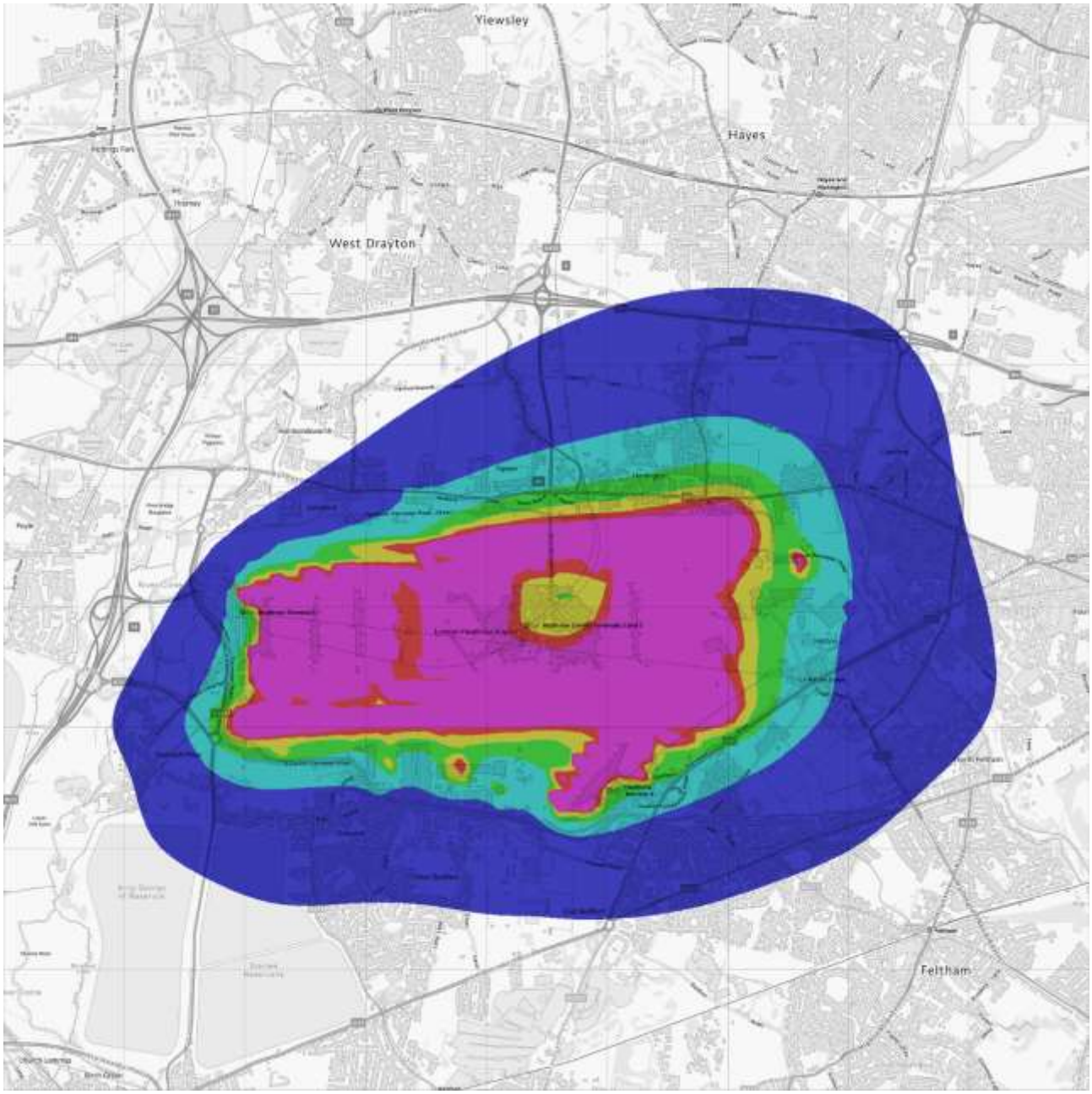

30 µg m^{-3}
25 µg m^{-3}
20 µg m^{-3}
15 µg m^{-3}
10 µg m^{-3}
5 µg m^{-3}

EVALUATION OF THE MODELLING FOR THE ROAD-NETWORK

Section 3.2 dealt with airfield sources and this section deals with road-network sources. Road vehicle emissions on the road network around Heathrow play an important role in determining the total concentration of NO_x in residential areas close to the airport, so concentration differences were analysed separately with a focus on the road-network contribution.

Table 20 shows wind directions and data related to the particular wind directions for pairs of sites. The modelled and measured concentrations are the difference between the two concentrations from the two sites. The model is underpredicting for all pairs of sites, more so at those heavily influenced by road traffic. Further detailed analysis of each pair of receptors is discussed in the following sections.

Table 33 Comparison of modelled and measured contributions to the annual mean difference in NO_x concentration between pairs of analysers, for selected sector ranges chosen to highlight the road network source contribution.

Site difference	Sector range[1]	Modelled NO_x (µg m^{-3})	Measured NO_x (µg m^{-3})	Discrepancy (µg m^{-3})	Model bias (%)
Hillingdon - Harmondsworth	100° - 270°	16.2	42.6	-26.4	-62.0
Hillingdon - Harlington	100° - 270°	12.7	38.0	-25.3	-66.6
Green Gates - Oaks Road	200° - 290°	4.2	7.3	-3.1	-42.2
Green Gates - Harmondsworth	0° - 90°	-0.3	6.3	-6.6	-104.7
Harmondsworth - Lakeside 2	200° - 290°	2.9	-0.4	3.3	-822.9
Oxford Avenue - Oaks Road	90° - 180°	1.3	1.9	-0.7	-35.0
LHR2 - Harlington	270° - 100°	6.1	24.1	-18.0	-74.6
Hayes - Cranford	90° - 210°	6.0	22.8	-16.8	-73.5

[1] Angle is the direction from which the wind blows, clockwise from north; sector ranges are inclusive.

Hillingdon–Harmondsworth; Hillingdon–Harlington

The Hillingdon site is 40 m north of the nearest lane of the M4, so receives a substantial contribution from the motorway when the wind blows from southerly directions. Over part of the range of southerly wind sectors, the site also receives a contribution from the airport, but at this distance the modelled contribution is small. By choosing a 'difference' site that is also north of the airport (and without a large airfield contribution), the potentially confounding effect of differences in non-road contributions can be reduced: Harlington and Harmondsworth are appropriate 'difference' sites.

Figure 59 gives the Hillingdon–Harmondsworth difference rose. Both the modelled and measured concentration differences are large for southerly winds, typically around 20–40 µg m^{-3} from modelling and 40–100 µg m^{-3} from measurement, but the model systematically underestimates the concentration difference over the whole range of sectors for which the motorway is expected to give a major contribution, in particular for south-easterly wind directions. An underestimation of this magnitude is very unlikely to be attributable to measurement uncertainty alone. Table 33 compares the measured and modelled differences for the sector range 100° to 270°, showing that the model underestimates the contribution to the annual mean concentration difference by 62%, a discrepancy of 26.3 µg m^{-3} on a measured total of 42.6 µg m^{-3}. Table 34 gives the breakdown by source of the contribution to the annual mean concentration difference from these sectors, showing that airfield sources account 1% of the total difference, with the road network accounting for 102%. (N.B. a value greater than 100% is possible when other sources counteract the differences.)

Figure 59 The average difference in NO_x concentration (µg m^{-3}) between Hillingdon and Harmondsworth as a function of wind direction

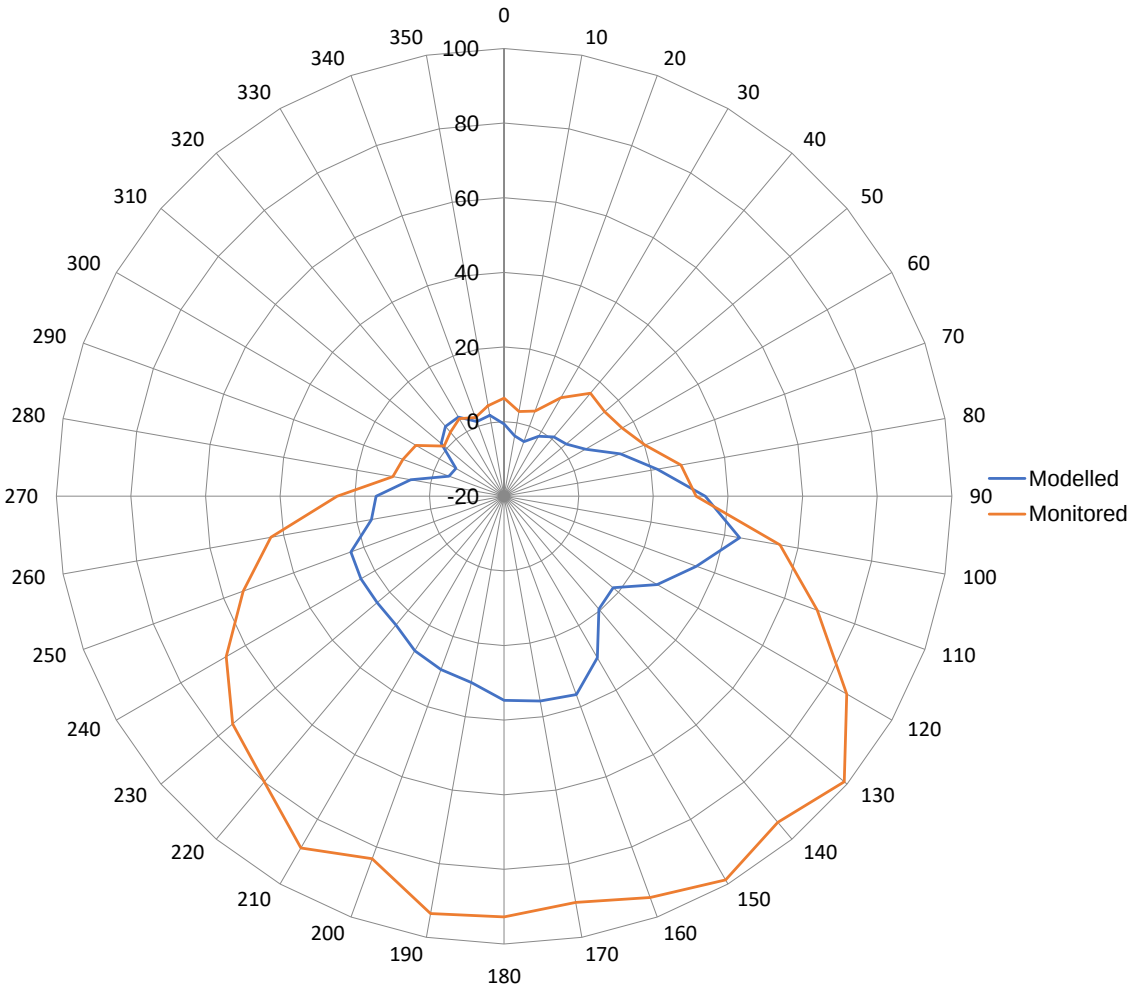

Table 34 Breakdown by source category of the contribution to the annual mean Hillingdon–Harmondsworth NO_x concentration difference from wind direction sectors 100° to 270° inclusive

Site	Aircraft	Background	Carparks	GSE	Roads	Stationary Sources	Total	Monitored
Hillingdon	3.2	7.1	0.1	0.2	19.4	0.1	30.2	65.7
Harmondsworth	3.0	7.7	0.1	0.3	2.8	0.1	14.0	22.7
Difference	0.2	-0.5	0.0	-0.1	16.6	0.0	16.2	42.6

Figure 60 shows the contribution/wind-speed comparison for the 100° to 270° sector range. There is an under-prediction in the total area, in line with the discrepancy in the difference rose.

Figure 60 Hillingdon–Harmondsworth concentration difference contribution from wind sectors 100° to 270° inclusive as a function of wind speed

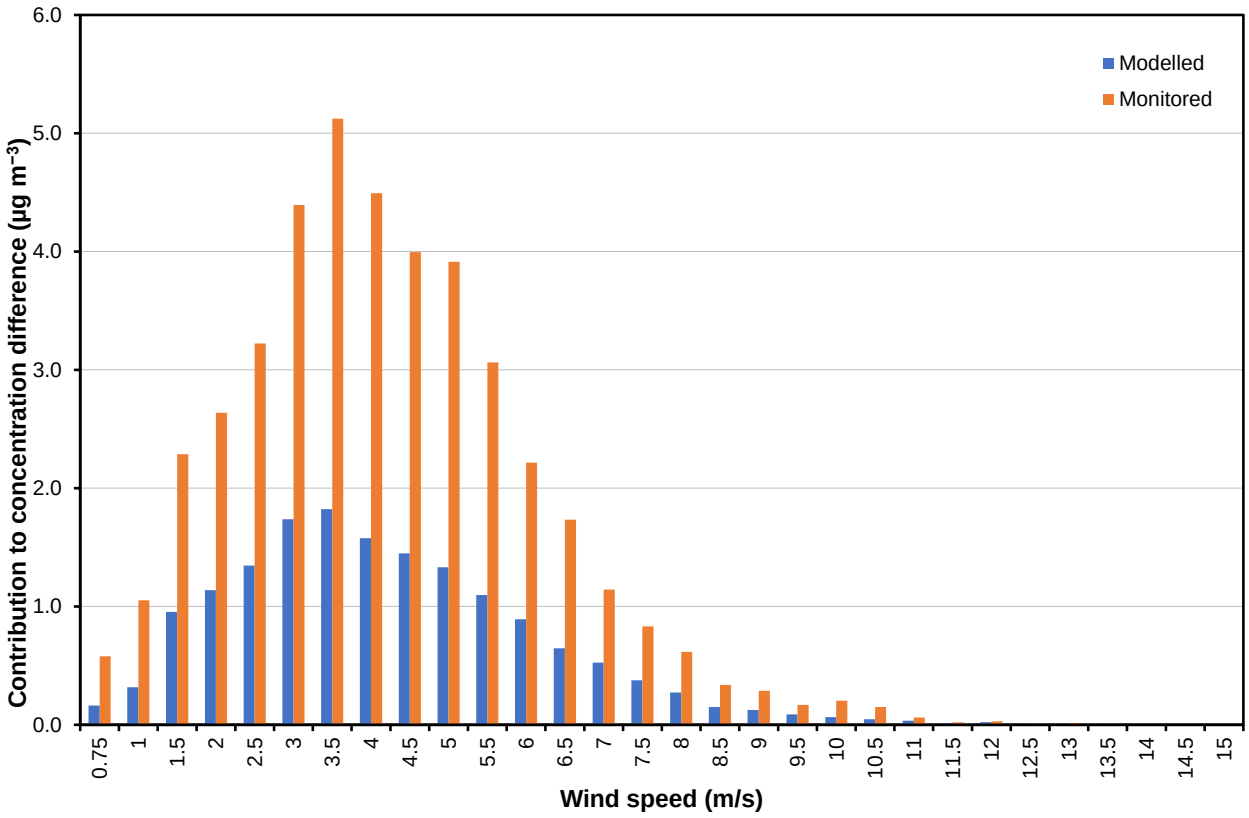

Figure 61 gives the Hillingdon–Harlington difference rose, which has similar features to those for Hillingdon–Harmondsworth. In this case, the fractional discrepancy between modelled and measured values for the contribution from sectors 100° to 270° to the annual mean concentration is a 66% under-prediction, a discrepancy of 25.2 µg m^{-3} out of a measured total of 38.0 µg m^{-3}.

Figure 61 The average difference in NO_x concentration (µg m^{-3}) between Hillingdon and Harlington as a function of wind direction

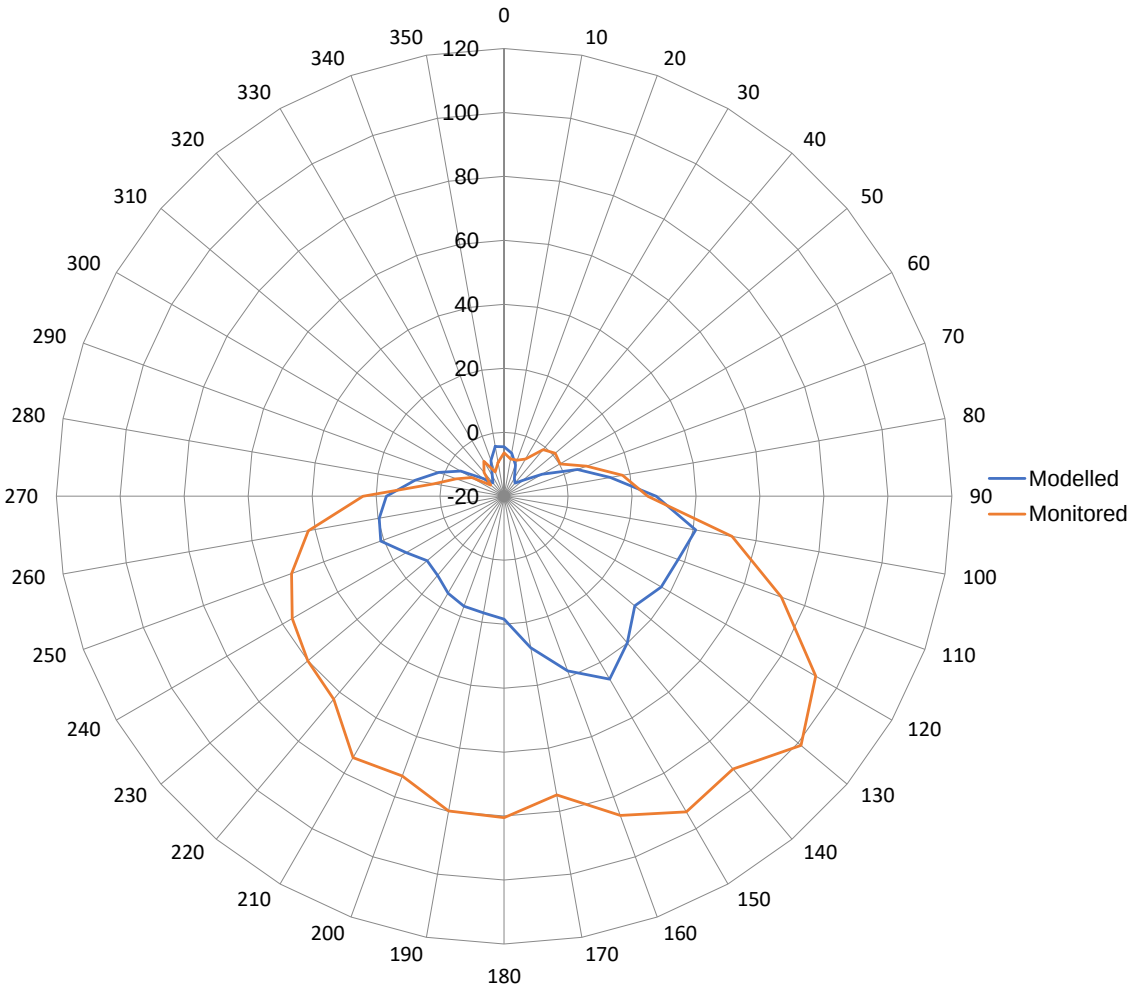

There is continuing major interest in whether the present methodologies for quantifying road vehicle NO_x emissions are leading to systematic under-prediction of traffic-related emissions, and it is tempting to interpret the above results for the Hillingdon site in this light. However, before conclusions can be drawn from these results about the current set of emission factors, it is necessary to evaluate the basic traffic data used in the emissions quantification. There are several discrepancies between the flows in the traffic model and those measured by the Department for Transport in 2019[33], as shown in Table 35 and Table 36 for two key motorway links. The model significantly underpredicts the number of HGVs and buses and coaches.

The measured data does not give any information on the accuracy of modelled traffic speed, also a parameter of key importance for emissions. Hourly average speed may not be enough to characterise the traffic state in relation to emissions if there are periods of flow breakdown and queuing (such as at major junctions).

[33] https://roadtraffic.dft.gov.uk/#6/55.254/-6.064/basemap-regions-countpoints

Table 35 Comparison of measured[34] and modelled traffic flows on the M4 between junctions 4 and 4B.

	Direction	Motorcycles	Cars and taxis	Buses and coaches	LGVs	HGVs	All motor vehicles
Traffic model	Eastbound	368	63397	188	10619	2981	77554
	Westbound	369	65203	169	11036	2978	79755
	2 Way	738	128600	357	21655	5959	157309
DfT	2 Way	999	131399	955	20237	8217	161807

Table 36 Comparison of measured[35] and modelled traffic flows on the M25 between junctions 14 and 15.

	Direction	Motorcycles	Cars and taxis	Buses and coaches	LGVs	HGVs	All motor vehicles
Traffic Model	Northbound	484	86539	158	17401	4556	109137
	Southbound	495	88964	80	17381	4485	111405
	2 Way	978	175503	238	34782	9041	220542
DfT	2 Way	1094	165759	741	30194	18320	216108

Green Gates–Oaks Road (road-network contribution)

As noted earlier, there is particular interest in the NO_x and NO_2 concentrations at Green Gates in view of the potential introduction of full runway alternation in easterly operations. In relation to the road-network contribution, the Green Gates–Oaks Road difference rose (Figure 51) indicates significant discrepancies for north-westerly quadrant.

It is difficult to identify a 'clear' difference for the road-network contribution at Green Gates. For angles giving a significant network contribution at the site, most other sites also have a significant network contribution. However, the key wind direction quadrants at Green Gates from this perspective are westerly (bringing pollutant from the M25 and the A3044), so the Green Gates–Oaks Road difference itself can be used if the sector range is restricted to around 200° to 290°: at greater angles Oaks Road starts to 'see' the nearby southern perimeter road and the various junctions with the A3044 and the M25 (J14); at smaller angles Green Gates starts to 'see' airfield sources. Table 37 gives the breakdown by source of the modelled contribution to the annual mean concentration difference from these sectors, showing that the road network accounts for 62% of the total difference; the relevant entry in Table 33 gives the model–monitoring comparison for this sector range, showing that the model contribution to the annual mean concentration difference is only 54% of the measured contribution, equivalent to a discrepancy in annual mean concentration difference of 3.9 µg m^{-3}.

Table 37 Breakdown by source category of the contribution to the annual mean Green Gates–Oaks Road NO_x concentration difference from wind direction sectors 200° to 290° inclusive

Site	Aircraft	Background	Carparks	GSE	Roads	Stationary Sources	Total	Monitored
Green Gates	0.4	5.8	0.1	0.0	4.0	0.1	10.3	20.3
Oaks Road	0.1	4.4	0.0	0.0	1.6	0.0	6.1	12.3

[34] https://roadtraffic.dft.gov.uk/manualcountpoints/16012
[35] https://roadtraffic.dft.gov.uk/manualcountpoints/27923

Site	Aircraft	Background	Carparks	GSE	Roads	Stationary Sources	Total	Monitored
Difference	0.3	1.3	0.1	0.0	2.4	0.1	4.2	7.3

Green Gates–Harmondsworth

There are other, more puzzling discrepancies associated with Green Gates for winds from northerly sectors, which can be examined most effectively using Green Gates–Harmondsworth differences. Figure 62 presents the difference rose for this site pair. The discrepancy in the westerly sectors has been discussed above using other differences. For the sectors 0° to 90° the model difference in Table 33 is effectively zero whereas the measured difference is 6 µg m^{-3}. Figure 62 show a large discrepancy for all northerly wind sectors. The magnitude of discrepancy is unexplained. Green Gates is too far from the A4 (around 200 m at closest point) and from the M4 (1.5 km) to expect a significant difference contribution from the road network. The nearby Bath Road (nearest edge is 16 m from the monitor) carries little traffic and is unlikely to be the origin of the excess concentration.

Figure 62 The average difference in NO_x concentration (µg m^{-3}) between Green Gates and Harmondsworth as a function of wind direction

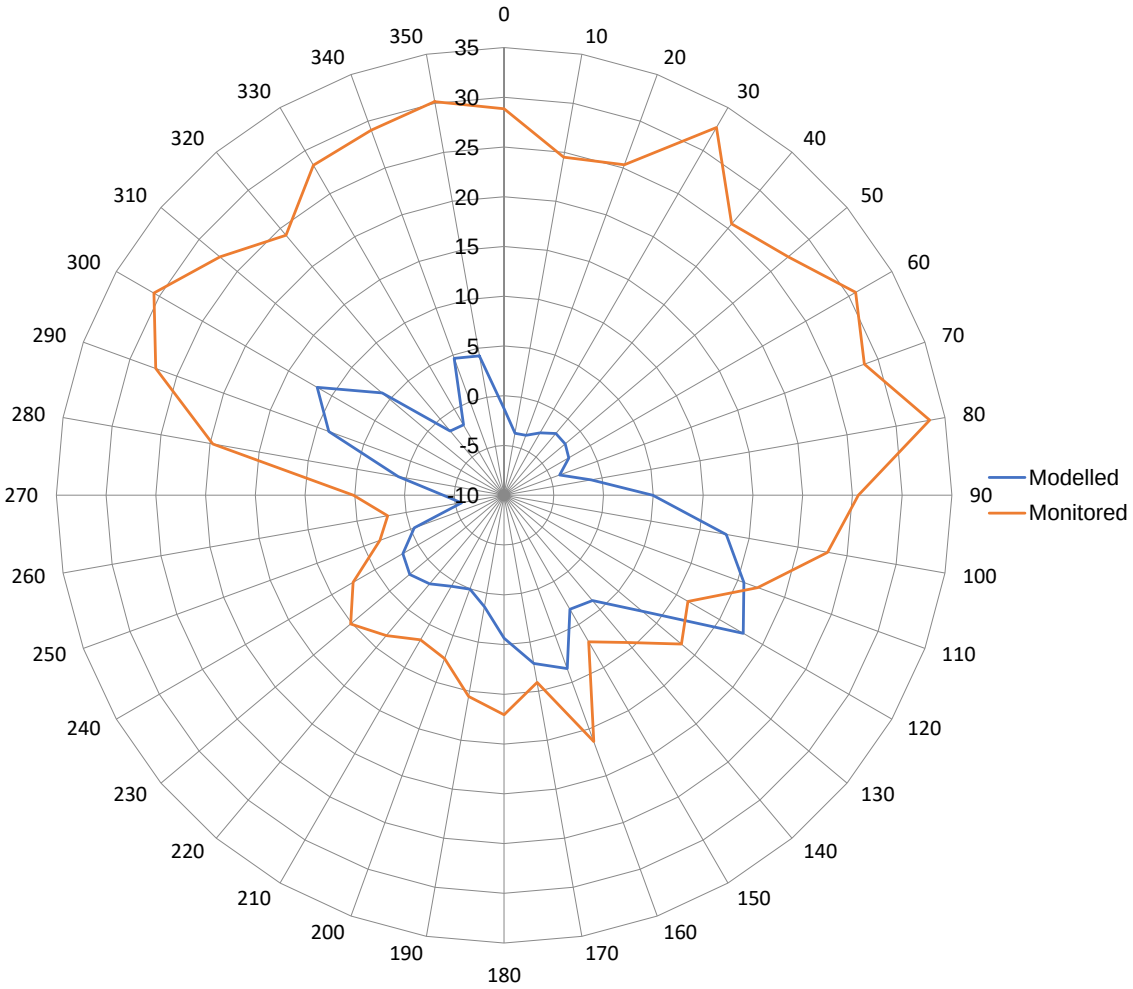

Harmondsworth–Lakeside 2

It is important to identify if the discrepancy at Green Gates in westerly winds arises from a source very local to the site or relates to the contribution from the western parts of the road network in general. To shed light on this, concentration differences were taken between Harmondsworth and Lakeside 2 for westerly wind sectors, restricting the (northerly) angular range to reduce the contribution at Lakeside 2 from the M4 (and A4). The

range 200° to 290° was selected. Figure 63 presents the difference rose for this pair of sites, showing that the model slightly overpredicts the difference over the pertinent angular range. The relevant entry in Table 33 compares the modelled and measured values of the contribution to the annual mean concentration from this sector range, showing that the model overestimates the contribution by 3.2 µg m^{-3}.

Figure 63 The average difference in NO_x concentration (µg m^{-3}) between Harmondsworth and Lakeside 2 as a function of wind direction

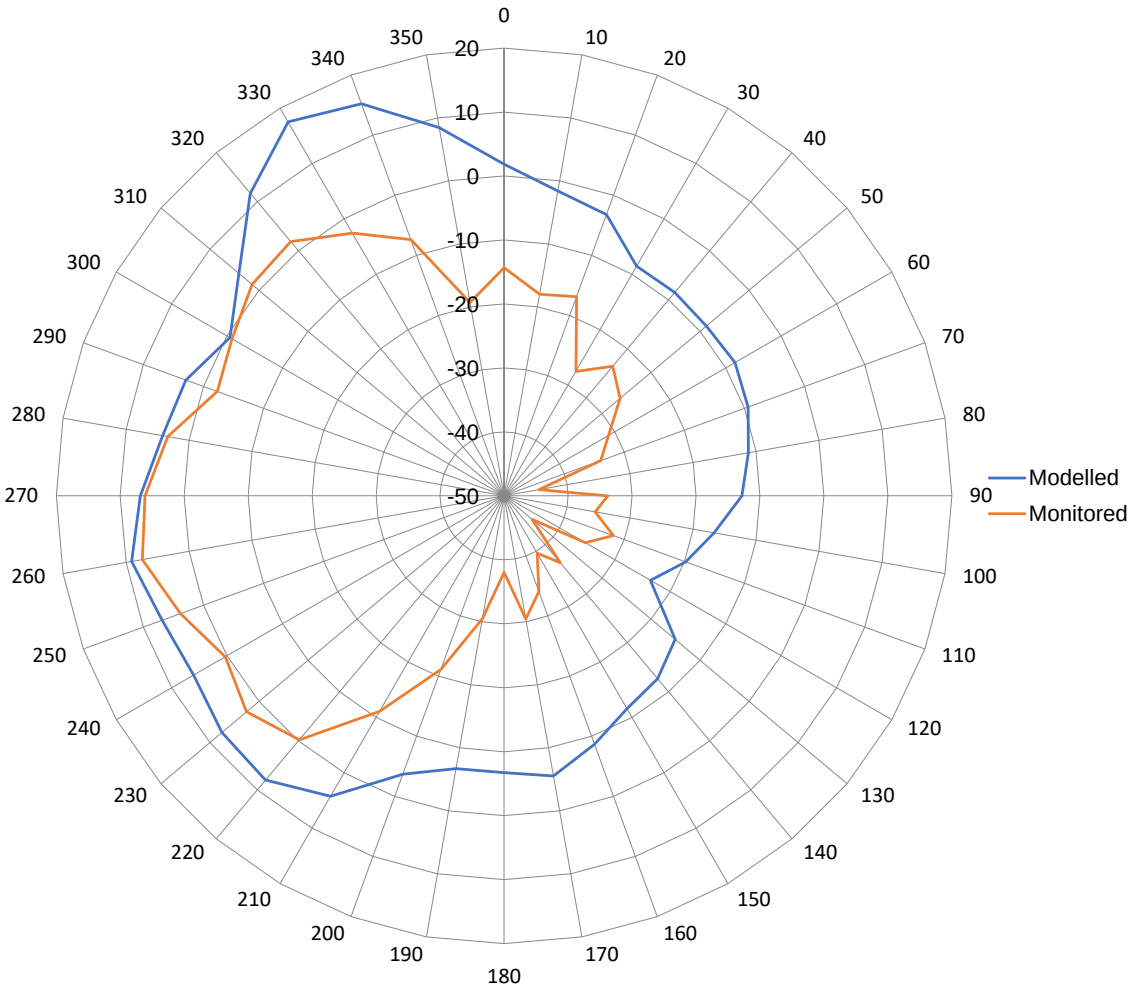

Again, before conclusions can be drawn about the emission factors in current use, the fidelity of the traffic data must be considered. Thus, it would be premature to draw conclusions from the present NO_x concentration comparisons about the performance of current methodologies for estimating road-vehicle emissions in situations where the traffic is well characterised from an emissions perspective.

Oxford Avenue–Oaks Road (road-network contribution)

As noted earlier, besides receiving a substantial contribution to annual mean NO_x concentration from airfield sources, Oxford Avenue is located close to the A4 and receives a moderate contribution from the road network. Choosing the sector range from 90° to 180° avoids the major airfield sources (although includes the long-stay carpark south of Oxford Avenue). Table 38 shows that the road network accounts for 86% of the modelled contribution to annual mean concentration difference for this range of sectors.

Table 38 Breakdown by source category of the contribution to the annual mean Oxford Avenue–Oaks Road NO_x concentration difference from wind direction sectors 90° to 180° inclusive

Site	Aircraft	Background	Carparks	GSE	Roads	Stationary Sources	Total	Monitored
Oxford Avenue	0.1	3.2	0.0	0.0	1.4	0.2	5.0	10.9

Site	Aircraft	Background	Carparks	GSE	Roads	Stationary Sources	Total	Monitored
Oaks Road	0.3	2.8	0.0	0.0	0.5	0.1	3.7	8.0
Difference	-0.2	0.4	0.0	0.0	0.9	0.1	1.3	1.9

The relevant entry in Table 33 shows that the model underpredicts by 44% for this range of sectors, equivalent to an under-prediction of 0.9 µg m^{-3}. Taken together with results quoted earlier for Oxford Avenue–Oaks Road (200°–260°), this suggests that the underestimation of the contribution from the road network for southerly wind sectors (which includes the contribution from the nearby A4) can account for around 2 µg m^{-3} (from Table 26 and Table 33) of the 19.5 µg m^{-3} discrepancy in total annual mean concentrations at Oxford Avenue (Table 25), with the remainder deriving from neither the airport nor the A4 and coming from the north.

LHR2–Harlington

As noted in the earlier discussion of the difference rose for LHR2–Oaks Road, the measured concentration difference shows a strong peak for northeast wind sectors, which requires further investigation. LHR2–Oaks Road is not the best site pair for examining these wind sectors, given that Oaks Road receives a substantial airfield contribution from the relevant sectors, which complicates the interpretation. Thus, a difference site north of the airport is preferable for investigating the contribution from northerly sectors to the annual mean concentration at LHR2. Harlington was chosen for this purpose, and Figure 64 gives the LHR2–Harlington difference rose, clearly showing the excess contribution for northeast sectors and peaking at 50°. For the sector range 270° to 100° (for which the road network dominates the contribution to the annual mean concentration difference), Table 33 shows that the model underestimates the difference contribution by 72%, equivalent to an under-prediction of 17.4 µg m^{-3}. This underestimation of the road-network contribution is more than enough to account for the under-prediction in total annual mean NO_x at LHR2 shown in Table 25.

Figure 64 The average difference in NO_x concentration (µg m^{-3}) between LHR2 and Harlington as a function of wind direction

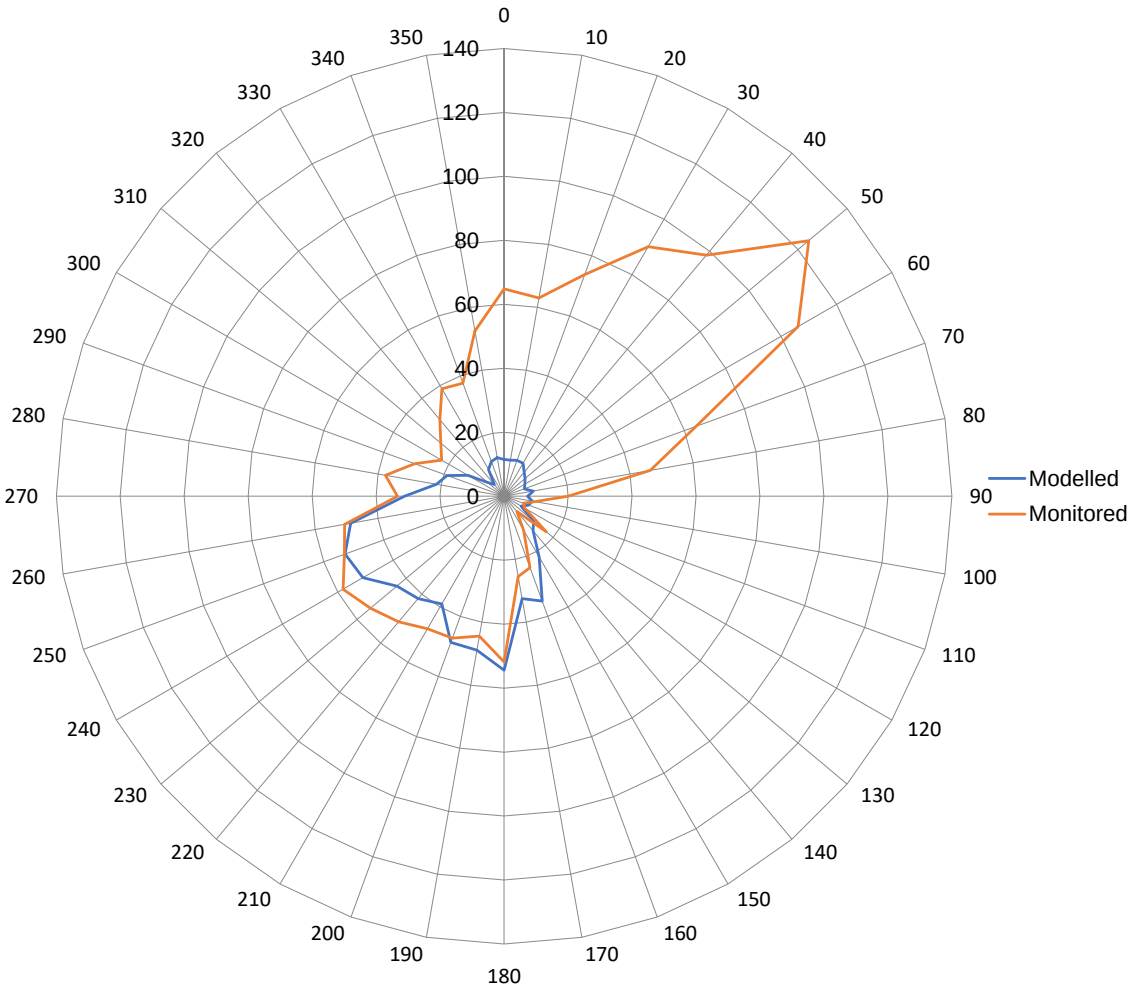

The relatively narrow angular range associated with the excess contribution and the fact that it does not appear for other monitoring sites suggests that it derives from a local source. Although there are several potential sources immediately northeast of LHR2, including carparks and the taxi feeder park, the most likely candidate is traffic on the Northern Perimeter Road (NPR), around the (signalised) junction with Neptune Rd.

Traffic queues were not explicitly recognised in the traffic data set available for this study. Instead, inventory junction delays were incorporated into the effective speed associated with the road link. This procedure does not necessarily lead to underestimation of total emissions on the link, but it does redistribute any increased emissions arising at/near junctions along the whole link. In the case of LHR2, this would reduce the modelled concentrations at the site. Such considerations indicate that detailed model–monitoring comparisons at sites close to road junctions require particular attention to how junction delays are to be represented from an air quality perspective.

Hayes–Cranford

The Hayes site has a large discrepancy between modelled and measured annual mean NO_x concentrations, according to Table 25 (−53.2 µg m^{-3}). To investigate the road-network contribution to this discrepancy, concentration differences between the Hayes and Cranford sites were examined. A site north of the airport was (marginally) preferred to Oaks Road as the difference site because of the north/south gradient in the NAEI contribution, although it restricts the angular range available to avoid the airfield contribution at Cranford.

Figure 65 gives the Hayes–Cranford difference rose, showing that the model significantly underestimates the difference for all sectors, but particularly so for southerly and easterly sectors, when the wind blows from the adjacent junction between the North Hyde Road and North Hyde Gardens towards the monitoring site. Restricting attention to sectors less than 220° to avoid the airfield contribution at Cranford, Table 33 compares the modelled and measured contribution to the annual mean concentration difference from the sectors 90° to

210°. The model underestimates the contribution by 74%, equivalent to 16.9 µg m^{-3}. It can be inferred, therefore, that the under-prediction of the contribution from all southerly sectors broadly speaking accounts for around a third of the total discrepancy in annual mean concentration at Hayes, with the remaining two-thirds deriving from northerly sectors.

Figure 65 The average difference in NO_x concentration (µg m^{-3}) between Hayes and Cranford as a function of wind direction

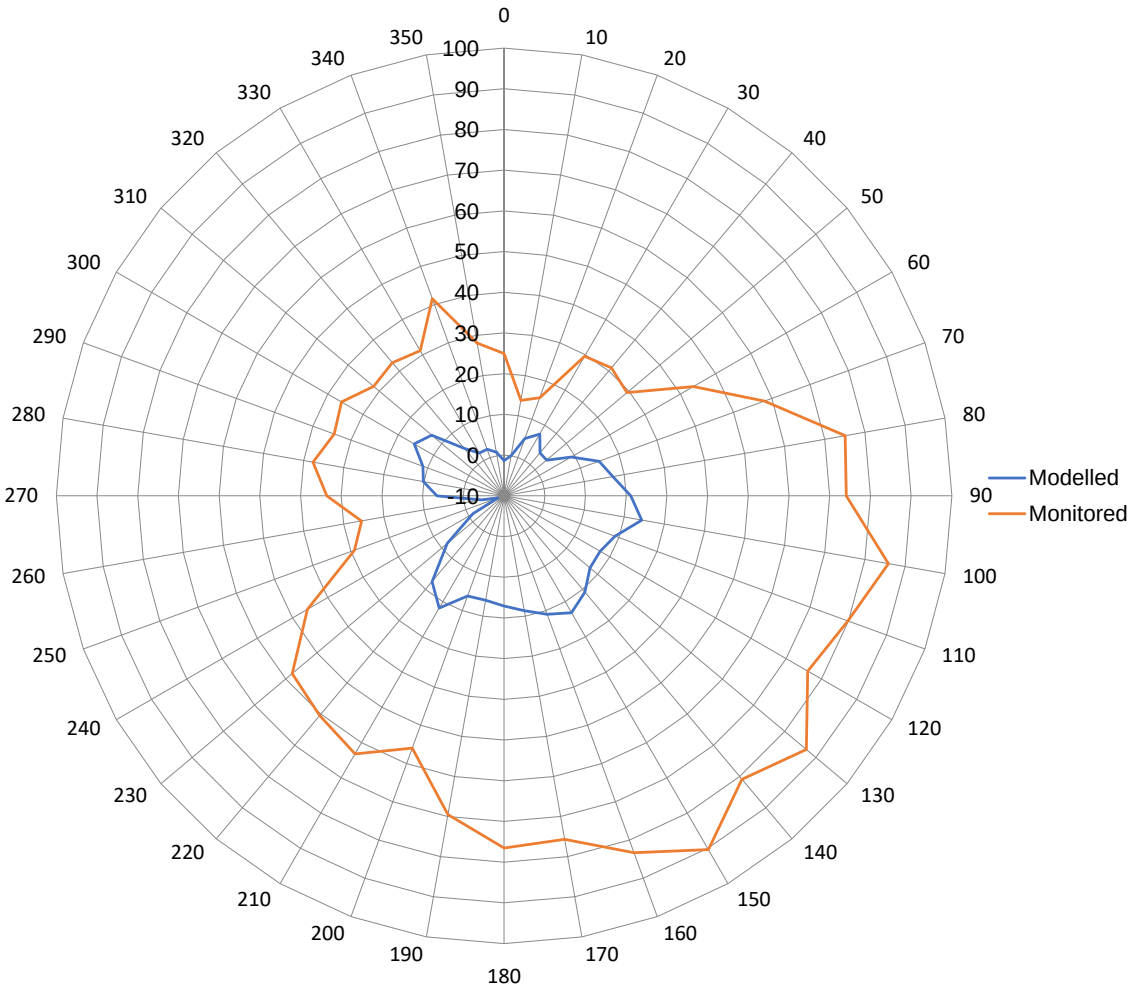

The location of the Hayes monitor is challenging from an air quality modelling perspective, situated at the kerbside of the North Hyde Road and on the junction with North Hyde Gardens. Table 39 compares measured and modelled traffic flows on North Hyde Road. The model significantly underpredicts the number of HGVs and buses and coaches. There is no information on the fidelity of the modelled traffic flows on North Hyde Gardens, nor on the accuracy of modelled traffic speeds on either road link. Earlier comments about the modelling of junction delays apply here also.

Table 39 Comparison of measured[36] and modelled traffic flows on North Hyde Road

	Direction	Motorcycles	Cars and taxis	Buses and coaches	LGVs	HGVs	All motor vehicles
Traffic model	Eastbound	368	63397	188	10619	2981	77554
	Westbound	369	65203	169	11036	2978	79755
	2 Way	738	128600	357	21655	5959	157309
DfT	2 Way	999	131399	955	20237	8217	161807

ROAD-NETWORK ADJUSTMENT FACTOR FOR NO_X

One aim of the modelling study, besides evaluating model performance, is to generate contours of total annual mean NO_2 concentration to gauge the spatial extent of any residential areas in which the concentration exceeded the limit value of 40 µg m^{-3}. If the model reproduces well the concentrations at the monitoring sites, this process can be viewed as an 'intelligent' way of interpolating and extrapolating from the measured data, guided by an understanding of source contributions, to generate the best estimate of the overall spatial distribution of concentration.

The difficulty that arises in the present study, therefore, is the evidence for a consistent underestimation of the contribution from the road network. Concentration contours derived from the raw modelling results, therefore, will underestimate NO_x concentrations and thus the extent of any NO_2 exceedance area.

A procedure has been devised that seeks to make best use of the information currently available to estimate the NO_x concentration field within the study area. This procedure attributes the non-zero average fractional discrepancy across the monitoring sites entirely to an underestimation of the road network (and background roads) contribution everywhere within the area. Thus, an adjustment factor is applied uniformly to the road network (and background roads) contribution at all points, with the magnitude chosen so that the average fractional discrepancy in total annual mean NO_x concentrations across the continuous monitoring sites reduces to zero. Applying an adjustment in this form automatically generates a larger absolute change in concentrations at sites close to roads, which is consistent with the results of the evaluation.

The required factor is found to be 1.6435, i.e., the modelled road-network contribution is increased by 64% everywhere in the study area. This compares with a factor of 1.385 which was the result of the 2013 modelling evaluation. The resulting scatter plot is shown in Figure 66. After application of the scaling factor, the correlation between modelled and measured values increases slightly from 0.69 to 0.78. It cannot be ruled out that this adjustment of the road-network contribution may be partly compensating for a systematic over- or under-prediction of the NAEI/background contribution, given that the combined contribution from these components is only slowly varying across the study area so cannot be readily evaluated by difference analysis. However, this additional uncertainty is intrinsic to the simple scaling approximation.

[36] https://roadtraffic.dft.gov.uk/manualcountpoints/811130

Figure 66 Effect on NO_x scatter plot of including the road-network scaling factor.

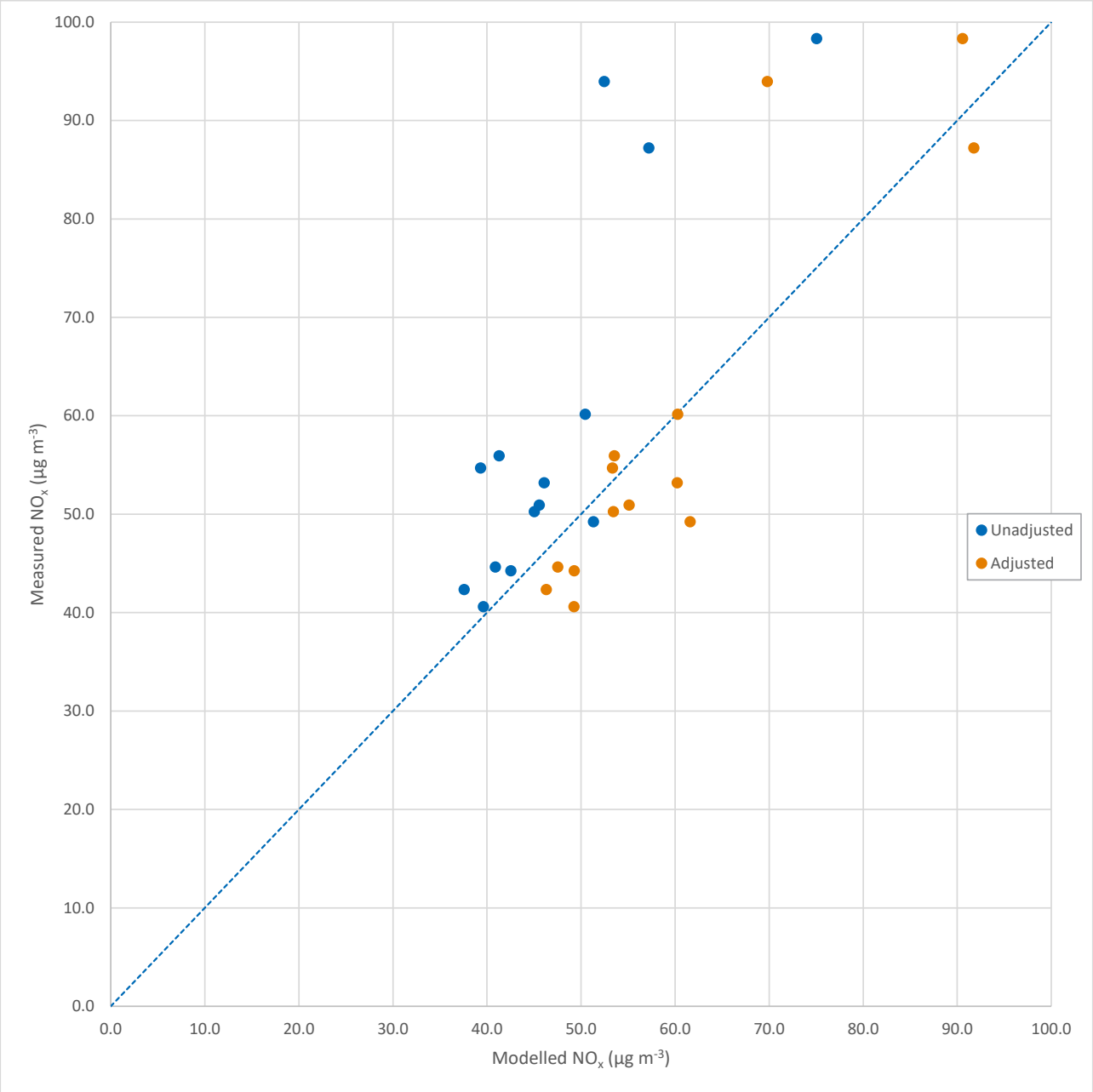

Although the average discrepancy across the sites has been reduced to zero, this does not imply that there cannot be a systematic spatial variation in the residual discrepancy across the study area.

The above simple scaling adjustment is unlikely to remove all the discrepancy relating to the road network at sites such as Hayes and LHR2, but at least some of the discrepancy at these sites is likely to be due to features specific to the site and not necessarily generalisable to other receptor locations. Nevertheless, the adjusted NO_x concentration field may underestimate concentrations at near-road receptor locations that are strongly influenced by traffic queuing at junctions or are situated close to areas of the network subject to other types of flow disruption.

Figure 67 to Figure 74 show the impact of applying the road-network scaling factor on the concentration difference roses. For most pairs of sites, the adjustment leads to a substantial improvement in the agreement between modelled and measured differences. However, as expected, the scaling does not explain the puzzling discrepancies associated with Green Gates for winds from northerly sectors (Figure 70), nor does it explain the discrepancies associated with sources immediately northeast of LHR2 (the relatively narrow angular range seen in Figure 73).

Turning to Figure 71, the difference rose for Harmondsworth–Lakeside 2, for easterly winds, where Lakeside 2 is influenced by emissions from the M25, the scaling shows an improvement in the agreement between modelled and measured differences. However, this is not the case for westerly winds.

Finally, as suggested previously, the scaling only partially explains the discrepancies associated with Hayes (Figure 74), reinforcing the view that the location of the Hayes monitor is challenging from an air quality modelling perspective.

Figure 67 Effect of including the road-network scaling factor on the average difference in NO_x concentration (µg m^{-3}) between Hillingdon and Harmondsworth as a function of wind direction.

Unadjusted

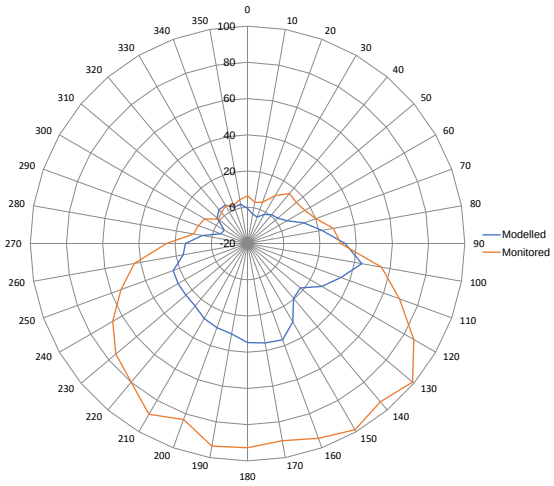

Adjusted

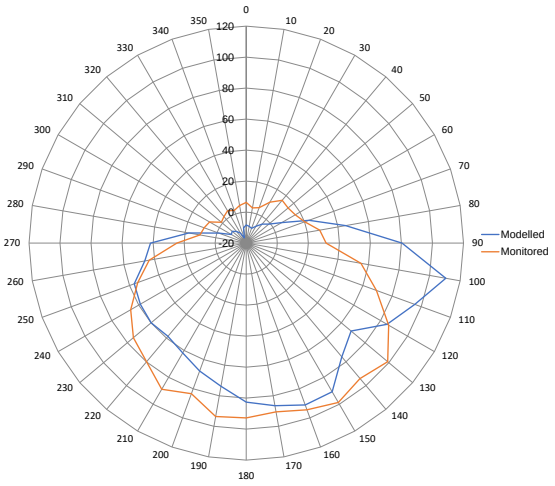

Figure 68 Effect of including the road-network scaling factor on the average difference in NO_x concentration (µg m^{-3}) between Hillingdon and Harlington as a function of wind direction.

Unadjusted

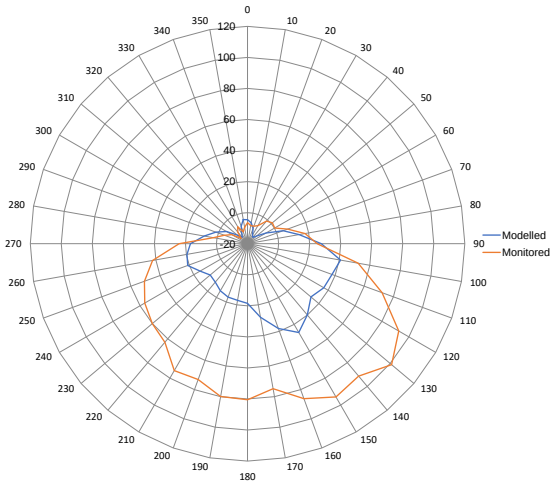

Adjusted

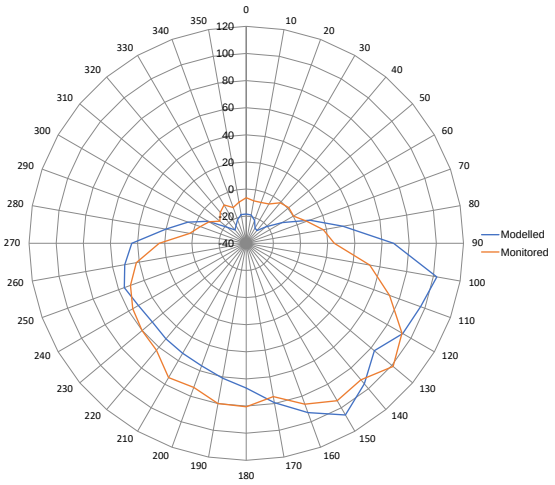

Figure 69 Effect of including the road-network scaling factor on the average difference in NO_x concentration (µg m^{-3}) between Green Gates and Oaks Road as a function of wind direction.

Unadjusted

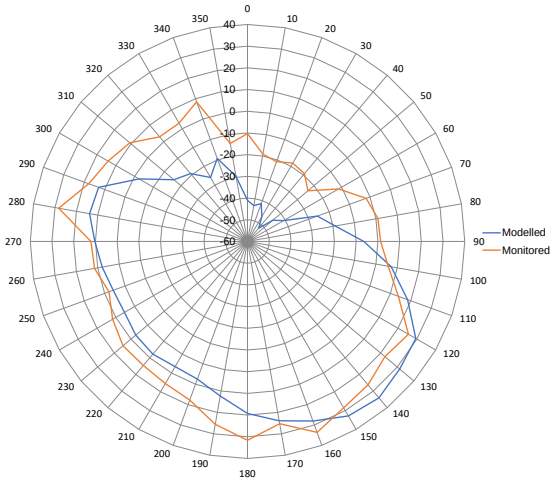

Adjusted

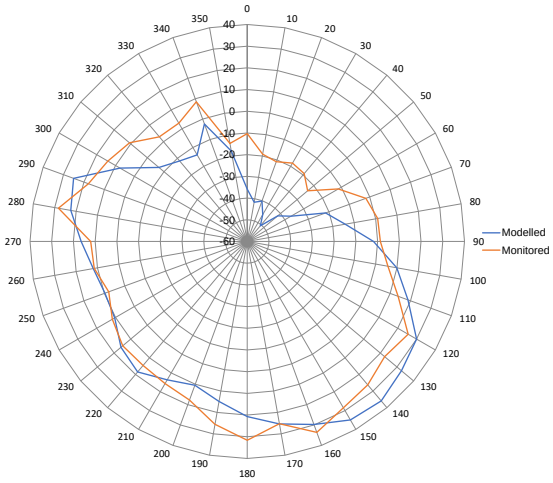

Figure 70 Effect of including the road-network scaling factor on the average difference in NO_x concentration (µg m^{-3}) between Green Gates and Harmondsworth as a function of wind direction.

Unadjusted

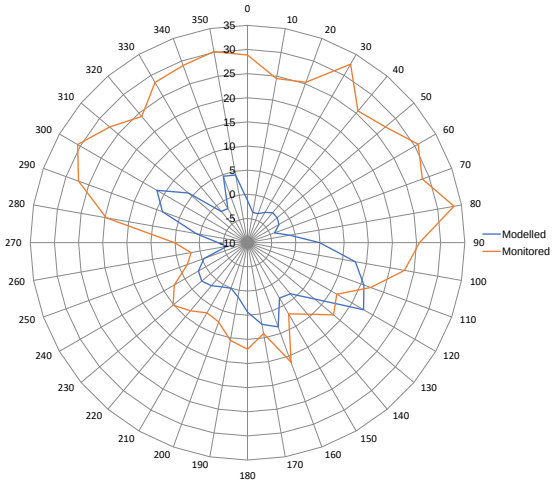

Adjusted

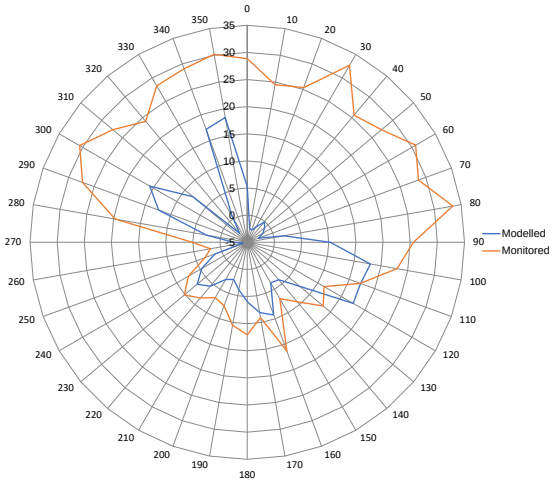

Figure 71 Effect of including the road-network scaling factor on the average difference in NO_x concentration (µg m^{-3}) between Harmondsworth and Lakeside 2 as a function of wind direction.

Unadjusted

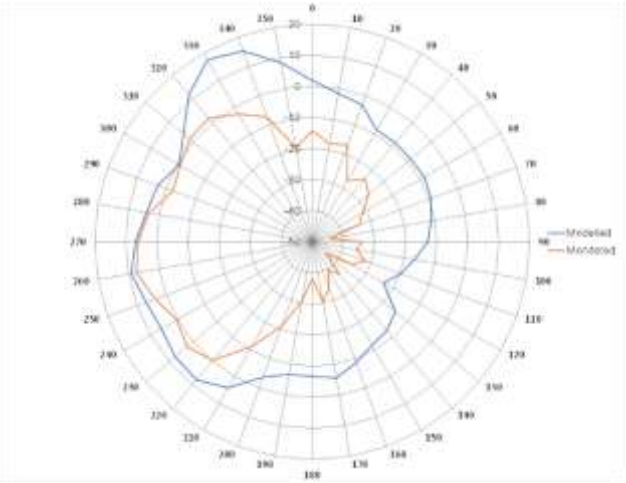

Adjusted

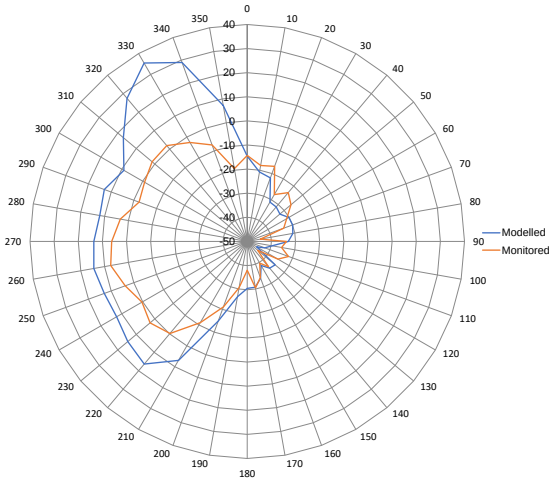

Figure 72 Effect of including the road-network scaling factor on the average difference in NO_x concentration (µg m^{-3}) between Oxford Avenue and Oaks Road as a function of wind direction.

Unadjusted

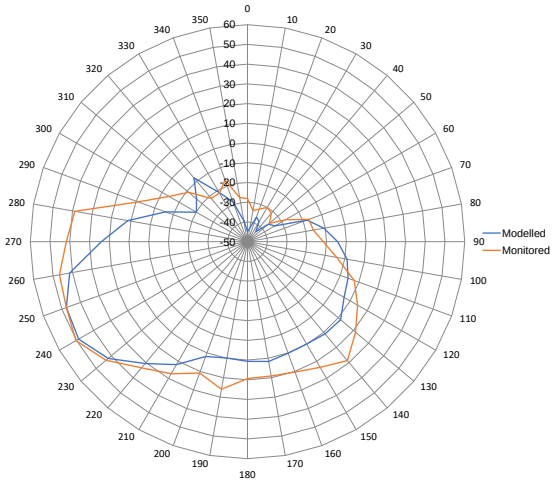

Adjusted

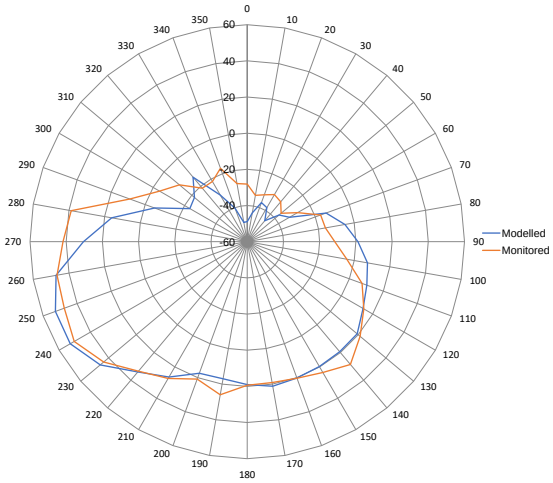

Figure 73 Effect of including the road-network scaling factor on the average difference in NO_x concentration (µg m^{-3}) between LHR2 and Harlington as a function of wind direction.

Unadjusted

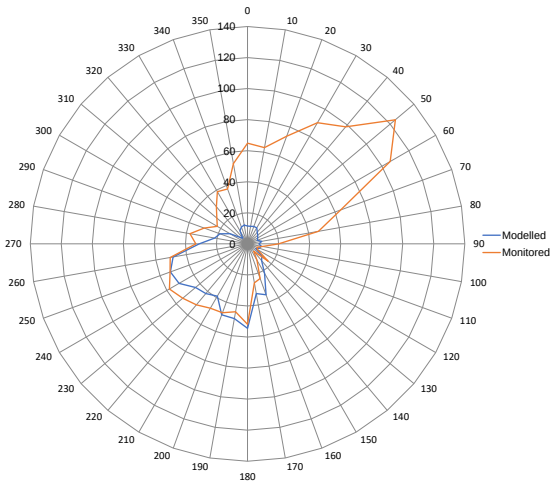

Adjusted

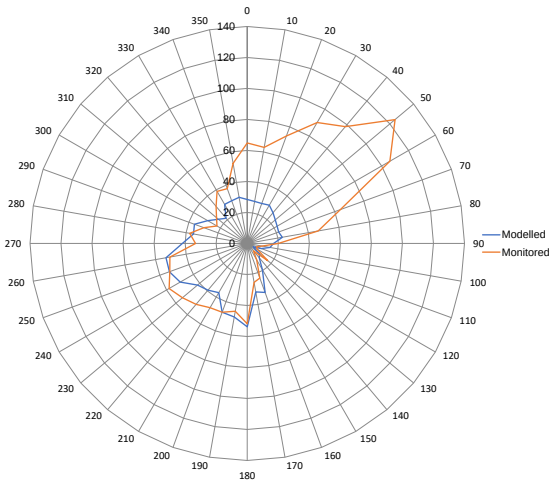

Figure 74 Effect of including the road-network scaling factor on the average difference in NO_x concentration (µg m^{-3}) between Hayes and Cranford as a function of wind direction.

Unadjusted

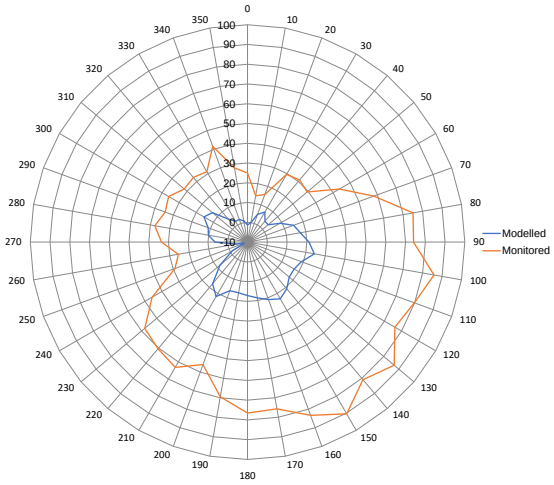

Adjusted

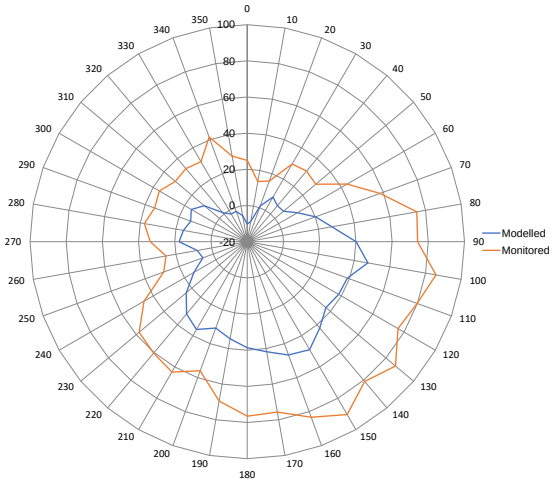

CONTOURS OF ANNUAL MEAN NO_X CONCENTRATION

Contours of annual mean NO_x concentration after applying the road-network adjustment factor discussed above are shown in Figure 75. Figure 76 shows the equivalent results without applying the road-network adjustment factor, to enable the impact of the adjustment to be visualised.

Figure 75 Modelled annual mean NO_x concentration (µg m^{-3}) (with adjusted roads contribution)

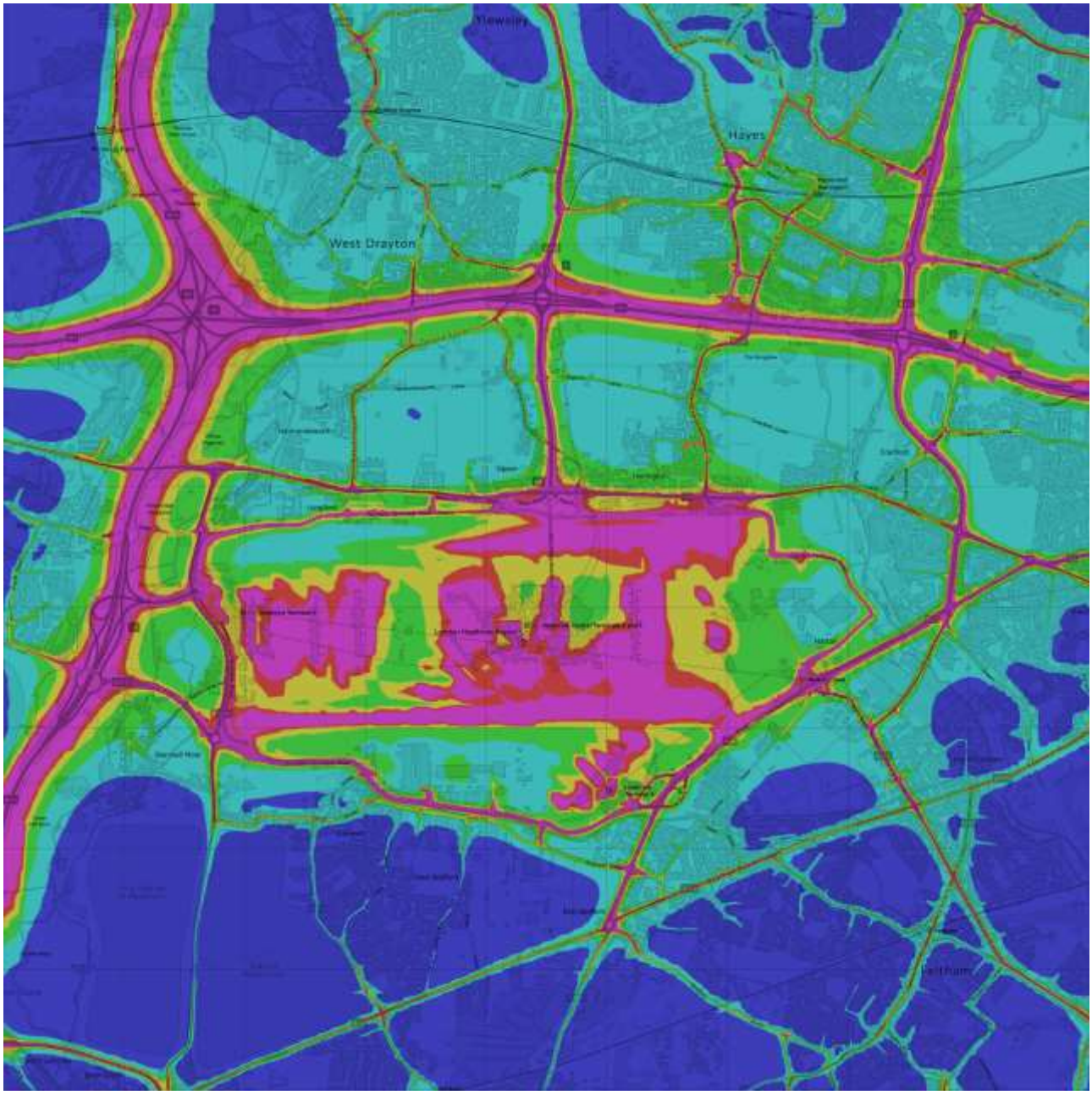

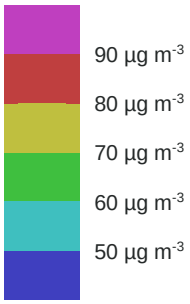

Figure 76 Modelled annual mean NO_x concentration (µg m^{-3}) (with unadjusted roads contribution)

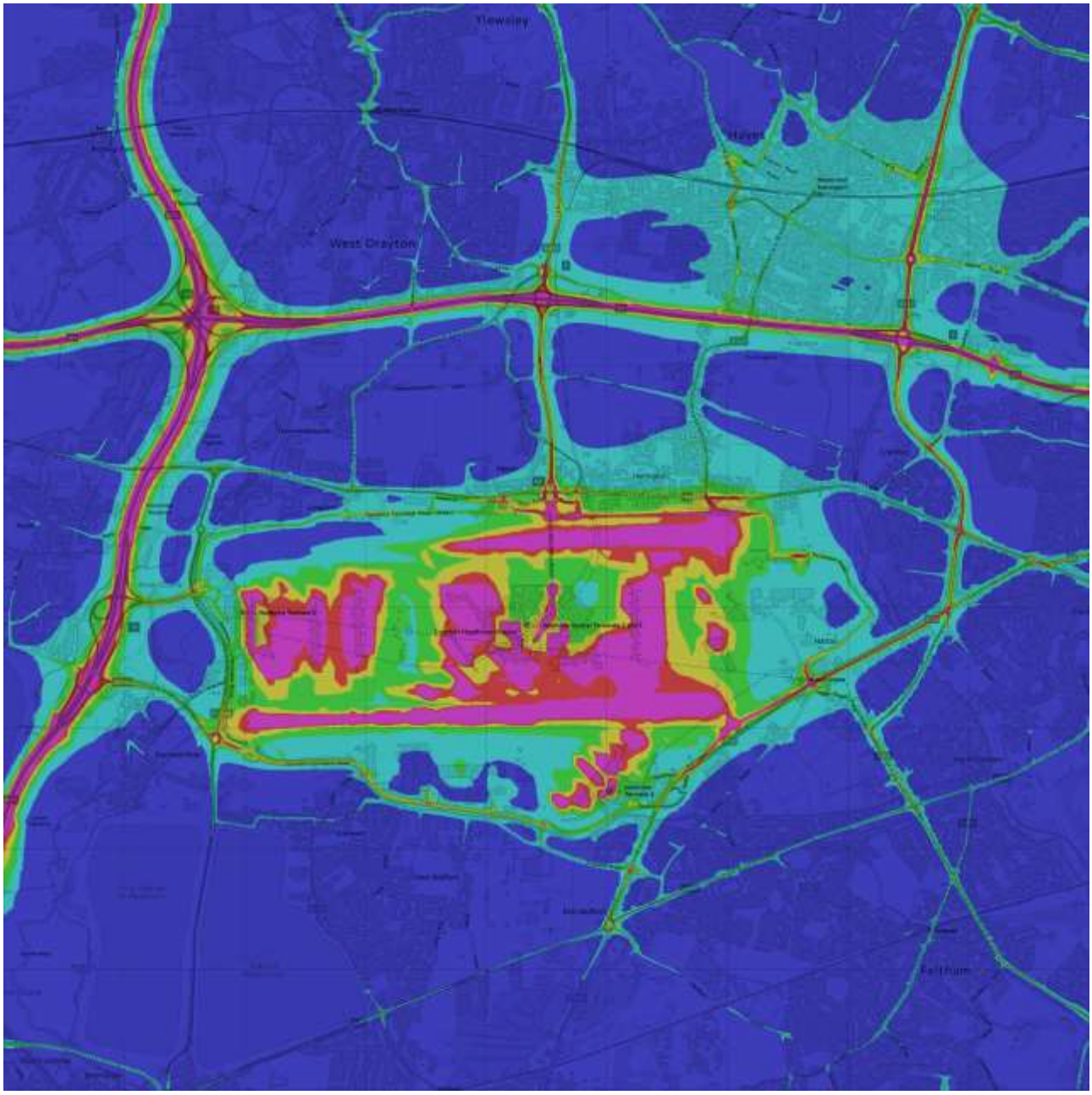

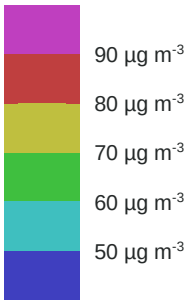

It should be noted that the spatial representation of sources has been judged in relation to the impact on off-airport concentrations, so spatial variations within the body of the airport are less reliable. In particular, the chosen spacing of the discrete jet sources on the runway and taxiways should be borne in mind. Also, the density of the grid receptor points results from a compromise between model run time and the smoothness of

contours, so that some features of the contour shapes at the sub-100 m scale may be artefacts of the finite resolution of the grid.

NO_2

OXIDANT LEVELS USED TO DERIVE NO2 CONCENTRATIONS

The concentration of NO_2 depends on the concentration of NO_x in a complex way, involving the chemical interaction of NO, NO_2 and ozone. The Jenkin model used in the 2013 assessment was retained for the 2019 assessment. The Jenkin model uses a procedure for estimating the interaction using the concentration of background oxidant as a parameter. Current recommendations from Defra indicate that background oxidant levels are falling and therefore the oxidant levels were updated based on local monitoring data from London Hillingdon and London Harlington. Once the total oxidant (the sum of the NO_2 and O_3 concentrations) level is calculated, the primary modelled NO_2 must be removed to avoid double counting. This resulted in estimated background oxidant concentrations around Heathrow to be 28.5 ppb (adjusted roads) and 32.6 ppb (unadjusted roads). The values used for the 2013 assessment for background oxidant were 31.8 ppb (adjusted roads) and 33.9 (unadjusted roads). It should be noted that the lower the background oxidant level the lower the resulting NO_2 concentrations will be (as the oxidant level acts as a limit to the amount of oxidation that can occur).

ANNUAL MEAN NO_2 CONCENTRATIONS

Table 40 compares the modelled and measured annual mean NO_2 concentrations. The model results are shown both with and without the application of the NO_x road-network scaling factor discussed earlier.

Table 40 Comparison of modelled and measured annual mean NO_2 concentrations (µg m^{-3})

Site	Without roads adjustment factor			With roads adjustment factor		
	Modelled	Measured	Bias (%)	Modelled	Measured	Bias (%)
Green Gates	26.0	30.6	-15.1	29.0	30.6	-5.3
LHR2	38.6	42.5	-9.1	40.6	42.5	-4.5
Oaks Road	25.5	26.3	-3.0	25.8	26.3	-1.8
Harmondsworth	25.0	23.7	5.2	26.9	23.7	13.3
Hayes	30.7	41.2	-25.3	35.1	41.2	-14.9
Oxford Avenue	29.7	33.1	-10.3	30.8	33.1	-7.0
Sipson	27.5	29.7	-7.4	28.4	29.7	-4.4
Cranford	26.1	26.9	-3.1	26.3	26.9	-2.2
Feltham	27.9	29.1	-3.9	31.2	29.1	7.4
Hatton Cross	30.1	27.9	7.9	31.3	27.9	12.3
Harlington	27.6	30.7	-10.1	29.0	30.7	-5.7
Hillingdon	34.0	44.7	-23.9	45.3	44.7	1.4
Colnbrook	23.9	24.5	-2.5	25.5	24.5	4.1
Lakeside 2	25.1	27.6	-9.1	29.2	27.6	5.8
Average			**-7.8**			**-0.1**
Standard deviation			**9.4**			**7.9**

Before applying the roads adjustment factor, the average fractional discrepancy in the NO_2 concentration (defined as *(modelled−measured)/measured*) is −8.2% (with a standard deviation of 9.6%), i.e., the model underestimates on average by 8.2%. After applying the roads scaling factor, the average fractional discrepancy is 3.5% (standard deviation 9.8%). Neither of these values of average fractional discrepancies can be interpreted as a significant model bias.

Figure 77 shows a scatter plot of modelled versus measured annual mean NO_2 concentrations, both with and without the application of the road-network scaling factor. The correlation coefficient is 0.70 without application of the road-network adjustment factor and 0.84 including the factor.

Figure 77 Scatter plot of modelled versus measured annual mean NO_2 concentrations, before and after applying road-network NO_x adjustment factor

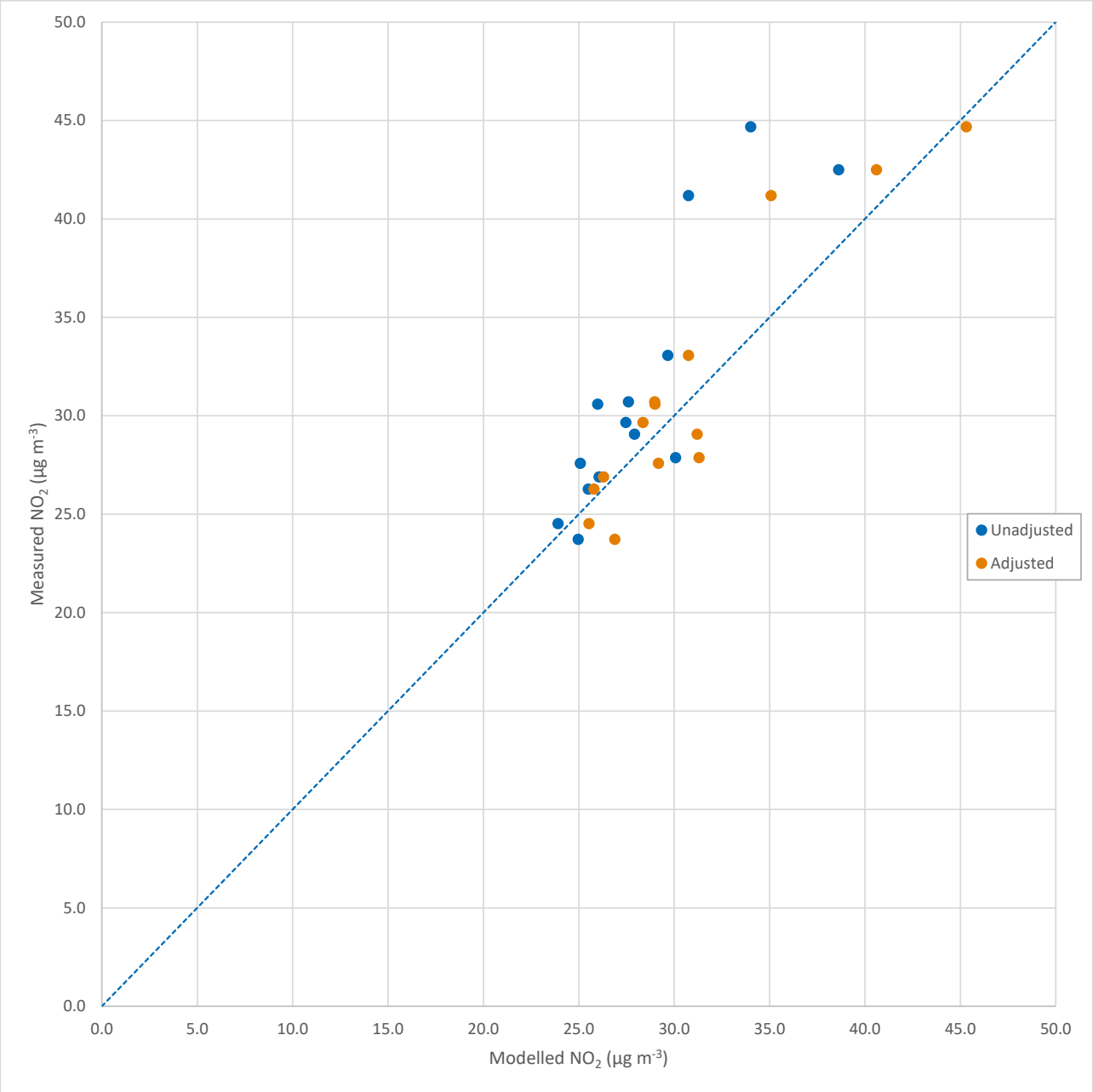

NO_2/NO_X RATIOS

The NO_2 comparison reflects partly the underlying NO_x comparison, whereas a comparison of NO_2/NO_x ratios provides a more specific test of the Jenkin methodology for deriving annual mean NO_2 concentrations from annual mean NO_x concentrations (although this test does not remove entirely the dependence on the absolute NO_x values because of the non-linearity of the relationship). Table 41 shows the modelled and measured values of this ratio, both with and without the roads scaling factor. Before applying the roads adjustment, the modelled ratios range from 0.55 to 0.68 across the sites, with the measured ratios ranging from 0.43 to 0.61. After adjustment, the modelled ratios range from 0.45 to 0.55.

Table 41 Comparison of annual mean NO_2/NO_x ratios

Site	Without roads adjustment factor			With roads adjustment factor		
	Modelled	Measured	Difference (%)[1]	Modelled	Measured	Difference (%)[1]
Green Gates	0.63	0.55	15.0	0.54	0.55	-1.0
LHR2	0.51	0.43	19.1	0.45	0.43	3.7
Oaks Road	0.62	0.59	5.9	0.54	0.59	-7.8
Harmondsworth	0.63	0.58	7.9	0.55	0.58	-6.6
Hayes	0.59	0.44	33.7	0.50	0.44	14.6
Oxford Avenue	0.59	0.55	7.0	0.51	0.55	-7.2
Sipson	0.61	0.59	3.4	0.53	0.59	-10.0
Cranford	0.61	0.61	0.8	0.53	0.61	-12.1
Feltham	0.61	0.55	10.9	0.52	0.55	-5.1
Hatton Cross	0.59	0.57	3.5	0.51	0.57	-10.2
Harlington	0.61	0.60	0.5	0.53	0.60	-12.8
Hillingdon	0.59	0.51	16.0	0.49	0.51	-3.6
Colnbrook	0.64	0.58	9.9	0.55	0.58	-4.8
Lakeside 2	0.64	0.50	26.5	0.55	0.50	8.4
Average			11.4			-3.9
Standard deviation			9.8			8.0

[1] Fractional Discrepancy = 100 * (modelled−measured) / measured

Without the roads adjustment factor, the average fractional discrepancy in the NO_2/NO_x ratios is 11.6% (i.e., the model on average overestimates the ratio by 11.6%) with a standard deviation of 10.1%. After adjustment, there is an average underestimation to 1.5% (standard deviation 8.9%). This level of agreement is within what is expected from the (semi-empirical) Jenkin methodology, judging from the scatter on the data points used to derive the underlying $[NO_2]/[OX]$ relationship. Thus, the results indicate that the Jenkin methodology does not introduce any significant bias into the model results, so that once the bias in NO_x concentrations has been removed no further model adjustment is necessary.

ANNUAL MEAN NO_2 CONTOUR PLOTS

As noted earlier for NO_x, although the primary purpose of the modelling study was to provide a basis for model evaluation, a subsidiary aim was to provide a more complete picture of the spatial variation in near-airport concentrations in 2019 than available from monitoring data alone.

Figure 78 shows contours of modelled annual mean NO_2 concentration on a map background, with the NO_2 concentrations derived from NO_x results that include the roads adjustment factor. For comparison, Figure 79 shows the equivalent results based on the NO_x concentration values without the roads adjustment factor.

Figure 78 Modelled annual mean NO_2 concentration (µg m^{-3}) (using adjusted roads NO_x contribution)

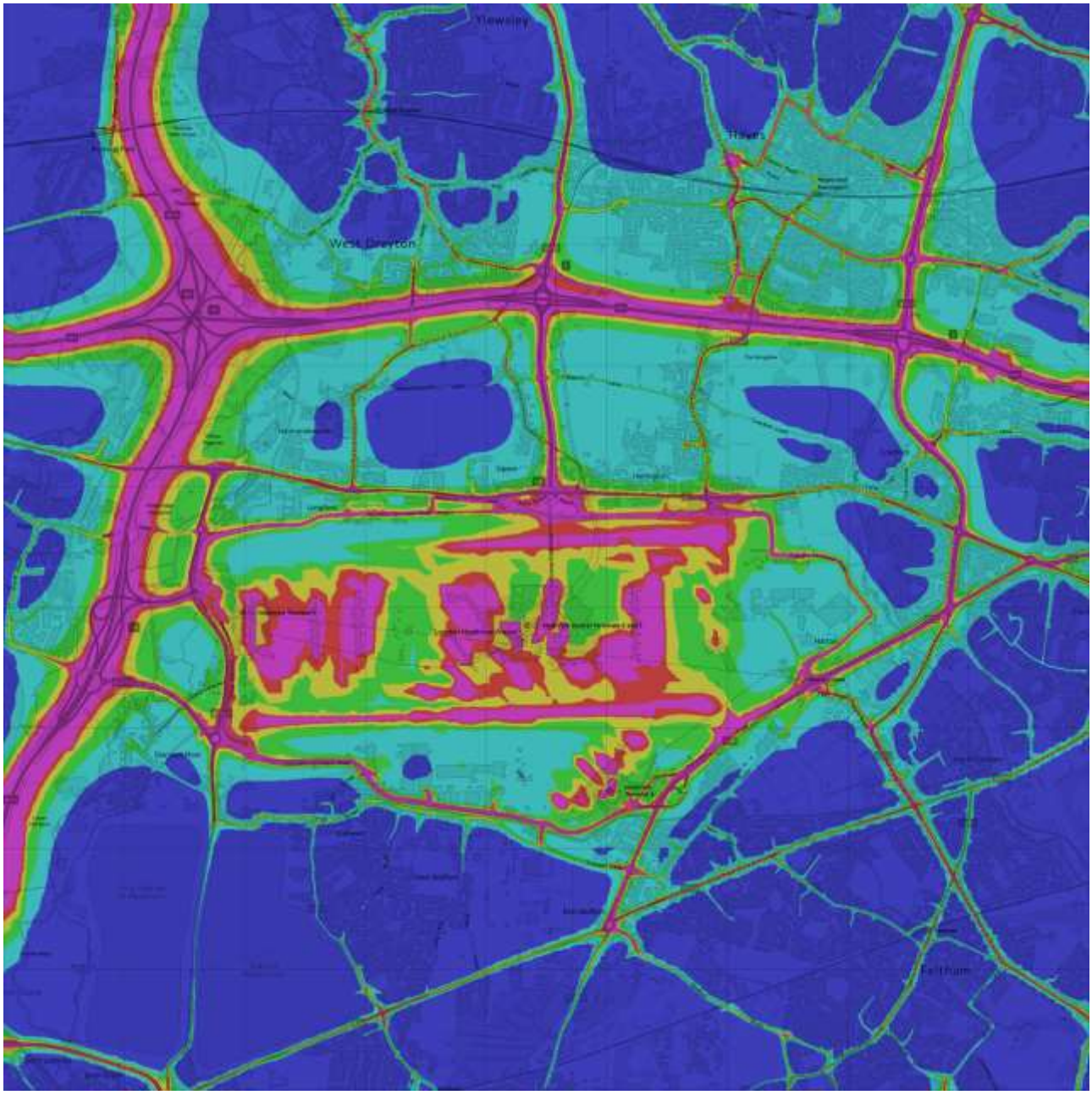

44 µg m^{-3}

40 µg m^{-3} (the annual mean limit value for NO_2)

36 µg m^{-3}

32 µg m^{-3}

28 µg m^{-3}

Figure 79 Modelled annual mean NO_2 concentration (µg m^{-3}) (using unadjusted roads NO_x contribution)

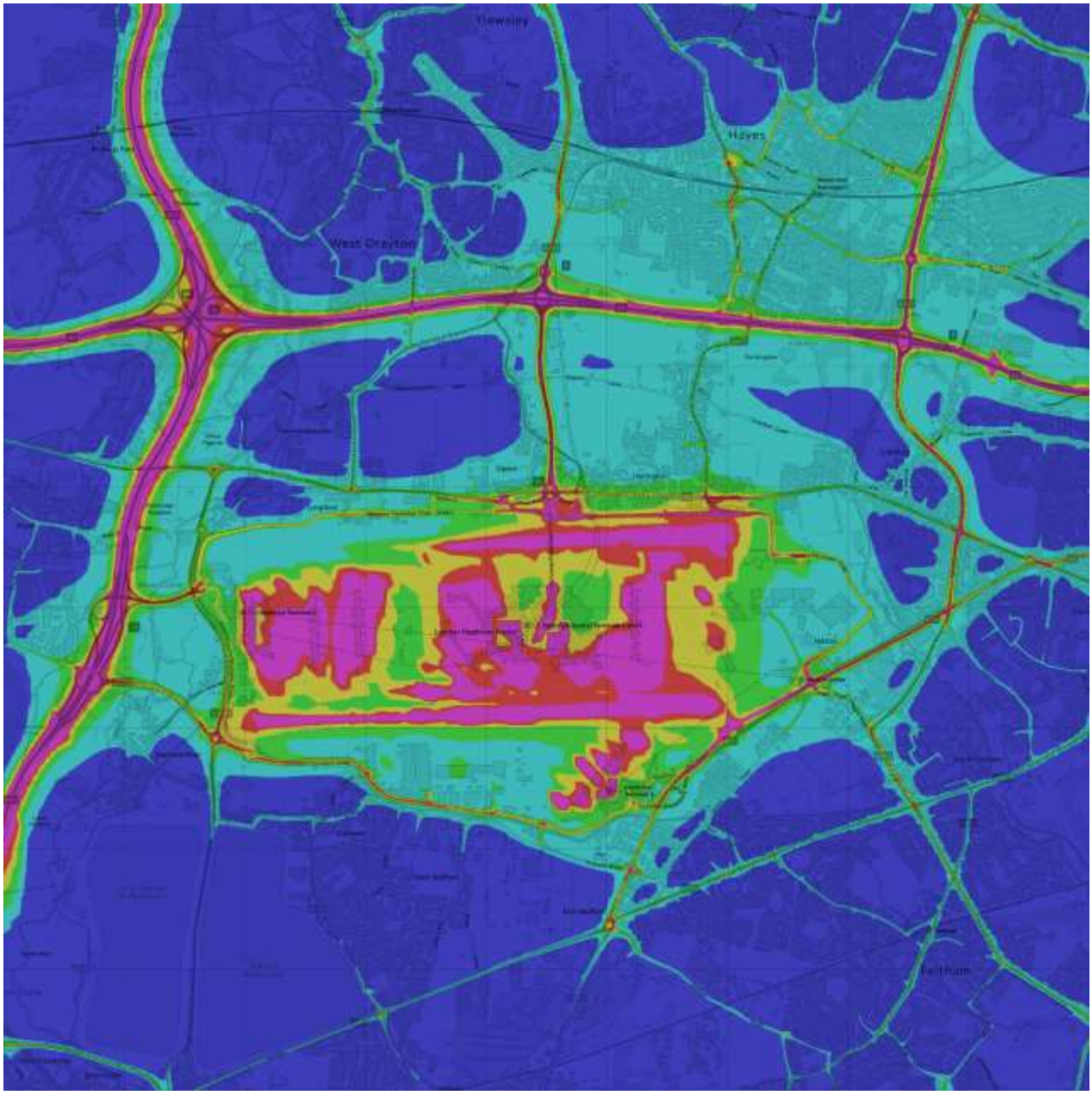

44 µg m^{-3}

40 µg m^{-3} (the annual mean limit value for NO_2)

36 µg m^{-3}

32 µg m^{-3}

28 µg m^{-3}

The 40 µg m^{-3} contour should be taken as indicative of areas vulnerable to exceedance, but the grid results may not have the spatial resolution to determine if individual receptor locations close to the contour are within or outside the exceedance area, which would require closer investigation on a receptor-by-receptor basis. The

limitations of the NO_2 contour plots in relation to spatial resolution are similar to those discussed earlier for the NO_x contours.

PM_{10}

TOTAL ANNUAL MEAN

Table 42 compares the modelled total annual mean PM_{10} concentrations at the continuous PM_{10} analysers with the measured values. It also shows the breakdown of the modelled total by source category. The average fractional discrepancy between modelled and measured total annual mean PM_{10} concentrations is 24.4%, with a standard deviation of 23.7% (14 sites). Figure 80 shows a scatter plot of modelled versus measured annual mean PM_{10} concentrations. The correlation coefficient including all data points is quite low at 0.55.

Figure 80 Scatter plot of modelled versus measured annual mean PM_{10} concentrations.

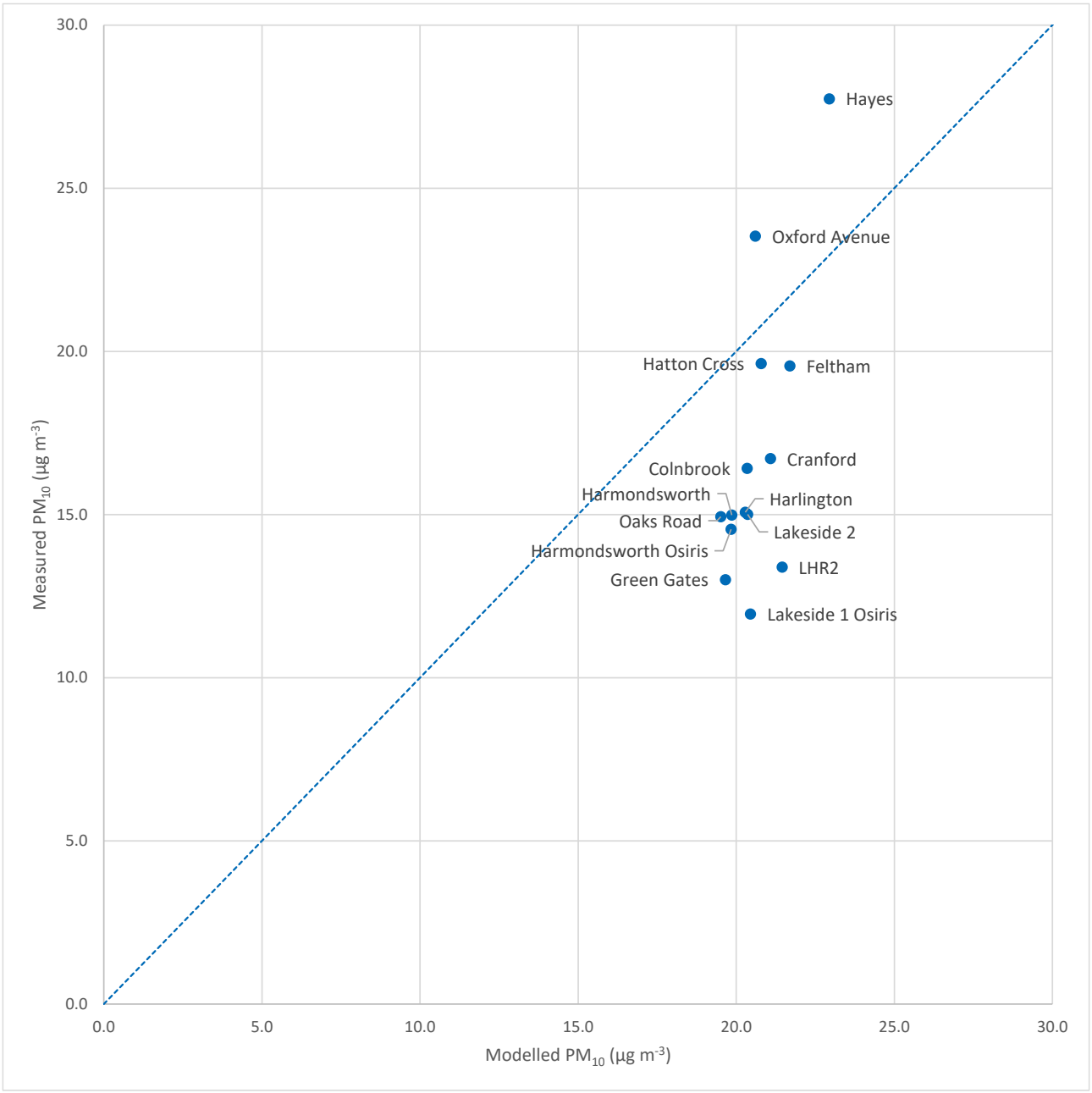

Table 42 Comparison of modelled annual mean PM_{10} concentrations with measured values for continuous PM_{10} analysers

Receptor name	Modelled annual mean PM_{10} concentration (µg m^{-3})							Measured PM_{10} (µg m^{-3})	Model bias (%)
	Aircraft	Background	Carparks	GSE	Roads	Stationary sources	Total		
Green Gates	0.2	18.1	0.0	0.0	0.6	0.0	19.0	13.0	46.1
LHR2	0.7	18.8	0.0	0.1	1.0	0.1	20.7	13.4	54.6
Oaks Road	0.2	18.4	0.0	0.0	0.4	0.1	19.0	14.9	27.4
Harmondsworth	0.1	18.7	0.0	0.0	0.4	0.0	19.3	15.0	28.7
Harmondsworth Osiris	0.1	18.8	0.0	0.0	0.4	0.0	19.3	14.5	32.6
Hayes	0.1	21.3	0.0	0.0	1.0	0.0	22.4	27.7	-19.2
Oxford Avenue	0.3	19.0	0.0	0.0	0.6	0.1	20.1	23.5	-14.5
Cranford	0.1	20.0	0.0	0.0	0.4	0.1	20.6	16.7	23.5
Feltham	0.1	20.2	0.0	0.0	0.8	0.1	21.2	19.6	8.3
Hatton Cross	0.5	18.9	0.0	0.0	0.6	0.1	20.1	19.6	2.5
Harlington	0.2	19.0	0.0	0.0	0.5	0.1	19.8	15.1	31.1
Colnbrook	0.1	19.4	0.0	0.0	0.4	0.0	19.8	16.4	20.8
Lakeside 1 Osiris	0.0	18.6	0.0	0.0	1.0	0.0	19.7	12.0	64.4
Lakeside 2	0.0	19.0	0.0	0.0	0.5	0.0	19.6	15.0	30.5

The model underestimates most at Hayes (−19%), which was also the case for NO_x. This supports the idea that there is something local to this site that is not being captured by the model, most likely either the influence of traffic queues at the road junction, or the kerbside location which is not treated properly by the dispersion modelling (or both).

The average fractional discrepancy excluding Hayes is comparable to the accuracy of the measurement technique (see Section 4), so the comparisons can demonstrate only that any model bias for total annual mean concentrations is less than the uncertainty in the measurements.

The modelled contribution from the designated road network and airfield sources is on average only 0.9 µg m^{-3} (maximum 1.9 µg m^{-3}, at LHR2) compared to a background level of 19.2 µg m^{-3}. This shows that the above comparison of total annual mean concentrations essentially evaluates only the prediction of the background contribution.

There is the possibility that concentration-difference comparisons may be able to add additional information on model performance for airfield and road-network sources. However, PM_{10} concentration differences will be subject to systematic differences in measurement accuracy from one analyser to another. For analysers that use the same measurement technique and are part of the same network, some sources of inaccuracy are expected to cancel out. For example, all the TEOM analysers have been VCM-corrected using the same set of FDMS data. Nevertheless, systematic differences will remain, and are expected to be greater when the type of analyser is different. It is judged that the measurement uncertainties in differences are unlikely to be less than 2–3 µg m^{-3} even for instruments of the same type, although this judgement is not based on any specific analysis. Only if measured concentration differences within a range of angles selected to highlight particular source groups are significantly greater than measurement uncertainties will it be possible to extract additional information on model performance from difference comparisons.

Besides measurement uncertainties, it is also necessary to keep in mind the possibility of ‘natural’ variations in the background (i.e., site-to-site variations in the background that are not captured by the modelling), which may mask differences in the concentration contributions from local sources.

ON-AIRPORT SOURCES

Leaving aside measurement uncertainties, the comparison between modelled and measured total annual mean PM_{10} values is not likely to provide any detailed information on the performance of the modelling for airfield and road-network sources, given that their combined contribution is smaller than the uncertainty in the modelled value for the contribution from all other sources. The upper bound on the combined contribution is loosened further when measurement uncertainties are accounted for.

Similarly, PM_{10}, concentration differences will be unable to provide any detailed information on the contribution from airfield and road-network sources.

Based on the above, Figure 81 shows contours of the contribution from airfield sources to total annual mean PM_{10} concentrations, without any model adjustment. The contribution is less than 0.5 µg m^{-3} in the residential areas just north of the airport, reaching around 0.5 µg m^{-3} at the airport perimeter.

Figure 81 Airfield contribution to annual mean PM_{10} concentrations

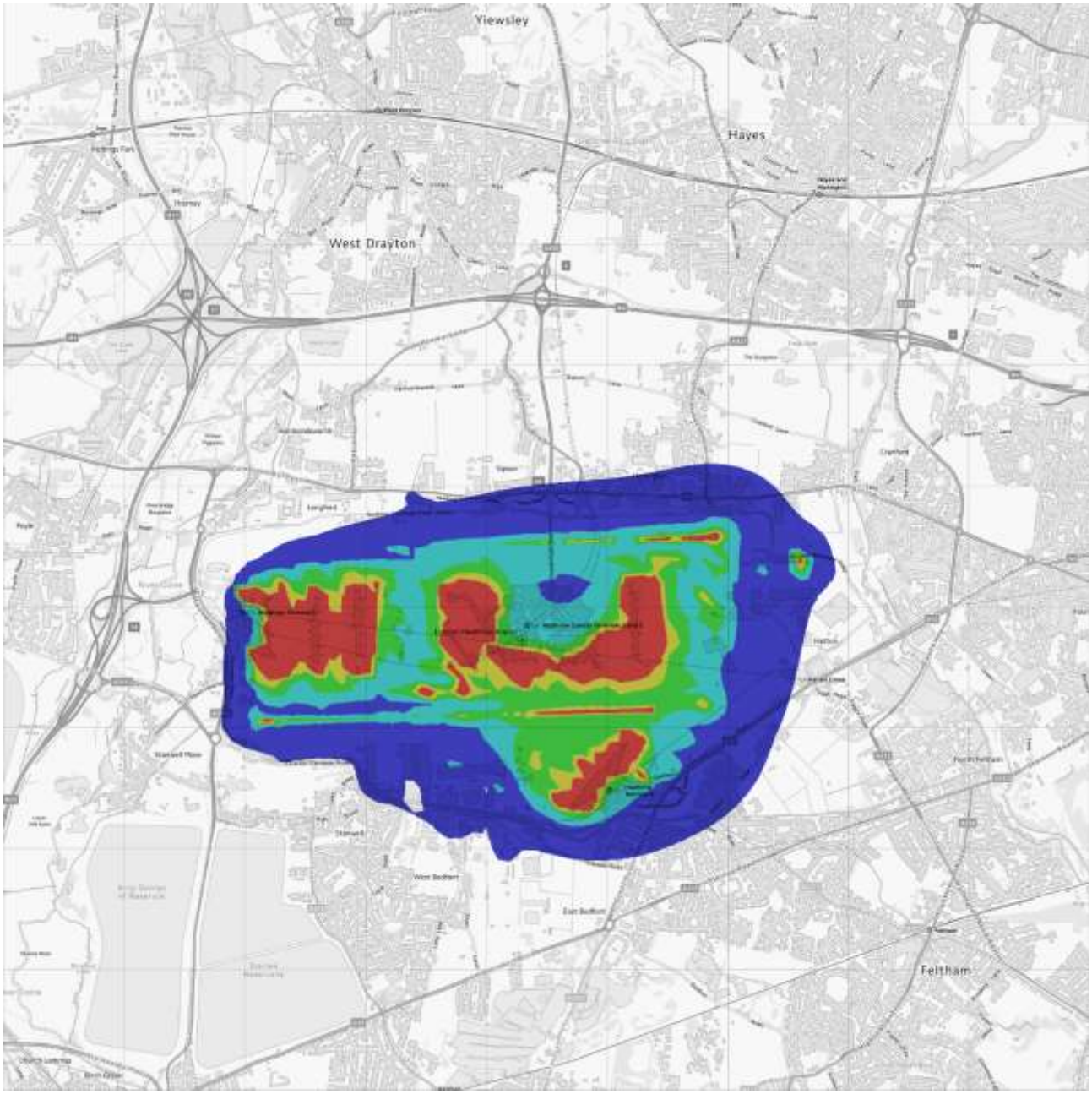

1.50 µg m^{-3}
1.25 µg m^{-3}
1.00 µg m^{-3}
0.75 µg m^{-3}
0.50 µg m^{-3}
0.25 µg m^{-3}

ANNUAL MEAN PM10 CONTOUR PLOTS

On average across the sites, total annual mean PM_{10} concentrations are overpredicted. However, there are sites where the model significantly underpredicts (e.g., at Hayes and Oxford Avenue). Given the dominance

of the background contribution to modelled PM_{10} concentrations and its inherent uncertainty, there is no adequate basis for making any model adjustment, so no adjustment factors have been applied to the model results used for generating contour plots.

Figure 82 shows contours of modelled annual mean PM_{10} concentrations.

Figure 82 Modelled annual mean PM_{10} concentrations.

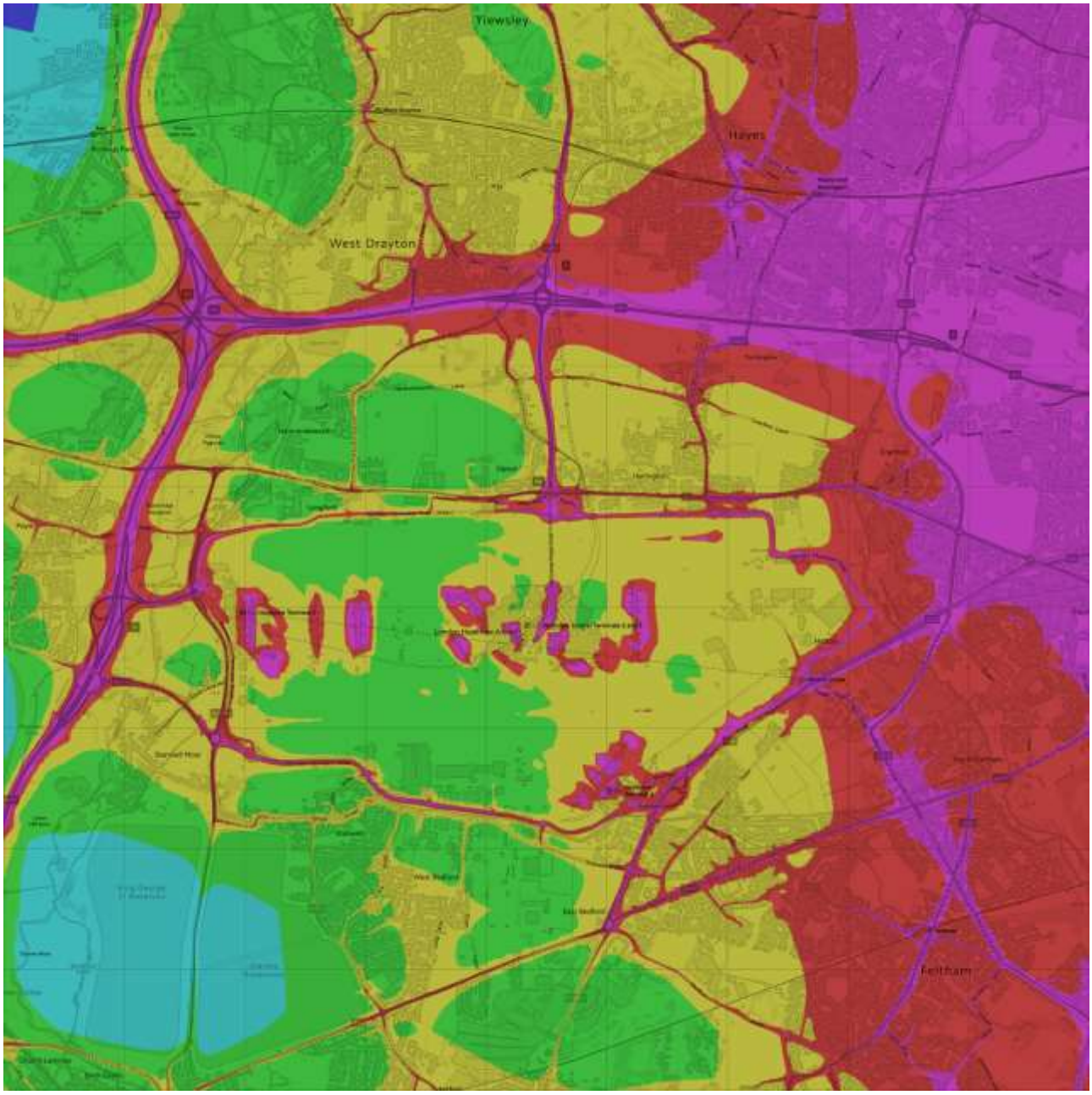

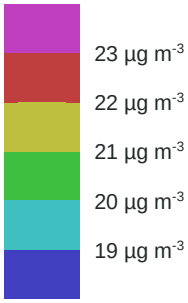

The annual mean AQS limit value for PM_{10} is 40 µg m^{-3}.
The 50 µg m^{-3} daily mean AQS limit value for PM_{10} is roughly equivalent to an annual mean of 31.5 µg m^{-3}.

$PM_{2.5}$

TOTAL ANNUAL MEAN

Table 43 compares the modelled total annual mean $PM_{2.5}$ concentrations at the continuous $PM_{2.5}$ analysers with the measured values. It also shows the breakdown of the modelled total by source category. Clearly, the background component is the dominant contributor (around 12 µg m^{-3}), with the airfield and road-network sources together contributing 1.2 µg m^{-3} at LHR2 and no more than 1 µg m^{-3} at off-airport sites. Figure 83 shows a scatter plot of modelled versus measured annual mean PM_{10} concentrations.

Figure 83 Scatter plot of modelled versus measured annual mean $PM_{2.5}$ concentrations.

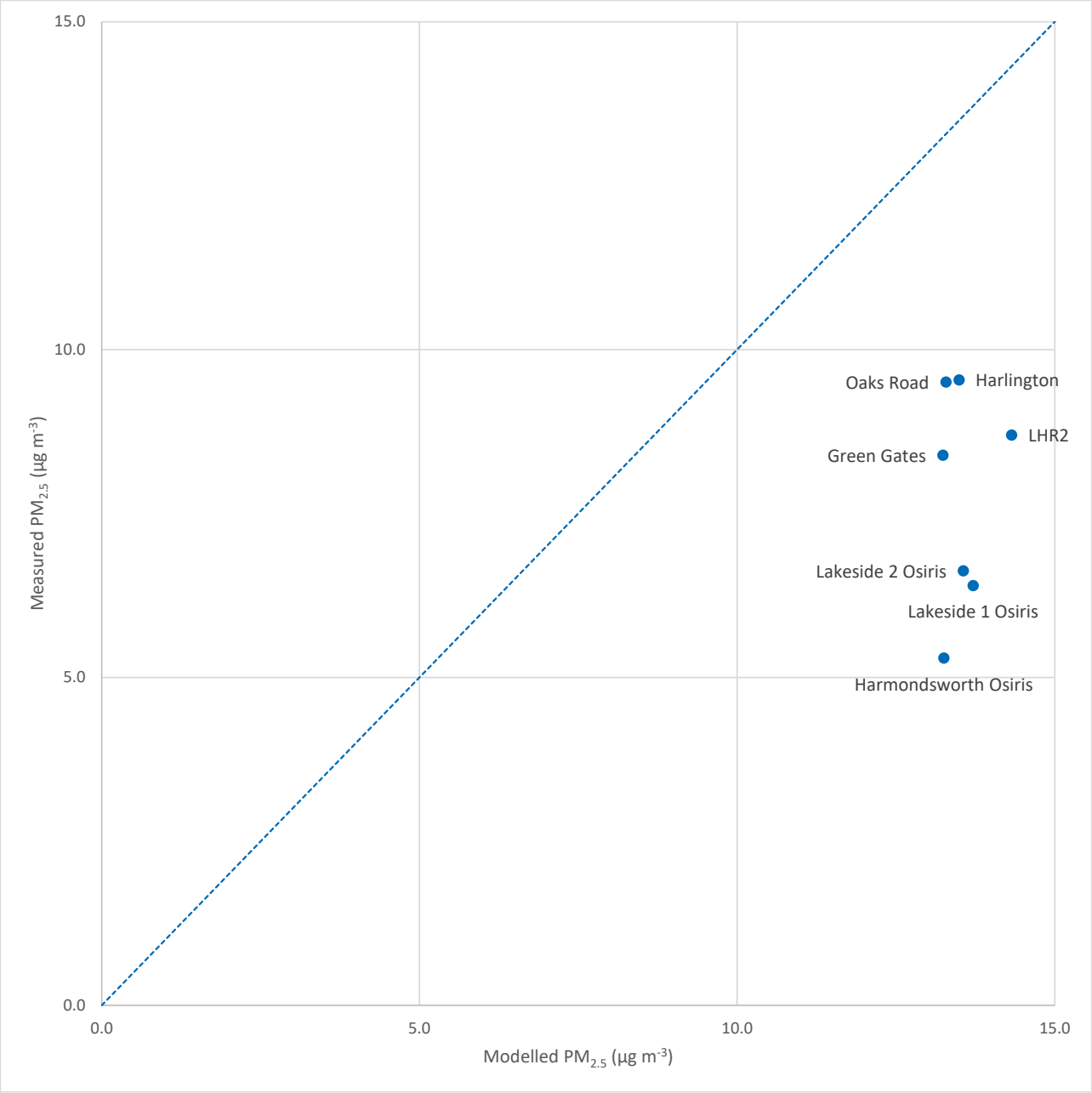

Table 43 Comparison of modelled annual mean $PM_{2.5}$ concentrations with measured values for continuous $PM_{2.5}$ analysers

Receptor name	Modelled annual mean $PM_{2.5}$ concentration (µg m^{-3})							Measured $PM_{2.5}$ (µg m^{-3})	Model bias (%)
	Aircraft	Background	Carparks	GSE	Roads	Stationary sources	Total		
Green Gates	0.1	12.2	0.0	0.0	0.4	0.0	12.8	8.4	52.8
LHR2	0.5	12.6	0.0	0.0	0.6	0.1	13.8	8.7	59.2
Oaks Road	0.1	12.5	0.0	0.0	0.2	0.1	13.0	9.5	36.5
Harmondsworth Osiris	0.1	12.5	0.0	0.0	0.3	0.0	12.9	5.3	143.3
Harlington	0.1	12.6	0.0	0.0	0.3	0.1	13.2	9.5	37.9
Lakeside 1 Osiris	0.0	12.5	0.0	0.0	0.6	0.0	13.2	6.4	106.1
Lakeside 2 Osiris	0.0	12.6	0.0	0.0	0.4	0.0	13.0	6.6	96.7

ON-AIRPORT SOURCES

Leaving aside measurement uncertainties, the comparison between modelled and measured total annual mean $PM_{2.5}$ values is not likely to provide any detailed information on the performance of the modelling for airfield and road-network sources, given that their combined contribution is smaller than the uncertainty in the modelled value for the contribution from all other sources. The upper bound on the combined contribution is loosened further when measurement uncertainties are accounted for.

Similarly, $PM_{2.5}$, concentration differences will be unable to provide any detailed information on the contribution from airfield and road-network sources.

Figure 84 Airfield contribution to annual mean $PM_{2.5}$ concentrations

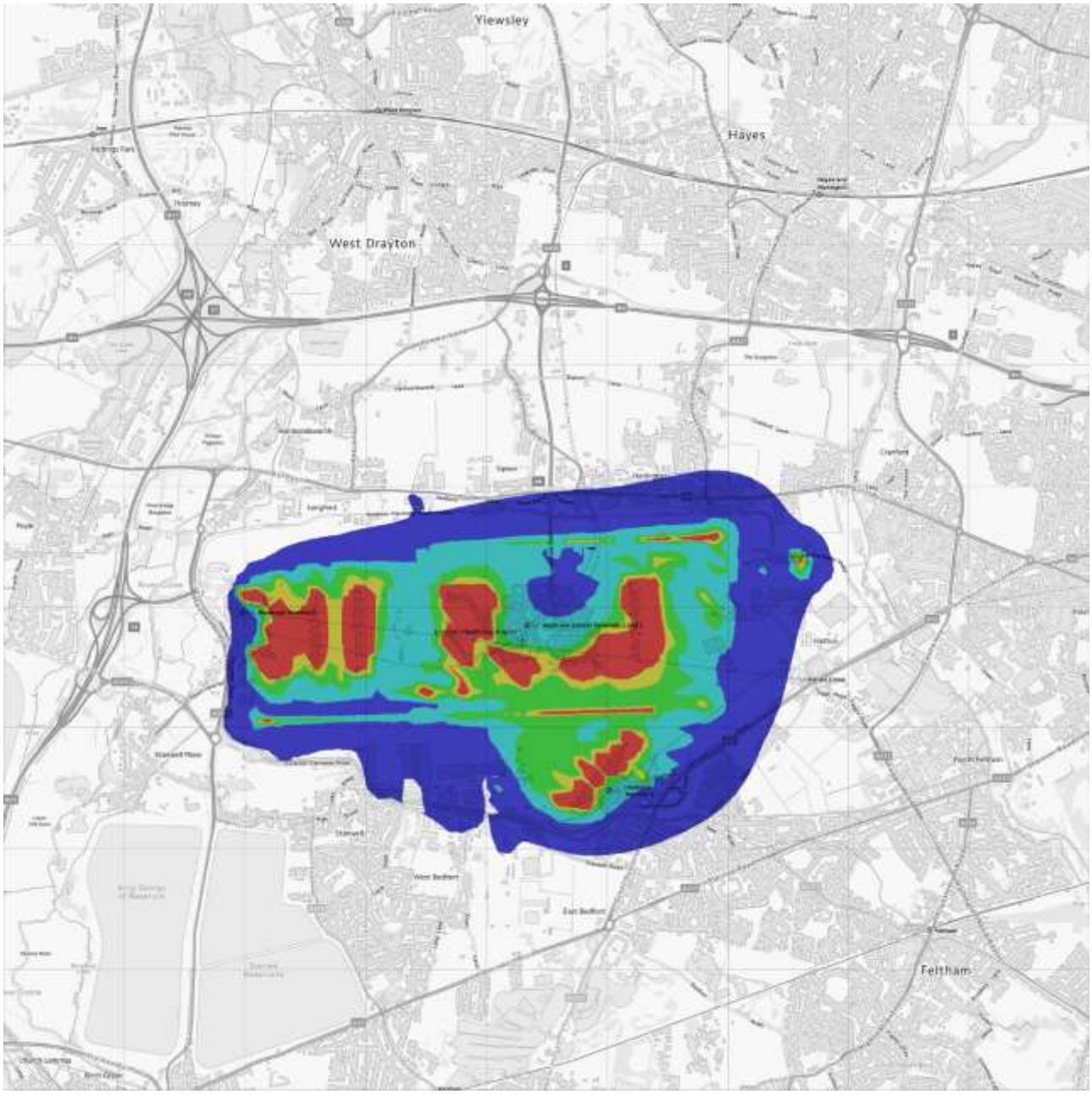

1.50 µg m^{-3}
1.25 µg m^{-3}
1.00 µg m^{-3}
0.75 µg m^{-3}
0.50 µg m^{-3}
0.25 µg m^{-3}

ANNUAL MEAN PM2.5 CONTOUR PLOTS

As was the case for PM_{10}, concentrations of $PM_{2.5}$ are overpredicted by the model. However, for $PM_{2.5}$, the overprediction is common across all sites. Again, as the background is the dominant contributor to modelled concentrations, no adjustment factors have been applied, but it should be noted that the contours of modelled annual mean $PM_{2.5}$ concentration presented in Figure 85 are an overestimate.

Figure 85 Modelled annual mean $PM_{2.5}$ concentrations.

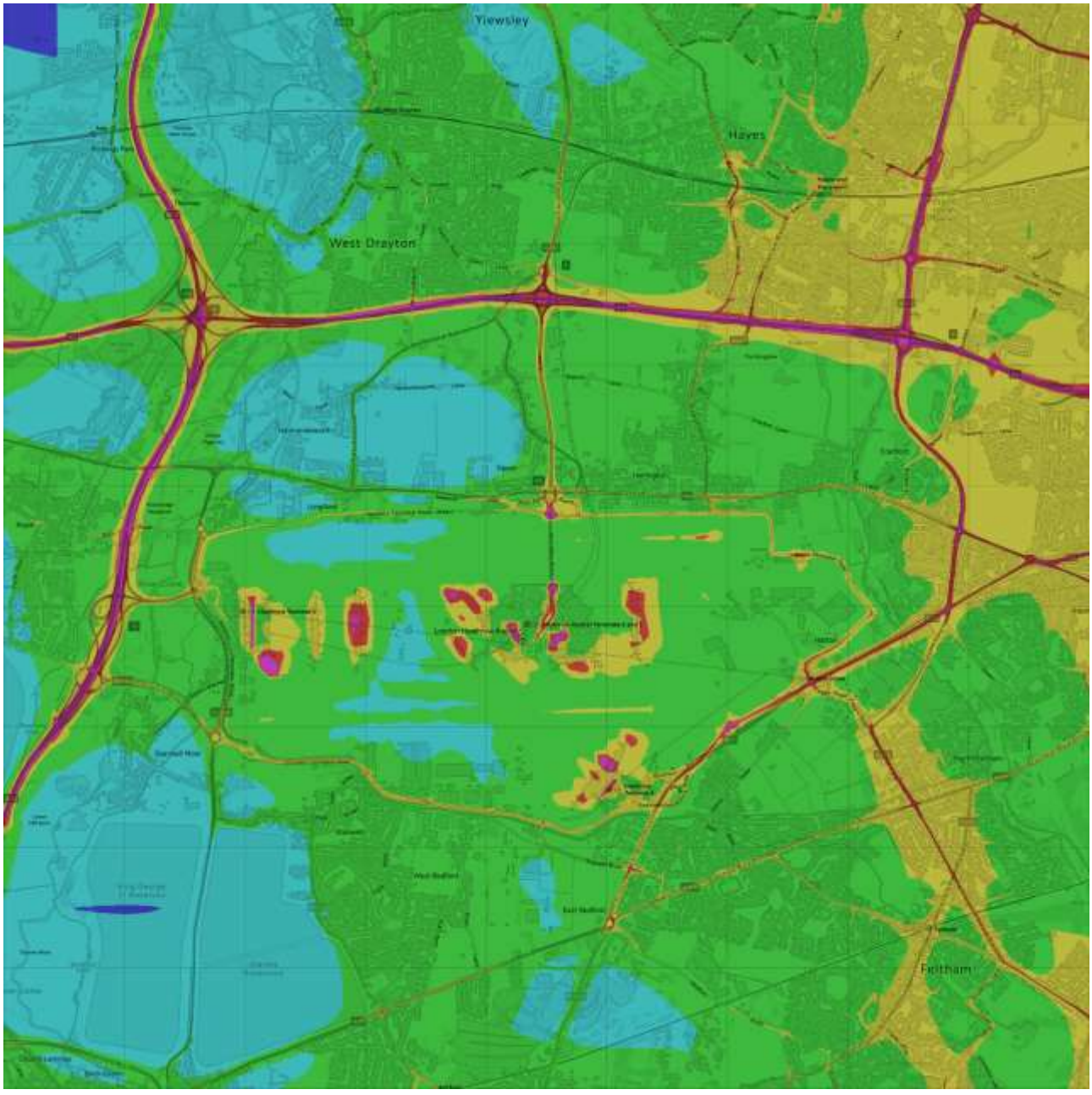

17 µg m^{-3}

16 µg m^{-3}

15 µg m^{-3}

14 µg m^{-3}

13 µg m^{-3} (the interim target for 2028)

The annual mean AQS limit value for $PM_{2.5}$ is 20 µg m^{-3}.

T: +44 (0) 1235 75 3000
E: enquiry@ricardo.com
W: ee.ricardo.com